Modelling the Interaction Between the Disease Microenvironment and Mesenchymal Stem Cells in Systemic Sclerosis

Zeinab Ahmad Taki

Supervisors

Dr Richard Stratton

Prof. Christopher Denton

Prof. Alan Salama

A thesis submitted for the degree of Doctor of Philosophy

UCL Centre of Rheumatology and Connective Tissue Disease

Division of Medicine

UCL Medical School- Royal Free

2018

Declaration

I, Zeinab Ahmad Taki, confirm that the work presented in this thesis is my own. Where information has been derived from other sources, I can confirm that this has been indicated in the thesis.

Zeinab Ahmad Taki

Abstract

Systemic sclerosis (SSc) is a complex autoimmune disease with unknown aetiology. While the presence of auto-antibodies classifies this disease as autoimmune, the issues concerning this disease extend much further with particular respect to inflammation and the gradually progressing internal and external organ fibrosis. If not lethal, at the very least, the symptoms of SSc are life-altering. Many potential driving forces are hypothesised to exacerbate pathology, one of which is the microenvironment in lesional skin, in which resident mesenchymal stem cells (MSCs), are exposed to aberrantly expressed growth factors and cytokines, and excessively stiffened and abundant extracellular matrix. In this thesis, it is hypothesised that MSCs adopt a pro-fibrotic, chronic, wound healing phenotype in response to the disease microenvironment.

Different representations of the disease microenvironment were assessed, including patient blister fluid, and some of its individual components, IL31 and lactate, in addition to the physical stiffness of the microenvironment. MSCs cultured in these conditions were assayed for migration, induced gel contraction, pro-fibrotic gene expression and differentiation. The presence of activated MSCs in patients' skin was also assessed and compared with healthy skin. Patient blister fluid induced MSC migration, collagen gel contraction and pro-fibrotic gene expression more than healthy blister fluid. Additionally, individual components of the SSc blister fluid accounted for at least some of these responses. Osteogenic differentiation of MSCs was enhanced by SSc microenvironments, both soluble and physical, whereas adipogenic differentiation was inhibited. Next-generation sequencing of treated MSCs highlighted fibrogenic and inflammatory pathways upregulated by SSc blister fluid.

The role of MSCs in SSc pathogenesis was until now relatively unexplored. The results of this thesis give new insight into the pathological part MSCs play in this disease and highly implicate MSCs in SSc related fibrosis, wound healing, tissue scarring and remodelling, calcinosis and loss of subcutaneous fat.

Impact Statement

The research presented in this thesis spans two fields of knowledge. The first being the current efforts to explain and understand systemic sclerosis and ultimately treat, and the second being the understanding of mesenchymal stem cell activity and function. This research fills a critical gap in the knowledge of the role of these cells in systemic Sclerosis, particularly with regards to early pathogenic phenomena and causative functions.

The findings strongly place mesenchymal stem cells as integral factors in pathogenicity. Widely viewed with optimism, to date, these cells have been studied as therapeutic agents to exploit for the treatment of systemic sclerosis, and this thesis essentially suggests the opposite. Evidence of these cells being at least partially responsible for many systemic sclerosis pathologies is demonstrated in this thesis. Systemic sclerosis is a relatively rare disease, and as such efforts in elucidating its cause still raise more questions than they answer. As such, while the findings of this research fill many gaps in this field, they also present many opportunities for further research in this discipline.

The findings of this research benefits academia in a number of ways. A novel method for visualising mesenchymal stem cells in dermal tissue, that maintains structural integrity of the cells and extracellular matrix, is presented. This alone will impact the way not only mesenchymal stem cells are visually analysed in the laboratory, but also the extracellular proteins of the environment. The large and extensive next-generation sequencing assay of this thesis has the potential for much further expansion and investigation. For the purpose of this thesis, a general approach was taken, however this assay presents many opportunities for further and more detailed studies.

On the other hand, the research also impacts fields outside academia. The strongest being the evidence against using mesenchymal stem cells indiscriminately as therapeutic agents in systemic sclerosis, as is currently being trialled. The studies also give insight into how lactate concentrations can be used as part of a minimally invasive technique to aid in systemic sclerosis diagnosis in the healthcare system. Additionally, IL31 was highlighted as a

major factor in pathogenicity, particularly with regards to pruritus, a symptom commonly suffered by patients. Inhibitors of IL31 and its receptors are being trialled in atopic dermatitis, and this thesis, shows evidence that the pruritus being studied in atopic dermatitis is similar to that of systemic sclerosis with regards to IL31.

The impact of the research is relevant on a global scale and has the potential to be delivered shortly, with regards to IL31 inhibition, or lactate measurement in diagnosis. Nevertheless, other aspects of the research will impact the broader field of research by filling in critical gaps in knowledge.

The work has been disseminated in national and international conferences and has also led to the collaboration with other academics internationally.

Acknowledgements

Firstly, I would like to thank the Royal Free Charity and Rosetrees Trust for the funding they were kind enough to donate, and UCL for giving me the opportunity to work on this wonderful and fruitful project.

I would like to express my sincere gratitude to Dr. Richard Stratton for his invaluable support and counsel, in addition to his motivation and immeasurable knowledge, during the course of this research. Together with Prof. Chris Denton and Prof. Alan Salama, I was in the hands of an enviable team.

I am forever indebted to my parents for their undying love, sacrifice and guidance, without which this PhD would have been impossible, my siblings for always keeping me sane and my in-laws for their continuous care and encouragement. Lastly, I would like to thank my husband for his endless support, patience and inspiration.

Abbreviations

αCHCA	α-cyano-4-hydroxycinnamic acid
ACAN	Aggrecan
ACTA2	Actin 2
ALCAM	Activated leukocyte cell adhesion molecule
ALPL	Alkaline Phosphatase
ANOVA	Analysis of Variance
ANXA	Annexin
α-SMA	α-smooth muscle actin
ATP	Adenosine Triphosphate
BCA	Bicinchoninic Assat
BMP2	Bone morphogenetic protein 2
BSA	Bovine Serum Albumin
CBF	Healthy control blister fluid
C/EBP	CCAAT enhancer binding protein
CEMIP	Cell migration inducing hyaluronan binding protein
CLA	Cutaneous lymphocyte antigen
Col1A1	Collagen Type 1A1
CSRP2	Cysteine and glycine rich protein 2
CTGF	Connective tissue growth factor
Dkk1	Dickkupf-1
DMEM	Dulbecco's Modified Eagle Medium
DNA	Deoxyribonucleic acid
DPBS	Dulbecco's phosphate buffered saline
EDTA	Ethylenediaminetetraacetic acid
ELISA	Enzyme linked immunosorbent assay
ENG	Endoglin
ERK	Extracellular regulated kinase
FAK	Focal adhesion kinase
FCS	Foetal calf serum
FGF	Fibroblast growth factor
FTL	Fingertip Lacticemy

GAPDH	Glyceraldehyde-3-Phosphate Dehydrogenase
GAS1	Growth Arrest 1
GM-CSF	Granulocyte-macrophage colony-stimulating factor
HC	Healthy control
HCl	Hydrochloric Acid
HGF	Hepatocyte growth factor
IBMX	3-isobutyl-1-methylxanthine
IFN	Interferon
IgG	Immunoglobulin G
IL	Interleukin
IL13RA2	Interleukin 13 Receptor A 2
IL31RA	Interleukin 31 Receptor A
ILK	Integrin Linked Kinase
IPA	Ingenuity Pathway Analysis
JAK	Janus Kinase
MAPK	Mitogen activated protein kinase
MHC	Major histocompatibility complex
miRNA	Micro-RNA
MLCK	Myosin light chain kinase
MRSS	Modified Rodnan Skin Score
MRTFA	Myocardin Related Transcription Factor A
MSC	Mesenchymal Stem Cell
NT5E	5'-nucleotidase-ecto
OCT4	Octamer binding transcription factor 4
OIM	Osteogenic induction media
PAH	Pulmonary Arterial Hypertension
PBS	Phosphate buffered saline
PDGF	Platelet derived growth factor
PDGFR	Platelet derived growth factor receptor
PI3K	Phosphoinositide-3-kinase
PPAR	Peroxisome proliferator activated receptor
qPCR	Quantitative polymerase chain reaction
RANKL	Receptor activator of nuclear factor Kappa-B ligand

RIPA	Radioimmunoprecipitation
RPM	Rotations per minute
RNA	Ribonucleic acid
RUNX	Runt related transcription factor
SEM	Standard error of mean
SSC	Saline Sodium Citrate
SSc	Systemic Sclerosis
SScBF	Systemic Sclerosis blister fluid
STAT	Signal transducer and activator of transcription
TBP	TATA binding protein
Th2	T helper 2
TIMP	Tissue inhibitor of metalloproteinase
TNF	Tumour Necrosis Factor
TGFβ	Transforming growth factor β
TWIST	Twist related protein 1
VEGF	Vascular endothelial growth factor

Table of Contents

List of Figures

List of Tables

Chapter 1 : Introduction

1.1 MSC definition and potential

Mesenchymal stem cells (MSCs) are heterogeneous, multipotent, committed progenitor cells with the ability to self-renew as well as differentiate into cells of mesenchymal origin, namely osteoblasts, adipocytes and chondrocytes. They were originally identified and isolated from bovine bone marrow by Friedenstein in the 1970s (Friedenstein et al. 1974). Cells with these properties can be derived from bone marrow, fat and umbilical cord and it has been proposed that the differently derived MSCs have some lineage commitment such that those in bone marrow do not act in skin; likewise those in fat do not travel to the bone marrow (Sacchetti et al. 2016a).

Much controversy surrounds the nomenclature, definition and origin of these cells. Two main theories exist; one is that they are a subset of specific pluripotent progenitor cells present only in bone marrow that give rise to skeletal cells. The role of these progenitors are mainly regarding differentiation and homeostasis of the bone marrow. The second possibility is that MSCs are a set of cells found in various parts of the body, otherwise known as 'pericytes'. These cells are pleiotropic and have functions other than differentiation. Simultaneously, they are thought to be myogenic in their pluripotency. This theory suggests that there was an original set of cells from which these different MSCs are derived that had all the possible roles assigned to MSCs, for example immunomodulatory as well as regenerative. On the other hand, the "pericyte" MSCs have not shown evidence of spontaneous self-renewal *in vivo* and their responses to tissue injury leads to fibrosis and scarring rather than regeneration, whereas the bone marrow MSCs spontaneously self-renew (Sacchetti et al. 2007). There is one explanation for the diverging theories. Caplan has suggested that there is a group of CD146 positive cells that have both skeletogenic and myogenic differentiation potential and fit the more blurred definition of MSCs (Caplan 2008). Others claim that that while there indeed is a cell type that is CD146-positive and myogenic, they differ from the CD146 positive bone marrow derived cell in their expression profile and

differentiation potential supporting the theory of distinct origins (Sacchetti et al. 2016).

For the purpose of this thesis, MSCs are defined as plastic adherent fibroblast-like cells of mesenchymal origin, shown to be multipotent and capable of differentiating down adipogenic, osteogenic and chondrogenic cell lineages. MSCs do not have specific surface markers and therefore, are characterised through combinations and elimination of markers, as well as differentiation capacity. *In vivo*, MSCs express variable markers dependent on the tissue they reside in and factors present in the surrounding environment. Then, following isolation and culture *in vitro*, the markers may vary even more depending on the method of isolation, together with culture material and cryo-preservation (Chamberlain et al. 2007). As such translating MSC surface expression findings *in vitro* to *in vivo* models holds some difficulty. To remove some of the confusion and variation, MSCs have been categorised as being negative for CD33, CD45, CD14, CD19, HLA-DR, CD105, and positive for CD73 and CD90, along with Stro1, NG2 and Gli1 (Uccelli et al. 2008).

Residing on the outside of blood vessels keeps MSCs close to the blood for easy migration to target sites of wounded or stressed tissue, consistent with the theory proposing that pericytes surrounding microvasculature are derived from MSCs. Physiologically quiescent, MSCs are triggered to activate when needed to differentiate into other cell types downstream of their lineage commitment. While these are of mesenchymal origin, some data suggests that MSCs can also be progenitors to endothelial cells during vasculogenesis and vasculature remodelling (Pittenger et al. 1999).

The multipotency, differentiation potential, self-renewal capacity, lack of teratoma formation and immune interaction makes MSCs of interest as therapeutic targets in diseases of degeneration, tissue injury and immune system deregulation. It seems to be their population heterogeneity that permits such a broad range of function (Meirelles et al. 2009;Tyndall 2014).

MSCs can inhibit the release of pro-inflammatory cytokines and interact with both the innate and adaptive immune system, giving rise to the modulation of several effector functions (Uccelli et al, 2008). Generally, they have a dampening effect on the innate and adaptive immune response. However, they can be induced to becoming more plastic in their effects. This plasticity depends on multiple factors such as cell-cell contact and the ratio of MSCs to target cells, possibly explaining how MSCs switch function, for example from anti-proliferative to anti-inflammatory (Glenn and Whartenby 2014). Furthermore, the microenvironment of the MSCs can dictate their plasticity and likely causes the switch from an immune-inhibitory state to an immune-stimulatory one. The anti-inflammatory effects of MSCs are directed at many immune cells. They can inhibit the respiratory burst of neutrophils after detection of a pathogen keeping the pathogen associated molecules hidden from the immune system. They can also inhibit monocyte differentiation into dendritic cells. Dendritic cells are antigen-presenting cells that engulf the pathogen and present the antigen on their cell surface to T-cells to provoke an inflammatory response. MSC inhibition of dendritic cell responses thereby stops the crossover from innate to adaptive immune systems. MSCs also have an effect on macrophage phenotypes and encourage M2 anti-inflammatory polarisation as opposed to the M1 pro-inflammatory phenotype through indoleamine 2, 3-dioxygenase and prostaglandin E2 (Uccelli et al. 2008). In the adaptive immune response, MSCs directly adhere to Th17 cells during inflammatory responses to resolve inflammation and reduce Th17 expression of pro-inflammatory cytokines (Ghannam et al. 2010).

There are a few major reservations regarding MSC usage as treatment therapies. The plasticity of MSCs means that their phenotype and activity can be readily altered *ex vivo.* Considering that before MSC administration into patients, MSCs need to be cultured for a minimum of 10 weeks in order to achieve sufficient MSC numbers, spontaneous differentiation and genomic instability affected by culture methods are concerns (Tarte et al. 2010). It is imperative to ensure that MSC phenotype and multipotency are unaffected before considering MSC administration as a treatment.

Animal models have shown that when MSCs are administered intravenously, few cells actually reach the target site, the majority being trapped in the small capillaries of the lungs (Lee et al. 2015;Tyndall 2014). As such, an alternative means of administration needs to be developed if they are to be used therapeutically. Homing of MSCs to their target site is believed to involve CXCR4 yet paradoxically, overexpression of CXCR4 does not seem to induce more efficient homing to injury (Gheisari et al. 2012). Since very few MSCs actually reach the target site following administration, it is safe to assume that the beneficial results of MSC infusion is not explained entirely by engraftment, differentiation and restoration or replacement of damaged tissue. It is thought that the short survival time cannot accommodate the lengthy process of differentiation and, as such, the paracrine secretions of MSCs in the target site are responsible for the results seen after infusion. In addition to mediating their immune effects through direct cell-cell contact, MSCs act on neighbouring cells in a paracrine fashion through their specific secretome. Extracellular vesicles are released from MSCs to their target immune cells. These vesicles are made from the MSC cell membrane and contain soluble factors, proteins, nucleic acids and lipids packaged in such a way that they are protected against cellular degradation. Such factors include micro-RNA (miRNA) molecules, proteins and lipids that are released in exosomes and act extracellularly to carry out MSC function. MSCs promote angiogenesis and neo-vascularisation; one way this is thought to occur is via exosome release (Bruno et al. 2015;Roccaro et al. 2013).

1.2 Adipogenic and osteogenic differentiation of MSCs

In order for MSCs to differentiate they need to be subject to very specific microenvironmental cues that span further than matrix stiffness and cytokine concentration. Adipogenic and osteogenic differentiation of MSCs are delicately balanced processes that almost oppose each other. Loss of osteogenic differentiation observed in the elderly coincides with an increase in adipogenesis of bone marrow derived MSCs (Nuttall and Gimble 2000). There are many common pathways involved in both differentiation lineages including Transforming Growth Factor β (TGFβ) and SMADs, canonical Wnt pathway,

Janus kinase/signal transducers and activators of transcription (JAK/STAT), phosphatidylinositol-4,5-bisphosphate 3-kinase (PI3K) and Mitogen-activated protein kinases (MAPK). However, the regulation of these pathways and the downstream transcription factors involved are thought to determine the direction of differentiation. For example, adipogenic differentiation relies on CCAAT-enhancer-binding proteins (C/EBP) and peroxisome proliferator-activated receptors (PPAR) transcription factors, whereas osteogenic differentiation involves Runt-related transcription factor 1 (RUNX) and OSX to induce expression of osteogenic genes (Bellido et al. 1997;Fritzius and Moelling 2008).

It is now thought that determination of differentiation direction begins at the gene expression level rather than through extracellular signalling cues and in particular, the gene expression is controlled by miRNA molecules. miRNAs are short RNA molecules transcribed predominantely from non-coding regions of the DNA. They function to inhibit mRNA translation into protein and ultimately gene expression by either, cleaving mRNA molecules resulting in degration, or inhibiting ribosome association and translation, thus ensuing cell-specific gene silencing (Figure 1.1). A differentiation study of MSCs showed that the expression of miR-17-5p, miR-17-10a and miR-17-20a was increased during adipogenic differentiation and decreased during osteogenic differentiation (Li et al. 2013). Furthermore, when these miRNA molecules were overexpressed, differentiation was able to be steered towards adipogenic lineages, whereas inhibiting them significantly reduced adipogenic differentiation. This study found that bone morphogenetic protein 2 (BMP2) was the target of these miRNA molecules at a post-transcriptional level and that its expression was decreased by miR-17s. BMP2 downregulation via miR-17-5p was shown to allow expression of C/EBP and PPAR. Inhibition of the miR-17 molecules showed opposing effects and initiated osteogenic differentiation (Li et al. 2013).

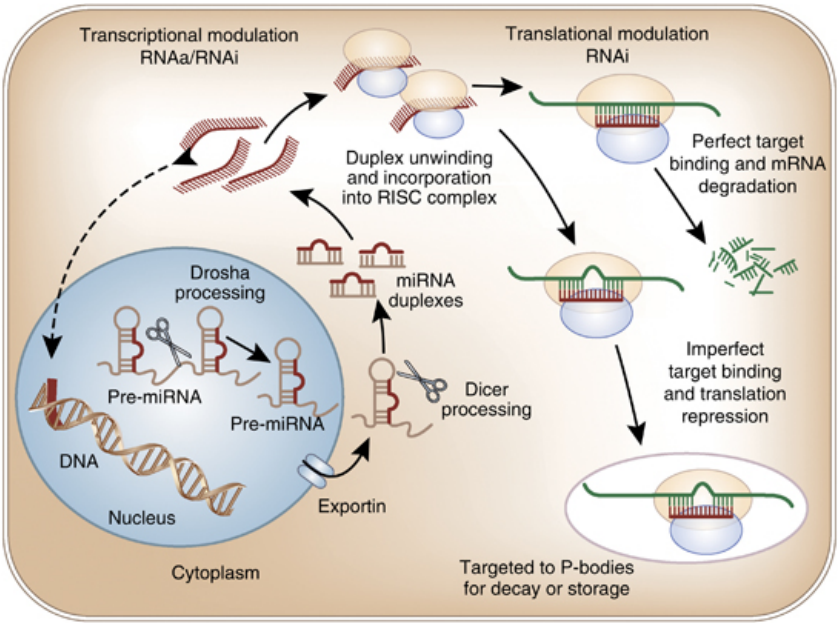

Figure 1.1 ***miRNA synthesis and function.*** *miRNAs are transcribed by RNA polymerase II in the nucleus and after association with modification complexes (DROSHA), the miRNA molecules are processed to adopt a hairpin loop structure denoted pre-miRNA. Pre-miRNA molecules are transported into the cytoplasm for further processing into single stranded miRNA molecules. Together with protein complexes (RISC), the miRNA molecules interfere with translation in one of two ways. They either have perfect complementary base pairing with a section of mRNA and thereby cleave the mRNA, resulting in its degration. Or, imperfect base pairing to mRNA sections can result in blockage of ribosome attachement and repression of translation (Karthikeyan et al. 2012).*

Hence MSCs are pluripotent tissue resident cells, quiescent under homeostasis, but activated following tissue injury and, therefore, of relevance to complex human diseases. Dysregulated activation of MSCs may lead to abnormal immunomodulation, wound healing and differentiation responses.

1.3 SSc as a disease

Systemic sclerosis (scleroderma, SSc) is an autoimmune, connective tissue disease of unknown aetiology, with skin thickening and fibrotic lesions being the primary manifestations (Gabrielli et al. 2009). Prevalence varies considerably across the world, but generally affects between 150-300 people per million (Barnes and Mayes 2012). It can be categorised into two types, diffuse and limited, defined by the pattern of skin involvement. In limited

cutaneous SSc (lcSSc) skin involvement is restricted to the extremities and face and does not extend proximal to the elbows, whereas diffuse cutaneous SSc (dcSSc) is characterised by more extensive skin involvement, spreading proximal to the elbows and often extending onto the trunk. DcSSc tends to be a more multi-systemic condition, affecting the skin, and linked to lung, heart, gastro-intestinal tract and kidney involvement, whereas in lcSSc, lung and kidney involvement are less frequent, but vascular manifestations such as pulmonary hypertension and critical digital ischaemia are more prominent (LeRoy et al. 1988;van den Hoogen et al. 2013). SSc is not considered to be primarily a genetic disease and does not follow a Mendelian pattern however, there does seem to be some level of genetic predisposition possibly followed by early environmental trauma. Polymorphisms in extracellular matrix genes such as Fibrillin 1 (*Fbn1)* and Connective Tissue Growth Factor (*CTGF)* have been associated with SSc manifestation along with exposure to silica dust, cytomegalovirus and vinyl chloride (Eckes et al. 2014). SSc progression leads to many life-threatening complications including cardiac complications, renal failure and the most common cause of death in SSc patients, pulmonary arterial hypertension (PAH) (Barnes and Mayes 2012).

One of the most common and ubiquitous symptoms of SSc is Raynaud's phenomenon, a syndrome that presents itself throughout the SSc pathology timeline and is essentially the constriction of blood flow to acral regions, particularly digits. It can be described as the result of an imbalance between vasodilation and vasoconstriction and in more severe cases, like those seen in SSc, digital ulcers and eventual amputation are common results of this imbalance. Furthermore, the digital ulcers that occur in SSc patients often remain unhealed due to dysregulated tissue repair as a complication of SSc. SSc patients face limitations in daily life activities that rely on finger and digit dexterity, and this is particularly noticeable during the colder seasons where the physiological vasoconstriction makes the underlying Raynaud's symptoms more severe. Blood perfusion can be detected by laser speckle contrast analysis and the difference between healthy and SSc images are stark. Healthy images show blood circulation across the entire palm, concentrating in the fingers, as represented by the red patches, while SSc palms are shown

as blue, indicating very little blood perfusion, and this is exaggerated in the fingers (Figure 1.2). The Raynaud's phenomenon in SSc patients essentially stops normal blood circulation resulting in the white appearance of the fingers which then turn blue and eventually red after reperfusion. While Raynaud's phenomenon can occur in otherwise healthy people, known as primary Raynaud's, secondary Raynaud's is associated with underlying autoimmune conditions. Approximately 95% of SSc patients present with secondary Raynaud's phenomenon (Velayos et al. 1971).

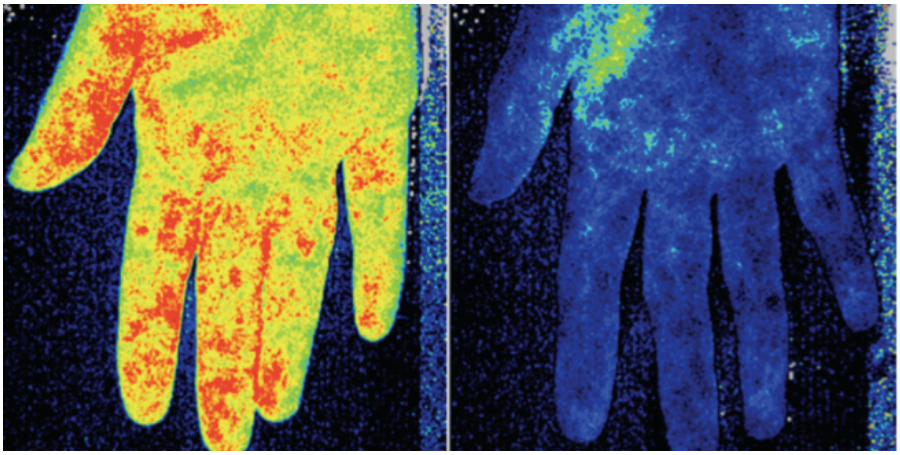

Figure 1.2 ***Raynaud's Phenomenon in SSc.*** *Laser speckle contrast imaging of healthy (left) and SSc patient (right). SSc patients show considerably less cutaneous blood perfusion (Ruaro et al. 2015).*

SSc-associated Raynaud's phenomenon is characterised by the loss of capillaries and vascular architecture in the acral regions particularly in the nail fold capillary beds found in the fingertips. As SSc pathophysiology progresses, the receding microvasculature then becomes that of enlarged microcapiliaries and microhaemorrages, eventually resulting in areas completed void of vasculature (Lambova and Muller-Ladner 2017) (Figure 1.3).

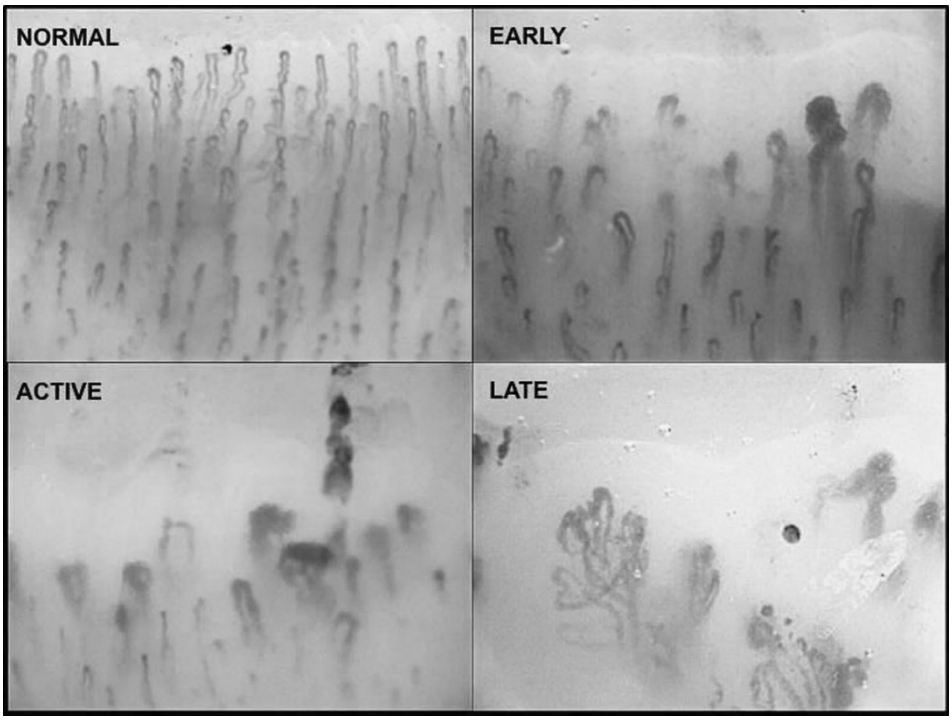

Figure 1.3 ***Nailfold capillaries of healthy and SSc individuals.*** *Capillaroscopic images (200x magnification) of healthy normal nailfold capillary beds, and SSc patients with progressive symptoms from early, active and late SSc patients (Lambova & Muller-Ladner 2017).*

Autoantibodies are characteristic of SSc, detected in more than 95% of cases, and thought to be products of chronically hyperactive plasma cells (Sato et al. 2001). They are against ubiquitous nuclear components; topoisomerase, RNA polymerase III, centromere proteins as well as some against endothelial (EC) and fibroblast cells, possibly explaining how SSc is a multi-systemic disease (Baroni et al. 2006;Cepeda and Reveille 2004;Ronda et al. 2002).

The route of pathology of SSc can be simplified down to microvascular damage followed by an uncontrolled inflammatory response that gives rise to fibrosis. Effective treatments are available for vascular complications including endothelin antagonists, prostacyclin derivatives, and phosphodiesterase inhibitors (Kahaleh and LeRoy 1999). SSc-related fibrosis continues to be a challenging condition to treat and as of yet, no therapy has

been shown to benefit (Denton 2015). Fibrotic lesions are caused by a continuous aberrant tissue repair process and extracellular matrix deposition. The matrix stiffness, caused by extracellular matrix deposition and the excess collagen, is enough to induce myofibroblast differentiation and activation (Shiwen et al. 2015). Myofibroblasts are the major producers of collagen and other extracellular matrix proteins, overproduced in response to TGFβ (Lafyatis 2014;Hinz 2009;Shiwen et al. 2015).

Cells typically undergo anoikis, a form of apoptosis, once they are functionally redundant. For example, myofibroblasts are removed, avoiding inappropriately prolonged tissue repair (Juric et al. 2009;Shiwen et al. 2015). Anoikis depends on cell detachment from the extracellular matrix, blocking pro-survival pathways. However, in SSc, cells are often resistant to anoikis and can remain viable following detachment for a prolonged amount of time. This could be one explanation of the chronic nature of the disease (Santiago et al. 2001).

1.4 SSc microenvironment

1.4.1 The role of growth factors and cytokines

The microenvironment in SSc lesions is believed to have a unique composition of cytokines and growth factors. The blister fluid method of sampling allows direct analysis of the microenvironment in fibrotic lesions, rather than the global analysis serum would achieve (Sondergaard et al. 1998). The SSc microenvironment consists of chemokines released by damaged resident cells, growth factors and cytokines produced by immune cells recruited into the lesions as well as growth factors secreted by a variety of cells including activated resident cells, which auto-stimulate as well as influence the immune cells infiltrating the lesions. Together, these factors all contribute to the pathogenesis. The combination of soluble factors present in the lesions is believed to contribute to fibroblast stimulation and differentiation to myofibroblasts, leading to the fibrosis seen.

Multiple lines of evidence support the notion of an altered growth factor and cytokine profile in the disease microenvironment, including published microarrays based on tissue samples, *in vitro* studies using cultured cells from the lesions as well as analysis of the extracellular fluid from the lesions using the blister fluid method as a minimally invasive technique to sample the lesions (Higashi-Kuwata et al. 2009; Sondergaard et al. 1998).

TGFβ, CTGF and platelet derived growth factor (PDGF) are the most widely studied growth factors implicated in SSc. They are linked in many ways. TGFβ stimulates the expression of TGFβ and PDGF receptors on the cell surface of fibroblasts, and also stimulates their production of CTGF and the vasoconstrictor, endothelin-1. The CTGF induced by TGFβ can promote fibroblast proliferation and migration to sites of inflammation. Excess PDGF signalling in the microenvironment caused by upregulation of the receptor and an increase in the growth factor itself, induces fibroblast chemotaxis and further TGFβ production. All three of these interlinked growth factors can act independently and together in their promotion of collagen synthesis along with other extracellular matrix proteins, fibronectin and proteoglycans. Moreover, they also inhibit extracellular matrix degradation by stimulating production of tissue inhibitors of metalloproteanases (TIMPs), enzymes involved in the breakdown of extracellular matrix proteins (Eckes et al. 2014).

Furthermore, fibroblasts respond to the excess TGFβ in SSc microenvironment, resulting in PDGF Receptor (PDGFR) upregulation which in turn causes a stronger reaction to PDGF, known to be increased in the microenvironment, creating a chronic feedforward cycle (Ball et al. 2010). Also, anti-PDGFR autoantibodies, found in SSc patients, may bind to the upregulated PDGFR and via the Ras/extracellular signal-related kinase (ERK) pathway, produce collagen Type I and reactive oxygen species, resulting in fibroblast to myofibroblast differentiation (Baroni et al. 2005; Ho et al. 2014).

The importance of TGFβ and PDGF in SSc fibrotic progression has led to the hypotheses that their inhibition is a possible therapeutic target in SSc treatment and fibrosis management. *In vitro* experiments have highlighted the

role of TGFβ signalling in fibrosis. Treatment of human dermal fibroblasts with TGFβ increases α-smooth muscle actin (α-SMA) expression indicating myofibroblast presence and activation. The canonical Wnt pathway is proposed to be one of the ways in which TGFβ causes myofibroblast differentiation. Nuclear accumulation of β-catenin confirms Wnt pathway activation in the SSc microenvironment (Bergmann and Distler 2016).

Wnt treatment of dermal fibroblasts resulted in a similar α-SMA response, indicating its role downstream of TGFβ in addition to nuclear accumulation of β-catenin. Inhibiting TGFβ pathway activation with a TGFβ receptor inhibitor SD-208 and inhibiting the Wnt pathway with Dickkopf-1(Dkk1) leads to a decrease in nuclear β-catenin presence. Dkk1 is found to be decreased in fibrosis and therefore is an interesting target to exploit in fibrosis treatment. *In vivo* mouse models of fibrosis also showed comparable results. Translating this into clinical trials has proven more difficult with less than convincing results (Bergmann & Distler 2016). Autoantibodies activating PDGFR can be found in some SSc patients and can explain the chronic over-stimulation of this pathway and the resulting collagen and α-SMA expression in SSc (Gabrielli et al. 2009). As such, targeting these activating antibodies was thought to be a potential therapy for SSc. Imatinib mesylate inhibits the activating autoantibodies, via its effect on the PDGF receptor tyrosine kinase. *In vitro* mouse studies of imatinib mesylate showed promising results by alleviating skin fibrosis in an SSc mouse model through PDGF signalling inhibition (Akhmetshina et al. 2009). Translation of this into SSc patients has proved less than successful. In a Phase 2 trial, the adverse effects of imatinib mesylate meant that only 12/20 SSc patients completed the trial. Furthermore, in another randomised control trial, no improvement of skin fibrosis was detected, although there was some indication of improved pulmonary function (Prey et al. 2012).

T-cells play an important role in SSc (O'Reilly et al. 2013). Histopathology of SSc skin biopsies show T-cell infiltrates before evidence of fibrosis suggesting they may be involved in the cause of SSc development (Roumm et al. 1984).

Moreover, their presence in lesions corresponds to the level of skin thickening and inflammation. Physiologically, following inflammatory resolution, T-cells are removed by apoptosis or migration. This process becomes pathological when they remain chronically activated and their wound repair function is not switched off. Experiments in mouse models have demonstrated their role in SSc. In mice with bleomycin induced fibrosis, T-cell depletion alleviates fibrosis (Huaux et al. 2003). Likewise, removal of T-helper cells before radiation reduces the amount of resultant pulmonary fibrosis, demonstrating their function in chronic wound repair and fibrosis (Westermann et al. 1999). Of the different T cell subsets, T helper 2 (Th2) cells are significantly implicated in SSc development considering the elevated levels of Th2 cytokines in SSc serum and not in healthy serum (Higashi-Kuwata et al. 2009;Sakkas et al. 2006).

Interleukins 4, 5 and 6 are all Th2 derived cytokines associated with SSc. IL4 has been found to induce fibroblast proliferation and chemotaxis and together with IL6, collagen production and collagenase inhibition. IL6 has been associated with SSc since it was discovered that SSc patients have elevated IL6 serum levels correlating significantly with skin thickness and severity of fibrosis (Khan et al. 2012a; O'Reilly et al. 2013). The increased IL6 is coupled with the inflammatory response seen in the early stages of SSc even prior to any noticeable fibrosis. Furthermore, metaanalysis genetic studies showed a significant association between a minor allele of the IL6 gene and both limited and diffuse SSc susceptibility and reassuringly to this finding, downstream of IL6 are pathways highly implicated in SSc pathogenesis including JAK/STAT, RAS/MAPK and PI3K/AKT (Cenit et al. 2012). IL6 staining is present in SSc patient epidermis and this can be extended by the finding that IL6 itself can induce collagen expression in SSc. In confirmation of this, even though typically fibroblasts are not found to express IL6 receptor, in SSc, dermal fibroblasts can be activated to produce collagen by the addition of IL6 (Khan et al. 2012a;Hugle et al. 2013). In fact, many cells lacking the IL6 receptor on their cell membrane can respond to IL6. This is due to the fact that IL6 signalling occurs via one of two ways; classic signalling where by IL6 binds to its receptor on cell membranes, and transsignalling. The latter is a process

where the IL6 receptor can be found in soluble form, produced by T-cells. In this soluble form, IL6 can bind to its receptor to form a dimer which in turn binds to membrane bound co-receptor gp130 (Figure 1.4).

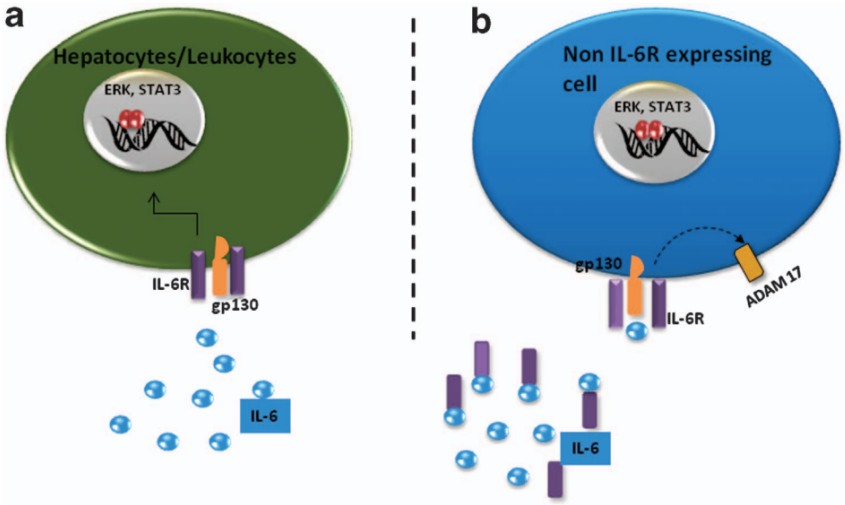

Figure 1.4 ***IL6 classic and transsignalling.*** *Cells expressing membrane bound IL6 receptor, including hepatocytes and leukocytes respond to IL6 by classic signalling. IL6 binds to its receptor and gp130 on the cell membrane inducing ERK and STAT3 signalling pathways and activation (a). Many cells do not express IL6 receptor and thereby respond to IL6 via transsignalling. This occurs when IL6 binds to a soluble form of its receptor which in turn, dimerises with membrane-bound gp130 (b) (O'Reilly et al. 2013).*

In vivo studies on different SSc mouse models showed that IL6 knockout resulted in a reduction of the fibrosis and the aggravated autoimmune response. While these findings implicate the elevated IL6 in SSc as being at least partially responsible for the fibrotic response, controversially, there may be inherent differences in the SSc derived cells themselves. Fibroblasts derived from pulmonary fibrosis lesions respond to IL6 treatment by proliferation and activation of collagen expression, whereas the same treatment on healthy lung fibroblast induced an opposite result. Rather apoptosis was induced in the healthy lung fibroblasts together with inhibition of proliferation (Moodley et al. 2003).

IL31 is an inflammatory cytokine only recently implicated in fibrosis. It is a 4-helix bundle Th2 cytokine and is related to IL6. IL31 signals by binding to the heterodimeric receptor complex of IL31 receptor A (IL31RA) and oncostatin M receptor and initiating pathway transduction via PI3K, MEK/ERK and AKT (Ip et al. 2007;Kasraie et al. 2013a). In addition to IL31 activating these pathways, it also has chemokine activity. Th2 cells often express cutaneous lymphocyte antigen (CLA). It was found that IL31 mRNA levels were significantly higher in CLA+ cells than in CLA-negative cells. Therefore, it is likely that CLA+ Th2 cells are recruited to sites of inflammation, subsequently releasing IL31 and inducing TARC and MDC expression which in turn; facilitate the recruitment of immune cells to the site of inflammation (Bilsborough et al. 2006). Transgenic mice overexpressing IL31 exhibited excessive scratching resulting in skin lesions. By 2 months this was accompanied by conjunctivitis and eye swelling in 67% of mice. By 6 months, pruritus was considered severe in almost 100% of mice and skin lesions showed inflammatory and mast cell infiltration (Dillon et al. 2004). Skin biopsies taken from patients suffering from atopic dermatitis showed keratinocyte expression of IL31RA at a higher level than biopsies from healthy controls. This indicates that in dermatitis, cells respond to IL31 more readily (Bilsborough et al. 2006). In addition to keratinocytes, macrophages respond to IL31 by expressing a relatively high amount of IL31RA and also express and secrete the ligands oncostatin M and IL31 (Hermanns 2015;Kasraie et al. 2010;Kasraie et al. 2013b). Although pruritus has been linked to over-expressed IL31 in mice, in humans it does not seem to have the same immediate effect. IL31 administration into humans by skin pricking did not evoke an immediate pruritic effect, rather itching was a late-onset phenomenon up to 72 hours after initial exposure to IL31 (Hawro et al. 2014). As such, this study concluded that rather than IL31 causing itching by directly acting on afferent and cutaneous nerve receptors, it works by binding to its receptor on keratinocytes and other IL31 receptor expressing cells, which in turn cause the pruritus (Hawro et al. 2014).

Pruritus is a severe and resistant symptom of SSc (Razykov et al. 2009). Since IL31 has a key role in driving pruritus and because Th2 cytokines are known to have an important role in SSc, IL31 is a candidate factor which may

be acting within the SSc microenvironment to promote inflammation and fibrosis.

1.4.2 The role of metabolites in the SSc microenvironment

The vascular damage and ischaemia predicted to be one of the earliest symptoms of SSc, are likely to result in a change in the biochemical balance of the ischaemic area. The chronic tissue hypoxia may result in a switch to anaerobic metabolism by resident cells, a phenomenon observed in the hypoxic microenvironment of tumours (Warburg effect) (Pavlides et al. 2010). The resulting accumulation of intracellular pyruvate leads to increased lactate production and release, and the lactate is believed to be a critical soluble metabolite acting within tumour microenvironments. Furthermore, low pH, increased protons, hypoxia and elevated extracellular purines such as adenosine triphosphate (ATP), are all characteristic of ischaemic disease microenvironments, which could contribute to biomechanisms of disease.

Lactate itself has been implicated in SSc as a novel marker of secondary Raynaud's Phenomenon and ergo, the structural abnormalities of the vasculature. Lactate levels in the blood can easily be determined by a Fingertip Lacticemy (FTL), where a blood drop from a small puncture on a fingertip can be assayed for lactate using a lactate strip and spectrophotometer. A method was developed where lactate levels were measured in this way before and after a cold stimulus, such as immersion of hands in 10°C water. Typically, following a cold stimulus and resulting vasoconstriction, effective perfusion occurs to wash away the lactate that accumulated in the ischaemic tissue as a result of the anaerobiosis that occurs in the cold. However, it was shown that this perfusion was absent in SSc patients with Raynaud's, and those with secondary Raynaud's Phenomenon (Pucinelli et al. 2002). Rather than the expected decrease in lactate levels, these patients showed a significant increase in blood lactate after a cold stimulus. Interestingly, those with primary Raynaud's Phenomenon showed a significant decrease in blood lactate after cold stimulus similar to that of control subjects. This shows that the Raynaud's phenomenon diagnosed in people with no other related medical condition is

distinct to that observed in secondary Raynaud's and SSc. In the latter cases, Raynaud's is caused by structural abnormalities and deformities in the vasculature rather than temporary dysregulation of the vasculature. Increased plasma lactate levels have also been recorded in SSc patients with PAH along with other metabolities detected by H-NMR spectroscopy. The authors of this study suggest that SSc patients with PAH have distinct metabolic abnormalities that differ from SSc patients without PAH (Deidda et al. 2017). Therefore, lactate merits further study as a soluble metabolite in the SSc microenvironment, which may be altering or activating cells. Furthermore, the increased mechanical stress within SSc fibrotic lesions merits study as a potentially important microenvironment factor causing or contributing to the cellular activation.

Feed forward loops of mechanical cues coupled to autocrine stimulation may play a major role in disease exacerbation and progression, and considering the similarities between MSCs and fibroblasts, these pro-fibrotic processes may apply to MSCs. Therefore, proteins in the form of growth factors and cytokines, metabolites including lactate, and mechanical stress responses may all be acting on cells within the SSc microenvironment. Because of their wide distribution and perivascular location in skin and internal organs, it is likely that MSCs will be influenced by these changes and the response of MSCs to SSc-like microenvironments should be studied further.

1.5 MSCs in Systemic Sclerosis

As described above, the SSc microenvironment contains many factors with the potential to interact with MSCs in various ways, many of which have not been elucidated (Figure 1.5). As such it seems possible that the process of disease progression is not linear, nor cyclical; rather it has many factors that come into play at different stages of the process. MSCs can fit into many of these stages both as primary pathogenic drivers and secondary downstream target cells.

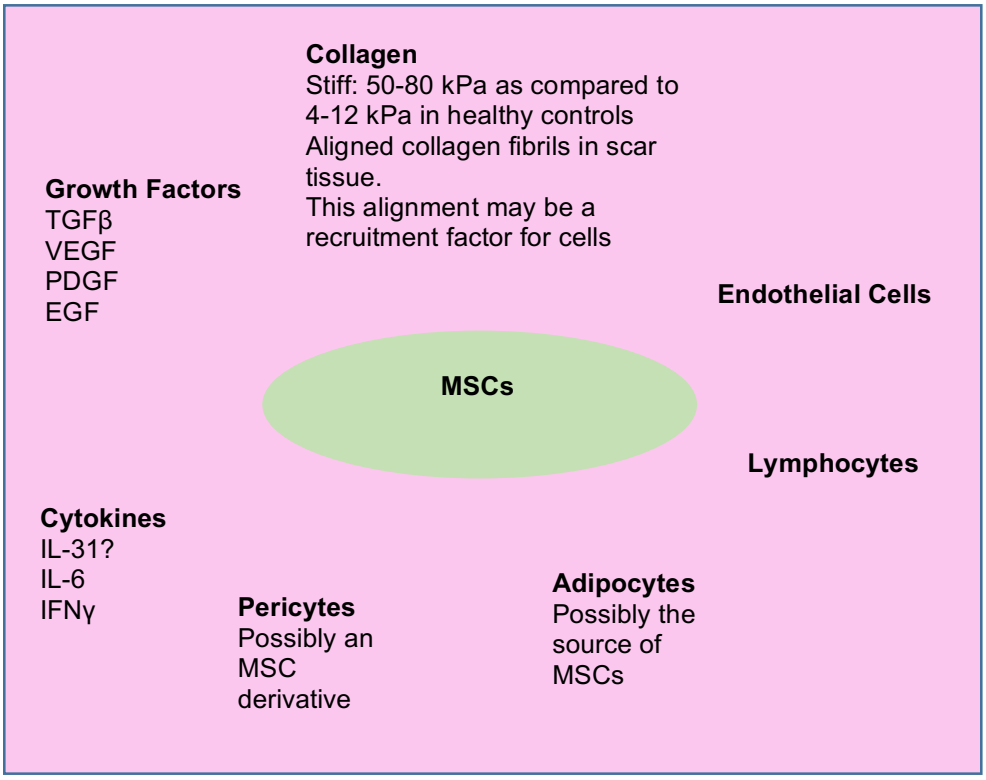

Figure 1.5 ***Proposed interaction between SSc microenvironment and MSCs.*** *Some of the factors implicated in the SSc microenvironment (Pink) are shown with MSCs (Green). Growth factors induce cell activation, expression, secretion, and migration. Cytokines act in a mostly paracrine manner and allow for cellular communication and recruitment. Pericytes reside on the outside of blood vessels, close to MSCs. Adipocytes, particularly in the subcutaneous fat may be one source of MSCs in fibrotic lesions. Immune cells are recruited to the fibrotic lesions and induce an inflammatory response. They may also respond to the characteristic autoantibodies. Endothelial cells and MSCs have a feed forward relationship, which may be responsible for MSC differentiation. Dermal fibroblasts and MSCs may have a direct correlation in that aberrantly activated MSCs differentiate into the fibroblasts that then go on to be responsible for the collagen deposition and extracellular matrix formation, creating the scarring.*

1.5.1 MSCs and vasculature in SSc

It has been established that one of the earliest pathogenic features of SSc is vascular damage whereby a microvascular injury and impaired compensatory angiogenesis leads to a reduction in endothelial density and resultant ischemia and hypoxia. What causes the injury is still unknown. Physiologically, pericytes and endothelial cells interact to maintain the vasculature through reparative angiogenesis. During development, a paracrine signalling mechanism

between endothelial cells and pericyte progenitor cells has been identified. These progenitor cells are thought to be of mesenchymal origin and differentiate into pericytes under the influence of TGFβ1 (Ding et al. 2004). There is evidence to suggest that pericyte differentiation into myofibroblasts is occurring in SSc and, since MSCs reside in the perivascular niche, these pericytes may actually be MSCs, supporting the idea that MSC activation has a role in promoting fibrosis in SSc (Rajkumar et al. 1999). On the other hand, MSCs physiologically can have a pro-angiogenic and pro-neovasculogenic role. They can directly differentiate into cells that maintain vasculature homeostasis, but more than that, the MSC secretome contains factors that have been found to induce the migration, proliferation and activation of endothelial cells, while inhibiting their apoptosis. Such pro-angiogenic factors include vascular endothelial growth factor (VEGF) and hepatocyte growth factor (HGF). Conversely, and reflective of the heterogeneity of MSC potential, anti-angiogenic factors have been identified in the MSC secretome, such as tissue inhibitor of metalloproteinase-1 (Zanotti et al. 2016).

Typically, endothelial cells inhibit MSC-myofibroblast differentiation. In SSc however, it has been suggested that the damaged endothelial cells induce a pathogenic pathway in which they cause MSCs to switch from supporting architectural cells to migratory and pro-fibrotic cells, exacerbating vessel instability. Healthy control endothelial cells' ability to form organised tube-like structures is enhanced when co-cultured with MSCs from both healthy and SSc donors. However, SSc-endothelial cells' ability to form tubules is impaired when cultured with MSCs. This result, together with SSc-endothelial cell hyporesponsiveness to pro-angiogenic induction, is consistent with a major defect in endothelial cells in SSc (Hegner et al. 2016a). SSc MSCs cultured alone, express higher basal levels of VEGFA than their healthy counterparts, and this is further exacerbated when they are cultured with SSc-endothelial cells compared with healthy endothelial cells. This may be significant since it highlights the paradox of increased VEGF, known to induce angiogenesis, and an overall reduction in vasculature in SSc. Of interest, SSc-endothelial cells induce MSC migration and differentiation as well as collagen and α-SMA production. This process is inhibited when healthy control endothelial cells are

added to the co-culture (Cipriani et al. 2014). This places abnormal endothelial cells as possible inducers of MSCs, in SSc pathology.

Many of the growth factors and cytokines in the microenvironment of SSc are implicated in the loss of blood vessel stabilization, possibly causing myofibroblast differentiation, fibrosis and scarring (Goritz et al. 2011). The imbalance in concentration of these proteins is likely to be a contributing factor in the pathology. SSc MSCs show similar immunomodulatory effects as those from healthy controls. However, interestingly, SSc MSCs have an impaired ability to differentiate into progenitor endothelial cells and partake in vasculogenesis (Capelli et al. 2017). This may be significant since failure of vascular repair by progenitor cells could explain the severe loss of microvasculature, a characteristic feature of SSc.

1.5.2 MSC differentiation in SSc

Osteopenia is a common symptom of SSc where patients start to lose bone integrity, particularly of vertebrae (Valenzuela et al. 2016). Conversely, calcinosis is also a feature of SSc where bone mineral is aberrantly deposited, particularly in the digits. Considering that MSCs differentiate into osteoblasts, there is conflicting evidence over how this differentiation is involved in SSc pathogenesis. It could be upregulated to account for the calcinosis and likewise, be inhibited to explain the osteopenia. The SSc mouse model *Fbn1* mutant tight skin mouse also exhibits osteopenia-like features. Studies on this model have shown that this loss of bone density is accounted for by increased IL4 signalling through PI3K-p100 complex, pAKT and phosphorylated mTOR. A study conducted by Chen et al, showed that this IL4 signalling occurs in the bone marrow derived MSCs of tight-skin mice and transplantation of healthy MSCs reverses the IL4 signalling as well as the osteopenia (Chen et al. 2017b). The adipogenic-osteogenic balance was studied and they found that these mice have high bone marrow stem cell adipogenesis which coincided with the osteopenia. Furthermore, when the bone marrow MSCs of the tight-skin mice were cultured *in vitro* it was found that their osteogenic differentiation potential was impaired even in induction media, whereas their ability to

differentiate into adipocytes was unaffected. This altered differentiation was confirmed with Western blot analysis of the implicated genes. RUNX2, alkaline phosphatase (ALP) and osteocalcin (OCN) protein expression was reduced while PPARγ and lipoprotein lipase (LPL), increased. Healthy MSC transplantation regulated the balance to reduce adipogenesis and increase osteogenic differentiation. The transplanted healthy MSCs were found to do this by secreting miR-151-5p in exosomes onto the bone marrow MSCs. miR-151-5p acted on the bone marrow MSCs by inhibiting IL4 signalling. Further, overexpression of miR-151-5p itself in tight-skin mice, without MSC transplantation reduced the IL4/IL4R expression of bone marrow MSCs and also improved their osteogenic differentiation potential. These results were reflected in humans. SSc patients have significantly reduced levels of miR-151-5p in their serum and supporting the hypothesis, bone marrow MSCs of these patients showed increase IL4/IL4R mTOR signalling (Chen et al. 2017b).

The loss of subcutaneous fat in SSc patients is an early phenomenon suggesting that rather than being merely a secondary symptom, it may be an initial event increasing the differentiation of myofibroblasts, and thereby promoting fibrosis (Bogatkevich 2015; Marangoni et al. 2015). It is even claimed that before fibrosis is noticeable by the patient, a pathogenic process has already been initiated in the subcutaneous fat in SSc (Fleischmajer and Perlish 1984). The idea that adipocytes are terminally differentiated has been contested since it was found that they have cellular plasticity enabling them to differentiate into osteogenic and angiogenic cells (Sugihara et al. 1986). As such, it is yet to be determined whether adipose derived MSCs are a source of myofibroblasts, or if the myofibroblasts differentiate directly from adipocytes. The Wnt2a pathway has been found be involved in both pathways leading to myofibroblast differentiation. This pathway inhibits adipocyte differentiation from MSCs in addition to both activating MSC to myofibroblast differentiation and adipocyte to myofibroblast differentiation. Chia et al, used flow cytometry to determine, in mouse models, that upon fibrosis induction with bleomycin, the number of adipose derived MSCs found in the hypodermal adipose tissue

decreased together with the decrease in the amount of hypodermal adipose tissue in the back skin of the mouse, particularly at bleomycin injection sites (Chia et al. 2016). Furthermore, they observed that the rate at which MSCs were lost in the adipose tissue does not fully explain the rate of myofibroblast gain at the start of fibrosis. This suggests that while MSCs could be partially responsible for differentiation into myofibroblasts, this alone does not account for myofibroblast action in fibrosis and the resultant α-SMA expression.

TGFβ is known to be a significant player in fibrosis and is implicated in SSc, and has varying biological effects, dependent on cell type (Massague 2012). MSC capacity to differentiate into chondrocytes is dependent on TGFβ and conversely, osteogenic and adipogenic differentiation is dependent on a lack of TGFβ (Walenda et al. 2013). As such, it may be possible that due to TGFβ elevation in SSc, MSCs are less able to remain quiescent and rather, are more inclined to adopt a pro-fibrotic phenotype. It was demonstrated that TGFβ expression was markedly increased in SSc endothelial cells in comparison with healthy control endothelial cells. This expression was further increased when SSc endothelial cells were co-cultured with MSCs from both SSc and healthy controls (Cipriani et al. 2014;Talele et al. 2015). Furthermore, MSC α-SMA expression is enhanced by TGFβ (Talele et al. 2015). This expression could be responsible for the pro-fibrotic nature of MSCs in SSc, placing TGFβ as an important factor in the SSc microenvironment. Conversely, it has been demonstrated that physiologically, MSCs express TGFβ when taking part in inhibitory immunological processes (Di et al. 2002). TGFβ treatment induces upregulation of TGFβ receptor 1 expression by SSc derived MSCs while the opposite is seen in healthy MSCs. It may be possible that the negative feedback loop that describes the healthy MSC reaction to TGFβ is dysregulated in SSc MSCs (Hegner et al. 2016).

Of importance to note, no differences in clonegenic potential of osteogenic/adipogenic/chondrogenic pluripotency have been detected between healthy and SSc derived MSCs, and as such it seems to be the case that the SSc microenvironment itself is pathogenic. In response to PDGF-BB

and b-fibroblast growth factor (bFGF) treatment, the MSC phenotype changes and they become much longer and slimmer with fewer α-SMA stress fibres. However, treatment with TGFβ elicited an increase in α-SMA positive stress fibres and a myofibroblast-like cell morphology. On the other hand, while phenotypic similarities are detected between healthy and SSc derived MSCs, they have been found to respond differently to SSc microenvironment components with respect to expression of contractile proteins. PDGF-BB and FGF reduced α-SMA and myosin light chain kinase (MLCK) expression, however this reduction was more prominent in healthy MSCs significantly with regards to α-SMA expression under PDGF-BB treatment conditions. Furthermore, TGFβ increased α-SMA expression of SSc MSCs significantly more than their healthy counterparts, indicating SSc MSCs being more readily differentiated into myofibroblast cells. TGFβ also was found to inhibit MSC differentiation into vascular smooth muscle cells while CTGF and b-FGF induced vascular smooth muscle cell differentiation of healthy MSCs only. SSc MSCs were also found to respond to TGFβ by producing collagen type I, significantly implicated in SSc, whereas healthy MSCs produced collagen type III. Together, with downregulation of the collagen degrading enzyme MMP9, SSc MSCs are candidate cells implicated in excess collagen deposition associated with SSc (Hegner et al. 2016). The results of this study indicate an endogenous abnormality in the regenerative potential of SSc MSCs such that it stands to reason that the microenvironment itself is not the only offender in SSc pathology.

	SSc MSCs	Healthy MSCs
Increased TGFβ Receptor II expression	✓	×
Increased collagen 1A1 expression	✓	×
Increased TGFβ induced α-SMA expression	✓	×
Differentiation into vascular smooth muscle cells	×	✓
Increased α-SMA in response to PDGF	✓	×
Growth and proliferation	✓	✓
CD73, CD90, CD105, CD26 expression	✓	✓
Adipogenic differentiation	✓	✓
Osteogenic differentiation	✓	✓
Chondrogenic differentiation	✓	✓
Immunosuppression	✓	✓
Support of endothelial cell tubule formation	✓	✓

Table 1.1 ***Summary of comparative effects of SSc and healthy MSCs.*** *SSc MSCs express more TGFβ Receptor II and collagen 1A1 and α-SMA in response to TGFβ treatment than healthy MSCs. SSc MSCs show reduced propensity to differentiate into vascular smooth muscle cells than healthy MSCs. Healthy MSCs show reduced α-SMA expression in response to PDGF than do SSc MSCs. Both healthy and SSc MSCs show similar growth and proliferative capacities, express similar amounts of MSC proteins CD73, CD90, CD105 and CD26. Differentiation capacities of both SSc and healthy MSCs are similar as well as their immunosuppressive functions. Finally, both SSc and healthy MSCs support endothelial cell tubule formation. (Capelli et al. 2017;Hegner et al. 2016;Vanneaux et al. 2013)*

1.6 MSCs in skin

1.6.1 MSCs and Wound healing

MSCs play an important role in tissue renewal and wound healing through their regenerative properties. In the skin, MSCs may be recruited from surrounding tissue, possibly adipose tissue, to a site of inflammation where they differentiate into the cells needed for tissue repair, for example keratinocytes in the skin (Borue et al. 2004). This has made them of interest in tissue engineering after burn injuries. Conversely, MSC effects on wound healing in animal models have suggested that their role is of a paracrine and secretory nature rather than direct engraftment and replacement of damaged tissues in wounds. MSCs can secrete anti-fibrotic factors together with angiogenic factors which induce wound healing and acting together with the anti-inflammatory effects of MSCs, resolve the inflammation surrounding the wound. These roles of MSCs work in syncytium resulting in the overall reduction of fibrosis and scar tissue. Perhaps in SSc, rather than MSCs themselves being inherently dysfunctional, it could be that their inability to resolve the tissue damage results from changes induced in the disease microenvironment. There is now interest in using MSC secretome transplantation as therapy rather than the cells themselves. This has been conducted by culturing MSCs in serum free media and exposing them to hypoxic conditions to pre-condition them to becoming more migratory and stimulate their expression of growth factors (Zhou et al. 2013). Hypoxic pre-conditioning also maintains stem cell pluripotency and their undifferentiated phenotype, important factors when considering the use of MSCs in therapy (Hawkins et al. 2013). The MSCs secrete soluble factors into the media which is then used as a representation of the secretome. This conditioned media was applied topically onto induced wounds of otherwise healthy individuals to assess wound healing. It was found that application of the MSC conditioned media to wounds, reduced erythema and redness of the wound as well as pigmentation, consistent with resolution of inflammation. The reduction of hyperpigmentation was attributed to the inhibition of the melanogenic enzymes expressed by the melanophages, induced to phagocytose the damaged keratinocytes. Moreover, transepidermal water loss was used as a

measurement of skin barrier function. Unhealed wounds have a high level of transepidermal water loss. Treatment with MSC conditioned media significantly reduced the amount of transepidermal water loss indicating quicker and more effective wound healing. The reduction in the transepidermal water loss could also be an explanation for the reduced hyperpigmentation observed (Zhou et al. 2013). Physical changes in skin elasticity and collagen content was not observed in this study. The presence of MSCs may be responsible for these recovery mechanisms, possibly through cell differentiation or direct cell-cell contact rather than paracrine signalling. Myofibroblasts are cells known to be involved in skin contractility in wound healing, differentiating from fibroblasts in subepithelial skin layers. They express α-SMA which induces skin contraction in order to close the wound, by pulling on the neighbouring healthy skin in a mechanism that leads to scar formation. Uysal et al, found that following injection into wounds in rats, MSCs played an immunoregulatory role and reduced α-SMA and TGFβ expression thus, reducing wound contraction. This is in conflict with the proposed idea that MSCs promote wound healing. Perhaps there is a fine line between wound healing and scar formation whereby MSCs induce healing of the wound via transdifferentation and tissue regeneration but, revert the exaggerated response of skin contraction and scarring following more severe wounds (Uysal et al. 2014). TGFβ is the growth factor found to be at least partially responsible for fibroblast to myofibroblast differentiation during wound healing. Addition of TGFβ to fibroblasts induces a significant increase in α-SMA expression indicating myofibroblast differentiation together with upregulation of fibronectin and vitronectin receptors. Inhibition of these receptors with antibodies inhibited the fibroblast to myofibroblast differentiation process observed by a decrease in α-SMA production. TGFβ also inhibited fibroblast migration and wound repopulation in a scratch wound assay, the hypothesis being that this was caused by myofibroblast differentiation (Lygoe et al. 2007). Conversely, in collagen gel contraction assays, the addition of TGFβ induced cell contraction indicating cell migration. In this case, the contraction was proposed to be due to cell matrix collagen reorganisation by myofibroblasts which by inhibiting fibronectin and vitronectin, reversed this matrix

reorganisation. If MSCs are a source of myofibroblasts, TGFβ could hypothetically act on MSCs and alter their integrin receptor expression profile causing differentiation into the myofibroblasts needed for wound healing.

1.6.2 MSCs and SSc extracellular matrix (ECM)

The combination, presence and concentration of the growth factors and cytokines present in the SSc microenvironment not only depends on their production and degradation, but also on the physical environment they act in. The SSc extracellular matrix is a product of the aberrant wound healing process. The chronic tissue repair is not resolved and results in excessive collagen deposition, dermal thickening, scarring and eventually fibrosis. The accumulation of collagen is due to both excessive production and inhibited degradation. Collagen type I, the main constituent of human extracellular matrix, is more readily expressed in SSc since the CCAAT binding transcription factor (CBF) responsible for its expression has a higher binding affinity for the collagen promoter region in SSc fibroblasts. Binding of CBF to the *COL1A1* promoter was found to be 3-5 times stronger in SSc dermal fibroblast nuclear extracts compared with age-matched healthy control extracts (Saitta et al. 2000).

The stiff microenvironment and disturbed organisation of the collagen fibrils in SSc has an effect on the activity of the SSc microenvironment constituents. Myofibroblasts are the cells responsible for tissue remodelling and extracellular matrix deposition in fibrosis. Continuous extracellular matrix deposition promotes further myofibroblast differentiation from fibroblasts through positive feedback mechanical signalling. The resultant extracellular matrix and its stiffness can effectively modulate MSC function and phenotype. This occurs through sensing of the microenvironment by MSCs whereby cells must create physical contacts with the matrix by a receptor-substrate complex that induces signal transduction to the MSC nucleus, instructing the appropriate cell response. Such transducers possibly include myocardin related transcription factor-A (MRTFA) and non-muscle myosin isoforms, which act on cellular transcription and gene expression to alter the actin

cytoskeleton and focal adhesions in order to “feel” the extent of possible deformity of the matrix, and thereby gauge its potential phenotypic change (Engler et al. 2006). MRFTA is a cytoplasmic transcription factor found in dermal fibroblasts, keratinocytes, endothelial cells and MSCs, that is induced to translocate to the nucleus under conditions of mechanical stress. Cytoplasmic to nuclear translocation occurs by actin cytoskeleton remodelling and polymerisation mediated by Rho GTPases. Once in the nucleus, MRTFA is involved in the transcription of genes involved in further cytoskeleton remodelling. In SSc, MRFTA is implicated as the mechanosensing mechanism by which SSc myofibroblasts are activated and synthesise collagen type I in response to stiff surroundings and interestingly, is itself further activated by elevated TGFβ. Thus it is not surprising that MRTFA knockdown alleviates skin stiffness in SSc mouse models and inhibits pro-fibrotic protein expression (Shiwen et al. 2015).

In healthy MSCs, it is possible that inhibition of the mechanosensing transducers will strongly inhibit the differentiation response of the MSCs to stiff extracellular matrix. Such responses include neurogenic differentiation when cultured on soft substrates, osteogenic on stiff substrates and myogenic on substrates between soft and stiff. The stiffness is measure in kilopascals (kPa) according to Young’s Modulus and essentially measures the ability of the cell to deform the substrate it is attached to. A stiff substrate, like SSc skin, is typically considered to be between 50-80 kPa while healthy skin, or soft matrices, range from 4-12 kPa (Sackson et al. 2013).

Interestingly, while *in vitro* differentiation studies most often are conducted using treated media conditions, matrix stiffness is a more selective inducer of cell differentiation. Furthermore, cells primed for lineage commitment in this way are less able to switch lineages than cells primed using soluble factors (Engler et al. 2006). The effect of the matrix microenvironment on the differentiation potential of MSCs seems to be stronger and more long-lasting than that of conditioned media. MSCs differentiated via matrix stiffness initially are passive in their responses and do not take an aggressive differentiated

committed profile automatically. Rather they seem to hover between their former ‘stemness’ state and their new commitment. Perhaps at this stage the soluble factors of the microenvironment play the more important role in cementing their new phenotype (Engler et al. 2006).

Although the majority of the myofibroblasts are believed to be derived from tissue resident fibroblasts, this is not proven, and MSCs may play a role in adding to the myofibroblast population. The relationship between MSCs and myofibroblasts is of considerable interest in SSc. It has been hypothesised that MSCs expressing α-SMA are somewhat lineage committed and have restricted self-renewal capacity while those lacking α-SMA retain pluripotency. These different phenotypes can be controlled by matrix stiffness. Physiologically, skin has a stiffness measured at 4-12kPa, however, SSc patients have skin stiffness ranging from 50-80 kPa. A study showed that α-SMA positive MSCs can lose their commitment when cultured on a soft matrix (3 kPa) that inhibits differentiation to myofibroblasts. In concordance; culture on stiff substrates (65 kPa) increases α-SMA expression (21.9% compared to 3.1% expression on stiff and soft substrates respectively). α-SMA positive MSCs are pro-fibrotic as suggested by their elevated collagen, CTGF and TGFβ2 expression, however, whether α-SMA causes expression of these pro-fibrotic factors has not been established (Talele et al. 2015). As such, it was concluded that α-SMA targeting could be a valid strategy in increasing MSC transplantation efficacy and reducing the likelihood of MSC induced fibrosis. Park et al, used qPCR to determine MSC expression of α-actin and calponin (smooth muscle cell markers) as well as collagen type II and LDL (chondrogenic and adipogenic markers), in response to matrix stiffness. Stiff matrices induced MSC α-actin and calponin-1 expression, while soft collagen gel matrices did not induce expression of smooth muscle cell markers. Conversely, collagen type II was expressed on soft matrices while stiff substrates inhibited this expression (Park et al. 2011). These results show how MSC lineage commitment is determined by matrix stiffness. The difference in stiffness values between extracellular matrix in SSc and healthy skin are very marked and likely to influence MSC differentiation.

In addition to the stiffness of the extracellular matrix, cellular motility is affected by the "roughness" of the surface it resides on. Since one of the major limitations of MSC clinical trials is the extremely low proportion of MSCs reaching the target site in order to perform therapeutic functions, enhancing MSC inherent ability to migrate is one potential way of resolving this issue. The positive results from MSC clinical trials can be explained by the quick migration to the target site rather than a high proportion of viable MSCs targeting the site. While pre-conditioning MSCs *in vitro* can be done using specific cytokine exposure, such as IL6 treatment, there are several limitations to this. Cytokine signalling is usually short-lived but more concerning is the potential effect of the cytokines or growth factor molecules on MSC phenotype and lineage commitment. Since MSC therapeutic strategies depend on pluripotency potential, it is important that MSCs injected retain the phenotype they are cultured towards. The effect of culture substrate on MSC activity seems to be much more long-lived than soluble factor treatment and thus it is being investigated as a mechanism of enhancing MSC migration potential *in vitro*. Nanoscale "roughness" has been described to be a potent enhancer of MSC motility (Jingjing Han et al. 2014). A study was conducted culturing adipose derived human MSCs on substrates of different "roughness" labelled R0, R1 and R2 ranging from completely flat to increasing roughness respectively, and observing cell migration and focal adhesion kinase (FAK) and mitogen activated protein kinase (MAPK) expression (Li et al. 2017). The roughness of the substrates also corresponded to increasing Young's Modulus, with rougher substrates also being calculated as stiffer. FAK is a molecule that when phosphorylated is activated and is involved in focal adhesion turnover, creating focal adhesions at the leading edge of the cell and detachment of them at the rear end, thereby creating tension from the leading end pulling the cell forward (Li et al. 2017). FAK is also involved in the activation of MAPK which when phosphorylated in turn phosphorylates myosin light chain, further enhancing cell motility. Cells were cultured on these different substrates before detaching and seeding onto a 24 well plastic plate for a scratch wound assay. Cells pre-conditioned on the completely flat R0 substrate were significantly slower at migrating across the scratch in

comparison to cells cultured on R1 and R2 substrates. Further, R1 pre-conditioned cells were even faster than R2 cells. This finding was reflected in the amount of focal adhesions on the leading edge, R1 and R2 pre-conditioned cells had significantly more focal adhesions present than MSCs cultured on R0 surfaces. FAK expression and MAPK phosphorylation were also significantly higher in cells cultured on R1 substrates and were maintained for 14 days after reseeding. This underlines the controversial issue of MSC memory, a concept that states that MSCs can remember mechanical signalling even after the signal is removed depending on the length and exposure of the signal. Yang et al, assign this to the effects of the YAP/TAZ mechanotransduction pathway and the long lasting presence of YAP in the nucleus, suggesting that once YAP has been shuttled to the nucleus it stays there even after the resolution of the signal, and continues is transcriptional effects (Yang et al. 2014). The effect of soluble factors on MSC activity and phenotype can be overridden upon a change in culture conditions, however, the effect of culture substrate seems to be more long-lasting. Worth noting is the fact that this "memory" was only apparent when cells were pre-conditioned for more than 4 days suggesting that there is a dose threshold of the signalling cues that determines the longevity of the signal and permanence of its effect.

1.7 Clinical trials involving MSCs

The therapeutic potential of MSCs is being investigated in degenerative, ischaemic, inflammatory and autoimmune conditions due to their regenerative, immunoregulatory and repair functions. They are relatively easy to isolate and expand while keeping their stem-cell identity. An additional advantage is that they do not induce immune responses upon intravenous administration, through lack of major histocompatibility complex (MHC) expression, and as such, issues regarding rejection of transplantation are not of concern. Conversely, rather than MSCs being completely hypoimmunogenic, they may be adept at evading the immune system and their long term beneficial effects may work via releasing their secrotome rather than direct MSC action. This theory is with support from the finding that injected MSCs become trapped in

micro-capillaries of the lungs and exert brief therapeutic effect before undergoing cell death (Ankrum et al. 2014).

Lung injury was induced in mice before MSC injection at 4 hours, 60 days and 120 days post injury. Cells injected 4 hours after injury were able to differentiate into functional epithelial and endothelial lung cells, highlighting MSC pluripotency and the fact that their regenerative potential can indeed be exploited therapeutically. However, MSCs injected at the later time points were found to have myofibroblast-like properties due to the TGFβ mediated inhibition of differentiation. The difference in lung microenvironment at the different time points emphasises how the microenvironment, in particular TGFβ concentration and matrix stiffness, determines MSC function (Yan et al. 2007). Clinical trials investigating the potential of MSC transplantation have been of particular interest with regards to autoimmune diseases, where rejection and histocompatibility are of major concern. The ability of MSCs to evade the host immune system grants much more liberty in the case of transplantations. Pre-clinical mouse models of autoimmune diseases have given rise to conflicting results, and one factor to consider is the lack of mouse models that mimic all aspects of the modelled disease. Two different systemic lupus erythematosus mouse models have different responses to allogeneic MSC administration (Theofilopoulos and Dixon 1985;Youd et al. 2010). Likewise in rheumatoid arthritis mouse models, MSC treatment was found to both alleviate arthritic symptoms and tissue damage yet also exacerbate T-cell proliferation and autoimmunity (Schurgers et al. 2010). Often in these studies, the encouraging *in vitro* studies were not reflected *in vivo*, and as such it can be hypothesised that the MSC activity is being altered *in vivo,* possibly by microenvironmental factors of the disease, or alternatively, the stage of disease progression is thought to play a role in determining MSC activity and function. This suggests that there are microenvironmental changes throughout disease progression to which MSCs respond, and that such changes are often not accounted for in the time-limited *in vitro* preliminary studies. Injecting MSCs into rheumatoid arthritis mouse models after inflammation was induced showed opposite and ineffective results when compared with MSC

transplantation early in the modelled disease progression, where MSC injection was found to ameliorate collagen-induced arthritis (Schurgers et al. 2010).

In humans, MSCs injected directly into the heart of patients with ischaemic cardiomyopathy showed regenerative improvement and an overall benefit in myocardial contractility and remodelling (Behfar et al. 2014). In autoimmune diseases like systemic lupus erythematosus, intravenous administration of MSCs elicited improved renal function and restoration of normal cytokine concentrations. The immunomodulatory function of MSCs was highlighted in this study by the finding that after transplantation, the typically increased levels of Th2 cytokines was reduced relative to Th1 cytokines (Liang et al. 2010). In this case, the role of MSCs was not of a differentiation nature and did not exploit pluripotency, rather their ability to influence and drive specific immune responses was of interest. How the MSCs are influenced to dictate functional polarisation is still unknown and how MSCs can be primed to carry out specific roles is yet to be elucidated.

In contrast to these positive results, administration of human MSCs into fibrotic tissue of a liver injury mouse model exacerbated the fibrosis (di Bonzo et al. 2008). Homing of the MSCs to the site of injury was encouraging, however, engraftment of these cells in mice with acute liver injury was minimal when the mice were assayed for GRP-labelled human derived cells. In contrast, MSCs were found in significantly higher amounts in mice with chronic liver injury. The engrafted cells however, were not found to differentiate into hepatocytes in order to replace damaged tissue, rather there was evidence of their differentiation into myofibroblast-like cells, thereby exacerbating the injury and fibrosis. This points to there being something in the chronically injured liver microenvironment that may induce MSCs to become pathogenic and possibly more myofibroblast-like.

In SSc cases, clinical trials have resulted in some reduced necrosis but with considerably varying persistence and efficacy. Allogeneic MSCs were transplanted into a 41-year-old female SSc patient with 6 digital ulcerations.

She was observed for one year, after which she reported warmer hands and 5/6 healed ulcers. Vascular ultrasound showed improved blood circulation in her hands (Christopeit et al. 2008). In another study, 5 SSc patients were treated with bone marrow derived MSCs, administered intravenously. Their skin thickness score (MRSS) was determined prior to and post transplantation. Digital photographs were taken of ulcers. MRSS scores for all patients were at least temporarily improved and necrosis was reduced in 3 of 5 patients. However, within 12 months post MSC transplantation, ulcers recurred (Keyszer et al. 2011;Todorovic et al. 2005). A clinical trial using adipose derived MSC transplantation in SSc was conducted on 12 patients diagnosed with limited cutaneous SSc (Granel et al. 2015). Autologous MSCs were used, obtained by extracting adipose tissue from the patients and isolating and culturing characterised MSCs. MSCs were injected directly into affected fingers, and the presence and state of digital ulcers was used as a measure of MSC efficacy, together with finger circumference to measure oedema and fibrosis. Although not found to be statistically significant, a trend was observed towards reduced finger size but more encouragingly, Raynaud's associated hand pain was significantly reduced. On the other hand, no change was seen in capillary formation and structure in the nail beds. As such it is still difficult to draw meaningful conclusions about the role injected MSCs are playing; is the reduction in finger size a reduction in fibrosis or merely resolution of oedema through MSC anti-inflammatory actions? Likewise, is there any data to suggest MSC differentiation into pericytes or other vasculature supporting cells?

The systemic nature of SSc means that while MSCs may be temporarily effective at symptom amelioration, as seen in acral regions, the effect of them on the systemic fibrosis and chronic inflammatory response is still unknown. In fact, considering that SSc derived MSCs are not entirely identical to their healthy counterparts, autologous transplantation may not actually be beneficial in the long term. To date the most successful MSC clinical trials in SSc have been based on localised injections into hands, fingers and extremities. Intravenous MSC infusion trials seem to show variable and temporary improvement at best.

1.8 Identifying MSCs in disease tissue

One difficulty with identifying MSCs in this project is the lack of specific MSC cell surface markers. Together with fibroblastoid morphology, there are cell surface marker combinations that suggest MSC presence. These include CD70 and CD93 together with Gli1. MSCs are physiologically quiescent and do not divide until activated, often to participate in acute wound repair. As such MSCs are not expected to be dividing in healthy control skin biopsies. Dividing MSCs have been named metakaryotes due to their cytology and behaviour in nuclear fission. Metakaryotic cell divisions are amitotic processes such that the nucleus divides without nuclear envelope breakdown. DNA replication also occurs after division via a double stranded pangenomic RNA/DNA intermediate that separates and becomes 2 double stranded DNA replicates. Divisions are determined by a large, hollow, bell shaped nuclear morphology, with a dense chromatin ring at the 'open' end (Figure 1.6). Such nuclear division is observed in adenomatous tumours and in early embryogenesis where they represent the presence of stem cells during growth and differentiation (Thilly et al. 2014). Further, metakaryotic stem cells have been observed to be recruited to wounds within 24 hours of trauma. Due to the physiological wound repair function of MSCs, this finding was of significant interest (Gostjeva et al. 2009). In this thesis the property of metakaryotic cell division will be used to identify proliferating, activated MSCs in the SSc disease tissue.

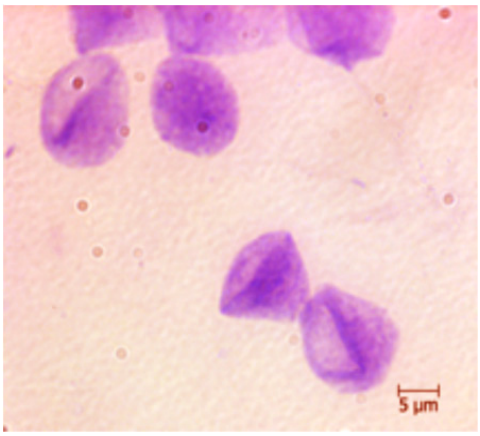

Figure 1.6 ***Metakaryotic stem cell in 9 week old human foetal kidney artery section.*** *Bell shaped nucleus with a dense ring of chromatin at the open end is the typical nuclear morphology of metakaryotic stem cells (Thilly et al. 2014).*

1.9 Conclusion: possible role of MSCs activated within the disease microenvironment in SSc

MSCs are undoubtedly an important cell type of relevance to SSc, and their almost ubiquitous presence in the human body is a highly attractive quality when considering their therapeutic use and potential. They are a highly plastic cell type and can readily change phenotype, morphology and expression profile in response to different environmental cues ranging from soluble factors to physical and mechanical stress. This plasticity allows them to be involved in many different roles that are both their own entities as singular signalling processes, yet can also be roles that lead into others, with cross talk with other cells, altering the microenvironment they reside in, which in turn may act through both positive and negative feedback to the MSCs themselves.

This heterogeneity in their characteristics, together with the wide range of derivations and expression profiles is also reflected in the controversy surrounding their definition. In this thesis, MSCs will be defined as fibroblast-like cells that can be derived from adipose tissue, bone marrow and the umbilical cord, with the ability to differentiate into osteoblasts, adipocytes and chondrocytes. Their differentiation into the former two lineages is of importance in SSc.

As described above, SSc is an autoimmune connective tissue disease with a wide range of symptoms, but ultimately systemic fibrosis is the undoubted main characteristic (Gabrielli et al. 2009). Understanding of the pathophysiology of this disease is still very much incomplete, with potential mechanisms of its cause ranging from genetic susceptibility and environmental exposure to inherent vascular dysfunction and abnormal microenvironment constituents (Eckes et al. 2014). As such treatments are merely to alleviate symptoms, particularly those regarding Raynaud's phenomenon and the resulting digital ulcers. To date, in regards to this disease, MSCs have been largely been proposed to be a benefit with their exploitation as therapies being investigated. This thesis investigates the opposite, suggesting a more pathological role for these cells. Just as the different roles of MSCs can be used as advantageous, explaining and

supporting their therapeutic use, this thesis aims to place MSCs as major players in the SSc pathogenesis, synergising with the pro-fibrotic factors of SSc. This flip-side to MSC function has been largely overlooked in the pathophysiology of SSc, especially following somewhat encouraging results of preliminary clinical trials using these cells.

As mentioned, MSCs can fit into SSc pathology as osteoblast cell precursors. Osteoblast presence and atypical deposition of calcium minerals is responsible for the calcinosis seen in approximately 22% of SSc patients (Valenzuela et al. 2013). Calcinosis is a painful symptom of SSc and results in inflammation and loss of dexterity particularly in the fingers. Conversely, SSc patients often present with osteopenia, a loss of overall bone density, suggesting that rather than there being a generalised systemic increase in osteoblasts through MSC differentiation, it is more likely that osteoblasts are abnormally regulated locally within the SSc microenvironment, inducing their production and secretion of bone mineral. Likewise, MSCs can also be thought of as adipocyte precursors. Loss of subcutaneous adipose tissue is a common symptom of SSc, such that mouse models often mimic this symptom in addition to fibrosis. Conceivably, if MSCs are otherwise induced, their physiological role of adipocyte and fat tissue homeostasis is disrupted.

The two differentiation pathways oppose each other to some extent where an increase in one lineage induction coincides with a reduction in the other (Nuttall & Gimble 2000). Perhaps, an imbalance between the two lineage routes is of importance of SSc and is in turn, a result of SSc microenvironment constituents, namely, TGFβ, and members of the canonical Wnt pathway, MAPK and PI3K pathways as candidate factors, coincidently all pathways highly associated with SSc pathology.

Further support of the role of MSCs in SSc is their ability to influence, maintain and differentiate into cells involved in vasculature homeostasis (Ding et al. 2004). With Raynaud's and microvascular dysfunction being such a universal feature of SSc and chiefly responsible for the occurrence of slow-healing

digital ulcers, it is not inconceivable that abnormal MSC function can result in a reduction in neo-vascularisation and angiogenesis.

Together, such data more than hints at MSC involvement in SSc causation, progression and symptoms. In addition to the direct involvement of MSCs themselves, is the issue of their interaction with the unique composition of the SSc microenvironment. Principally, MSCs both secrete and respond to the pro-fibrotic growth factor TGFβ. This alone is supportive for some form of MSC-caused exacerbation of SSc. Furthermore, and as investigated in this thesis, MSCs may have distinct responses to SSc related cytokines and metabolites such as IL31 and lactate. The potential importance of IL31 in SSc is relatively new and its relationship with MSCs is uninvestigated. Notably, many SSc mouse models available do not take into account the pruritus and often omit modelling the effect of cytokines on collagen production, loss of subcutaneous fat as well as dermal thickening. The results of this thesis have led to the investigation of the the use of a new SSc mouse model that resolve some limitations of other models such as bleomycin treated mice, described in the manuscript in the Appendix.

The approaches used in this thesis aim to place MSCs in SSc pathophysiology by elucidating their role in wound healing responses, adipogenic and osteogenic differentiation in SSc, together with measuring SSc microenvironment induced RNA expression and protein synthesis. Different representations of the SSc microenvironment were used in an attempt at identifying key factors which may be promoting MSCs in SSc. Blister fluid was considered to the be the fullest available representation of the SSc microenvironment, containing all the relevant soluble factors. Individual “players” such as IL31, lactate and matrix stiffness were also used.

1.10 Hypothesis

As a result of the research questions identified by the literature review, this thesis attempts to test the following hypothesis.

The abnormal microenvironment in systemic sclerosis fibrotic lesions leads to the reprogramming of mesenchymal stem cells to a persistent tissue repair phenotype.

1.11 Aims and objectives

To test the above hypothesis methodological approaches in this study mainly tried to model the role of MSCs in SSc *in vitro*. SSc blister fluid was used as the main representation of microenvironment and the response of MSCs to the blister fluid was measured. Migratory ability in response to blister fluid and its constituents was measured by scratch wound assays as well as floating cell populated collagen lattice structures. Differentiation assays were conducted, not only as quality control methods to ensure pluripotency of the MSCs, but also modelling possible differentiation responses relevant to SSc. RNA and protein expression were measured by quantitative polymerase chain reaction (qPCR), next generation RNA sequencing and Western blotting to see whether the changes in MSC phenotype and function in response to blister fluid can be explained by and reflected in their expression profile. And lastly, the presence of MSCs in SSc skin was confirmed by a novel histological staining technique, using metakaryotic nuclear divisions as a marker of activated MSC presence.

Through these methodological approaches, the overall aim of the studies in the thesis is to model the interaction between the disease microenvironment and MSCs in SSc by achieving the following objectives:

1) To determine whether activated MSCs are present within the fibrotic microenvironment of SSc patients' skin lesions.
2) To use profiling of tissue fluid to determine which factors are present in the SSc disease microenvironment.
3) To fully evaluate the effects of the disease microenvironment on MSC phenotype and gene expression
4) To understand the relevance of the enhanced extracellular matrix stiffness of the SSc microenvironment to MSC activation

Chapter 2 : Materials and Methods

2.1 Culturing cells

2.1.1 Buffers and culture media

All cells were cultured in Dulbecco's modified eagle medium (DMEM; Gibco) with or without foetal calf serum (FCS) on plastic T75 flasks (Corning; New York, USA). Negative serum controls were represented by either serum free DMEM, or DMEM supplemented with 0.2% serum. Positive serum controls were represented by 10% serum in DMEM. All media was supplemented with 1% penicillin/streptomycin. Dulbecco's Phosphate Buffered Saline (DPBS; Life Technologies, Paisley, UK) was used to wash cultured cells. Where specified, MSCs were cultured in osteogenic (OIM) or adipogenic induction media (Gibco, UK). Cells were trypsinised and passaged by incubation with Trypsin/EDTA (Life Technologies, Paisley, UK).

2.1.2 Culturing dermal fibroblasts

Primary cultures of skin fibroblasts were obtained from 4mm punch biopsies sampled from forearm skin of SSc patients. Biopsy material was minced and cultured in 20% serum. Cultures were inspected daily by light microscopy and when a fibroblast outgrowth was detected, cells were washed with DPBS and contaminating epithelial cells were detached by Trypsin/EDTA. Fibroblasts were cultured further and then subcultured in T75 tissue culture flasks. Passaged cells were cultured further in DMEM supplemented with 10% FCS and 1% penicillin/Streptomycin solution, incubated at 37°C 5% CO_2 in T75 flasks. All fibroblasts were used at passage 3-5 for experiments to correspond with MSC passage numbers and to avoid the effects of senescence.

2.1.3 Culturing MSCs on plastic

Human adipose-derived MSCs, isolated from liposuction fat, were obtained commercially (ATCC PCS-500-011, Lonza PT-5006). DMEM supplemented with 20% serum was used to culture MSCs for three days in plastic T75 flasks (Corning; New York, USA), before replacing media with 10% serum. In other experiments, MSCs were also cultured from healthy and SSc skin biopsies.

Biopsies were washed and minced in DPBS before being kept for 7 days in 10% serum, replacing media every 3 days. Sheets of keratinocytes were seen to spread out from the biopsy with MSC-like cells on their surface. Media and non-adherent cells were aspirated before washing cells with DPBS. Trypsin/EDTA was added to the flask before incubation at 37°C 5% CO_2. 10% serum DMEM was added to neutralise the Trypsin/EDTA activity and the detached cells, thought to be MSCs, were centrifuged at 1250RPM for 5 minutes before sub-culturing. These primary cultures were used only to test for pluripotent, osteogenic differential capacity, but for the purpose of the *in vitro* studies in this thesis, only commercially obtained adipose derived MSCs were used.

2.1.4 Culturing MSCs on Softwell plates

Extracellular matrix stiffness was modelled *in vitro* by culturing cells on Softwell collagen hydrogel coated plates (Cell Guidance Systems SW12-COL-50, SW12-COL-4). These 12 wells are collagen coated hydrogels at specific stiffness's to model the stiff skin of SSc patients. Stiffness of the gels is determined by their elastic modulus and are available with 4 kPa and 50 KPa gels mimicking healthy and SSc skin, respectively. MSCs were seeded at a density of 1 x 10^5 cells per well and incubated in DMEM supplemented with 10% serum, with media being changed every 3-4 days, being careful not to disrupt the hydrogel layer.

2.2 Patient samples

Patients studied gave informed written consent for the use of donated blister fluid, blood and skin biopsies. Ethical committee approval was obtained under "NHS Health Research Authority, NRES Committee London-Hampstead, HRA, reference number 6398- "Elucidating the pathogenesis of scleroderma".

2.2.1 Blood collection

Blood from SSc and healthy individuals was taken by a phlebotomist. For plasma analysis, purple topped blood tubes were used containing EDTA anticoagulant. After centrifuging the tubes for 10 minutes 1710 g at 4ºC, plasma was aspirated with a sterile Pasteur pipette and transferred to PT4

tubes before being frozen at -80ºC. Being a potential biohazard, handling the blood required wearing a lab coat, gloves and goggles. Used materials and equipment were disposed of in a clear plastic autoclave bag. Liquid waste was disposed and decontaminated using Virkon dispersible tablets and any spillages were immediately cleaned using bleach or Virkon.

2.2.2 Blister fluid collection and profiling

SSc patients with dcSSc were selected for blister fluid donation. Using a dermal suction apparatus (Ventipress, Upsalla, Sweden) and a technique originally devised by Sondergaard et al, an 8mm blister was formed on the anterior forearm of patients and healthy controls under negative pressure (280-310 mmHg) over 3 hours (Sondergaard et al.1998). The interstitial fluid in the blister was aspirated using a 23-gauge needle. 100-250 µl of fluid is collected per blister and stored in 1.5 ml Eppendorf tubes following centrifugation at 4°C for 10 minutes and decantation of the supernatant. Samples were kept in 20 µl aliquots at -80°C until needed.

2.2.3 Blister fluid Luminex assay

Profiling of blister fluid constituents was conducted in collaboration with Henry Lopez (Murigenics, US) using a Luminex bead array with EMD Millipore MILLIPLEX MAP human cytokine/chemokine bead panel (Billerica, MA) for 41 SSc-related soluble factors (EGF, Eotaxin, FIT-3L, Fractalkine, GRO, G-CSF, FGF-2, GM-CSF, IFNα2, IFNγ, IL-1RA, IL-1α, IL-1β, IL-2, IL-3, IL-4, IL-5, IL-6, IL-7, IL-8, IL-9 IL-10, IL-12p40, IL-12p70, IL-13, IL-15, IL-17A, IP-10, MCP-3, MDC, MCP-1, MIP-1α, MIP-1β, PDGF-AA, PDGF-AB/BB, RANTES, sCD40L, TGF-α, TNFα, TNFβ, and VEGF). Blister fluid samples from 26 SSc and 10 healthy control individuals were assayed. The Luminex bead panel was washed with wash buffer (200 µl/ well) before the addition of 25 µl Human Cytokine Standards (10,000 pg/ml) or SSc and healthy blister fluid samples (diluted 1:100 for RANTES, PDGF-AA and PDGF-BB). The plate was incubated rocking at 4ºC overnight. The wells were aspirated and washed with 200 µl wash buffer before the addition of 25 µl detection antibody per well for 1 hour and room temperature. 25 µl streptavidin-phycoerythrin was added to

each well for 30 minutes at room temperature before washing with 200 µl wash buffer followed by 150 µl sheath fluid per well. Using a Luminex plate reader, a laser excites fluorescent dyes on the bound reporter molecule. The amount of fluorescence is processed and quantified.

2.2.4 Blister fluid and plasma IL31 ELISA assay

A Human IL31 DuoSet enzyme linked immunosorbent assay (ELISA) kit (R&D systems) was used to assay the amount of IL31 in 43 SSc and 21 healthy control blister fluid samples as well as 23 SSc and 27 healthy control plasma samples. A 96 well ELISA plate coated with 100 µl capture antibody per well diluted in reagent diluent (0.8 µg/ml) was incubated at room temperature overnight before blocking with 300 µl reagent diluent for 1 hour (1% BSA in PBS, 0.2 µm filtered). A serial dilution of standards was prepared ranging from the 8000 to 0 pg/ml. 100 µl of standard or blister fluid/plasma sample was added to each well and incubated for 2 hours at room temperature before adding 100 µl IL31 detection antibody provided with the kit (55.56 µl in 10 ml reagent diluent). The plate was left covered at room temperature for 2 hours before 100 ml streptavidin HRP was added to each well for 20 minutes. 100 µl Glow substrate A and B (3 ml A: 7 ml B) was pipetted onto each well before reading optical density using a microplate reader at a wavelength of 450 nm.

2.2.5 Blister fluid Lactate assay

A L-lactate Colorimetric Assay (Biovision, CA, USA) used to detect the amount of lactate in SSc and healthy control blister fluid. Using the manufacturer's protocol, lactate standard provided in the kit was diluted (10 µl in 990 µl, lactate Assay Buffer) to a concentration of 1 mM. In a 96 well plate, 0, 2, 4, 6, 8 and 10 µl of the diluted lactate standard was pipetted into wells in duplicates before further diluted by adding 50 µl lactate assay buffer per well such that final concentrations were 0, 2, 4, 6, 8 and 10 nmol per well respectively. 50 µl of 10 healthy control and 8 SSc blister fluid samples were also pipetted in individual wells of the plate. 50 µl of the lactate reaction mix (46 µl lactate assay buffer 2 µl lactate substrate mix 2 µl lactate enzyme mix) was added to each well of

the standards and test samples. Lactate znzyme and lactate substrate mixes were reconstituted in 0.22 ml lactate assay buffer. After 30 minutes' incubation at room temperature, optical density was measured using a microplate reader at 450 nm. A standard curve of nmol/well vs optical density of the diluted lactate standards was plotted and used to determine the amount of lactate in each test sample.

2.2.6 Skin biopsy collection and metakaryotic staining

Skin punch biopsies of 4mm diameter and 5mm depth were taken from the lower arm of 5 patients with diffuse SSc and 5 healthy controls. Biopsies were fixed in Carnoys fixative (3 parts ethanol to 1-part glacial acetic acid, mixed immediately before adding the tissue). The biopsies were stored at 4°C with fixative being replaced three times, once every hour before being stored long term in 70% ethanol at 4°C. Using a method developed by Dr Elena Gostjeva (Gostjeva et al. 2009), tissues were assessed for the presence of metakaryotic stem cells. Biopsies were cut laterally into 3 pieces using a scalpel and each piece digested in collagenase II (0.8mg/ml) at 37°C for two hours. Sections were then placed in 1M HCL at 60°C for 8 minutes for hydrolysis to occur. Acid treatment releases the aldehydes by cleavage of the N bases and formation of aldehyde groups to which Schiff's staining binds. Schiff's staining is DNA specific and staining intensity is proportional to DNA concentration. After hydrolysis, sections were rinsed in distilled H_2O and placed into a Petri dish at room temperature containing 45% acetic acid for 15-30 minutes. Individual sections were placed on glass microscope slides and 5 µl acetic acid pipetted on top before covering with a glass coverslip and spreading the section with slight pressure until a thin uniform layer was achieved. Slides were placed on dry ice until frozen, before immersion in Schiff's reagent for one hour, and then rinsed twice in 2 x saline-sodium citrate (SSC) buffer, once for 30 seconds, once quickly. Slides were then rinsed well with distilled H_20 and dipped in 1% giemsa solution for 5 minutes before rinsing in sorenssen buffer and distilled H_2O. Slides were allowed to dry fully before being immersed in xylene for 3 hours and mounting with dpx mountant. Slides were scanned with a LEICA SCN400F scanner. Quantification of metakaryotic nuclei was conducted by

counting the number of bell-shaped nuclei in 10 randomly selected 20x magnification field views per slide and determining the average number of MSCs per section.

2.3 Differentiation

2.3.1 Osteogenic differentiation

Adipose derived MSCs were cultured in a T75 flask until ~70% confluent before being seeding in 12 well plates, with either soft or stiff matrices at a seeding density of 50000 cells per well. They were cultured in 10% serum for 4 days until 70% confluent before serum starving overnight and switching media to osteogenic induction media (OIM) with or without treatments; TGFβ (R&D Systems, Minneapolis, USA), IL31 (R&D Systems, Minneapolis, USA) and MRTFA inhibitor CCG-1423 (R&D Systems, Minneapolis, USA) (Figure 2.2). Media was changed every 3 days for 12 days and cells were retreated at every media change. Cells were imaged with Axioscope Light microscope at a magnification of 2.5x every 3 days to observe changes in cell morphology. At day 12, cells were washed thoroughly with DPBS before fixing with 4% formaldehyde for 10 minutes. Cells were then carefully washed with distilled water without disturbing the monolayer. 350µl of 1% Alizarin Red S solution at pH 4.2 was added to the wells and left at room temperature for 20 minutes before thoroughly washing with deionised water and observing red staining of osteoblasts.

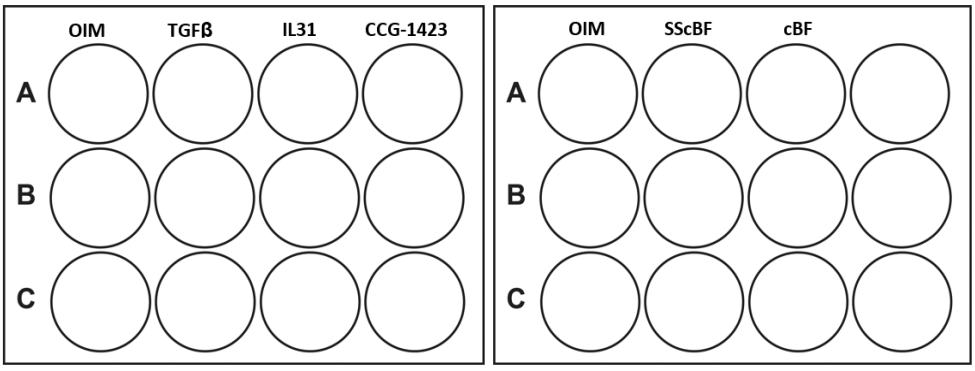

Figure 2.1 ***Plate map of osteogenic differentiation assay.*** *MSCs cultured in Osteogenic Induction media (OIM) treated with TGFβ (4 ng/ml), IL31 (50 ng/ml), MRTFA inhibitor CCG-1423 (10 µM) or blister fluid (SScBF/cBF at a dilution factor of 1:50).*

2.3.2 Adipogenic differentiation

Adipose-derived MSCs were cultured in a 12 well plastic plate (4 x 10^4 cells per well) in 10% serum until ~60% confluent. After overnight serum starvation cells were treated as follows in replicates of three: adipogenic media only, adipogenic media plus SSc blister fluid (1:125), adipogenic media plus healthy control blister fluid (1:125), DMEM supplemented with 10% serum (Figure 2.3). A different blister fluid sample was used for each replicate. Cells were imaged with an Axioscope microscope at 2.5x magnification on days 4 and 10. On day 10, cells were rinsed well with 2 ml DPBS per well before fixing with 2 ml 10% formalin per well. Cells were fixed at room temperature for 60 minutes. Adipogenic differentiation was measured using Oil Red O staining. A stock solution of the stain was made by dissolving 300 mg Oil Red O in 100 ml 99% isopropanol. 3 parts stock solution to 2 parts deionised water were mixed and filtered through Whatman filter paper. After washing cells with DPBS, 1 ml of the diluted Oil Red O stain was added to each well and left at room temperature for 15 minutes before washing again with deionised water. For semi-quantification of adipogenic differentiation, dye was eluted by adding 1 ml 100% isopropanol to each well and rocking for 15 minutes. 100 µl of the isopropanol from each well was pipetted into a 96 well plate using fresh isopropanol as blank standards and absorbance was measured at 490nm using a plate reader. Absorbance was corrected for controls and standards. Absorbances which are greater than 3 times standards and controls were considered positive for adipogenic differentiation. Less than 2 times the standards and controls were considered negative for adipogenic differentiation (Strutt et al. 1996).

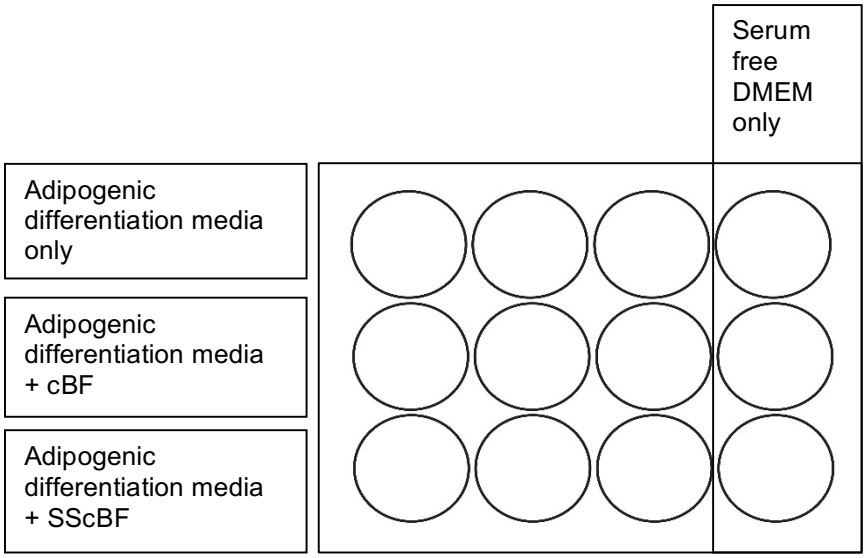

Figure 2.2 ***Plate map of adipogenic differentiation assay.*** *MSCs cultured in adipogenic differentiation media supplemented with SSc blister fluid (SScBF) or control blister fluid (cBF) at a dilution factor of 1:125. Serum free DMEM was used as a control.*

2.4 qPCR

2.4.1 RNA extraction

For qPCR assays, RNA was extracted using the RNeasy Plus Mini Extraction kit protocol (Qiagen #7414). Cells were lysed with 350 µl Buffer RLT Plus per well and scraped using a cell scraper before aspirating lysates into 1.5ml eppendorfs per sample and vortexing. Lysates were pipetted into a QIAshredder spin column per sample and centrifuged for 2 minutes at 13,200 RPM. 350 µl of 70% ethanol was added to the flow-through before pipetting 700 µl of each sample lysate into an RNeasy spin column. Each sample was centrifuged for 15 seconds at 10,000 RPM and flow-through was discarded. 500 µl of Buffer RPE was added to the spin column for each sample and centrifuged for 15 seconds at 10,000 RPM. This was repeated twice, discarding the flow-through after each centrifugation. 30 µl RNase-free water was added to each spin column and centrifuged for 1 minute at 4ºC at 10,000 RPM to collect RNA. RNA concentrations were measured using a Nanodrop 2000 spectrophotometer. RNA were diluted to yield a loading concentration of

100 ng RNA per sample. All primers used in qPCR assays were created using Integrated DNA technologies PrimerQuest.

2.4.2 Primers

All primers were purchased from Integrated DNA technologies. Primers used in the studies were Tata Binding Protein (TBP) Forward sequence AGTGACCCAGCATCACTGTTT, reverse sequence GGCAAACCAGAAACCCTTGC, IL31 Receptor pair 2, forward sequence TGTGCGGTCAAGGAGTCAAA, reverse sequence AGGCCACATGGAGCTTCTTC, α-SMA forward sequence CCGACCGAATGCAGAAGGA, reverse sequence ACAGAGTATTTGCGCTCCGAA, and collagen type 1α1, forward sequence TGCTTGCAGTAACCTTATGCCTA, and reverse sequence.

2.4.3 IL31 Receptor

RNA from four SSc and healthy control, dermal and lung fibroblast cell lines, plus two MSC cell lines was extracted using the RNeasy extraction kit. To assay IL31 receptor mRNA concentration, qPCR was performed using the Qiagen QuantiFAST SYBR Green kit and protocol. Two primer mixes were prepared, IL31 receptor (IL31R2) and the housekeeping gene primer TATA binding protein (TBP). Forward and reverse primers for each primer, were mixed with the QuantiFAST SYBR green master mix, reverse transcriptase and water at a ratio of 0.12: 0.12: 6: 0.12: 3.64 respectively. 10 µl of the primer mixes were added to the appropriate PCR tubes with 2 µl RNA per sample in duplicates bringing the concentration to 100 ng RNA per sample. The PCR tubes were loaded into the Rotorgene 6000 machine and set to the following: hold time 50ºC for 15 minutes, hold time 95ºC for 5 minutes, 40 cycles of 95ºC for 10 seconds, 60ºC for 10 seconds and 60ºC for 20 seconds, melt, ramp from 74ºC to 95ºC, rising by 0.5, wait for 90 seconds, wait for 5 seconds, acquire to melt A on Green. Results were collected using Rotorgene6000 analysis software and relative expression was calculated by subtracting TBP CT values from the IL31R2 CT values for each sample to obtain ΔCT, then

calculating $2^{-\Delta CT}$ and plotting the average for replicates of each sample. Graphpad Prism 7.0 was used to conduct a two-way ANOVA with Tukey's post hoc test to correct for multiple comparisons and determine statistical significance. IL31RA expression was also measured on one MSC cell line treated with one SSc or control blister fluid sample (1:50), using the same method.

2.4.4 α-SMA expression and blister fluid

MSCs seeded in 2 x 6 well plates at a density of 3 x 10^5 cells per well were cultured in 10% serum DMEM until full confluency before serum starving overnight and treating for 16 hours as follows: serum free DMEM, TGFβ (4 ng/ml), SSc/healthy control blister fluid (1:50), SSc/healthy control blister fluid (1:50) + TGFβ inhibitor 1D11 (10 µg/ml), SSc/healthy control blister fluid (1:50) + Wortmannin (100 nM), SSc/healthy control blister fluid (1:50) + U0126 (5 µM) and SSc/healthy control blister fluid (1:50) + 1D11 (10 µg/ml)+ Wortmannin (100 nM) (Calbiochem, San Diego, California CAS 19545-26-7) + U0126 (5 µM) (Calbiochem, San Diego, California). Blister fluid, TGFβ and inhibitor treatments were in serum free DMEM. The same blister fluid sample was used in all blister fluid treatments in order to validly compare inhibitor action. After RNA extraction, using the Qiagen RNeasy Mini extraction kit as outlined above, 100 ng of RNA was loaded into each PCR tube together with TBP or α-SMA primers. The Qiagen QuantiFAST SYBR Green kit was used to make the primer mixes. Samples were loaded in duplicates into the Rotorgene 6000 and the PCR run was set to the same template used for the IL31 receptor assay. The Rotorgene 6000 analysis software was used to determine CT values of each primer for each sample.

2.4.5 α-SMA expression and lactate

MSCs were cultured in a 24 well plate in 10% serum until fully confluent. After overnight serum starvation, all 24 wells were treated as follows in replicates of three: serum free DMEM, 10% serum, sodium L-lactate (25 µM) (Sigma-Aldrich; Dorser, UK), sodium L-lactate (25 mM) + lactate inhibitor α-cyano-4-hydroxycinnamic acid (αCHCA 5 mM) (Sigma-Aldrich; Dorser, UK) , SSc or

control blister fluid (1:50), SSc or control blister fluid (1:50) + αCHCA (5 mM). Lactate, blister fluid and inhibitor were all added to serum free DMEM. Cells were treated for 16 hours before cell lysis and RNA extraction as detailed above. 20 ng RNA was loaded for each sample in duplicates. TBP and α-SMA primers were used in this assay using the Qiagen QuantiFAST SYBR Green kit. Results were analysed using the Rotorgene 6000 analysis software.

2.4.6 Pro-fibrotic gene expression on Softwell collagen plates

Adipose-derived MSCs cultured until confluency on either soft (4 kPa) or stiff (50 kPa) Softwell collagen coated plates were serum starved overnight. Cells were treated with 0.2% serum, TGFβ (4 ng/ml) or CCG-1423 (10 μM) with 4 replicates of each condition for 20 hours. As above, RNA was extracted and diluted in order to load 20 μg of RNA per sample. qPCR was run using the primers of two pro-fibrotic genes, α-SMA and CTGF in addition to the housekeeping gene TBP. Expression was analysed using the Rotorgene 6000.

2.4.7 α-SMA dose response of blister fluid

Adipose-derived MSCs were cultured in 10% serum on a 24 well plastic plate until fully confluent. After serum starvation overnight and washing with DPBS, cells were treated with SSc or control blister fluid at the following dilution factors: 1:5, 1:10, 1:20, 1:50, and 1:125. All concentrations were using the same blister fluid sample. Cells were treated for 16 hours before RNA extraction and qPCR for α-SMA using Rotorgene 6000. 15 ng of RNA was loaded into each reaction tube in duplicates and expression was compared to TBP housekeeping protein.

2.5 Western Blotting

2.5.1 α-SMA protein expression on Softwell collagen plates

MSCs cultured on soft (4 kPa) and stiff (50 kPa) matrices were serum starved on 0.2% serum overnight, washed with DPBS and treated as follows for 24 hours: 0.2% serum, TGFβ (4 ng/ml) and CCG-1423 (10 μM) (Cayman

Chemical; Michigan, USA). Treatments were added to 0.2% serum with 4 replicates of each condition. 10 μg of protein extracted was assayed per sample.

2.5.2 Pro-fibrotic protein expression of MSC in SSc microenvironments

MSCs cultured on plastic 6-well plates (Corning; New York, USA) were grown in 10% serum until 80% confluent. Following serum starvation overnight and washing with DPBS, cells were treated for 24 hours as follows, 0.2% serum, 10% serum, SSc or control blister fluid (1:125), IL31 (50 ng/ml), TGFβ (4 ng/ml). 50 ng/ml IL31 was used as the optimum concentration for all experiments in this thesis following experiments conducted by others in the lab whereby a Western blot of pro-fibrotic proteins in response to IL31 concentrations of 1, 2.5, 5, 10, 50 and 100 ng/ml showed that expression did not increase when treated with IL31 concentrations above 50 ng/ml, and was less than optimal at lower concentrations. Blister fluid, IL31 and TGFβ treatments were in 0.2% serum conditions. Dependent on protein concentrations obtained, either 4 or 10 μg of protein was run per sample.

2.5.3 Protein extraction

Cells were washed thoroughly with DPBS and lysed with 120 μl lysis buffer per well (1 tablet complete mini, 100 μl Phosphatase inhibitor 2 and 100 μl Phosphatase inhibitor 3 in 9.8 ml RIPA buffer, Sigma-Aldrich; Missouri, USA). The lysed cells were scraped off using a cell scraper. The protein concentrations of each sample was determined with the Bicinchoninic Acid Assay Kit and protocol (BCA) (Life Technologies; Paisley, UK). 10 μl of Bovine Serum Albumin (BSA) standards found in the kit, of known protein concentrations were added to the 96 well plate as a standard curve. The lysed cell samples were also pipetted into the remaining wells of the 96 well plate. 200 μl of colour change Working Reagent was added to each sample and incubated while covered for 30 minutes at 37°C 5% CO_2. Protein concentrations were measured using a Mitras LB940 Multimode Microplate Reader (Berthold Technologies, Bad Wildbad, Germany) at 570 nm.

Absorbance readings of the BSA standards were plotted and used to determine the protein concentrations of the unknown samples.

2.5.4 Western blot electrophoresis

The same amount of each protein sample was aliquoted into a 1.5 ml eppendorf tube together with 3.5 µl NuPAGE LDS sample buffer and 1.5 µl reducing agent (Life Technologies; Paisley, UK). Proteins were denatured at 95°C for 5 minutes and centrifuged at 13,500 RPM for 15 seconds. 15 µl of each protein sample was loaded into individual wells of NuPAGE Novex 4-12% Bis-Tris, 1.0mm 12 well gels (Life Technologies; Paisley, UK) in addition to loading 9 µl of SeeBlue marker plus2 Pre-stained Protein Standard ladder (Life Technologies; Paisley, UK). Western blot electrophoresis tanks fitted with the gels were filled with Running Buffer (50ml NuPAGE MOPS SDS Running Buffer (20X) (Life Technologies; Paisley, UK) and 950ml distilled water) and run for 1.5 hours at 200V. The gels were removed from the cassettes and immersed in Transfer Buffer (50 ml NuPAGE Transfer Buffer 20X (Life Technologies; Paisley, UK) in 200 ml 70% Methanol and 750 ml distilled water). While immersed in the buffer, gels were placed over chromatography paper and sponges. A membrane was placed over the gel, followed by chromatography paper and more sponges. Any bubbles between layers were carefully rolled out before placing the whole gel/membranes/sponge 'sandwich' in a transfer cassette and running it for 2 hours at 35 V. The proteins now transferred to the membrane were stained using Ponceau Red S Solution (Sigma-Aldrich; Missouri, USA) to ensure complete protein transfer. The Ponceau Red S Solution was washed off with DPBS before rocking in blocking agent (5 g semi-skimmed milk powder in 100 ml DPBS) for 1 hour to block non-specific antibody binding.

2.5.5 Antibodies

All antibodies were diluted in 5% semi skimmed milk. Primary antibodies used were monoclonal mouse anti human-α-SMA (Dako, Cambridgeshire, UK) diluted 1:500-1:1000, monoclonal mouse anti human-GAPDH (Abcam; Bristol, UK) diluted 1:50000, polyclonal goat anti human-CTGF (1:500/ 1:1000) (Santa

Cruz Biotechnology; Milan, Italy) and polyclonal goat anti-human collagen (1: 3000) (Merck Millipore). Membranes were left rolling in diluted primary antibodies at 4°C overnight. Membranes were washed with PBS-Tween (10% PBS, 0.05% tween) for 10 minutes three times before probing with anti-mouse/goat HRP-conjugated IgG secondary antibodies (Cell Signalling Technology; Massachusetts, USA) diluted 1:1000. Membranes were rolled in the secondary antibody for 1 hour at room temperature before washing with PBS-Tween.

2.5.6 Developing

Amersham ECL Western Blotting detection kit (GE Healthcare Life Sciences; Buckinghamshire, UK) was used on the membranes as instructed by the kit before covering the membrane with cling film. Membranes were developed using Xograph Compact X4 Automatic Processor and Hyperfilms. α-SMA films were developed for 30 seconds to 1 minute while CTGF, Collagen and GAPDH proteins were visible after 1-2 minutes developing. NIH ImageJ software (National Institutes of Health (NIH), Bethesda, MD, USA) was used to conduct densitometric analysis on the Western blots.

2.6 Cell Migration Assays

2.6.1 Collagen Glass slide migration assay

Aligned collagen coated glass slides (manufactured by Fibralign, California, USA and provided by Sigma-Aldrich; Dorset, UK 5054-6EA) are glass slides coated with bovine collagen type I in an aligned conformation mimicking fibrotic skin as well as a woven mesh-like alignment which models healthy skin (Ahmed et al. 2017) (Figure 2.4). Collagen chips were washed in DPBS free of Ca^{2+} or Mg^{2+} for 5 minutes, to ensure collagen fibrils become resistant to changes in pH, before being immersed in deionised water for 10 seconds. They were covered with 70% ethanol for 1 hour in a tissue culture biosafety hood. After 1 hour the ethanol was aspirated and the chips left to dry fully by being placed at an angle in the culture dish. Once dry, chips were incubated in 2% serum for 45 minutes at 37°C, 5% CO_2 then taken out of the incubator

and allowed to dry at room temperature. A cell suspension of healthy dermal fibroblasts was made in 10% serum and 6 x 3 μl dots containing 12000 cells each were were pipetted onto the chips in a culture dish. 50 μl 10% serum was added to the culture dish to prevent dehydration of the cells on the chip. Culture dishes were incubated for 2.5 hours to allow for cell adhesion. Following incubation, the entire chips were immersed by flooding the well with serum free media, IL31 (50 ng/ml) in serum free media, SSc blister fluid (1:125) in serum free media or 10% serum. Chips were incubated and imaged at 0, 24 and 48 hours at 2.5x magnification using phase contrast Zeiss Axiocam to observe cell migration. The area the cell population inhabited was measured using Image J by setting the scale using the microscope field of view measurements of 3400μm x 2700μm and using the free hand tool to draw around the edge of the population.

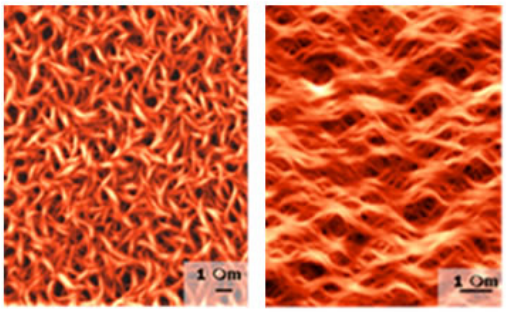

Figure 2.3 ***Alignment of collagen coated glass slides.*** *Woven (right) and aligned (left) collagen fibrils on glass slides (Fibralign)*

2.6.2 Scratch Wound assay

For these assays, dermal fibroblasts or MSCs were cultured in 24 well plates at a seeding density of $9x10^4$ cells per well until fully confluent in 10% serum. After washing with DPBS, a scratch of the diameter of the well was made in each well using a p200 pipette tip (Figure 2.5). DPBS was used to wash the cells to remove detached cell remnants. Cells were imaged at 2.5x magnification using phase contrast Zeiss Axioscope and Axiocam. Migration was measured as the area of the scratch left at each time point. The free hand tool on NIH ImageJ was used to draw around the scratch and area (mm^2) was measured after setting the field of view to 3400μm x 2700μm.

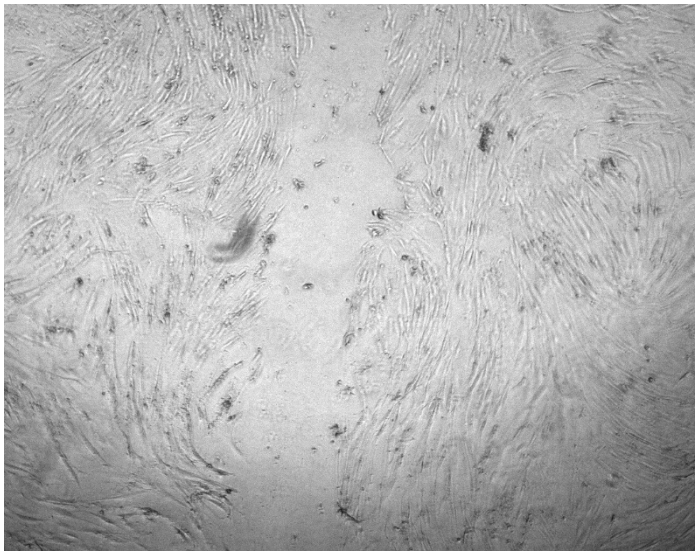

Figure 2.4 ***Scratch made by p200 pipette tip***

2.6.2.1 Dermal fibroblast scratch wound assays

Healthy control (NF25) and SSc (SScF1, SScF2) dermal fibroblasts were treated in replicates of 4 with 0.2% serum, or else media with 0.2% serum plus IL31 (10 ng/ml), IL31 (50 ng/ml), IL31 (50 ng/ml) + Wortmannin (100 nM), IL31 (50 ng/ml) + U0126 (5 μM) or 10% serum. Inhibitors was added to the cells 1 hour prior to IL31. Wells were imaged at regular intervals until the scratch was no longer visible.

2.6.2.2 MSC scratch wound assays

Cultured adipose derived MSCs were treated in replicates of three with 0.2% serum, as negative control, 10% serum, as positive control, IL31(50 ng/ml), IL31 (50 ng/ml) + Wortmannin (100 nM), SScBF (1:125) and cBF (1:125). IL31, Wortmannin and blister fluid treatments were under 0.2% serum conditions and a different sample of blister fluid was used for each replicate. Wortmannin was added to the MSCs 1 hour before the addition of IL31. Wells were imaged at 0, 8 and 24 hours.

2.6.3 Collagen Gel contraction assays

Adipose-derived MSCs cultured on T75 plastic flasks were trypsinised with Trypsin/EDTA, centrifuged at 1250 RPM and suspended in serum free DMEM.

Collagen gel suspensions were made using HEPES buffer pH 8.9, Rat Tail Collagen I (First Link Ltd, UK) and cell suspension at a ratio of 1:4:5 parts respectively. 1 ml of this mixture was added to each coated well of a 24 well plate such that the final concentrations in each well were 80,000 cells and 1.2 mg collagen/ml. The collagen gels polymerised after 2-3 hours of incubation at 37°C 5% CO_2. Gels were detached from the edges of the well by adding 2 ml serum free media per well treated with 10% serum, blister fluid (1:125 or 1:50), IL31 (50 ng/ml), Wortmmanin (100 nM), U0126 (5 μM), TGFβ (4 ng/ml), 1D11 (10 ng/ml), αCHCA (5 mM) or lactate (25 mM). Cells were incubated with the treatments for 24 - 48 hours before thoroughly aspirating all media and weighing the gels.

2.7 Next Generation Sequencing (NGS)

One healthy dermal fibroblast and one MSC cell line were cultured in 24 well plastic plates until fully confluent. After overnight serum starvation, both cell lines were treated in replicates of 4 as follows; 0.2% serum, SSc or healthy control blister fluid (1:125), or IL31 (50 ng/ml). Blister fluid and IL31 were added to 0.2% serum conditions. A different sample of blister fluid was used for each replicate for both cell lines. Cells were treated for 16 hours and lysed for RNA extraction using Qiagen RNeasy extraction kit and protocol. In collaboration with UCL Genomics, RNA extractions were assayed using Illumina TrueSeq standards library with 15 million reads per sample. Quality control of the samples was performed using the High Sensitivity Tapestation kit and 43 base pair paired end sequencing. Differential expression of each sample was analysed using principal components analysis. P-values were determined with Wald's statistic test. Transcriptome analysis was conducted using paired end reads and were mapped to the Ensembl human transcriptome reference sequence (latest version available during analysis: GRCh38 (84)). Mapping and generation of read counts per transcript were done using Kallisto (Bray et al. 2016), based on the novel idea of pseudoalignment. R/Bioconductor package tximport was used to import the mapped counts data and summarise the transcripts-level data into gene level as described in this paper (Soneson et al. 2015). Further analyses were run

using DESeq2 package (Varet et al. 2016). Some advantages of this method includes (i) correction for potential changes in gene length across samples (i.e. from differential isoform usage), (ii) Kallisto is faster and requires less memory and disk usage compared to alignment-based method. Normalisation and differential analysis are carried out according to the DESeq2 model by use of negative binomial generalized linear model. The estimates of dispersion and logarithmic fold changes incorporate data-driven prior distributions. Using this method, we compared the two conditions for each experiment and we extracted a result table with log2fold changes, Wald test p values and adjusted p values (according to false discovery rate). Mapped reads for each sample ranged between 12 and 21 million. Principal component analysis was used as a quality control assessment. Functional classification of genes' list was performed using Ingenuity Pathway analysis (IPA, https://www.qiagenbioinformatics.com/). The "core analysis" function was used to interpret the data in the context of biological processes, pathways and networks. Both up and down regulated identifiers were defined as value parameters for the analysis. Significance of the biofunctions and the canonical pathways were tested by the Fisher Exact test p-value. Pathway analysis was performed and highlighted predicted pathways involved in the context of their physiological significance. Countplots of differentially expressed genes were produced using Graphpad prism 7.0.

2.8 Statistical analysis

Two statistical analysis softwares were used; IBM SPSS 22 and GraphPad Prism 7.0. Unless stated otherwise, a unvariate, one-way Analysis of Variance (ANOVA) with Tukeys Post hoc test was conducted on the majority of *in vitro* quantitative assays. Some exceptions include, the students T-Test for the Lactate and IL31 concentration assays, and multivariate ANOVA and are indicated when used.

Chapter 3 : Determining whether activated MSCs are present within the fibrotic environment of SSc patients' skin lesions

3.1 Introduction

As discussed in the literature review in Chapter 1, relatively little data exists surrounding the role of MSCs in SSc. The majority of the published work attempts to evaluate their beneficial uses in potential transplant therapies in many autoimmune diseases, including SSc. However, even less data exists on the role of the endogenous tissue resident MSCs in these diseases, particularly SSc and how MSCs function in these pathological microenvironments. MSCs are proposed to partake in metakaryotic stem cell division, which is an amitotic process giving rise to both symmetrical and asymmetrical division. This potentially is what allows for the MSCs to self-renew and differentiate simultaneously. Bell-shaped nuclei are proposed to be indicative of metakaryotic stem cells. Their behaviour with regards to cell division differs from eukaryotic mitosis or meiosis and is, therefore, termed metakaryotic. This type of division is suggested to be a driving force for growth and differentiation. Thus far, this is well documented in early embryogenesis, and in adult tumours, but their presence in SSc has not been studied (Thilly et al. 2014).

Physiologically, MSCs can be found in the subcutaneous fat under and since the majority of the studies of this thesis concern skin pathology and fibrosis, in the *in vitro* experiments undertaken, commercially available adipose-derived MSCs were used rather than bone marrow or umbilical MSCs. This was an attempt to model as closely as possible the interaction between MSCs and the SSc microenvironment, considering the recent discovery that not all MSCs from the different derivatives are identical and that they seem to function in the tissue environment from which they are derived.

In order to begin to understand how MSCs are behaving within the disease microenvironment, taking an *ex vivo* approach to visualise resident MSCs in SSc patient skin samples was considered a reasonable starting point. DcSSc patient biopsies were taken and after fixing them in Carnoys fixative and storing in 70% ethanol, biopsies were stained for metakaryotic cell division. Such nuclear divisions are not reported to be seen in healthy tissues but are present in tumour and during embryogenesis, and may represent MSCs

undergoing activation and division. The histology was conducted in collaboration with Dr Elena Gostjeva, Boston, MIT, a cytopathologist who first described this form of cell division (Gostjeva et al. 2009). Four healthy and four SSc biopsies were treated as described in the methods to investigate the presence of such nuclei. Feulgen staining methods of acid hydrolysis followed by Schiff reagent treatment, allowing for semi-quantitative measurement of DNA content by measuring the amount of aldehydes released upon DNA hydrolysis, were used previously by Dr Gostjeva's group in developing this technique. Staining intensity of the aldehydes released from DNA is directly proportional to DNA concentration (Chieco and Derenzini 1999). In this Chapter, the nuclear morphology associated with metakaryotic cell division is used to identify dividing MSCs in the SSc tissue.

3.1.1 Aim: To use a novel histologic technique which identifies metakaryotic cell division to identify activated dividing MSCs in SSc and healthy skin biopsy material

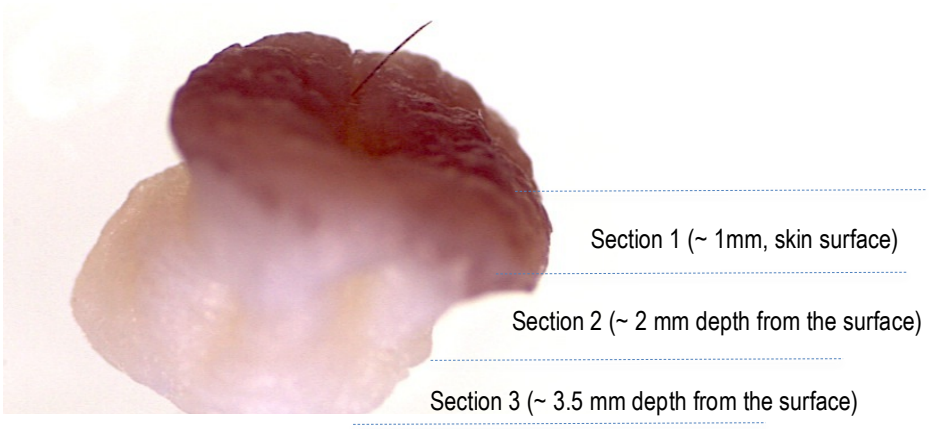

Figure 3.1 ***Biopsy taken from the forearm of SSc patient with indications of the lateral sections cut with a scalpel.***

Figure 3.1 illustrates how the fixed skin biopsies were cut laterally so that each section could be spread individually onto slides to assess differences in metakaryotic cell division at the different skin levels.

3.2 Feulgen's Staining of SSc biopsy

Four different SSc biopsies from four different patients were analysed in same way and similar trends were observed in all four. For the purpose of this Chapter, representative images are presented as well as quantitative analysis of all the sections studied.

In the uppermost layer of the SSc biopsies, section 1 (Figure 3.2), epithelial cells (purple) are found embedded within a thin collagen network (pink) (Figure 3.3). The collagen fibres are evenly interspersed across the section with no evidence of metakaryotic stem cells. In fact, in all four SSc biopsies, only 1 bell shaped nucleus was observed in the uppermost section. Also, in healthy control sections, no metakaryotic divisions were seen. Altered collagen orientation was found in SSc skin. Typically, collagen fibres are braided and woven together, but in one SSc biopsy, collagen was found in an abnormal aligned parallel configuration in keeping with a recent paper describing aligned collagen in SSc fibrosis (Figure 3.4) (Cao et al., 2017).

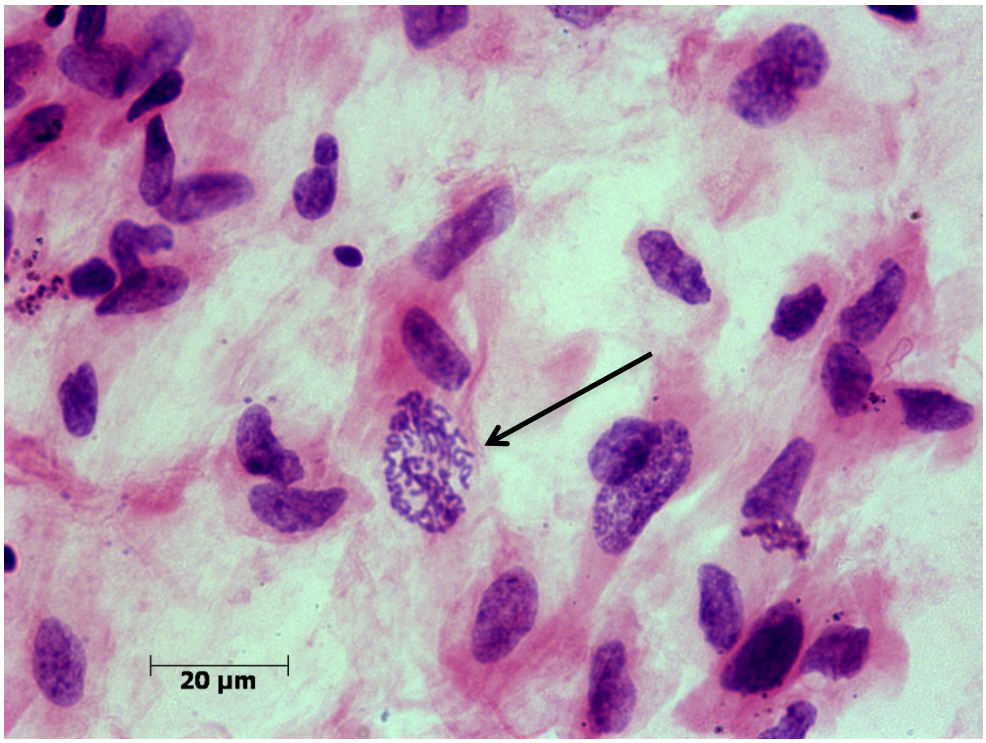

Figure 3.2 ***Mitotic proliferative epithelial cells (arrow) can be identified.***

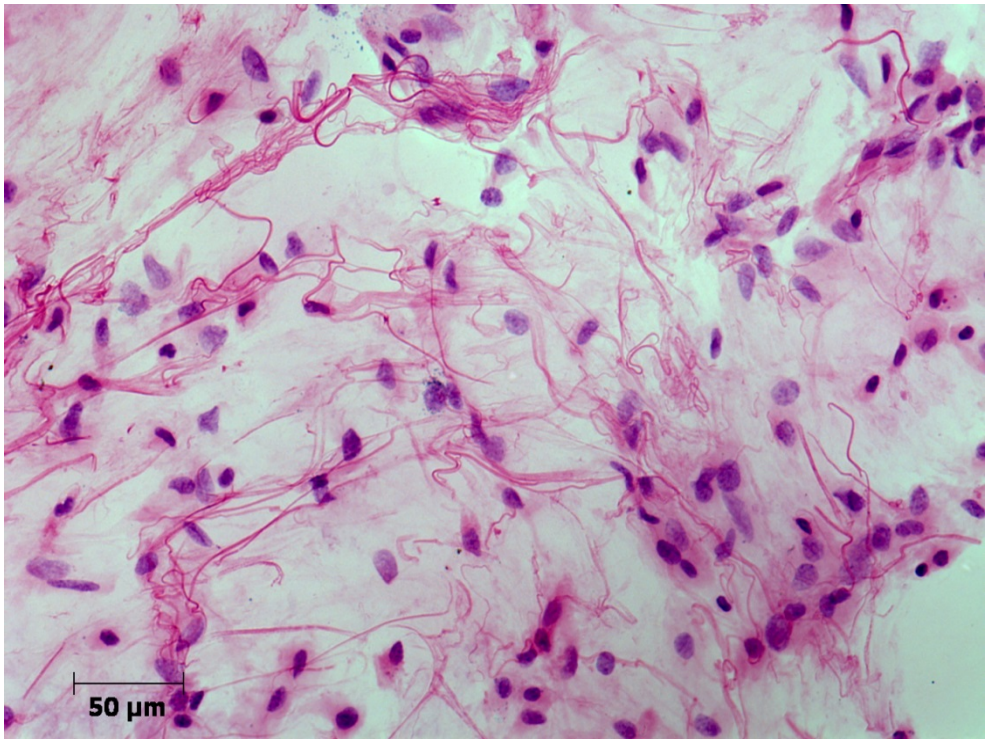

Figure 3.3 ***The collagen fibres of the top 1mm section of an SSc biopsy are thinly spread.*** *Collagen bundle structures are not seen. There is no evidence of metakaryotic nuclei in this section.*

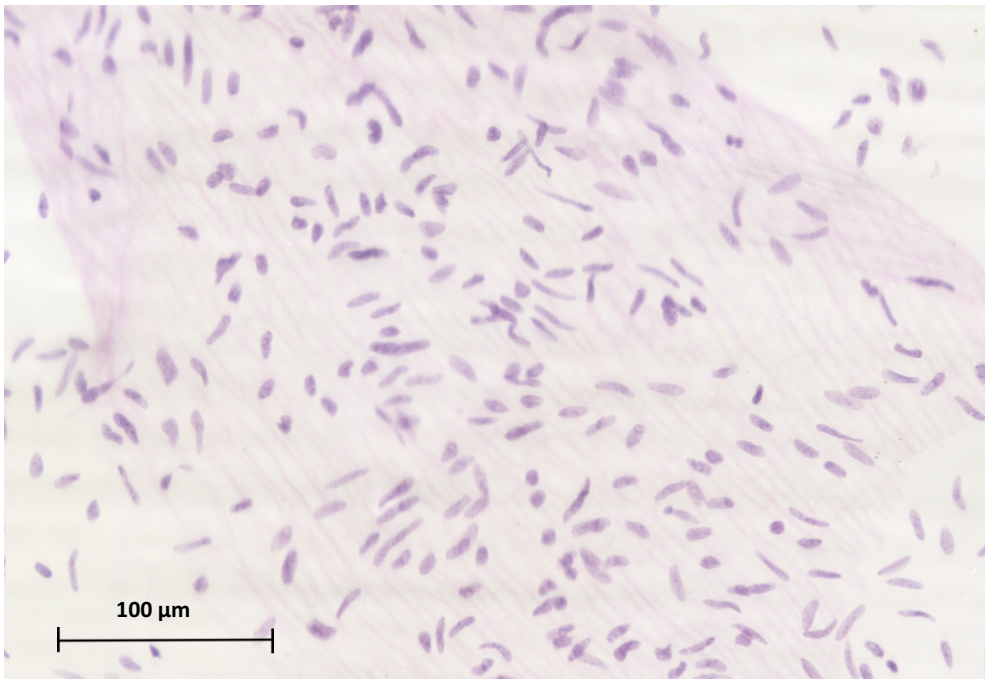

Figure 3.4 ***Aligned collagen fibres (above) are seen only in SSc skin.*** *Healthy skin shows no evidence of such alignment in the collagen structures.*

Feulgen's staining stains DNA content and thereby allows identification of mitotically dividing cells. Figure 3.5 shows a mitotically dividing epithelial cell in section 1 of the skin biopsy. The epithelial cell nuclei show no structural abnormalities, no sign of apoptosis and show mitotic cell divisions indicating physiologic cell turnover with regards to epithelial cell function.

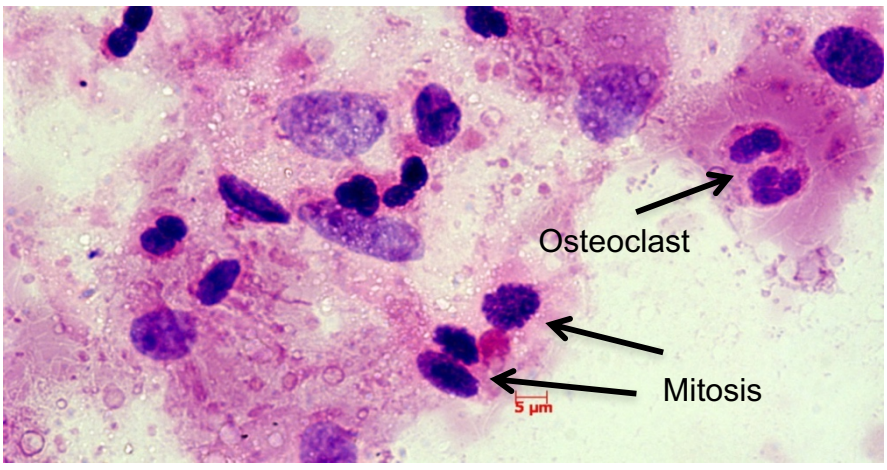

Figure 3.5 ***Bi-nucleated cells, identified as osteoclasts, and mitotically dividing epithelial cells (arrows) can be seen in the uppermost section of SSc skin, particularly in the hyper-pigmented top section.***

In addition to epithelial cells, other cells are identified in section 1 of the biopsy on the basis of their nuclear morphology (Figure 3.5). Many bi-nucleated cellular nuclei can be observed in the SSc biopsies, indicating the presence of osteoclast cells. The presence of these cells was particularly seen on the pigmented skin surface of section 1, responsible for the darker background of this slide. Osteoclasts are not generally seen in the skin and were not found in the healthy control sections examined. They derive from differentiation of peripheral blood mononuclear cells and monocytes in response to RANKL and macrophage colony-stimulating factor which are induced by pro-inflammatory cytokines involved in SSc including, IL33, IL17 and TNFα (Raimondo et al. 2017). Some SSc patients suffer from acroosteolysis, bone resorption of the digits. It was found that this bone resorption is a result of increased osteoclastogenesis and is found in SSc patients with acroosteolysis significantly more than in healthy control individuals and SSc patients without acroosteolysis (Park et al. 2016).

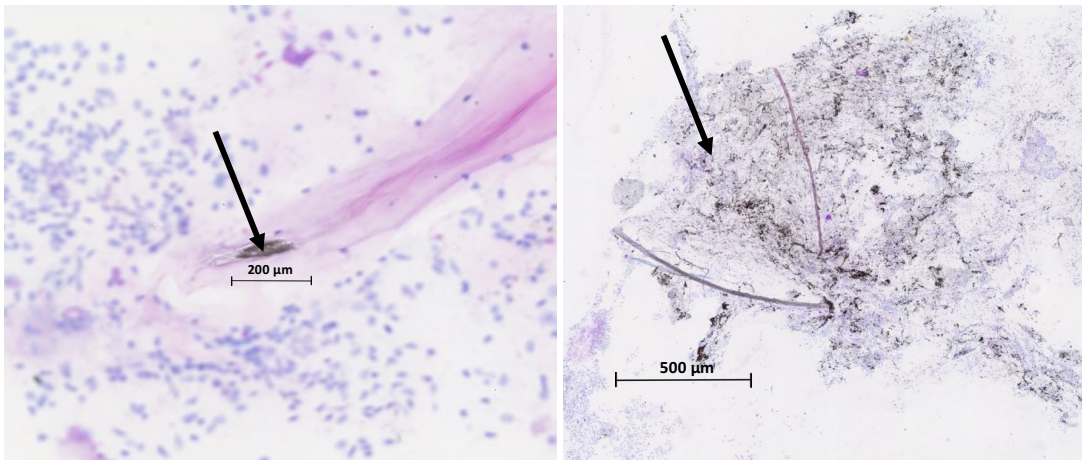

Figure 3.6 ***Bone material (left) and calcinosis (right) indicated by arrows are observed in SSc skin biopsy sections only.*** *Healthy skin biopsy sections showed no evidence of calcified bone material not black stained calcinotic lesions.*

Strikingly, bone material was identified in a top section of an SSc biopsy, together with calcinosis present in three out of the four SSc sections (Figure 3.6). The presence of calcinosis was determined by the amount of blackened staining and this was not found in any of the healthy skin sections. Bone material is not a normal constituent of skin and therefore its presence is highly

abnormal. The piece of bone seems to be embedded deep in collagen possibly hinting that the precursor the bone material produced, or induced nearby production of collagen.

Moving down the biopsy to section 2, indicating depth of 1-2 mm into the skin, mitotically dividing pigment producing cells were seen (Figure 3.7) as well as fibroblasts associated with slightly thicker collagen fibres than those seen in section 1 (Figure 3.8). The fibroblast cells can be seen embedded into the collagen fibres highlighting their symbiotic relationship.

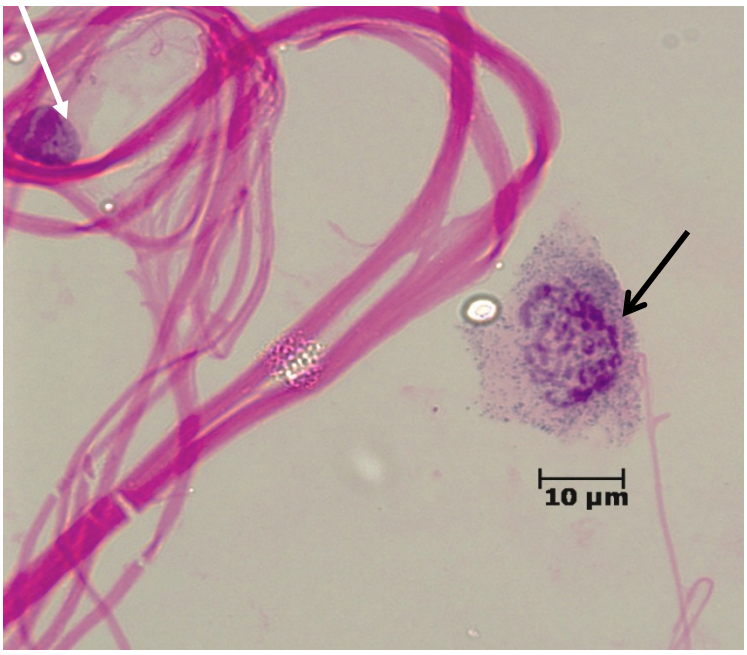

Figure 3.7 ***Pigment producing cells (black arrow) can be identified in the middle section of SSc skin.*** *Non-pigment producing cell (white arrow). Pigment producing cells in SSc skin may indication the presence of wound healing activity since scarred tissue is often hyper-pigmented.*

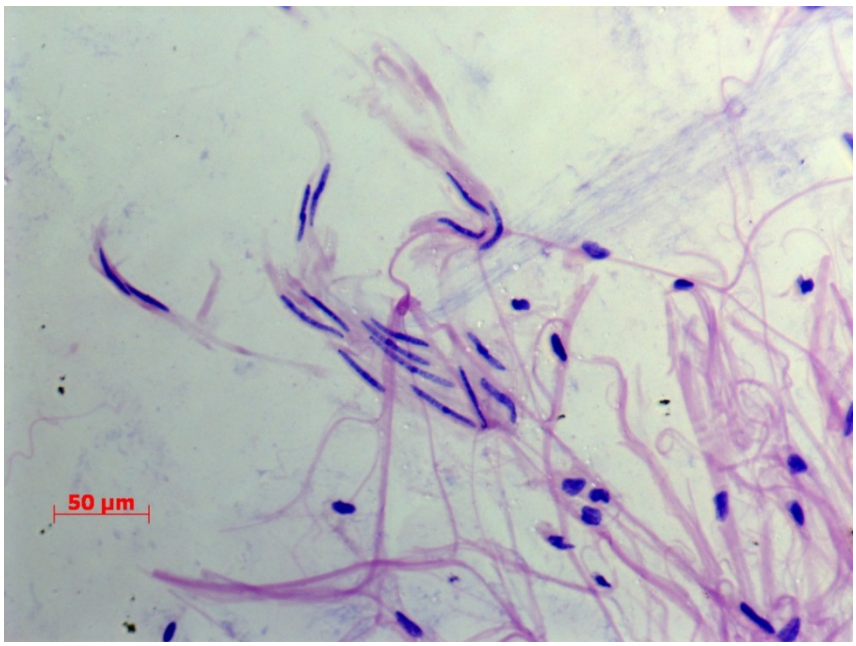

Figure 3.8 ***Fibroblast nuclei stained blue, and collagen fibres stained pink, are present in SSc skin biopsies in the middle section.***

In this section, the first appearance of metakaryotic stem cell were detected by their bell shaped nuclei (Figure 3.9) and their presence was associated with thicker collagen fibres and bundles. The Feulgen staining clearly shows the denser ring of chromatin on the open end of the 'bell'.

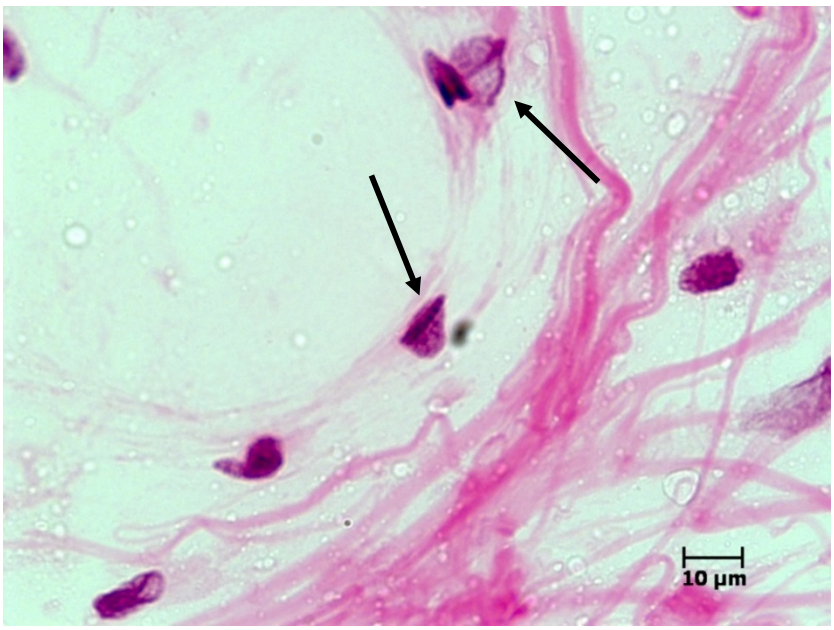

Figure 3.9 ***The first appearance of metakaryotic stem cells (arrows, bell shaped nuclei) in the middle section of the biopsy coincides with denser collagen in SSc skin only.*** *Such nuclei were not found in healthy skin biopsies*

Conversely, in all the healthy control biopsies, regardless of the layer, metakaryotic divisions were not seen and the collagen fibres were much less noticeable, and no individual fibres were observed, rather the collagen was arranged in a smooth network appearing as one whole sheet (Figure 3.10).

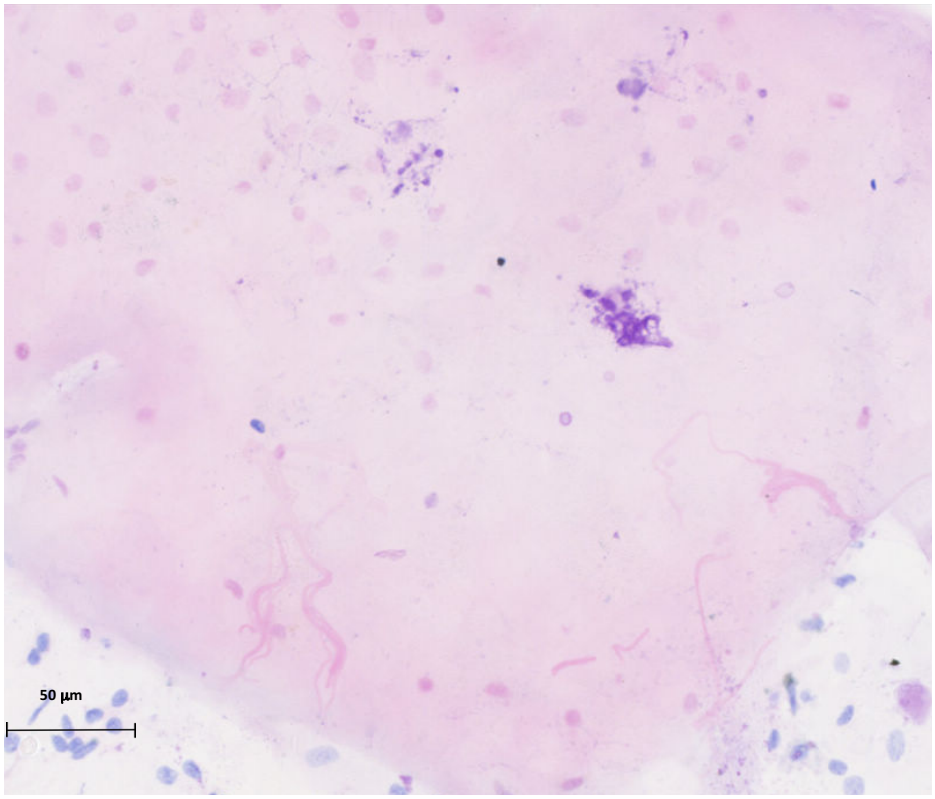

Figure 3.10 ***Fine, thinly spread collagen in healthy biopsy sections.*** *The collagen in healthy control biopsy sections is much more homogenous, less intensely stained and no thick fibres are seen.*

The third (bottom) section, indicating a depth of 2-3 mm features many bell-shaped nuclei (Figure 3.11).

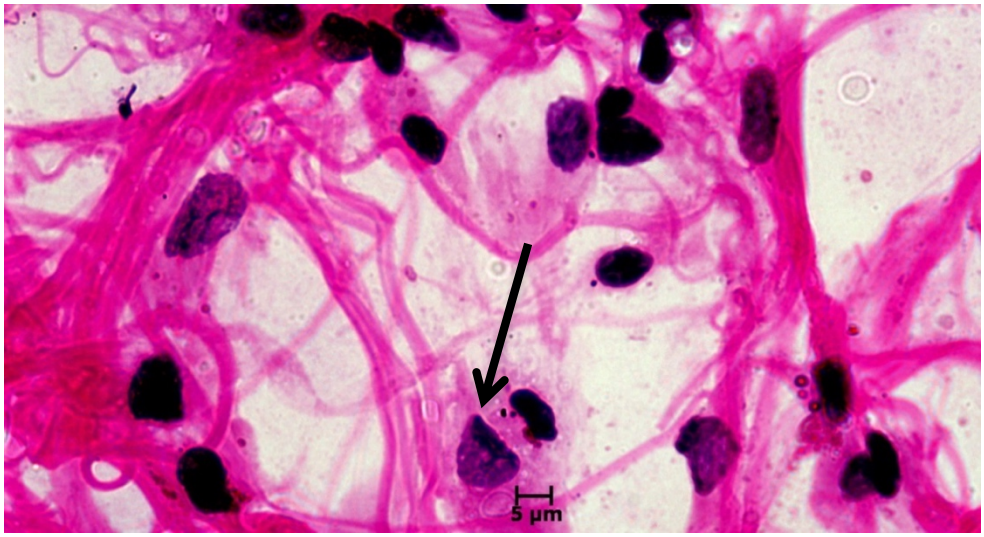

Figure 3.11 ***Metakaryotic stem cell with bell shaped nucleus (arrow) embedded in collagen fibres in the middle layer of an SSc skin section.***

Collagen in this section was not arranged in a mesh-like network like that seen in the uppermost 1 mm of the biopsy. Deep into the dermis, the collagen is arranged in fibres that in turn, are woven into thick bundles. It is these bundles that are reflective of the fibrosis in SSc and the thickening of the collagen layer in the skin. The metakaryotic nuclei in this section do not appear to be undergoing apoptosis.

Figure 3.12 seems to show an individual cell with a metakaryotic nucleus surrounded by a cloud of collagen in its cytoplasm. This may be the first indication that MSCs in SSc synthesis collagen and implicates them in SSc as a pathological factor in an *ex vivo* way.

Figure 3.12 ***Possible cytoplasmic production of collagen in a metakaryotic cell.*** *The dark red fibres can be identified as collagen fibres upon a pink clearly defined background, possibly identified as cell cytoplasm. The multiple nuclei also are surrounded by the pink "cytoplasmic" material and therefore, may indicate multiple cells in close proximity.*

MSCs, when physiologically quiescent, would not be expected to be actively dividing, however, in the SSc skin biopsy, amitotic cell divisions of these metakaryotic nuclei was observed in the third section where the new nucleus emerges from the 'mother' nucleus (Figure 3.13). Again, metakaryotic cell divisions were not seen in healthy control sections.

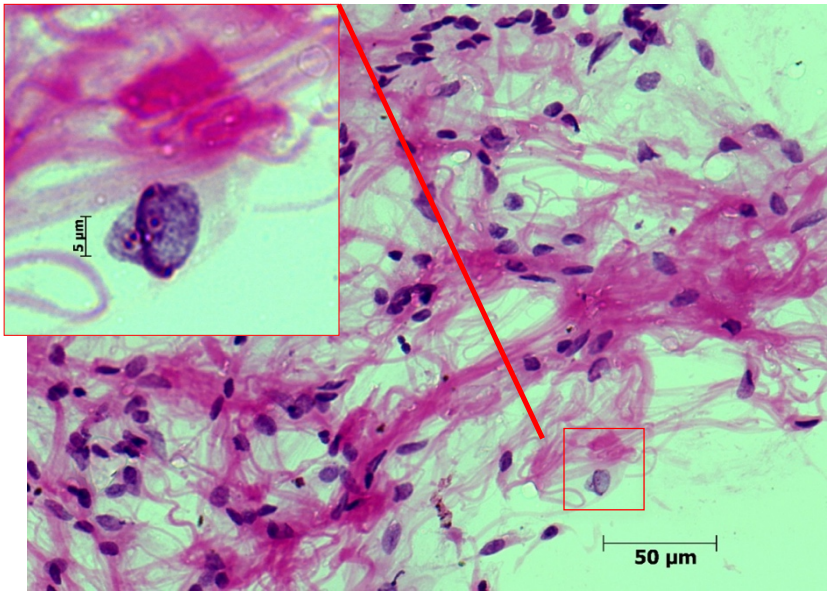

Figure 3.13 ***Metakaryotic stem cell dividing amitotically.*** *Magnification of symmetrical metakryotic cell division in the bottom section of an SSc skin biopsy. Collagen fibres are stained bright pink and cell nuclei stained purple by Schiff's staining.*

Metakaryotic cell divisions happen in different ways. Amitotic cell divisions are symmetrical and described in Figure 3.13. Another cell division is termed the syncytial stage and can be described as multiple bell-shaped nuclei arranged in a head to toe formation inside a tubule. Previously, this has been seen in developing foetal tissues, and now, in SSc skin biopsies.

In the deepest layer of the SSc skin biopsy, approximately 5 mm deep, thick rope-like structures were seen that do not resemble collagen (Figure 3.14). Rather this well-structured thick fibre is possibly elastin and is supported by the finding of a higher amount of soluble elastin derived peptide found in SSc patients compared with controls (Hong et al. 2012).

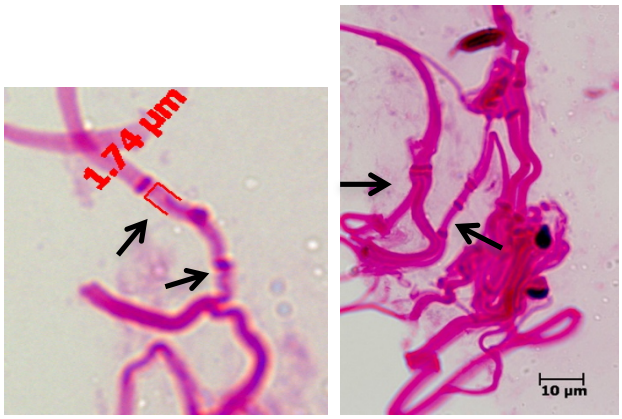

Figure 3.14 ***Thick elastin-like fibres found in SSc skin.*** *Dark pink stained fibrils (arrows) found in only SSc skin biopsies deep in the tissue can possibly be identified as elastin considering morphology and thickness of the fibres.*

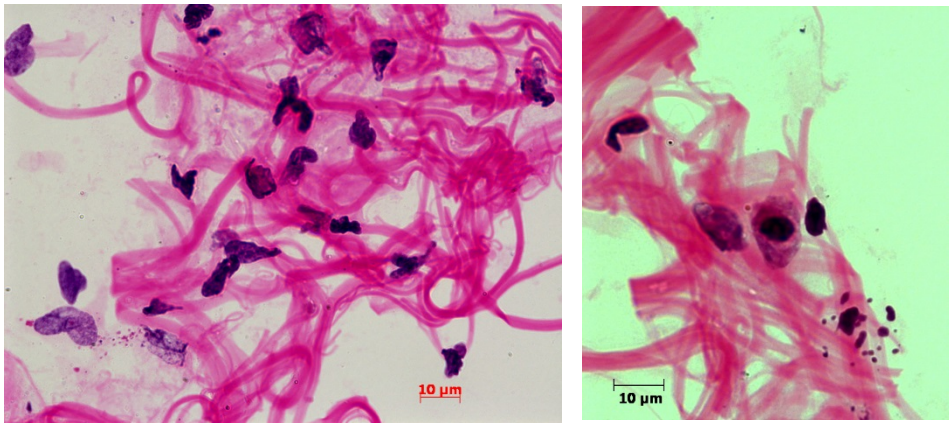

Figure 3.15 ***Apoptotic cells observed deep in SSc skin.*** *Deep in SSc skin biopsies, cell morphology was identified as abnormal and apoptotic, with many picnotic nuclei, possible indicating the damaged nature of SSc skin. Thick collagen fibres stained pink and cell nuclei stained purple by Schiff's staining.*

Approximately 3-4 mm deep in the biopsy, many abnormal looking dying cells were observed, identified by their heterochromatic and picnotic nuclei (Figure 3.15). Such apoptotic cells were not observed in any healthy control tissue section.

In addition to the increase in apoptotic cells, an increase in mitotically dividing cells was also observed, this could indicate the possible compensatory cell

divisions being induced in an attempt to reverse the apoptotic effects in the skin. More interestingly, metakaryotic stem cells with bell shaped nuclei were observed in a small blood vessel (Figure 3.16). This result, together with the potential role of MSCs in SSc vasculature and their relationship to pericytes, explained in Chapter 1, is further support that MSCs are not merely bystanders in SSc and their involvement in SSc is more than just as a therapeutic transplantation. Furthermore, it was noted that some of the vasculature in the biopsy contained abnormally looking, possible apoptotic cells with condensed, heterochromatic nuclei. Normal looking blood vessels were not observed to contain such cells (Figure 3.17). This possibly illustrates the abnormal angiogenesis and vasculogenesis, in SSc, particularly associated with Raynaud's Phenomenon leading to avascular regions in SSc skin.

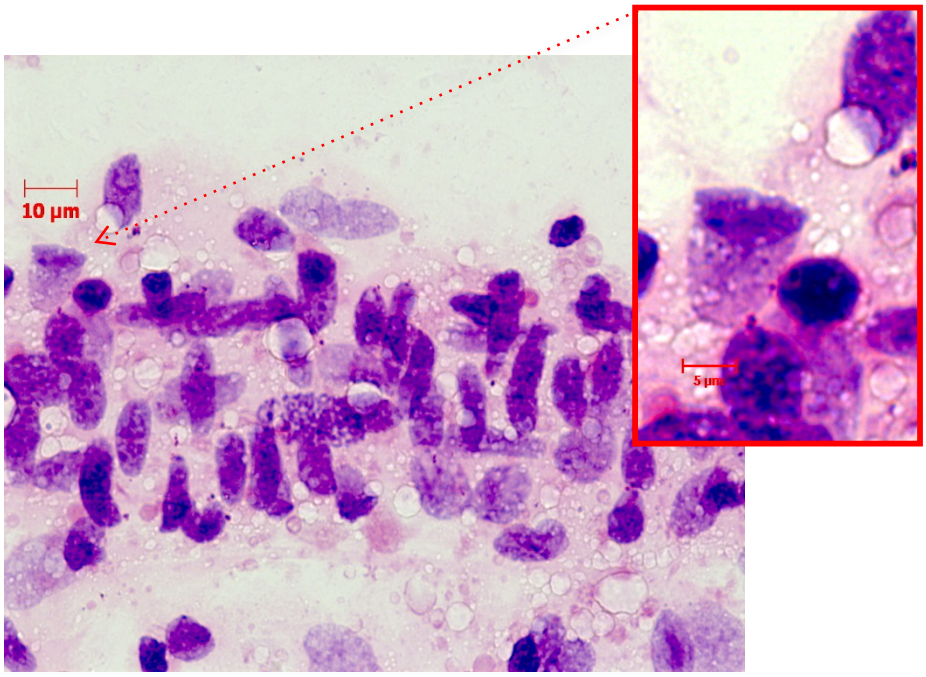

Figure 3.16 ***Bell shaped nucleus in small blood vessel.*** *Metakaryotic nuclei were found in the blood vessels of SSc skin biopsies with a bell shaped nuclear morphology.*

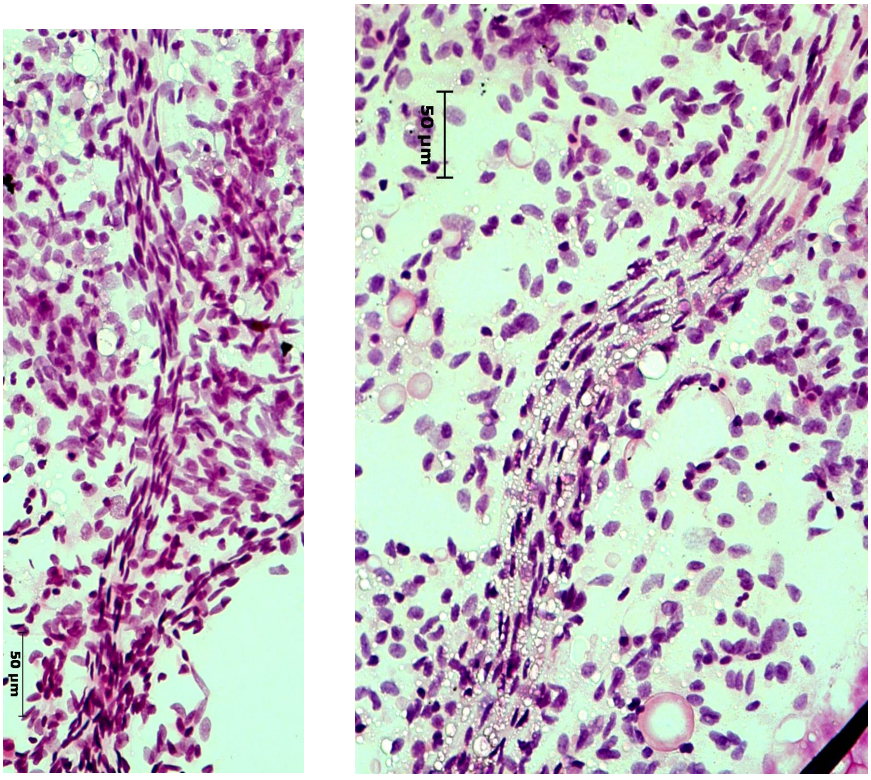

Figure 3.17 ***SSc skin blood vessels are abnormal.*** *Healthy (left) and abnormal SSc (right) blood vessels. Abnormal looking blood vessels contain unstained 'bubbles' not seen in healthy blood vessels. Such vessels were seen in approximately 3/5 SSc skin sections indicating it may be more than an artificact of the staining process.*

Quantification of the number of metakaryotic nuclei in each section was conducted by counting them in ten randomly chosen 20x magnification field views per section per biopsy (Figure 3.18). No bell-shaped nuclei were detected in any of the healthy control sections. In contrast, up to four nuclei were detected in any one 20x magnification field view of the middle and bottom section of SSc biopsies. Only one metakaryotic cell was detected in the top section of all the SSc biopsies. Middle and bottom SSc biopsy sections contained significantly more metakaryotic nuclei than the uppermost section ($p<0.0001$) and slightly more metakaryotic nuclei were detected in the deepest section than the middle section (bottom 1.45±0.16 (SEM), middle 1.225±0.06 (SEM)).

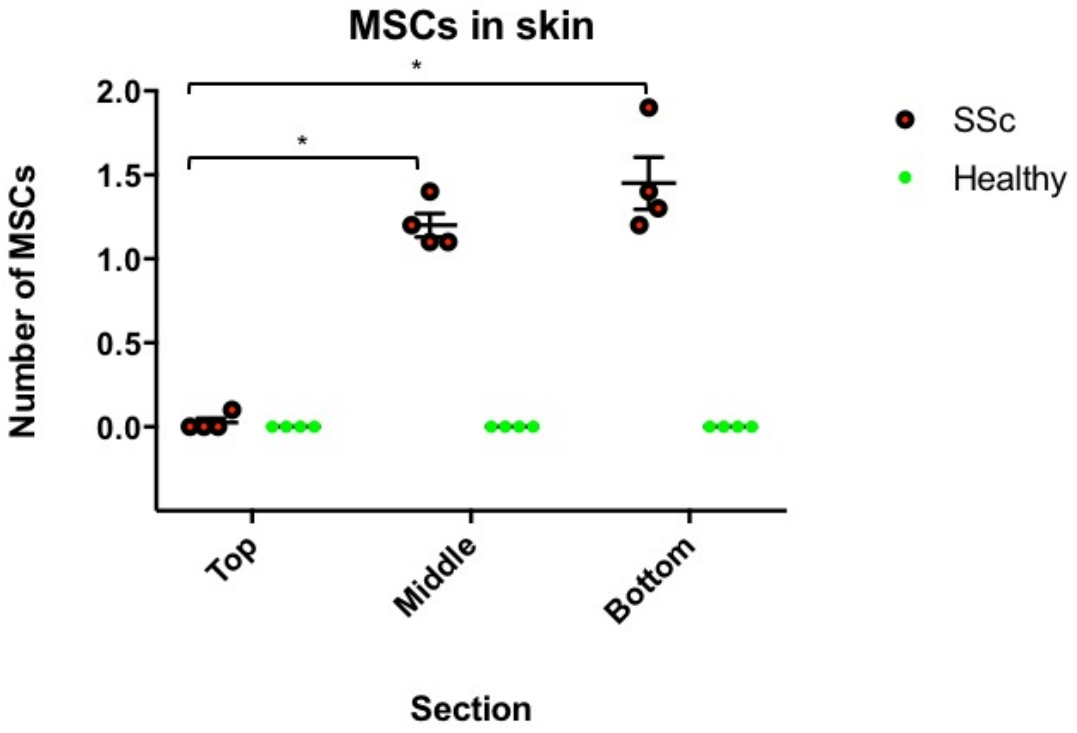

Figure 3.18 ***Metakaryotic stem cell nuclei can be detected in the lower two sections of SSc skin.*** *Biopsies sectioned laterally into top, middle and bottom thirds (Figure 3.1). Middle and bottom skin sections contain more metakaryotic nuclei than the top section ($p<0.0001$). $P<0.0001$ between healthy biopsies and SSc biopsies in all layers. No significant difference detected between the middle and bottom sections ($p=0.285$). n=10 high power fields per section per biopsy were examined. Magnification x20 per high power field. *$p<0.05$ using two-way ANOVA with Tukey's post hoc test.*

3.3 Conclusion

In this Chapter, Feulgen's Staining of SSc skin biopsies shows the definite presence of metakaryotic bell shaped nuclei assumed to be a marker of actively dividing MSCs' presence. Four SSc and four healthy control biopsies were analysed in this way. Feulgen's staining relies of the reaction of Schiff's reagent with DNA content, releasing aldehydes that are stained, and as such this method of staining is a semi-quantitative measure of DNA content with staining density proportional to amount of DNA (Chieco and Derenzini 1999). While physiologically, MSCs are not thought to be dividing until induced to partake in wound healing, immunomodulatory or differentiation function (Tyndall et al.2014), in SSc, these cells were shown to divide amitotically, and are present in this nuclear morphology, unseen in healthy tissue. This is the first piece in the puzzle of this study placing MSCs in SSc skin in a pathological manner.

Biopsies were cut laterally into thirds, and the tissue was expanded using a novel histologic method allowing visualisation of whole cells and the associated extracellular matrix. This was in order to elucidate any differences in their presence and location in different skin layers. The amount of such bell-shaped nuclei were found to increase deeper in the tissue. This is consistent with their possible origin in the subcutaneous layer of the skin (Bogatkevich 2015; Friedenstein et al. 1974). Furthermore, their increased presence is associated with much thicker collagen bundles, possibly indicating that they are either producing the collagen itself, or acting on collagen-secreting cells to induce collagen expression (Schurgers et al. 2010). Both of these explanations place MSCs as pathogenic cells exacerbating the abnormal collagen production and deposition that SSc is characterised by.

In addition to the collagen deposition and extracellular matrix thickening, the vasculature in SSc skin biopsies shows some abnormalities in the form of unstained bubbles, and heterochromatic apoptotic nuclei. This, together with the finding of a metakaryotic nucleus in a small blood vessel, neatly fits into the hypothesis of vascular deregulation and abnormal vasculogenesis being an important symptom of SSc and also the impression that MSCs could be

responsible for this deregulation. This is supported by literature stating that typically, MSC-derived pericytes are responsible for normal vasculature homeostasis and this is disrupted in SSc (Rajkumar et al. 1999). Finally, the finding of elastin-like structures deep in an SSc biopsy could be supportive of the increased elastin content found in SSc skin. Since MSCs could be found in SSc skin, the next step in painting the picture of their role in SSc is to reveal what the SSc microenvironment is made of in order to put the two together and model their interaction as is illustrated in Chapter 4.

Chapter 4 : Profiling systemic sclerosis tissue fluid to determine the factors present in the disease microenvironment

4.1 Introduction: examining the growth factor and cytokine microenvironment in SSc

The SSc microenvironment is multi-factorial, and this is perhaps an explanation for the heterogeneous nature of SSc and the large amount of theories and hypotheses surrounding its pathology. Many factors are thought to play a role, yet how significant that role is, together with how they interact with other known factors is still unknown to some extent. The SSc microenvironment consists of many cell types. These include immune cells such as Th2 cells, which exacerbate fibrosis, B-cells producing the autoantibodies, and macrophages and monocytes involved in inflammation and chemotaxis (Fuschiotti 2017; Raker et al. 2017). Arguably the most important cell type in SSc pathology is the fibroblast. These are thought to be activated by LAP bound TGFβ and induced to differentiate into myofibroblasts, the cells ultimately responsible for the collagen deposition and persistently unregulated fibrosis and scarring. The substrate these cells attach to is also of importance since the stiff nature of SSc extracellular matrix, ~50 kPa on the Young's Modulus Scale, can influence cellular function, namely fibroblast differentiation into myofibroblasts, but also MSC differentiation into myofibroblasts and osteoblasts (Shiwen et al., 2015;Olivares-Navarrete et al. 2017). The extra deposition of cross-linked collagen fibres makes up the scar tissue of SSc. Soluble factors are also important in SSc and make up a large portion of the microenvironment. Notably the most well-known and studied growth factor implicated in SSc is TGFβ, and together with other growth factors and other cells, it creates a pro-fibrotic and anti-inflammatory environment aiding the fibrosis. In addition to growth factors, cytokines are important in SSc, acting on the immune system to exacerbate inflammation, wound healing and migration of cells to the site of inflammation. Cytokines implicated in SSc are often Th2 cell derived and include IL6, IL2 and IL10 (O'Reilly et al. 2013).

One way of representing SSc microenvironment is by using blister fluid aspirated from suction blisters made in SSc and healthy individuals' normal forearm skin (Sondergaard et al. 1998). This gives an insight of the local factors around SSc lesions and in the skin rather than the global and systemic approach of blood and plasma samples. The components of blister fluid would be more dependent on inflammatory and fibrotic processes occurring locally, and is a method of examining the fibrotic lesions directly. Conversely, blood and plasma samples give rise to results representative of all physiological and pathological processes occurring in the body, which therefore makes it more difficult to infer site-specific SSc features.

The suction blister method relies on negative pressure pulling interstitial fluid into the blister (Sondergaard et al. 1998). This fluid is thought to contain the soluble factors involved in SSc. If the suction is left on for 24 hours rather than 3 hours, cellular components can be extracted too. For the purpose of this thesis, only 3-hour blister aspirates were used. A Luminex assay of the blister fluid as well as ELISAs and other assays for specific factors was used to profile the local growth factor and cytokine environment.

4.2 Specific analysis of IL31 as a candidate factor in the SSc microenvironment

After finding that MSCs were present in SSc skin, but before investigating their role in this microenvironment, the constituents of the microenvironment needed to be elucidated in the hope that factors could be identified as specific to MSC activation. As such, several representations of the SSc microenvironment were used in this thesis. Blister fluid from SSc and healthy individuals was used as a model of the SSc microenvironment as well as individual components of the fluid to ascertain their specific roles.

As mentioned in Chapter 1.4, IL31 is a candidate cytokine implicated in SSc since it promotes itching, a common symptom of SSc (Ip et al. 2007). IL31 has been shown to be a Th2 cell derived cytokine that promotes itching and

inflammation in mouse models. Since Th2 cell activation is implicated as an important driver of SSc, IL31 should be investigated in this disease. This cytokine was hypothesised to be a key component in the interstitial fluid of pruritic patients and, therefore, a potential microenvironment representation. Furthermore, key downstream target cells which are believed to be important effectors contributing to the pathology seen, may express the receptor for IL31, IL31RA, providing a mechanism through which multiple pathogenic steps can be activated. Therefore, IL31RA levels were analysed by qPCR, using RNA extracts from SSc and healthy control skin fibroblasts, lung fibroblasts, as well as MSCs themselves.

4.3 Possible role of products of anaerobic metabolism acting within the disease microenvironment

Lactate presence is an indication of anaerobic respiration, one of the consequences of vascular ischaemia. The loss of vasculogenesis in SSc causes Raynaud's Phenomenon due to avascular regions resulting in digital ulcers and ultimately amputation. Measuring lactate is relatively easily and can be conducted routinely using the Fingertip Lacticemy test. As such, if higher lactate concentrations are found in SSc patients, and since vascular damage is an early SSc pathological process, measuring concentrations could be a useful early diagnostic tool before progression to severe fibrosis. Furthermore, multiple lines of evidence indicate that raised levels of lactate might exert important biologic effects on target cells within the lesions including macrophages, fibroblasts as well as the MSCs. Previous published data suggests that lactate could be polarising macrophages as well as mobilising and activating MSCs (Errea et al. 2016). L-lactate is a stereoisomer of lactate (CH3CH(OH)COO-) and is found in the blood and as such was predicted to be the isomer present in blister fluid.

This Chapter hypothesises that multiplex and other assays of blister fluid from the lesional skin of SSc patients will identify key factors involved in MSC

activation within the disease environments. This hypothesis was studied through three aims:

1) Profiling the cytokines and growth factors present in SSc dermal tissue fluid using Multiplex
2) Specifically assaying the blister fluid levels of IL31 as a key candidate factor acting within the microenvironment
3) Determining the levels of lactate in SSc and healthy control blister fluid

4.4 Results: Profiling the cytokines and growth factors in SSc blister fluid

Initially multiplex (Luminex) assays were performed to investigate a wide range of 41 growth factors and cytokines. This assay revealed proteins with significantly elevated concentrations in SSc blister fluid compared to controls. PDGF-AA is one such protein, likely to be involved in fibroblast recruitment to fibrotic lesions (10.38pg/ml versus 6.94pg/ml p=0.03). Monocyte chemoattractant protein (MCP-1) is another chemoattractant, implicated in SSc mouse models. Its levels in SSc blister fluid negatively correlate with disease duration. By contrast in plasma, a different pattern was observed. Th2 cytokines, IL1a, IL2, IL10 and VEGF were all found to be increased more than 1.5 fold in SSc plasma compared to controls. Other cytokines significantly elevated include IL6 (38.78pg/ml versus 5.51pg/ml p=0.01) and IL15 (6.27pg/ml versus 4.38pg/ml p=0.03). Interestingly, IL17 was only found in SSc blister fluid from diffuse patients and not in healthy control or limited patient blister fluid (Clark et al. 2015a). The data is summarised in Table 4.1. Furthermore, an ELISA assay was used in a preliminary screen of 28 SSc and 15 healthy control blister fluid samples showing a significant difference between the two groups (p=0.0003) (Figure 4.1). When compared to the results of the Luminex assay of blister fluid, not only does IL31 show the most significant difference, but also was found to have the highest concentration of all the elevated factors (Table 4.1).

BIOLOGIC FUNCTION		MEAN HC CONCENTRATION	SEM HC	MEAN SSC CONCENTRATION	SEM SSC	T-TEST P-VALUE
INNATE IMMUNITY	IFNα2	5.7	1.17	6.83	0.63	0.41
	IL1a	97.09	29.67	84.51	19.15	0.73
	IL1B	0.2	0.2	0.7	0.41	0.28
	IL1Rα	115.1	244.71	1057.62	227.36	0.86
	IL6	17.85	6.86	77.22	20.5	0.01
	IL12p40	5.59	1.81	7.72	3.31	0.57
	IL12p70	1.73	0.36	1.86	0.24	0.77
	IL15	4.12	0.42	7.38	0.98	0.004
	IP10	921.8	156.24	1774.77	455.92	0.08
	TNFα	39.38	10.94	49.45	15.54	0.6
ADAPTIVE IMMUNITY	IFNγ	0.13	0.13	1.59	0.48	0.006
	IL2	0.37	0.37	1.03	0.54	0.31
	IL3	0.13	0.13	0	0	0.34
	IL4	2.3	1.06	4.04	2.01	0.44
	IL5	0.53	0.44	0.4	0.16	0.79
	IL7	4.48	0.57	6.16	0.69	0.07
	IL9	0.22	0.22	0.39	0.24	0.60
	IL10	29.99	5.99	32.96	4.15	0.69
	IL13	2.05	1.1	2.03	0.77	0.99
	IL17A	0	0.71	0.61	0.27	0.03
	IL31	**1.78**	**1.31**	**118.71**	**59**	**0.0003**
	sCD40L	380	85.66	361.95	49.9	0.86
	TNFβ	0	0	0.47	0.33	0.16
CHEMOKINES	Eotaxin	37.83	5.85	36.65	3.08	0.86
	Fractalkine	53.39	14.06	49.38	9.04	0.81
	GRO	143.61	42.1	173.4	24.12	0.55
	IL8	128.07	41.1	79.07	15.07	0.29
	MCP-1	1859.9	732.01	1316.88	323.52	0.51
	MCP-3	3.45	1	8.59	1.56	0.008
	MDC	1085.4	191.25	764.08	75.05	0.14
	MIP-1a	32.49	12.14	14.96	4.46	0.20
	MIP-1b	66.64	20.94	38.55	8.16	0.24
	RANTES	114.27	44.43	186.44	90.88	0.47
GROWTH FACTORS	EGF	0.96	2.08	3.41	1.22	0.56
	Flt-3L	65.7	12.09	60.42	10.65	0.74
	GCSF	10.53	3.33	9.85	2.29	0.87
	GMCSF	6.19	2.03	4.77	0.96	0.54
	PDGF-AA	7.54	0.97	16.37	4.28	0.05
	PDGF-BB	0.64	0.43	19.99	14.13	0.18

Table 4.1 ***IL31 is increased in SSc blister fluid.*** *All factors except IL31 were measured by Luminex assay and IL31 by ELISA. The data is presented as mean concentrations (pg/ml) with permutation analysis correcting for multiple comparisons. Signficant results where P<0.05 are highlighted in red. EGF, epidermal growth factor; FGF, fibroblast growth factor; Flt, FMS-like tyrosine kinase; GCSF, granulocyte colony-stimulating factor; GMCSF, granulocyte–macrophage colony-stimulating factor; GRO, growth regulated oncogene; IFN, interferon; IL, interleukin; IL-1RA, interleukin-1 receptor antagonist; IP-10, Interferon gamma induced protein 10; MCP, monocyte chemotactic protein; MIP, macrophage inflammatory protein; PDGF, latelet-derived growth factor; RANTES, regulated on activation normal T cell expressed and secreted; SSc, systemic sclerosis; TGF-α, transforming growth factor alpha; TNF-α, tumour necrosis factor alpha; VEGF, vascular endothelial cell growth factor.*

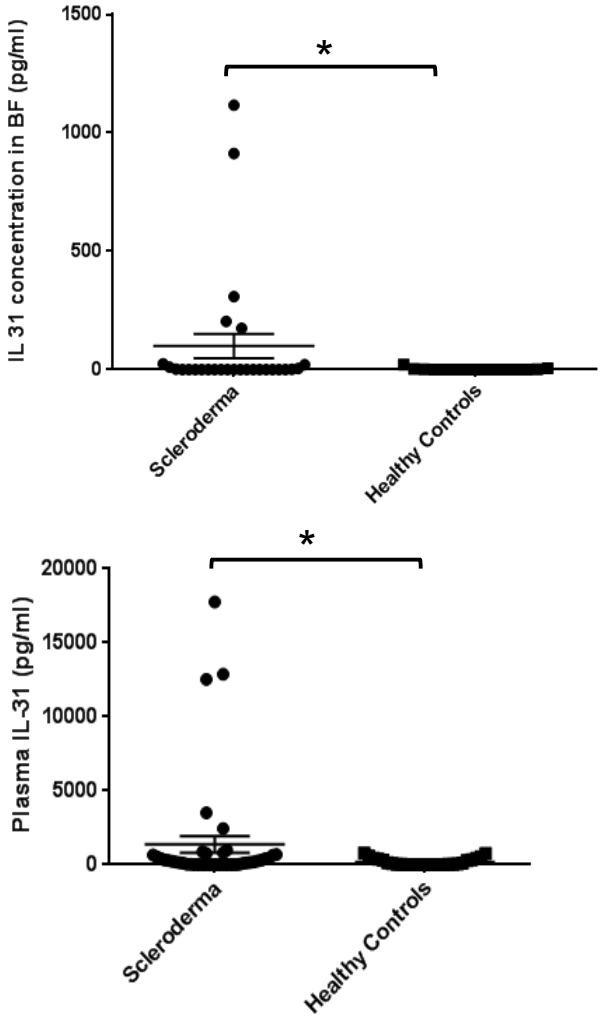

Figure 4.1 ***Preliminary ELISA assay of IL31.*** *Mean IL31 concentration in SSc blister fluid (top) is increased compared to healthy control samples (p=0.0003). Plasma IL31 levels showed the same trend with SSc concentrations significantly higher than healthy control samples (p=0.01). SSc n=27; Healthy Controls n=15. Blister fluid and plasma samples were from the same patients. P values were obtained using two tailed T-test.*

Because of these findings, IL31 was pursued further as a potentially important pathogenic factor driving cellular activation within the disease microenvironment. Conducting more extensive ELISA assays on 56 SSc and 22 healthy blister fluid samples found that while SSc samples trended towards increased IL31 concentrations, significance was no longer reached owing to a few healthy control samples with abnormally high levels (Figure 4.2). On the other hand, the significantly higher IL31 concentration found in SSc plasma remained in this larger sample size ($p<0.048$). Both data sets showed a skewed non-Gaussian distribution in a dimorphic pattern with IL31 levels being either virtually undetectable, or at levels higher than 500 pg/ml.

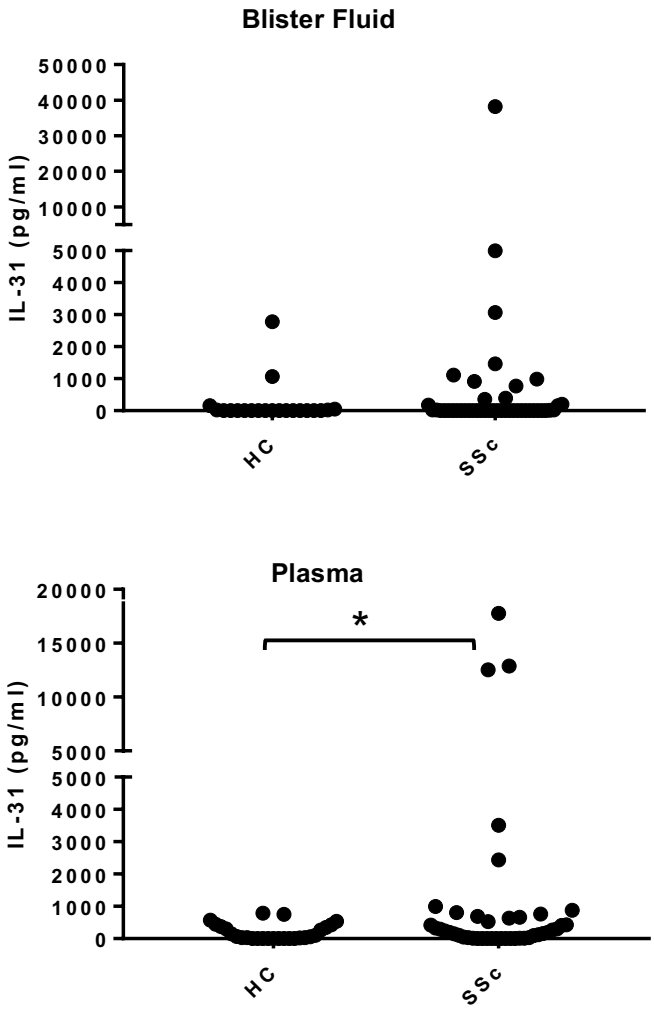

Figure 4.2 ***ELISA assay of IL31 in blister fluid and plasma.*** *Blister fluid from anterior forearm dermal lesions and corresponding plasma samples taken from SSc and healthy control (HC) individuals were assayed for IL31. Blister fluid (top) showed no significant difference between SSc and HC samples but lends itself to a trend of higher levels in SSc samples (HC 0-2777, median 0, IQR 0-23, SSc 0-38222, median 0, IQR 0-175 pg/ml, p= not significant). SSc n=43; HC n=21. Plasma IL-31 was elevated in SSc (HC 0-792, median 55, IQR 0-375, SSc 0-17764, median 193, IQR 13-658 pg/ml, p<0.048). SSc n=43; HC n= 27*

IL31 has been showed to be responsible for the pruritus in atopic dermatitis. Conducting a spearman's rank correlation showed a significant positive correlation between blister fluid IL31 and pruritus (R=0.72, p= 0.0038) as determined by itch scores (5-25 see appendix Figure S1) (Figure 4.3). On the other hand, no significant correlation was found between plasma IL31 levels and itch score (R= 0.0059, p= not significant).

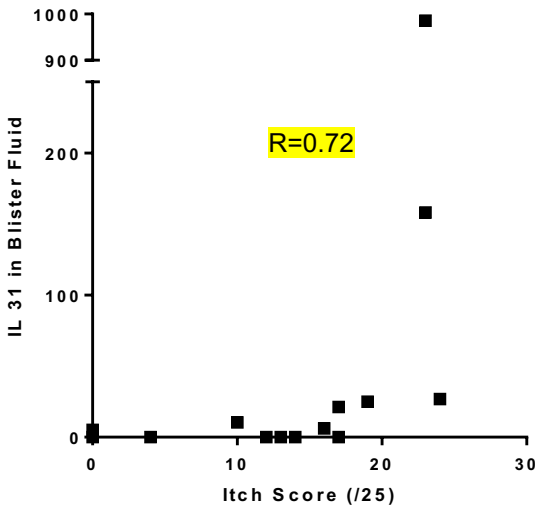

Figure 4.3 ***Increased IL31 correlates with itch score.*** *Blister fluid IL31 levels correlated with severity of itch as determined by an itch score questionnaire conducted by patients at the time of blister fluid aspiration. Spearmans rank correlation analysis determined R=0.72, p= 0.0038. (see appendix for questionnaire).*

Correlations between patients with high IL31 and disease classification, duration and autoantibody presentation were investigated and no significant correlations were found, although there was a trend towards a more diffuse SSc phenotype in these patients.

Also, a group of SSc patients were found to have blister fluid level of IL31 greater than 1000pg/ml. The characteristics of these patients are shown in Table 4.2. Interestingly these patients were from both limited and diffuse disease subset and from both early and late stage disease. However, all

patients demonstrated a high itch score (16-24) indicating severe pruritus in this group of patients.

Age	Gender	Disease	Antibody	Year of diagnosis	Itch Score	Hb (g/L)	Platelet ($x10^9$/L)	Skin Score
59	Female	Diffuse	Scl70, RF	2010	18	122	188	20
44	Female	Limited	ANA, ACA	2006	16	122	279	11
65	Male	Diffuse	RNA Pol III	2011	23	130	276	21
66	Female	Diffuse	RNA Pol III	2014	23	102	319	10
60	Male	Limited	ACA	2010	24	130	172	4

Table 4.2 ***Characteristics of patients with high IL31 levels correlating with high itch scores.*** *Gender, plasma antibody presence, disease duration, Hb (haemoglobin) levels, platelet levels, and skin score did not correlate with the high itch score. There was a slight tendency for those with high itch scores to have diffuse SSc rather than limited.*

4.5 Measuring Lactate in blister fluid

A lactate assay of 10 healthy and 8 SSc blister fluid samples, diluted 1:5 was conducted. The assay works on the basis of lactate oxidation by the enzyme lactate dehydrogenase, generating a colour change in the probe interacting with the enzyme product, measured at 450 nm. The optical density of the colour change is proportional to the lactate concentration. Average lactate concentration of SSc blister fluid was higher than that of healthy control blister fluid, although the difference between the SSc and healthy blister fluid was not significant (p=0.1001) (Figure 4.4). Also, the standard error of SSc data is larger than healthy controls, reflecting the heterogeneity of the disease whereby there is a large range in the severity of vascular ischemia and the resultant lactate produced. Although not statistically significant, the increased lactate in SSc blister fluid suggests the benefits of using lactate alone as an SSc microenvironment representation.

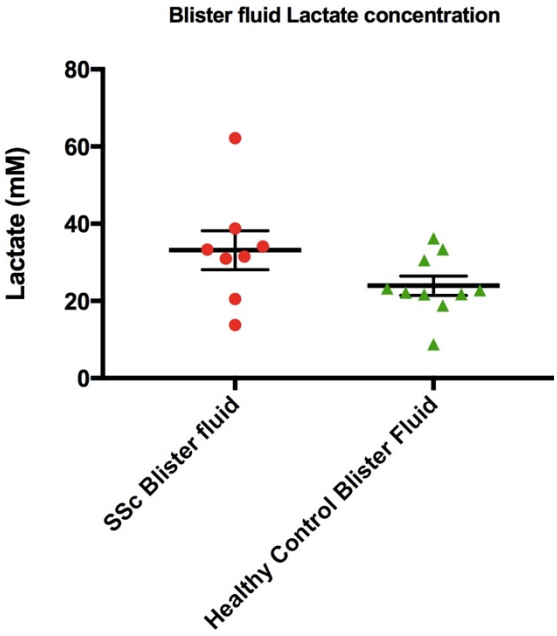

Figure 4.4 ***Lactate concentration of Blister Fluid.*** *SSc blister fluid contains more Lactate than healthy control blister fluid (SSc 33.14 ± 5.027 mM, n=8 vs Healthy Control 23.95 ± 2.484 mM, n=10; p=0.1001). Significance was calculated using a two tailed unpaired T-Test.*

4.6 Conclusion

There is no doubt that the soluble factors associated with SSc play a role in the disease and yet, to date, very little data exists on profiling the specific components of the SSc soluble dermal microenvironment. Rather, studies have focused on profiling of gene expression in involved tissue of cultured SSc cells (O'Reilly et al. 2013). Elucidating some of the components of blister fluid was essential when attempting to model different representations of the SSc microenvironment to be used in further experiments presented in the following Chapters. Adding to the preliminary assays, IL31 was found to be significantly increased in SSc blister fluid compared with healthy blister fluid to the extent that it has the highest concentration of all blister fluid components significantly increased in SSc blister fluid. When the sample size was made larger, significance was no longer reached but there was still a trend towards SSc blister fluid containing more IL31 than healthy control blister fluid samples. The

SSc patients with elevated IL31 in their blister fluid and plasma could not be categorised together based on disease duration, autoantibody production nor gender, but a subgroup with the highest levels appeared to experience higher levels of pruritus, consistent with the known prurigenic properties of this cytokine. Although not significant, results seemed to suggest there was more propensity for SSc patients with higher IL31 levels to have been diagnosed with dcSSc rather than be part of the limited subset.

These findings warrant IL31 being used as one of the ways SSc microenvironment is modelled in tissue culture in this thesis, with effects of IL31 treatment giving rise to conclusions regarding MSC response to cytokines. On the other hand, one limitation of this simple approach is that other soluble factors are being overlooked with this representation. Lactate is a metabolite present as a result of hypoxic conditions and ischemia, both of which are factors in SSc pathogenesis (Pucinelli et al. 2002). SSc blister fluid contained more lactate than healthy control blister fluid as measured by a lactate colorimetric assay. While the difference is not significant, the mean lactate concentration in SSc blister fluid was higher than in healthy control blister fluid and both the lowest and highest concentration in SSc blister fluid were higher than the respective values in healthy control blister fluid.

Together these findings bring about three different ways to model soluble phase SSc microenvironments; SSc blister fluid taking a holistic approach and the most accurate overall representation, culture media with additional IL31 alone signifying the effect of this Th2 cytokine and lastly, culture media plus lactate, representing potentially important metabolites. Not only were these microenvironments studied as models of SSc in this thesis, identifying key factors of SSc blister fluid meant that they could, in turn, be individually inhibited to robustly elucidate the extent of their role in blister fluid. This Chapter investigated the role of the soluble microenvironment of SSc. However, as explained in Chapter 1.4, many other factors come into play. The role of microenvironment stiffness is also likely to be important and is studied further in Chapter 5**.** All the models of SSc microenvironment were added to

MSCs using different *in vitro* techniques to investigate the different MSC responses to the microenvironment, as subsequently discussed in Chapter 5.

Chapter 5 : Evaluating the effects of the disease microenvironment on MSCs: phenotypic changes induced by SSc blister fluid and its key constituents

5.1 Introduction

From the literature review in Chapter 1, it stands to reason that MSCs are more than innocent bystanders of the SSc disease process, despite often being overlooked as pathological. From their potential role in vasculature deregulation, through their part in the osteogenic-adipogenic imbalance, to their differentiation into myofibroblast-like cells directly exacerbating the collagen deposition and fibrosis, it is possible that their heterogeneic phenotype is mirrored in the complex pathology of SSc. Although, there is evidence suggesting they have beneficial effects, they are anti-inflammatory and maintain vascular homeostasis. This Chapter attempts to evaluate the role of MSCs in the pathological cycle of SSc by modelling microenvironment-MSC interaction.

It has been shown that MSCs express α-SMA in response to pro-fibrotic microenvironments (Talele et al. 2015). MSCs expressing α-SMA were found to have reduced pluripotency potential further exacerbated by TGFβ treatment. Furthermore, they are less likely to differentiate into adipocytes and have a tendency to be more committed to myofibroblast lineages. α-SMA is hypothesised to have a strong effect on MSC fate. MSCs overexpressing α-SMA show significantly reduced clonogenicity and expression of stem cell specific RNA molecules, octamer-binding transcription factor 4 (OCT4) and SOX2, while the opposite is found upon knocking out α-SMA (Talele et al. 2015).

One of the roles played by MSCs both physiologically, and likely in SSc, is with regards to wound healing. Wound healing is a process in which skin contraction is induced by α-SMA-positive contractile bundles, pulling on the neighbouring healthy cells in an attempt to close the wound. This excessive pulling makes the surrounding skin tight and thicker and thereby results in

scars. This process is further affected by the cytokine, growth factor and cellular microenvironment. It is this microenvironment that is thought to be aberrant in SSc and as such is hypothesised to affect the physiological wound healing process and inflammation resolution.

MSC expression of α-SMA increases not only whole cell contractility and migration, but also the contractility of the cytoskeleton in the cytoplasm. α-SMA polymerisation to stress fibres in the cytoplasm was found to be the primary mechanism of α-SMA mediated contractility (Talele et al. 2015). YAP/TAZ are transcription factors predominantly found in the cytoplasm, which are shuttled to the nucleus where they regulate the transcription of genes highly associated with stem cell differentiation, fate and phenotype. This nuclear localisation was found to be mediated by α-SMA polymerisation to contractile fibres, as α-SMA knockdown reduced nuclear localisation of YAP. This experiment highlighted the possible mechanism by which MSCs differentiate, migrate, express α-SMA and altogether become myofibroblast–like cells in SSc.

In addition to α-SMA, MSCs have also been found to express other pro-fibrotic proteins such as collagen type I and CTGF (Battula et al. 2013;Cipriani et al. 2014). Since the work presented in the preceding Chapters has indicated that MSCs are active in SSc tissue, and has established some of the abnormalities of the SSc microenvironment, the two can be investigated together to discover the effect the disease microenvironment has on MSCs. The interaction between the microenvironment and MSCs was modelled in different ways in this Chapter including the addition of blister fluid and key constituent factors, protein and RNA expression, migration assays, contraction assays as well as differentiation assays to determine MSC responses.

5.2 Measuring SSc microenvironment: MSC interaction using pro-fibrotic protein expression

With α-SMA being not only one of the most important SSc markers of pathology, but also expressed by MSCs under pro-fibrotic conditions, this protein was used as a readout of MSC activation in response to SSc microenvironments. In this section, SSc blister fluid and key constituents of the blister fluid such as IL31, or lactate will be used as the SSc microenvironment representations, in comparison with serum controls and healthy control blister fluid. Quiescent MSCs should not typically express a high level of α-SMA without being activated. This protein is involved in SSc cell motility, contractility and migration and, therefore, was considered a useful readout for many SSc-associated cellular functions. In addition to α-SMA, collagen type I and CTGF were used as protein readouts for MSC pro-fibrotic activity. These proteins together are expressed by myofibroblasts, and as such, in these Western blots, their protein expression levels will be used as possible markers of MSC to myofibroblast differentiation. Furthermore, a characteristic of SSc myofibroblasts is their ability to contract collagen gels *in vitro*. MSCs were cultured in collagen gels and treated with SSc or healthy control blister fluid, or with the addition of IL31 or lactate. The role of signalling pathways was explored using small molecule inhibitors.

5.3 Hypothesis and aims

Given the above background, the overall hypothesis of this Chapter is that treatment of MSCs with SSc blister fluid, or with key constituents, will induce pro-fibrotic phenotypic changes. This hypothesis was tested using the following aims:

1) To model interaction of the disease microenvironment with MSCs using blister fluid and adipose-derived healthy MSCs
2) To investigate the effect of IL31, as a candidate key constituent of the SSc blister fluid, on MSCs
3) To determine whether lactate, as a metabolite raised in SSc blister fluid, will induce pro-fibrotic changes in MSC phenotype

5.4 Results

5.4.1 The effects of SSc blister fluid on MSCs

Initially the microenvironment-MSC cross talk was modelled using MSCs cultured in a monolayer and treated with SSc blister fluid, diluted in culture media. Figure 5.1 shows the first Western blot attempted on MSCs treated for 24 hours as follows; 0.2% serum as a negative control, 10% serum as a positive control, healthy control blister fluid (cBF), SSc blister fluid (SScBF), IL31 (50 ng/ml) and TGFβ (4 ng/ml). Blister fluid and IL31 treatments were in 0.2% serum conditions. TGFβ treated healthy dermal fibroblast protein lysates were used as an internal control sample for collagen type I and CTGF expression, because of the known strong induction of these factors in fibroblasts treated with this pro-fibrotic growth factor. GAPDH was used as the housekeeping protein loading control.

Relative density of the bands was calculated with Image J Software Densitometer and was plotted for each treatment and each protein readout (Figure 5.1B). Expression of all three pro-fibrotic proteins was most affected by SSc blister fluid treatment, with the strongest effect on α-SMA, although CTGF and collagen type I expression did not differ greatly between SSc and healthy control blister fluid treatments. Both blister fluid treatments did induce expression of all three proteins more than serum controls. Furthermore, IL31 treatment did not affect protein expression like the blister fluid treatments did and results from IL31 showed only a modest induction of α-SMA and CTGF, and no effect on collagen type I.

This Western blot protein assay was only a preliminary experiment which used protein samples from MSCs treated with only one SSc and one healthy control blister fluid sample and therefore, did not take into account the known large differences found in blister fluid constituent concentrations of growth factors and cytokines between individuals as established in previous Chapters. As such the assay was repeated using the same MSCs at the same passage number with blister fluid samples from different individuals. This was to try to assess to what extent variation in the patient sample can affect results and to

differentiate between protein expression as a result of blister fluid source and patient sample discrepancies.

The second attempt was conducted in exactly the same tissue culture method as the first experiment. However, as the Western blots in the first experiment appeared overloaded, leading to overexposed bands, the amount of protein loading per channel was reduced to 4 µg per well, resulting in technically improved blots. Readouts for this attempt were α-SMA and collagen type I (Figure 5.2). Again, IL31 was not found to affect expression of the pro-fibrotic factors more than serum controls and as such its elevation in SSc blister fluid cannot account for the full effects of blister fluid on pro-fibrotic protein expression. α-sma expression was induced by SSc blister fluid more than collagen type I, yet both were more highly expressed in response to SSc blister fluid than to healthy control blister fluid, further confirming a differential response of MSCs to the SSc microenvironment, and supporting the idea that there are biologically significant differences in the constitutions of the two blister fluids.

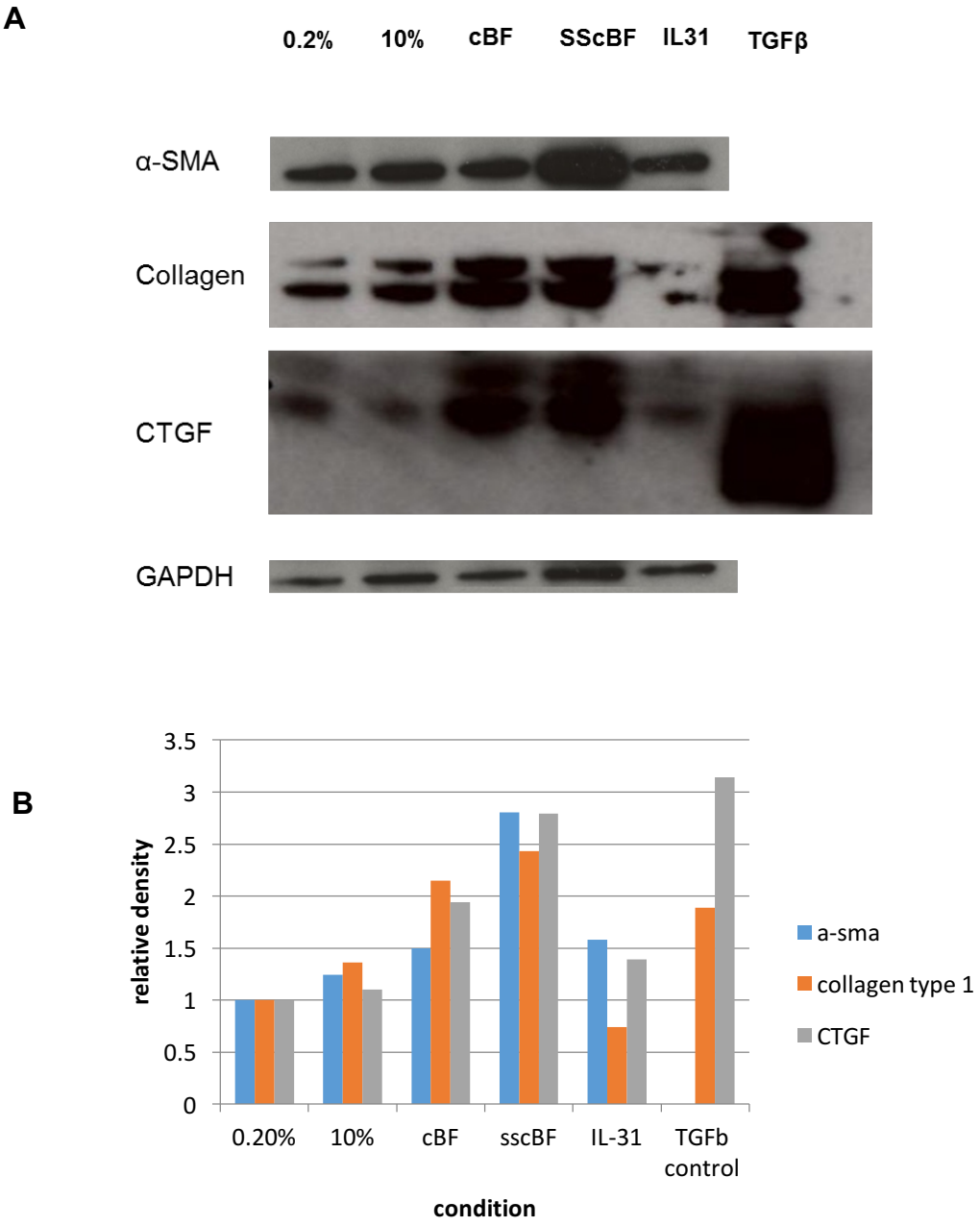

***Figure 5.1* α-SMA, collagen type I and CTGF protein expression of MSCs in response to blister fluid and IL31.** *A. Western blot of α-SMA, collagen type I and CTGF protein. B. Graphical representation using densitometry values. SSc blister fluid (SScBF), healthy control blister fluid (cBF) and IL31 (50 ng/ml) were used as microenvironment representations. Blister fluid was diluted 1:125 in 0.2% serum. TGFβ (4 ng/ml) treated dermal fibroblast lysate was used as a positive control for collagen type I and CTGF protein expression.*

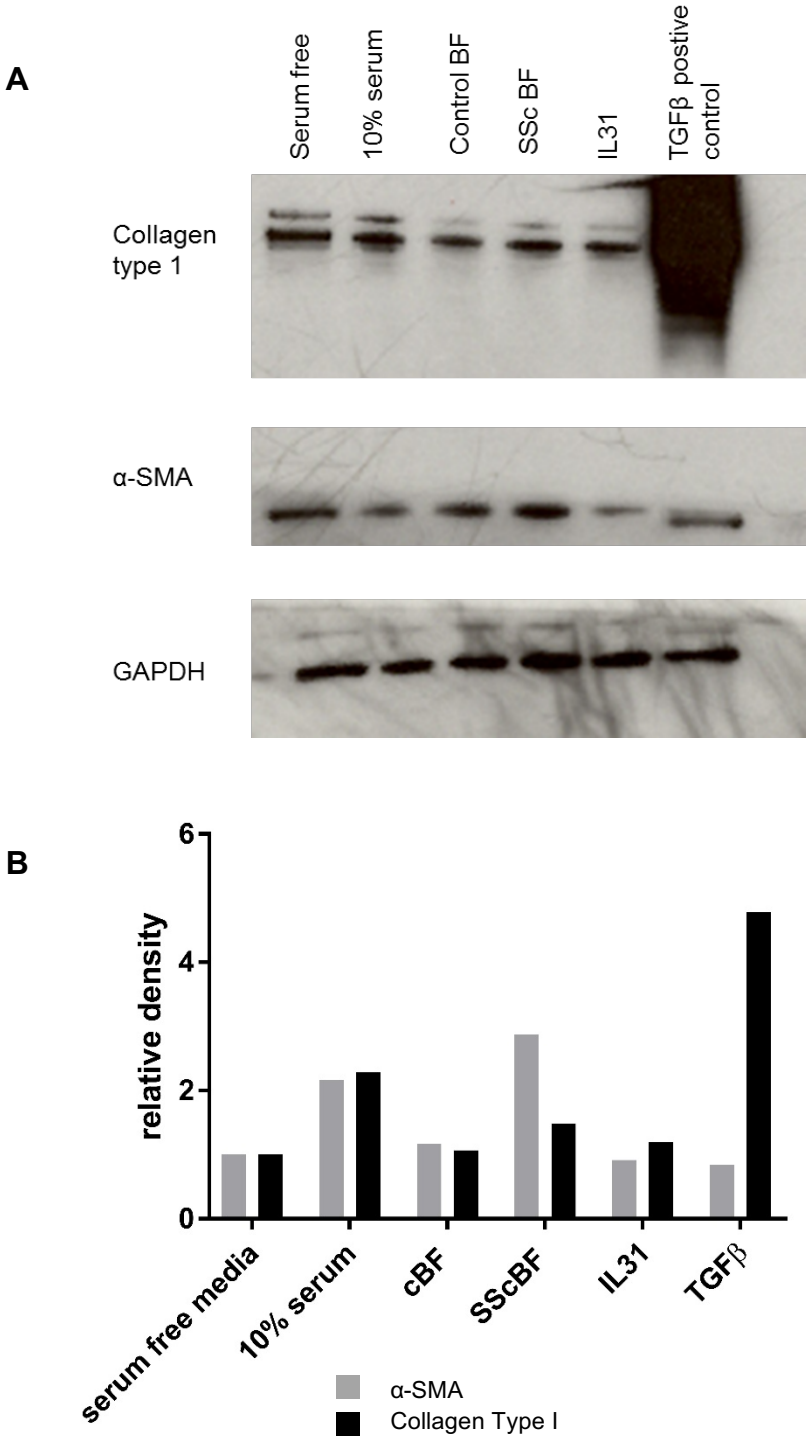

Figure 5.2 ***Western blot of MSC collagen type I and α-SMA expression in response to blister fluid and IL31.*** *A. Western blot of collagen type I and α-SMA. B. Densitometry results. Grey bars denote α-SMA and black bars, collagen type I. SSc (SScBF) and healthy control blister fluid (cBF) were diluted 1:125 in serum free DMEM. IL31 (50 ng/ml) was in serum free DMEM conditions. TGFβ (4 ng/ml) treated dermal fibroblast lysate was used as a positive protein expression control for α-SMA and collagen type I.*

Based on these preliminary experiments using Western blotting, α-SMA seemed to be the most prominent readout of the differential response of MSCs to SSc and healthy control blister fluid, since the two blister fluid derivations elicited the biggest difference in its expression.

As such α-SMA results from both assays were plotted on one graph (Figure 5.3) to compare the different effects of different blister fluid samples on its expression. While there was some variation between the two assays, the trend was expectedly the same and both assays resulted in the conclusion that SSc blister fluid contains some factor(s) responsible for the increase in α-SMA expression compared with healthy control blister fluid. Moreover, this difference cannot be fully accounted for by the increased IL31 in SSc blister fluid samples, since high dose IL31 treatment alone did not result in increased pro-fibrotic protein expression. A two-way ANOVA was conducted on the combined assays to determine statistical significance in α-SMA expression in response to SSc blister fluid, with Tukey's Post Hoc test to correct for multiple comparisons. Significance was achieved between the negative serum control, and SSc blister fluid treated MSCs ($p=0.0511$) however, no significant difference was detected between the two blister fluids. There is more α-SMA induced by SSc blister fluid than healthy control blister fluid and since IL31 treatment does not elicit any comparable responses, it stands to reason that other constituents of SSc blister fluid, not present or lesser in control blister fluid, may be responsible for this difference in protein expression, although these preliminary experiments were based on small sample numbers.

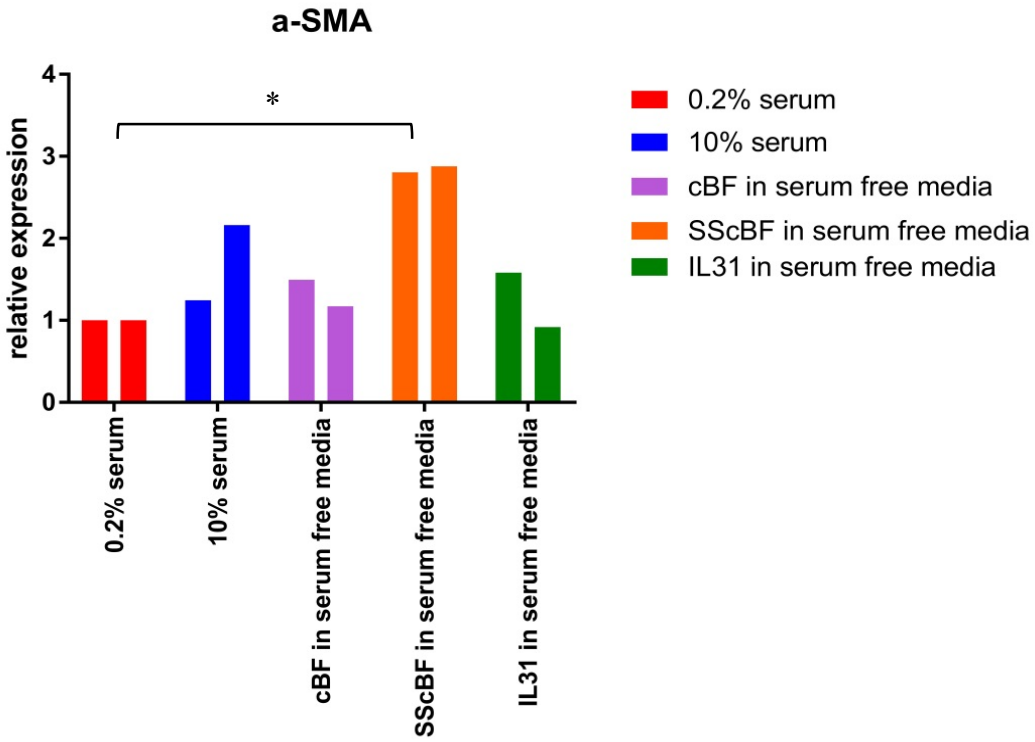

***Figure 5.3* α-SMA expression of MSCs in response to blister fluid and IL31.** *Data from both assays plotted together, each bar per treatment is for each assay (n=2). SSc blister fluid (SScBF) induced more α-SMA than 0.2% serum (p=0.0511). No significant difference was found between SScBF and control blister fluid (cBF) (p=0.0956). *p<0.05.*

The Western blot protein assays, most importantly illustrated that there is potentially a difference between SSc and healthy control blister fluid and their propensity to activate MSCs to express pro-fibrotic proteins, particularly α-SMA, associated with SSc. From this, it can be concluded that SSc blister fluid constituents not present in healthy control blister fluid, or at least at a much lower concentration, are responsible for the differential induction effects on MSCs. MSCs in low serum conditions express little α-SMA, collagen type I and CTGF in comparison and this expression is increased when MSCs are exposed to blister fluid. IL31, while increased in SSc blister fluid, cannot be solely responsible for the difference between SSc and healthy control blister fluid microenvironments and therefore, other factors are present in SSc blister fluid responsible for this higher level of expression. The increased expression of pro-fibrotic proteins by MSCs suggests possible activation, and looking at

the α-SMA induction in response to SSc blister fluid, MSC differentiation to a myofibroblast-like cell can be suggested. As such, α-SMA can be concluded to be a useful readout of MSC to myofibroblast differentiation and is used in subsequent experiments in this thesis. In order to provide a more quantitative and technically easier readout, qPCR for α-SMA is used in the subsequent experiments.

5.4.2 Dose response of blister fluid on α-SMA in MSCs

With blister fluid being a relatively precious material, high dilution factors were more attractive to use in the above preliminary modelling experiments. However, in order to ensure that the results obtained were reliable and were not a result of a low dilution factor, a dose response assay was conducted with MSCs treated with either one SSc or one healthy control blister fluid sample at dilution factors ranging from 1:5 to 1:125. After treatment for 16 hours, RNA extracted from the MSCs was assayed using qPCR for α-SMA expression, since this was considered the best expression readout for MSC response to blister fluid. Reassuringly, and confirming the protein assays, healthy control blister fluid induced considerably less α-SMA than SSc blister fluid at all doses (Figure 5.4).

Interestingly, it does not seem the simple case of higher blister fluid concentrations resulting in more α-SMA expression. This finding is possibly due to the large range of factors in blister fluid interacting in many different, both positive and negative ways. The biggest differential responses to the two blister fluid sources were at the higher dilution factors; 1:50 and 1:125 and the smallest difference at 1:20. As only 120-200 µl of blister fluid can be collected at one time, these high dilutions were used as a pragmatic approach in subsequent experiments.

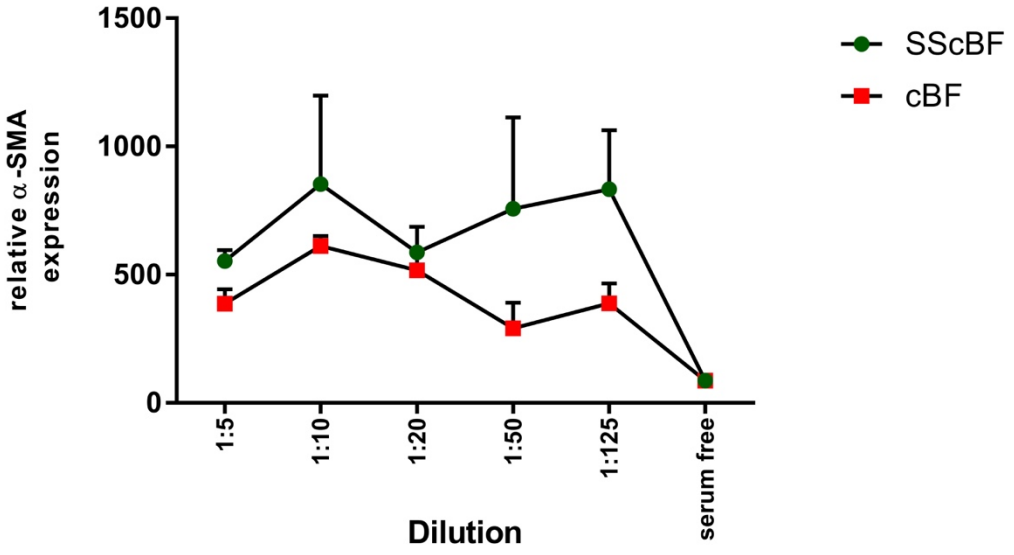

Figure 5.4 ***α-SMA dose response of blister fluid treated MSCs.*** *qPCR assay of α-SMA expression in response to different SSc (green) and healthy control (red) blister fluid dilution factors ranging from 1:5 to 1:125 in serum free DMEM. α-SMA expression was normalised to TBP housekeeping gene.*

5.5 The effect of IL31 on migration and wound healing

5.5.1 Aligned and woven collagen glass slide migration assays

The collagen fibres in SSc skin is proposed to be aligned in nature in comparison to the woven collagen configuration of healthy skin (Figure 2.4 and Figure 3.4). This difference was proposed to reflect the migratory capabilities of cells in SSc skin, possibly making migration to sites of inflammation, wound healing and fibrosis easier along aligned collagen.

Glass slides pre-coated with bovine collagen in woven or aligned configurations were used in these preliminary experiments with human dermal fibroblasts cultured on the slides, as a prelude to using MSCs. They allow close representation of cell migration through healthy or SSc tissue. Different treatments such as the SSc blister fluid or its constituents were added to the culture medium to assess the effect on migration and whether it can be assigned to the soluble factors of the microenvironment or the matrix on which the cells are attached. Theoretically, untreated cells should not migrate much

outside their original seeding area, and the addition of pro-migratory factors such as FBS, PDGF and potentially IL31 would induce migration.

Dermal fibroblast were seeded onto the slides in 3 μl foci, being allowed to adhere before flooding the slide with condition media. However, major technical problems were encountered with this assay, mainly the lack of adherence of the cells to the slides and their resultant death. Furthermore, when assaying the few foci that attached, very poor reproducibility was achieved regarding cell number per focus since the large amount of cell detachment resulted in unclear foci boundaries. Reducing the cell number from 12,000 to 4500 per focus, in an attempt to eliminate the possibility of contact inhibition was not successful, and the majority of cells detached from the collagen glass slides. Likewise, cells in complete serum free media seemed less likely to survive than those in 10% serum. In subsequent attempts, serum free media was replaced with 0.2% serum. Still, they were more likely to detach than those in 10% serum despite the fact that fibroblasts normally survive very well in 0.2% serum. As such, this methodology was not studied further and the scratch wound assay was proposed as the measure of cell migration in response to SSc microenvironments.

5.5.2 Dermal fibroblast scratch wound assay

Scratch wound assays mimic cell migration over a wound *in vitro,* modelling pathological fibroblast or fibroblast precursor recruitment into fibrotic lesions. This assay was used as a much more pragmatic measure of cell migration than the collagen glass slide migration assay. The scratch wound assay consists of creating a scratch through a well of confluent cells using a 200 μl pipette tip, and measuring how well the cells either side of the scratch migrate and refill the empty scratch.

The scratch wound assay was conducted initially with fibroblasts, which are readily available in our lab, to optimise the protocol and determine concentrations of conditions before using it as a model of SSc microenvironment and MSC interaction. Preliminary experiments were initially

conducted on healthy dermal fibroblasts treated with 0.2% serum, 10% serum, and IL31 at 10 ng/ml or 50 ng/ml, since blister fluid IL31 was elevated up into the ng/ml range in SSc patients, and previously published studies use IL31 at 50 ng/ml (Ip et al. 2007). With the course of this assay being over 30 hours, imaging at 0, 3, 6, 20 and 30 hours, 0.2% serum media was used as the negative control rather than complete serum free media to eliminate potential cell death seen in serum free conditions.

The area of the scratch imaged at each of these time points was measured using Image J software with a smaller area indicating migration across the wound. After 3 hours, the area of the scratch remained very similar to the initial area at the time the scratch was made (Figure 5.5) and this did not change significantly by 6 hours, although the smallest scratch at this time was under 50 ng/ml IL31 conditions. The most significant migration occurred by 20 hours and over the following 10 hours, changes were less obvious (0.2% serum; 1.51 mm^2, 50 ng/ml IL31; 0.85 mm^2; P=0.047). This suggests that the majority of migration occurs between 6 and 20 hours, presumably for the cells to respond to factors in the conditioned media, induce appropriate RNA and consequently protein expression, resulting in migration. IL31 treatments induced migration of dermal fibroblasts like, or more successfully than 10% serum. Considering serum contains many growth factors involved in migration such as PDGF and EGF, the fact that IL31 is just as potent, if not more, as serum at inducing migration, illustrates its possible role in cell migration in SSc wounds. The high IL31 levels in SSc microenvironments may induce neighbouring cells to migrate and, therefore, account for the high number of cell infiltrates in SSc wounds and sites of inflammation. 50 ng/ml was even more potent at inducing migration than 10 ng/ml and significantly more stimulatory than 0.2% serum (p=0.047).

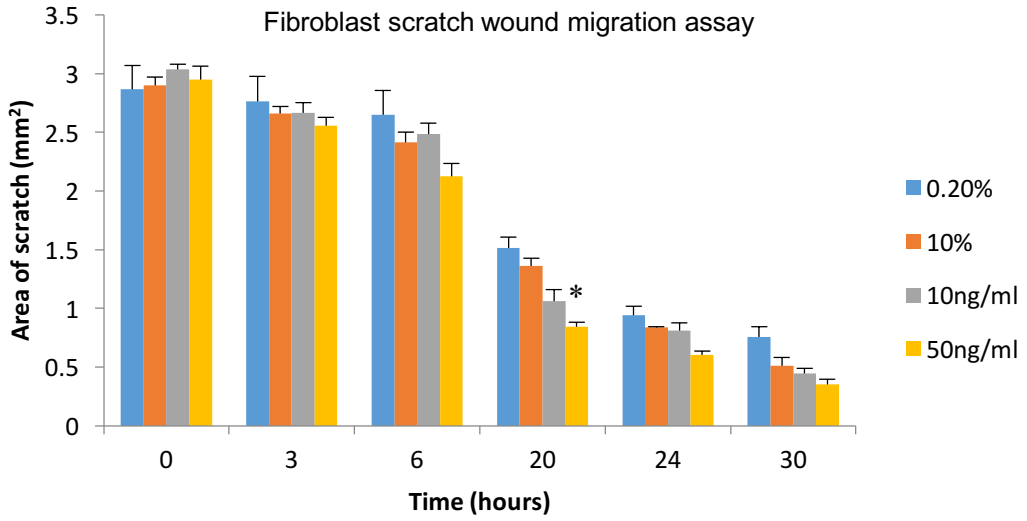

***Figure 5.5* Effect of IL31 on fibroblasts.** *Normal dermal fibroblasts were cultured in 24 well plates in DMEM with 0.2% serum (negative control), 10% serum (positive control), or with 0.2% serum plus additional IL31 (10 ng/ml or 50 ng/ml). Migration was assayed by taking images of the scratch at timepoints 0-30 hours. The area of the residual wound were compared by ANOVA. 50 ng/ml induces the most fibroblast migration across the scratch particularly at 20 hours. P=0.047 at 20 hours between 50 ng/ml IL31 and 0.2% serum. N=4 for each condition and average areas of the scratches were taken. Areas were measured in mm^2 by Image J software (see Appendix). P values were calculated using by a two-way ANOVA with Tukey's Post Hoc tests. *p<0.05.*

The dose response previously conducted by colleagues testing increasing IL31 concentrations on pro-fibrotic protein expression of fibroblasts also showed 50 ng/ml to be the optimum IL31 concentration (explained in Chapter 2.5.2). Because of this, together with findings from the scratch wound assay and published studies using 50 ng/ml IL31, this concentration was used for all *in vitro* IL31 experiments (Ip et al. 2007).

It is possible that SSc derived dermal fibroblasts may be more responsive to IL31 due to their previous exposure to higher levels of this cytokine, resulting in a differential activation state and elevated expression of IL31RA. As such, a scratch wound assay using one healthy control dermal fibroblast cell line (NF25) and two different SSc dermal fibroblast cell lines (SScF1 and SScF2) was conducted to test the difference between the cell lines in response to IL31.

In addition to IL31 treatments, the cells were also treated with two different IL31 related signalling pathway inhibitors; Wortmannin and U0126. Wortmannin is a non-specific covalent inhibitor of PI3 kinases and U0126 is an inhibitor of MEK1/2, which are MAP kinases. Two inhibitors were used in this assay offering two separate and different ways in which to downregulate the IL31 response. After making a scratch down the diameter of each well, cells were left under the treatment condition for 24 hours and images were captured at 0, 3, 6, 20 and 24-hour time points.

At 3 hours, IL31 treatment led to a significant difference between SSc cell lines and healthy control cell lines, with one SSc dermal fibroblast cell line (SScF1) migrating more than the healthy control (NF25) cell line (SScF1; 1.86 mm^2, NF25; 2.27 mm^2; p= 0.04) (Figure 5.6). One explanation for this rapidly evoked effect could be the differential expression of IL31RA or else a degree of pre-exposure to IL31 *in vivo,* may have made SSc fibroblasts more responsive to IL31.

By 6 hours post treatment, IL31 was shown to be clearly an effective cell migratory inducer, with migration being significantly induced by IL31 (0.2% serum; 2.07 mm^2; IL31 1.38 mm^2; p=0.001) and inhibited by both inhibitors (IL31; 1.38 mm^2 ; Wortmannin/U0126; 2.24/1.89 mm^2 ; p=0.001). Interestingly, at this point Wortmannin was a significantly more potent inhibitor of IL31 induced cell migration than U0126 across all cell lines (Wortmannin; 2.24 mm^2, U0126; 1.89 mm^2; p=0.033). On the other hand, no difference was found between responses of the different cell lines. Possibly, pre-exposure allows a more rapidly evoked, but not larger response, to IL31.

By 24 hours, IL31 significantly enhanced migration compared to the serum negative control (0.2% serum; 0.92 mm^2; IL31; 0.28 mm^2; $p<0.05$), an effect blocked by both of the inhibitors. Both inhibitors seemed to reverse migration to the same extent by this time although the area of the scratch under Wortmannin conditions was smaller than under U0126 (Wortmannin; 1.14 mm^2; U0126; 0.98 mm^2; p=0.61). Wortmannin and U0126 do not seem to be compensatory for each other in their inhibition of migration, and therefore, it

stands to reason that upon IL31 stimulation, the two pathways do not converge. However, they both completely reverse the migratory effect of IL31 to a similar extent. By 24 hours, the SScF2 cells had completely migrated across the scratch under 10% serum conditions rendering the area of the scratch as 0 (Figure 5.6)

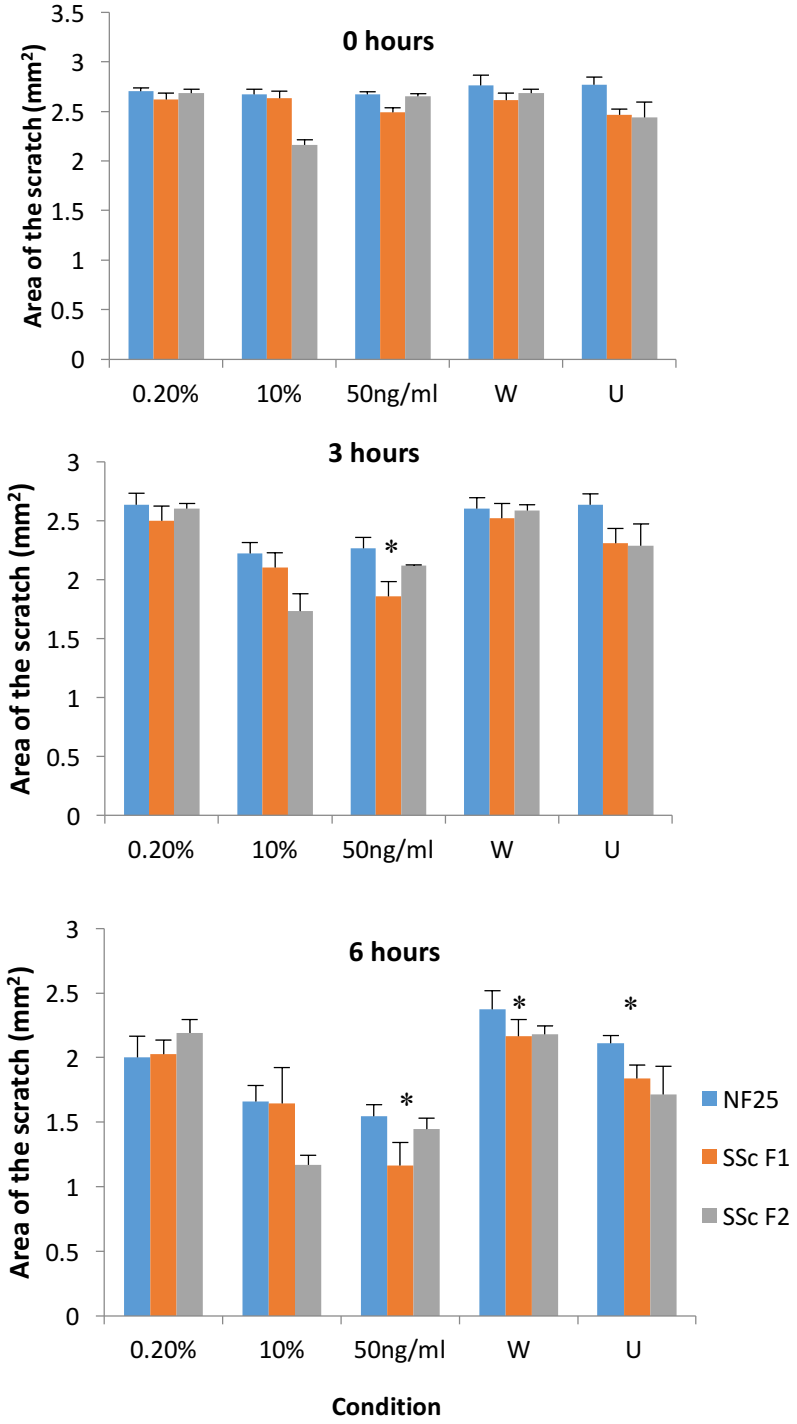
0 hours
3 hours
6 hours
Area of the scratch (mm²)
0.20%
10%
50ng/ml
W
U
Condition
NF25
SSc F1
SSc F2
*

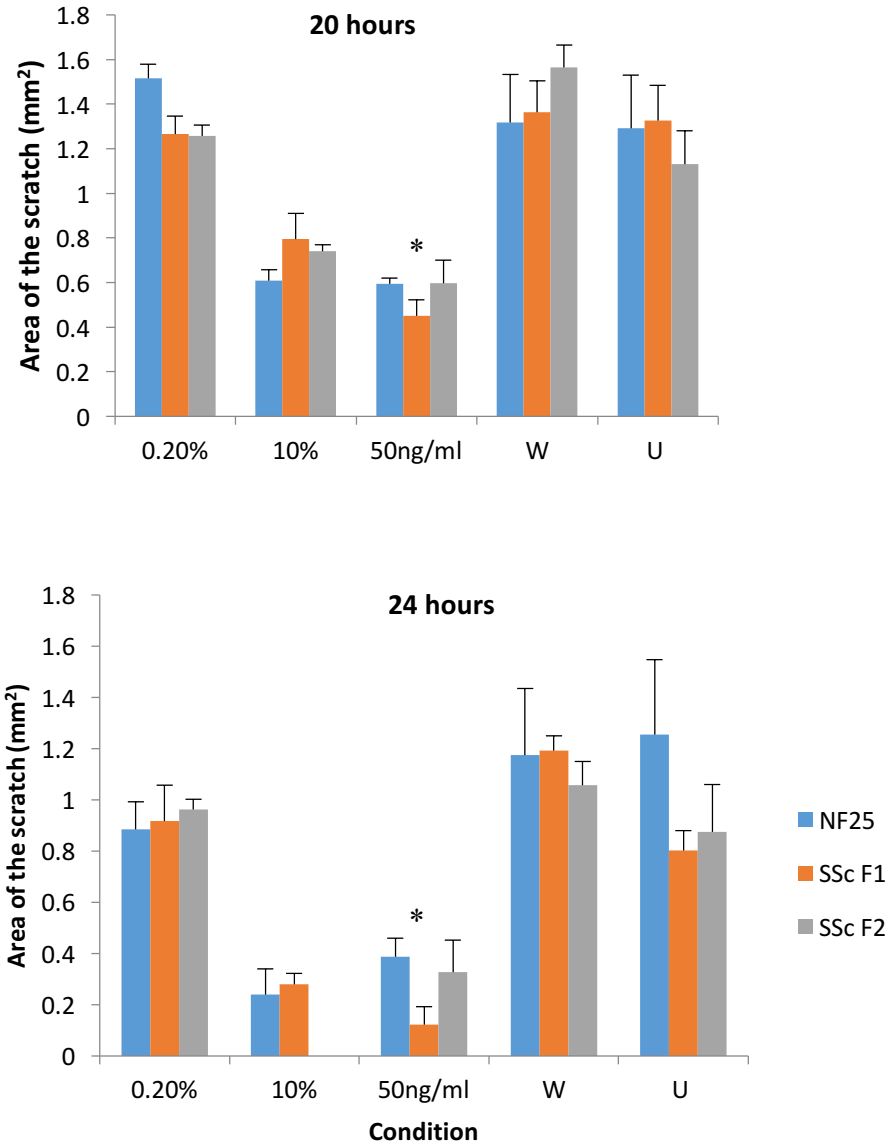

***Figure 5.6* IL31 induces migration of SSc and healthy control dermal fibroblasts.** *Area of the scratch measured at 0, 3 and 6 hours. Fibroblasts treated with 0.2% serum, 10% serum, IL31 at 50 ng/ml with or without either Wortmannin (W; 100 nM) or U0126 (U; 5 μM). P=0.04 at 3 hours comparing SSc and healthy fibroblast cell lines treated with IL31. SSc fibroblasts; SSc F1 and SSc F2. Healthy control fibroblasts; NF25. N=4. Area of the scratch measured at 20 and 24 hours. At both 20 and 24 hours, p<0.05 for IL31 vs 0.2% serum control and both inhibitors. No significant difference was found between the two inhibitors p=0.61. *p<0.05.*

The scratch wound assay was conducted initially with fibroblasts to optimise the protocol and determine concentrations of conditions before using it as a model of SSc microenvironment and MSC interaction.

5.5.3 MSC scratch wound assay

Having established the above protocol with fibroblasts, further experiments were performed with MSCs in order to model SSc environment interaction with MSCs undergoing migration. After 50 ng/ml was chosen as the optimum IL31 concentration, a scratch wound assay was conducted on adipose-derived, commercially obtained MSCs. This assay measured the effect of two SSc microenvironment representations, blister fluid, or else IL31, with or without Wortmannin inhibition, using MSC migration as the readout. *In situ*, MSCs are thought to be activated to migrate to sites of wounds to carry out their wound healing function and otherwise when unstimulated, do not move from their location. As such, SSc microenvironment was hypothesised to induce MSC migration and explain the activation of MSC wound healing responses in SSc pathology.

When considering MSCs as quiescent homeostatic cells, it was thought possible that conditioned media may not be enough to induce their migration. However, with MSCs being fibroblast-like in shape and substrate attachment, it was not implausible that they would respond to SSc microenvironment conditions in a similar way to dermal fibroblast.

MSCs were treated with serum controls, IL31 at 50 ng/ml with or without Wortmannin (100 nM), and SSc or healthy control blister fluid diluted 1:125. In each of three replicates, a different blister fluid sample was used to account for differences in blister fluid constitution between patients or healthy individuals. Since both signalling pathway inhibitors worked to a similar extent at inhibiting IL31 stimulated migration, only Wortmannin was used in this experiment as it seemed to be a slightly more potent inhibitor (Figure 5.6). The inhibitor was added to the cells 1 hour prior to IL31 to allow the cells to take

up the inhibitor, otherwise it was felt that the IL31 added may induce migration before the inhibitor has had time to carry out its inhibitory functions.

By 8 hours, no visible difference in the area of the scratch remaining was seen between the different treatment conditions, in that MSCs under all treatment conditions migrated similar amounts, resulting in similar scratch areas. Furthermore, although no statistical significance was reached, the blister fluid treated cells did seem to have migrated across the scratch slightly more than other treatments. Of note, by this time, fibroblasts had responded visibly to IL31 (Figure 5.6). By 24 hours, it was clear that SSc blister fluid had stimulated the most migration of MSCs compared to all other treatments and significantly more than the negative serum control ($p=0.016$) and notably, more than 10% serum conditions (Figure 5.7). As expected, 10% serum treatment was responsible for significantly more MSC migration than 0.2% serum ($p=0.03$). IL31 also induced MSC migration but less than SSc blister fluid. This finding, along with the Western blot of pro-fibrotic protein expression in Chapter 5.4 may indicate that elevated IL31 cannot fully account for the difference between SSc and healthy control blister fluid in their induction of MSCs. Like its effect on fibroblasts, IL31 induced migration was completely reversed by PI3K inhibition by Wortmannin ($p=0.027$) to an extent that the area of the scratch by 24 hours was larger than the scratches in wells treated with 0.2% serum alone. Microscope images are shown in Figure 5.8 with the remaining area of the scratch at each time point outlined in red.

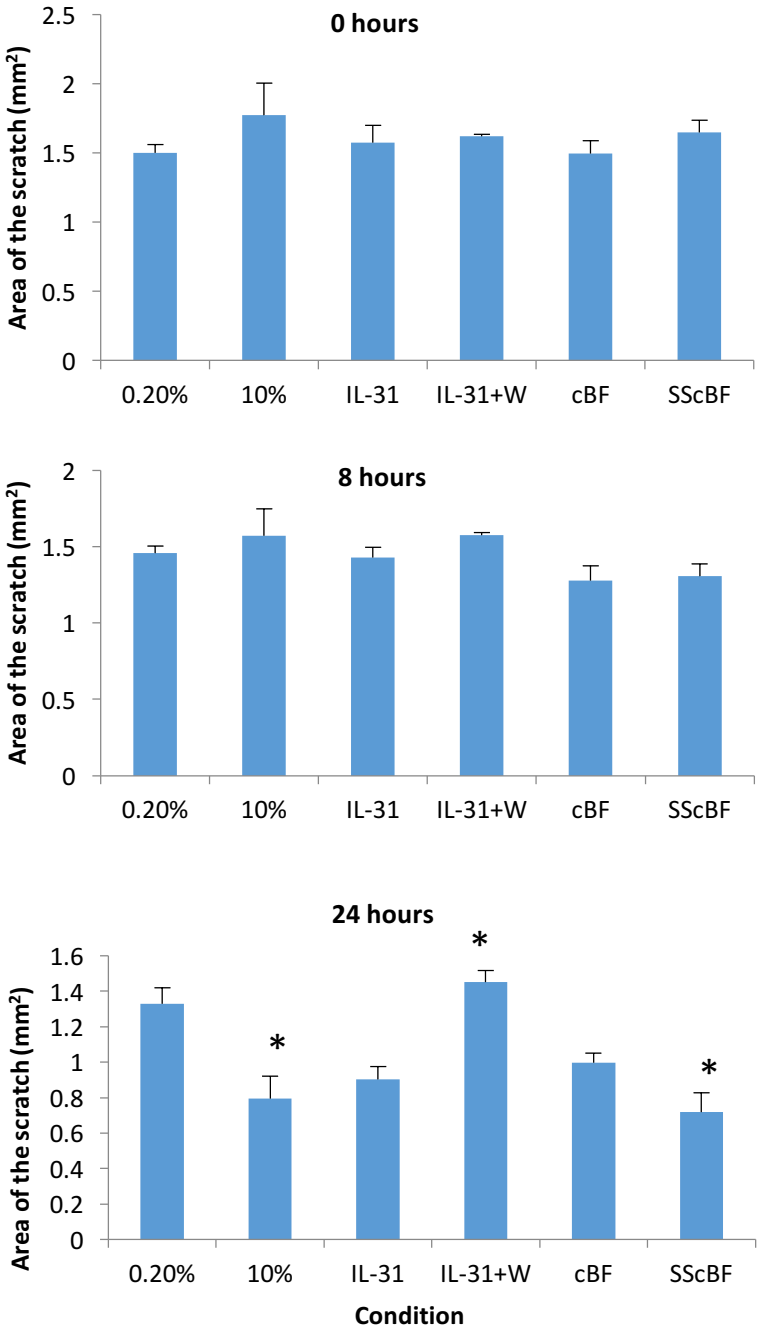

Figure 5.7 ***Blister fluid induces MSC migration.*** *MSCs seeded in a 24 well plate at a density of 50000 cells per well and treated with 0.2% serum, 10% serum, 50ng/ml IL31, 50ng/ml IL31 and 100nM Wortmannin (IL31 + W), SSc blister fluid (SScBF 1:125) and healthy control blister fluid (cBF 1:125). All treatment conditions were in 0.2% serum media. * p<0.05 using one-way ANOVA with Tukey's Post Hoc test. At 8 hours there was no significant difference between treatment conditions. By 24 hours p=0.03 0.2% vs 10% serum, p=0.016 0.2% vs sscbf. p= 0.027 IL31 vs IL31+W. N=3 for all conditions.*

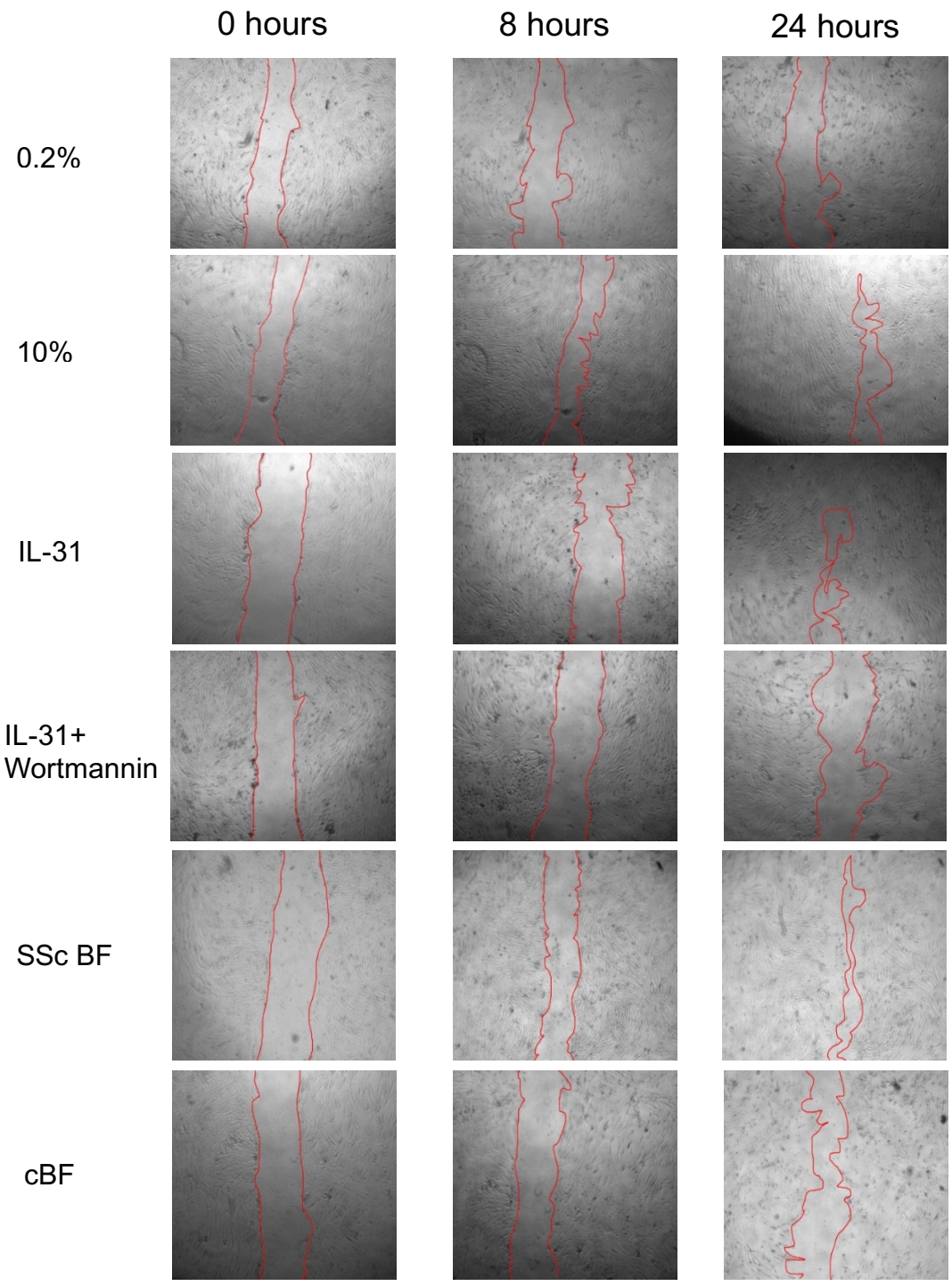

Figure 5.8 ***Microscope images of MSC migration in response to SSc microenvironments.*** *MSCs treated with 0.2% serum (negative control), 10% serum (positive control), IL31 (50 ng/ml), with or without wortmannin (100 nM) in 0.2% serum, SSc or control blister fluid in 0.2% serum (1:125). Wells were imaged at 0, 8 and 24 hours using at 2.5x magnification. ImageJ software was used to outline the scratch in red and measure the area of the scratch remaining at the time points. SScBF, SSc blister fluid. cBF, healthy control blister fluid.*

The scratch wound assays on both dermal fibroblasts and MSCs confirmed the use of IL31 as a model of SSc microenvironment however, when comparing the induction capability of IL31 on MSC migration to that of SSc blister fluid, it is clear that the latter contains a factor(s) that is not taken into account with the use of IL31 alone. The effect of IL31 alone on MSC migration was more akin to that of healthy control blister fluid rather than SSc blister fluid, not reflecting the elevated IL31 concentration in SSc blister fluid. On the other hand, inhibiting the PI3K pathway with Wortmannin did completely reverse the IL31 induced migration of MSCs and therefore the role of IL31 as a contributing factor in the SSc microenvironment on cellular migration cannot be overlooked or undermined.

For this reason, another assay was performed that models migration of cells in a 3D collagen matrix, which may be more suitable as a model mimicking SSc skin than monolayer on plastic substrates.

5.5.4 Collagen gel contraction and IL31

The scratch wound assays mimicked wound healing and migration on hard plastic 2D substrates, and while these assays showed encouraging results of the effect of SSc blister fluid on MSCs, it was considered not adequately representative of what occurs *in vivo*. In order to remove the effect the hard plastic has on the migration, a similar experiment was conducted using a collagen gel lattice as the extracellular matrix the cells migrate through. The collagen contraction assay is not only a model for individual cell migration, but also the bigger process of tissue contraction, more relative to wound healing. This model is more akin to *in situ* processes where the interaction between the soluble environment, modelled by the media in this case, and the cells in the skin, modelled by the collagen matrix, can be studied.

Furthermore, as α-SMA is a major protein involved in the contractile ability of cells, this assay ties in more closely with the Western blot of α-SMA expression. The collagen gel lattices are cell-populated and have been found

to contract relative to cell migration in a consistent manner, and are therefore, a good method to not only measure the extent of contraction, but also rate of gel contraction over time. Trapped inside the collagen gels, the cells attach to collagen fibres and affect their organisation. As the cells move through the gel, they pull on the collagen they are attached to, resulting in expelling media from the gel and contraction of the gel. Gel contraction is thought to be brought about by polymerisation of α-SMA positive contractile fibres that span the cells and affect the formation and maturation of focal adhesions which in turn influence cellular attachment to the substrate. Focal adhesion turnover involves the presentation and internalisation of integrins on the cell surface attaching to the extracellular matrix and this turnover controls the rate of cell migration.

Wound healing is thought to occur in two stages, the first is the formation of contractile forces induced by the effect of soluble factors in the environment on cellular contraction of the matrix. This results in closing of the wound by stretching the surrounding skin. The second and later stage involves maintenance of tension in the cytoskeleton and this process results in the formation of scar tissue (Grinnell 1994). The *in vitro* collagen lattice model can be used to represent both stages. Floating gels are detached from the plastic substrate of the culture plate and mimic the first and early stage of gel contraction. This model allows the study of interaction between the media and the cells in the gel. The second stage can be modelled by attached or tethered collagen gels. These gels are not detached from the plastic and as such the cells can form attachments between the gels, themselves and the plastic, resulting in tensile forces of the actin contractile bundles (Bell et al. 1979;Grinnell 1994).

Although the tethered gel lattice assay is a better representation of scar tissue, the free-floating method was used in order to investigate effects of specific microenvironment factors on cell migration rather than scar formation. For this assay, a solution of rat tail collagen and MSCs was prepared and allowed to polymerise in a 24 well plate. At this point the cell-populated collagen gels are attached to the walls of the plastic well and only began contraction after their

detachment. Adding 2 ml of treated media to each well detached the gel from the plastic, allowing them to float in the media. The gels were treated with serum free media, 10% serum, SSc blister fluid, healthy control blister fluid, and IL31 with or without Wortmannin. Again, a different blister fluid sample was used in each of the three replicates to account for differences in blister fluid constitutions as a result of differences in disease state. Contraction was measured as the weight of the gels after 48 hours of contraction rather than physical change in diameter of each gel. This was because when the gels were removed from the media in each well their shape flattened to some extent, and in particular with the gels treated with serum free media, they were not robust enough to hold their shape out of the media.

SSc blister fluid promoted contraction of MSC collagen gel matrices significantly more than serum free control media (Serum free; 0.11 g, SSc blister fluid; 0.07 g; p=0.002) (Figure 5.9). On the other hand, IL31 treatment alone was not sufficient to induce significant gel contraction. Inhibiting PI3K with Wortmannin however, prevented gel contraction below basal levels seen with serum free control media. This finding suggests that there is some basal MSC migration and contraction via the PI3K pathway. Although SSc blister fluid resulted in more gel contraction than did healthy control blister fluid, measured by lighter gel weight, this difference was not significant. Similar to the scratch wound assays, IL31 was as effective at inducing MSC migration as healthy control blister fluid supporting the conclusion that the elevated IL31 in SSc blister fluid cannot be solely responsible for their differing induction effects.

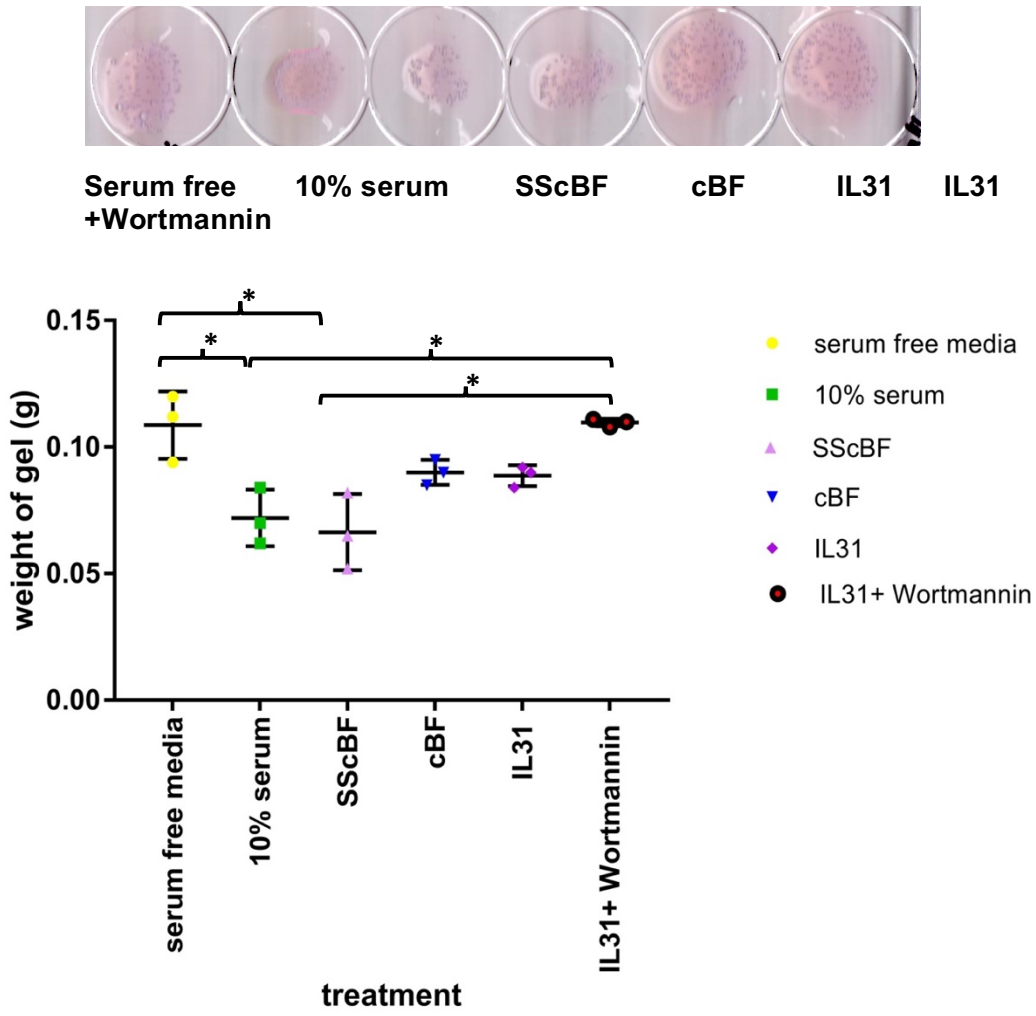

***Figure 5.9* Blister fluid induces MSC migration and contraction of collagen gels.** *MSC populated gels were treated with serum free media, 10% serum, SSc blister fluid (SScBF 1:125), control blister fluid (cBF 1:125) or IL31 (50 ng/ml) with or without Wortmannin (100 nM). Wortmannin was added 1 hour prior to IL31 and other treatments. SSc blister fluid treatment was responsible for the most gel contraction measured by loss of gel weight (g) (p=0.002). 10% serum was the next best treatment resulting in loss of gel weight (p=0.0062). IL31 and control blister fluid (cBF) did not result in significant gel weight loss. There was no difference between SSc and healthy control blister fluid (p=0.094). * p<0.05 determined by one-way ANOVA with Tukey's Post Hoc test for multiple comparisons. N=3 for each condition. See Appendix for statistical analysis.*

The studies conducted in Chapter 5.5 investigate the specific effect of IL31 on migration compared to complete blister fluid but not to what extent IL31 has a role on MSC function in the blister fluid itself. This is discussed in Chapter 5.6.

5.6 The effect of IL31 in blister fluid

5.6.1 Investigating the effect of signalling pathway inhibitors on blister fluid induced collagen gel contraction

Both SSc and healthy control blister fluid have a migratory-contractile effect on MSCs suspended in a collagen gel lattice, as does IL31. Potentially a number of signalling pathways could be involved in these effects, including canonical TGFβ signalling, PI3K or the ERK/MAPK. Use of specific pathway inhibitors might help define the nature of the active factors present in blister fluid responsible for the gel contraction seen.

As with the previous gel contraction assay, a suspension of MSCs and rat tail collagen was made and left to polymerise into gels in a 24 well plastic plate. After polymerisation, the gels were detached so that they were floating, by the addition of treated media. The positive control in this assay was TGFβ. Not only is this growth factor undoubtedly associated with and highly involved in SSc pathology, it is known to effectively induce cell populated collagen gel contraction. The media added to the gels were treated with TGFβ, SSc or healthy control blister fluid, with or without the following inhibitors, 1D11, a TGFβ neutralising antibody, Wortmannin, a PI3K inhibitor or U0126, a MAPK inhibitor. Inhibitors were added to the gels one hour before stimulating ligands. The inhibitors were used to assess the importance of the three different pathways on MSC migration and this way, possibly narrow down the nature of the factor in SSc blister fluid responsible for its difference from healthy control blister fluid. Blister fluid was diluted 1:50.

After 48 hours' incubation, the gels were removed from their respective wells and weighed with loss of gel weight being a measure of gel contraction. As shown in Figure 5.10, no single inhibitor fully blocked blister fluid induced gel

contraction enough to mimic serum free conditions. This may suggest that there is no one individual pathway involved in MSC migration in response to SSc microenvironment conditions. While all three inhibitors, 1D11, Wortmannin and U0126, caused some slight but noticeable inhibition of gel contraction, none significantly inhibited the loss of gel weight caused by blister fluid. In addition, no one inhibitor seemed to be more potent than another. Serum free media, as the negative control in this assay, resulted in the least contraction, as expected. This alone shows that any reduction in gel weight was a direct result of MSC interaction with factors in the media. When SSc blister fluid was inhibited with Wortmannin, there was no significant inhibitory effect, however the complete opposite was found when inhibiting IL31 with Wortmannin. A possible explanation for this is the relatively low IL31 concentration in blister fluid in comparison to 50 ng/ml IL31 treatment. Also, this confirms that the cause of contraction in blister fluid treated wells is not IL31 alone and is indeed another blister fluid derived factor. A possibility is that the collective power of the growth factors and cytokines present in the fluid work together to result in the migration, and it is the specific combination rather than the action of individual constituents, that causes SSc blister fluid effects. Although no significant difference was shown, there was a trend towards more gel contraction by SSc than healthy control blister fluid.

Such results seem to hint at the possibility of multiple pathways working together synergistically such that inhibiting one makes no significant difference, as the other pathways resulting in the same outcome will compensate. Another possibility is that there is a completely different pathway stimulated that has not been taken into account in this assay. To elucidate this, an Ingenuity Pathway Analysis (IPA) was carried out (Chapter 5.7)

The contraction ability of MSCs in the collagen gels partly depends on polymerisation of α-SMA positive contractile fibres and therefore, it would be plausible that the results of this collagen gel contraction assay be reflected in α-SMA RNA expression determined by qPCR.

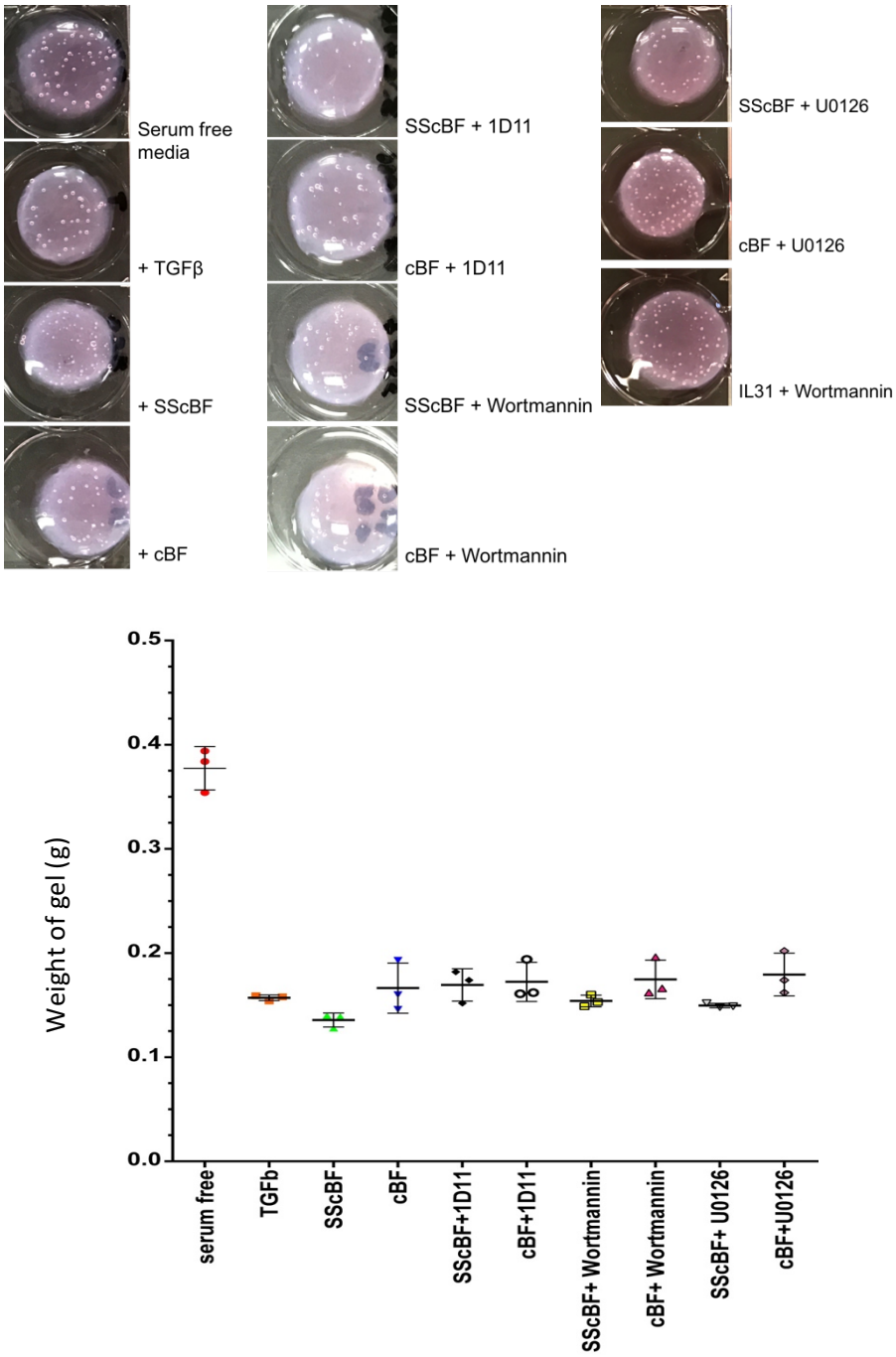

Figure 5.10 ***IL31 is not responsible for SSc blister fluid induced MSC migration in collagen gels.*** *MSC populated collagen gels were treated with serum free media, TGFβ (4 ng/ml), SSc blister fluid (SScBF 1:50) or healthy control blister fluid (cBF 1:50) with or without TGFβ neutralising antibody 1D11 (10 ng/ml), PI3K inhibitor Wortmannin (100 nM) or MAPK inhibitor U0126 (5 μM). All treatments were in serum free media conditions. A different blister fluid sample was used in each replicate. One-way ANOVA with Tukey's Post Hoc test found p<0.001 for serum free media vs all condition. N=3 for all conditions. See Appendix for raw data.*

5.6.2 Investigating α-SMA expression of MSCs treated with blister fluid and inhibitors

Regarding cell migration through a collagen matrix, no specific pathway was found to be responsible for the migration and gel contraction induced by SSc blister fluid. It was hypothesised that the pathways compensate of each other. In an attempt to find a pathway activated by SSc blister fluid more than healthy control blister fluid, cultured MSCs in monolayer were treated with serum free media, TGFβ, SSc and healthy control blister fluid (1:50) with or without 1D11, Wortmannin, U0126. Additionally, MSCs were also treated with blister fluid, plus all three inhibitors together. α-SMA RNA expression was used as the measure of MSC activation and the treatment with all three inhibitors simultaneously was a measure of the theorised compensatory effects of the pathways and their redundancy to each other.

RNA was extracted after a 16 hour treatment and α-SMA expression of the MSCs was measured against expression of the housekeeping gene TBP. α-SMA expression would highlight any contractile potential induced by the TGFβ, PI3K or MAPK pathways but does not account for migration stimulated irrespective of α-SMA. This assay illustrates the extent of MSC to myofibroblast differentiation promoted by SSc blister fluid via the individual pathways.

Illustrated in Figure 5.11, of all the treatments, the TGFβ positive control induced the most (2 fold increase) α-SMA expression (TGFβ; 32.7; serum free control; 16.84; $p<0.004$), closely followed by SSc blister fluid (serum free control; 16.84; SSc blister fluid; 29.4; 1.7 fold increase; $p<0.0004$) when compared with serum free media. All three inhibitors had a similar and marked effect on the α-SMA expressed by MSCs in response to SSc blister fluid, and no one inhibitor worked better than another ($p<0.0001$ for all SSc vs inhibitor comparisons). Furthermore, the addition of all three inhibitors simultaneously did not affect α-SMA expression any more than the use of each individually ($p>0.999$ for all individual vs simultaneous inhibitors). A significant difference between α-SMA expression caused by SSc blister fluid compared with healthy

control blister fluid was achieved (SSc blister fluid; 29.4, healthy control blister fluid; 22.4, p=0.048). Based on these experiments it was concluded that in monolayer culture, induction of α-SMA by SSc blister fluid is dependent on all 3 pathways studied, so that inhibiting any one pathway fully antagonises the α-SMA induction seen. This finding is contradictaory to the effects seen in 3D gels shown in Figure 5.10. Possible explanations include failure of the inhibitors to penetrate into the MSC collagen gels, or else different mechanisms induced in the 3D model compared to monolayer.

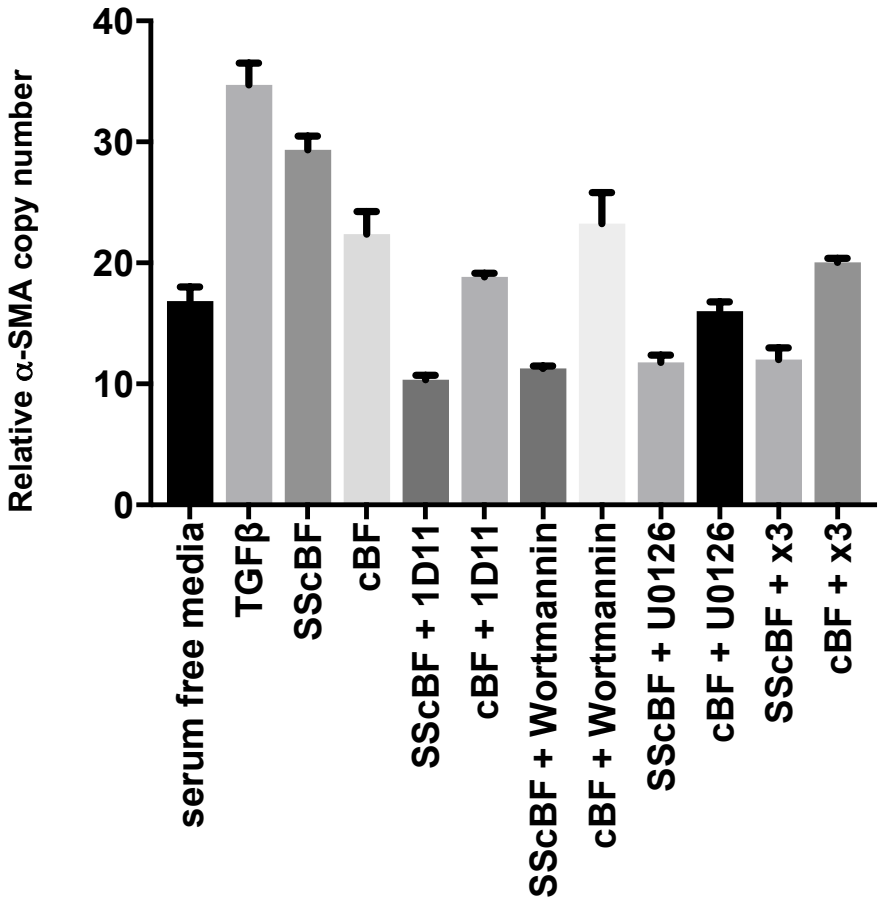

***Figure 5.11* α-SMA expression of MSCs in response to SSc blister fluid is not caused solely by IL31.** *Inhibitors of TGFβ, PI3K and MAPK pathways were more effective on SSc blister fluid (SScBF) treated MSCs than healthy control blister fluid (cBF) treated MSCs. MSCs were treated with serum free media, TGFβ (4 ng/ml), SSc and healthy control blister fluid (1:50) with or without 1D11 (10 μg/ml), Wortmannin (100 nM) and/or U0126 (5 μM). All treatments were in serum free media conditions. 10 ng/ml RNA was analysed per sample. SSc blister fluid significantly induced more α-SMA expression compared to serum free media (p=0.0004) and healthy control blister fluid (p=0.048). All three inhibitors, reversed SSc blister fluid induced α-SMA to the same extent (p<0.0001) and when treated with all three inhibitors together, the same extent of inhibition was observed (p<0.0001). No difference was seen between inhibitor effects on SSc blister fluid induced expression was measured (p>0.999 for all inhibitor comparisons). 1D11, Wortmannin and U0126 were less effective on healthy control blister fluid induced α-SMA expression (p=0.6653, p>0.999, p=0.0821 respectively. All three inhibitors together did not make a difference to the α-SMA expressed in response to healthy control blister fluid (p=0.9548). See appendix for full ANOVA multiple comparisons.*

5.6.3 IL31 Receptor expression in response to blister fluid

Considering the increased IL31 in SSc microenvironment, in addition to the quicker response of SSc fibroblasts to IL31 treatment in the scratch wound assay in Chapter 5.5.2, the amount of IL31RA expression was assessed on candidate cells thought to possibly respond to IL31 in the SSc microenvironment. Dermal and lung fibroblast cells were investigated as well as MSCs. Typically, fibroblasts express low to undetectable IL31RA levels and so this study sought to investigate whether these cells, commonly uninvolved in IL31 signal transduction, are receptive to the higher IL31 levels in SSc. While oncostatin M is also a ligand for the IL31RA-oncostatin M receptor dimer, the binding affinity of IL31 to the receptor is not dependent on its presence and as such oncostatin M was not assessed in these studies. qPCR was used to measure the amount of IL31RA expressed by four SSc and healthy control fibroblast dermal and lung cell lines, and two adipose derived MSC cell lines. Measurements were made in comparison to the housekeeping gene TBP (Figure 5.12).

To assess how blister fluid affects MSC expression of IL31RA, MSCs were also treated with SSc and healthy control blister fluid diluted 1:50 in serum free media. Healthy control dermal and lung fibroblast IL31RA expression was significantly lower than their SSc counterparts ($p=0.0148$ and $p=0.0163$ respectively). Both SSc lung and dermal fibroblasts expressed IL31RA to a similarly high level. Untreated healthy adipose-derived MSCs expressed IL31RA similar to SSc fibroblasts. Treating these MSCs with SSc blister fluid for 16 hours induced more IL31RA expression than untreated MSCs, and further, healthy control blister fluid (cBF) treated MSCs expressed IL31 receptor levels lower than their untreated equivalents.

Finding an increase in IL31 in SSc blister fluid led to the hypothesis that cells in the vicinity of this increased IL31 would express higher levels of IL31RA subunits on their cell membrane through a possible positive feedback response. While macrophages and keratinocytes typically express IL31RA subunits, if also expressed by SSc associated cells, a hypothesis that IL31 acts on SSc associated cells to conduct SSc associated processes could be

drawn. The finding that IL31 levels in SSc lung fibroblasts were similar to those in dermal fibroblasts may indicate that IL31 action is not limited to skin although for the purpose of the experiments of this thesis, this is the organ it was modelled in.

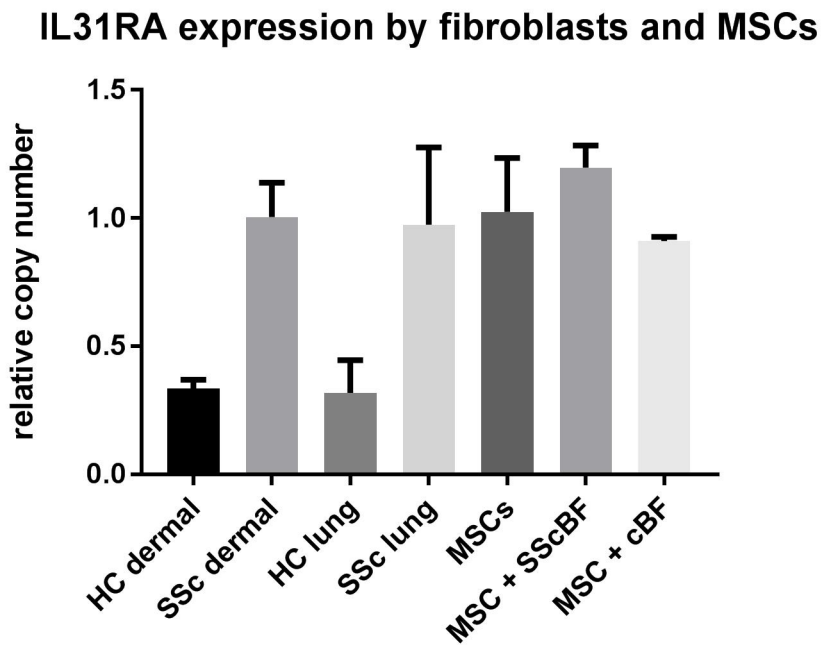

Figure 5.12 ***qPCR of IL31 Receptor A in fibroblasts and MSCs.*** *SSc dermal fibroblasts express more IL31 Receptor A than healthy (HC) dermal fibroblasts (SSc mean 1.00402 SEM 0.06734; HC mean 0.33619 SEM 0.0168; p=0.0148). SSc lung fibroblasts express more IL31 Receptor A than HC lung fibroblasts (SSc mean 0.97462 SEM 0.1506; HC mean 0.318 SEM 0.0637; p=0.0163). MSCs express IL31 Receptor A to levels similar to SSc fibroblasts and significantly different from HC dermal and lung fibroblasts (mean 0.98757 SEM 0.03799 p=0.0125 and 0.0107, respectively). SSc blister fluid (SScBF) increases expression in MSCs (mean 1.1965 SEM) while healthy control BF (cBF) reduces it (mean 0.91081 SEM 0.01116) although blister fluid had no significant effect on expression in comparison to untreated MSCs. * p<0.05 using ANOVA with Tukey's Post Hoc test. SSc and HC dermal and lung fibroblast n=4, MSC n=2.*

The results from SSc dermal and lung fibroblasts compared to healthy fibroblasts could indicate that since SSc fibroblasts were previously exposed to SSc microenvironment conditions, they may be primed to express IL31RA, enhancing responses to the high IL31 ligand in the SSc microenvironment. However, MSCs obtained from liposuction aspirates of healthy individuals and

have not been exposed to high IL31 levels, also express IL31RA levels similar to that of SSc fibroblasts. Exposing MSCs to SSc or control blister fluid in culture did not affect IL31RA expression significantly but did hint at higher expression levels in response to SSc blister and interestingly, lower levels than untreated MSCs in response to control blister fluid. So, while the increased IL31 in SSc blister fluid does not significantly affect migration or contraction, it does seem to have some involvement in α-SMA and IL31RA expression.

The inhibition experiments of this Chapter take into account the possible roles of the cytokine IL31 and growth factor TGFβ, but do not assess the importance of other blister fluid constituents, namely metabolites. Blister fluid is a result of cellular secretions in response to the environment. With the SSc environment being particularly anaerobic, lactate build up is not surprising and its effects on neighbouring cells should not be overlooked.

5.7 The effect of Lactate in blister fluid

5.7.1 Lactate in blister fluid and MSC collagen gel contraction

With lactate being higher in SSc blister fluid, experiments were conducted to assess the extent of the effect this elevation has on the differing inductions of SSc and healthy blister fluid. In other words, is the elevated lactate responsible for the differential responses to SSc blister fluid?

Lactate is transported into and out of cells via a lactate-protein co-transporter which is inhibited by α-cyano-4-hydroxycinnamic acid (αCHCA). MSC populated collagen gels were made and treated with media only as a negative control, 10% serum as a positive control, L-lactate with or without αCHCA and SSc or healthy control blister fluid with or without αCHCA. After 48 hours of incubation, contraction of the gels was measured as the gel weight, with a lower weight indicating more contraction. Shown in Figure 5.13, 10% serum caused the most gel contraction, closely followed by SSc blister fluid. Lactate treatment of MSCs induced some contraction (serum free; 0.13 g, lactate; 0.1 g; p=0.96) and this was completely inhibited by the addition of αCHCA to levels below the serum free negative control (serum free; 1.13 g, lactate; 0.1 g,

αCHCA; 0.18 g). SSc blister fluid induced gel contraction more than lactate, although not significantly, an effect that was partially inhibited by the αCHCA (SSc blister fluid; 0.08 g, lactate; 0.1 g, p=0.8259). While, lactate may indeed be involved in SSc blister fluid stimulated gel contraction, inhibition of its transport into MSCs by αCHCA only partially reversed the contraction. Like in previous collagen gel contraction assays, SSc blister fluid samples were significantly better at causing MSC migration and gel contraction than healthy control blister fluid (SSc blister fluid; 0.08 g, healthy control blister fluid; 0.16 g; p=0.023), which did not cause any gel contraction. These findings may suggest a shared component between 10% serum media and SSc blister fluid, not present in healthy control blister fluid, that has an effect on MSC migration and the subsequent collagen gel contraction.

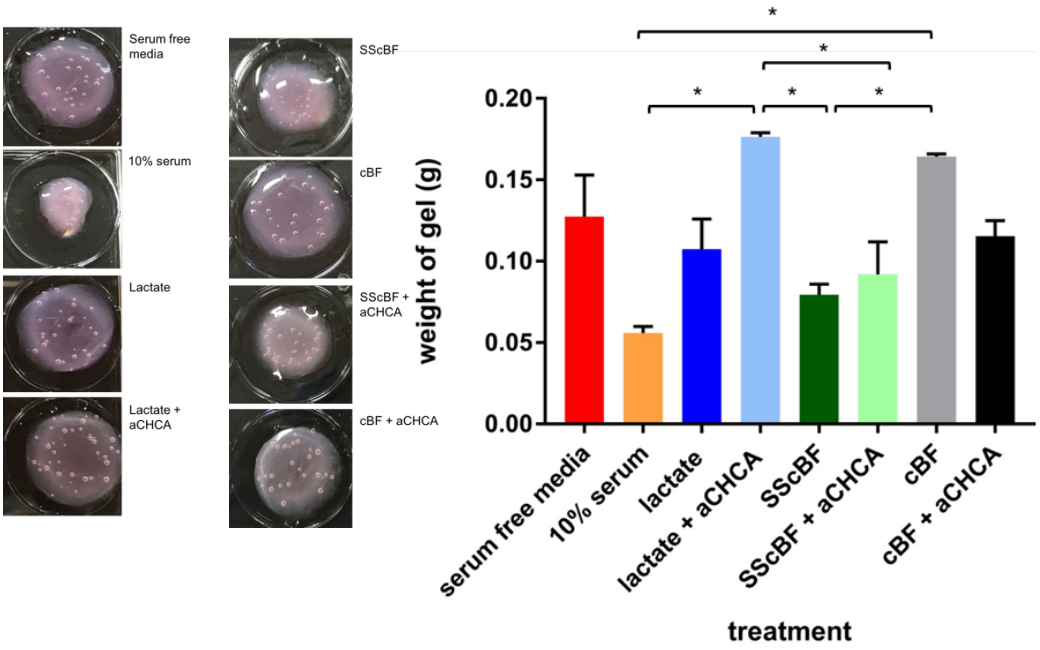

Figure 5.13 ***Lactate is only partly responsible for SSc blister fluid induced gel contraction.*** *MSC populated collagen gels were treated with serum free media, 10% serum, Lactate (25 mM) with or without αCHCA (5 mM) and SSc or healthy control blister fluid (diluted 1:50) with or without αCHCA. Lactate and blister fluid treatments were added to serum free media. Gels were incubated for 48 hours before being weighed (g). One-way ANOVA with Tukey's Post Hoc test was conducted to find statistical significance between multiple comparisons. * p<0.05. P=0.004 between 10% serum and Lactate + αCHCA, p=0.0078 between 10% serum and healthy control blister fluid (cBF). No significant difference found in contraction ability of SSc blister fluid (SScBF) compared with Lactate p=0.8259. Lactate + αCHCA was significantly worse at inducing gel contraction than SSc blister fluid (p=0.0152)*

but not different from control blister fluid (p=0.9973). SSc blister fluid was better than healthy control blister fluid at inducing MSC migration and gel contraction (p=0.0323). N=2 for each condition. See Appendix for full ANOVA results.

Similarly to when investigating the effect that IL31 has on blister fluid, α-SMA RNA expression was chosen as a measurement of the induction of α-SMA positive contractile fibres responsible for the MSC migration and collagen gel contraction, and as an indicator of myofibroblast differentiation of the MSCs.

5.7.2 Investigating α-SMA expression in response to Lactate

MSCs cultured as monolayers in 24 well plates were analysed for α-SMA expression by a qPCR assay. After 16 hours of treatment, RNA was extracted and α-SMA RNA in the lysates was compared to TBP expression. A higher α-SMA expression level was used as a readout of MSC fibrogenic activity. Kottmann et al, found that lactate dehydrogenase, the enzyme responsible for pyruvate to lactate metabolism, is an important mediator in activation of latent TGFβ. In turn, the anaerobic conditions of SSc, can explain the increased lactate concentration in SSc microenvironment. Increased lactate is responsible for a general decrease in pH levels and acidosis. It has been found that TGFβ is activated from its latent form under acidic conditions and as hypothesised, the TGFβ is a major inducer of MSC differentiation into myofibroblasts. Since myofibroblasts are predominant expressers of α-SMA, it stands to reason that increased lactate concentration can increase differentiation and thereby α-SMA. Adding to this, inhibition of the enzyme lactate dehydrogenase, by stopping pyruvate metabolism and lactate formation, has been shown to inhibit production of TGFβ mediated collagen type I, II and III expression as well as α-SMA expression. This result suggests using Gossypol, the lactate dehydrogenase inhibitor, as a pharmacological therapy for fibrosis (Kottmann et al. 2015). This experiment attempted to see how this TGFβ mediated lactate-induced α-SMA fits into MSC fibrogenic activity.

Baseline α-SMA expression of MSCs was determined by serum free media treatment (Figure 5.14). MSCs treated with 10% serum media expressed higher levels of α-SMA than any other treatment. Both SSc blister fluid and lactate treatment resulted in very similar levels of α-SMA (p=0.9999) which was significantly inhibited to levels below baseline by the addition of the lactate-protein co-transporter inhibitor αCHCA (p=0.0148 and 0.0078 respectively). The below baseline expression possibly suggests some autocrine stimulation of the cells by endogenous lactate. Healthy control blister fluid did not induce α-SMA expression in MSCs.

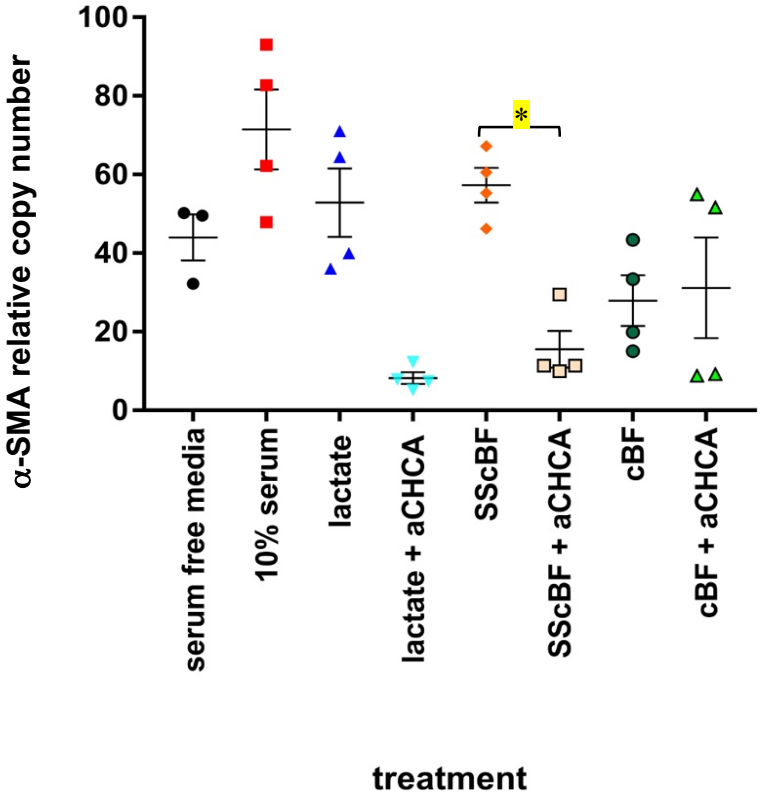

Figure 5.14 ***qPCR analysis of MSC α-SMA expression in response to αCHCA.*** *MSC α-SMA expression is inhibited by αCHCA.Confluent MSCs were treated with serum free media, 10% serum, lactate (25mM) with or without αCHCA (5 mM) and SSc or healthy control blister fluid (SScBF, cBF 1:50) with or without αCHCA. αCHCA significantly inhibits α-SMA expression in response to lactate (p=0.0079) and SSc blister fluid (p=0.0148). Healthy control blister fluid did not affect α-SMA (p=0.9999). All lactate and blister fluid treatments were diluted in serum free media. α-SMA expression is relative to TBP expression. N=4 for all conditions. Significant results p<0.05, as determined by one-way ANOVA with Tukey's post hoc tests. See Appendix for full ANOVA results.*

Lactate, therefore, undoubtedly has an effect on α-SMA expression by SSc blister fluid treatment of MSCs, but like IL31, does not seem to be the only factor. While inhibiting lactate transport significantly affected α-SMA expression, in monolayer cultures of MSCs, it did not fully inhibit the MSC gel contraction stimulated by SSc blister fluid. As hypothesised previously, it is unlikely that one individual component of SSc blister fluid is responsible for its effects on MSCs.

5.7.3 Investigating the collective effects of lactate and IL31 on MSC collagen gel contraction

The findings of this thesis so far have highlighted IL31 and lactate as being possible bioactive components of SSc blister fluid. They are both elevated in SSc blister fluid compared with healthy control blister fluid, both induced some form of MSC activation, migration or collagen gel contraction, and both, to some extent resulted in increased α-SMA expression. For this reason, their collective effects were analysed in order to test the hypothesis of multiple factors working together to bring about SSc blister fluid mediated pro-fibrotic functions.

MSC populated collagen gels were treated with serum free media, 10% serum, lactate and IL31, both alone and together. Again, the loss of gel weight was considered a measure of gel contraction and MSC migration, possibly through polymerisation of α-SMA positive contractile and stress fibres. Little contraction was observed by lactate or IL31 treated MSC populated collagen gels, as in the previous experiments presented above, and treating the MSCs with both lactate and IL31 together made no significant difference, although a very slight loss in gel weight was measured (Figure 5.15). This finding concludes that lactate and IL31 both have an effect with respect to promoting MSC collagen gel contraction.

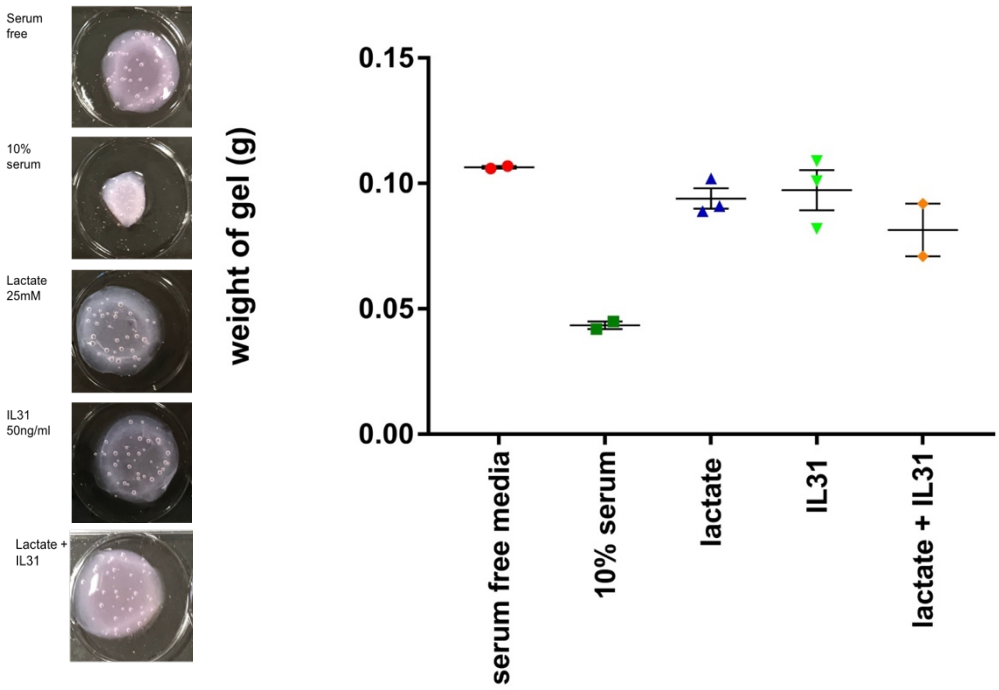

Figure 5.15 ***Lactate and IL31 do not work together to induce MSC gel contraction.*** *MSC populated collagen gels were treated with serum free media, 10% media, lactate (25 mM) and IL31 (50 ng/ml), both alone and together. Lactate and IL31 treatments were diluted in serum free media. Gels were left to contract for 48 hours before weighing (g). N=2 for all conditions. One-way ANOVA with Tukey's post hoc measured significance of p<0.05. The only significantly contracted gels were in 10% serum conditions (p=0.0026) in comparison with serum free media treated cells. The full ANOVA report can be seen in the Appendix.*

5.7.4 Conclusion

This chapter used many different models of interaction between different SSc microenvironments and MSCs in culture. SSc blister fluid, IL31, TGFβ and lactate represented the soluble SSc microenvironments while collagen gels mimicked the 3D matrix of skin. Interaction was modelled by western blots for pro-fibrotic protein expression and qPCR for pro-fibrotic α-SMA expression. In addition, scratch wound and collagen gel contraction assays modelled how MSCs migrate in response to SSc microenvironments. SSc blister fluid from patients was used as a direct representation of the growth, factors, cytokines and metabolites present in SSc interstitial fluid and therefore should, theoretically, contain all the soluble factors that affect MSCs in SSc skin, in turn, activating them to adopting a wound healing or myofibroblast phenotype.

The more specific microenvironment representations of IL31, lactate and TGFβ attempt to elucidate how big a role each of these individual factors play in SSc blister fluid induced responses.

SSc blister fluid induces the expression of three main pro-fibrotic proteins in MSCs, namely, α-SMA, collagen type I and CTGF. Healthy control blister fluid does not have this effect, although, some increase in expression compared with serum controls was observed in response to healthy control blister fluid. It can, therefore, be concluded that while blister fluid in general can have an effect on pro-fibrotic protein expression, SSc blister fluid is different to healthy control blister fluid in that it has a stronger effect on protein expression. With IL31 being elevated in SSc blister fluid compared to healthy control blister fluid, it would make sense that IL31 alone would induce similar expression levels as SSc blister fluid if concentration of this factor was the difference between healthy and SSc blister fluid. In fact, IL31 had little if any effect on pro-fibrotic protein expression and, therefore, it stands to reason that another factor(s) is responsible for the difference between the two blister fluid derivations.

Since the biggest difference in protein expression induced by SSc blister fluid was regarding α-SMA, this was used as the main readout of MSC activation by SSc blister fluid. This was indeed confirmed by the finding that at dilution factors ranging from 1:5 to 1:125, SSc blister fluid was better at inducing α-SMA RNA expression than control blister fluid. With most growth factors and cytokines present in blister fluid at picogram/ml concentrations, such high dilution factors, like 1:125 (used in the majority of experiments), make it unlikely that the culprit responsible for the differing actions of SSc and healthy control blister fluid is a simple protein factor present at slightly higher levels in SSc. In fact, considering the importance of the MSC microtome on MSC functions, miRNA molecules could account for the action of SSc blister fluid at high dilution factors. Mi-RNA molecules are needed in very small quantities to carry out their functions as they are not used up, silenced or inhibited (Chen et al. 2017).

Migration assays demonstrated the function of fibroblasts and MSCs during wound healing. IL31 was shown to work best at 50 ng/ml, inducing migration of dermal fibroblasts more than serum controls. Furthermore, SSc derived dermal fibroblasts seemed to be more responsive to IL31 induced migration. This is likely due to the increased IL31RA expression found in SSc dermal and lung fibroblasts. Increased receptor expression on SSc cells can be explained by their pre-exposure to increased IL31 *in situ.* More interesting is the increased receptor expression on healthy adipose-derived MSCs that have not been exposed to SSc microenvironments. This indicates that MSCs themselves are ready to respond to increases in IL31 and explains their migration across a scratch when treated with IL31. Furthermore, encouraging of the theory that pre-exposure to SSc microenvironments primes cells to respond to IL31 by increasing receptor expression, is the fact that MSCs pre-treated with SSc blister fluid, express even more IL31RA than those exposed to healthy control blister fluid or serum free media. As such, while IL31 was not wholly responsible for fibroblast and MSC migration, its role cannot be overlooked. This particularly resonates since MSC migration across a scratch in response to IL31 can be completely reversed by inhibition of the PI3K pathway.

Gel contraction assays bring together migration of cells with expression of α-SMA since it is via the formation of α-SMA positive contractile fibres that MSCs migrate in collagen gels and with them, pull collagen fibres, resulting in gel contraction. Reflective of the models of interaction explained thus far, SSc blister fluid was responsible for the highest degree of gel contraction observed, measured by loss of gel weight. Again, although IL31 has some effect, this is more akin to that of healthy control blister fluid and, therefore, it cannot be deemed as the defining factor differing the functions of the two blister fluid derivations, even though, treatment with the PI3K inhibitor Wortmannin did reduce gel contraction. Since TGFβ is known to influence fibroblast ability to contract collagen gels, this was used as a positive control on MSC gel contraction. TGFβ did indeed result in high levels of gel contraction, closely followed by SSc blister fluid, however, inhibiting the TGFβ receptor kinase

pathway in blister fluid did not largely inhibit MSC gel contraction in response to TGFβ, likewise, inhibiting PI3K and MAPK by Wortmannin and U0126, respectively, had only modest effects on inhibition of IL31 induced gel contraction. As such, it can be concluded that either these three pathways play no significant role in MSC migration, or that inhibition of one can be compensated for by another.

This theory was investigated when all three inhibitors were used together on SSc and healthy control blister fluid treated MSCs. α-SMA RNA expression was used as the measure of MSC activation in this assay. Like with gel contraction, blister fluid mediated MSC α-SMA expression was not highly inhibited by the use of the inhibitors, either alone or simultaneously. From this, it seems likely that these pathways converge at a common point and, therefore, can compensate for each other, without being additive in effects. In spite of this, SSc blister fluid still resulted in the most α-SMA expression and was more affected by inhibitors than healthy control blister fluid.

Chapter 4.5 showed that lactate levels were higher in SSc blister fluid compared to healthy control blister fluid samples. This fits into the hypothesis of anaerobic respiration taking place in avascular regions, particularly digits, due to Raynaud's phenomenon and vascular damage. The by-product of this process is the lactate anion, after its dissociation from the lactic acid produced by anaerobic glycolysis. The increase in lactate found in SSc blister fluid indicates a higher rate of production than removal in SSc patients. This could be due to the reduced oxidative capacity of the cells in these ischaemic regions. Lactate is reported to affect cell migration and invasion in cancer (Valvona et al. 2016). The increased lactate and decreased pH of the microenvironment activate metalloproteinases, which in turn affect extracellular matrix turnover and degradation. This remodelling of the extracellular matrix allows interactions with focal adhesions on cells and influences cell migration (Valvona et al. 2016).

SSc microenvironment is known to be hypoxic, and therefore, it is not surprising that SSc blister fluid contains more lactate than healthy control blister fluid. Lactate alone however, like IL31, does not fully account for the MSCs responses to SSc blister fluid since gel contraction in response to lactate was less than that of SSc blister fluid. On the other hand, inhibiting lactate transport in MSCs using αCHCA significantly reversed gel contraction and α-SMA expression as a result of SSc blister fluid. This inhibitor blocks lactate transport both into and out of cells. Since the inhibitor seems to have the highest effect on SSc blister fluid treated cells it can be concluded that lactate in blister fluid is partially responsible for both migration and α-SMA expression of MSCs to a some extent, similar to that of IL31. Following on from this, it was thought that IL31 and lactate could be working together in an additive manner to account for their effects on migration and α-SMA expression. As such a gel contraction assay was conducted with MSCs treated with lactate or IL31 together or alone. It was found that IL31 and lactate do not work together to mediate MSC migration and gel contraction since together their responses were only slightly stronger than alone. Interestingly however, both IL31 and lactate induced migration and contraction to very similar extents, and given that they have been found to work on different pathways, this poses the question of MSCs being induced to migrate by a variety of factors and as such elucidation of this factor in SSc seems to be relatively complicated.

Specific soluble factors in the microenvironments of SSc were investigated in Chapters 5.5, 5.6 and 5.7 with particular reference to their effect on MSC migratory ability and pro-fibrotic α-SMA expression. These readouts do by no means give complete insight into the whole effect of SSc microenvironment on MSCs. Taking a step back from these experiments on specific factors and their effects on MSCs, a more holistic approach was taken in the form of a large next generation sequencing assay as detailed in Chapter 6.

Chapter 6 : Next Generation RNA Sequencing of SSc microenvironment treated fibroblasts and MSCs

6.1 Introduction: Using Illumina TruSeq RNA sequencing to fully define altered patterns of gene expression in MSCs

The assays conducted so far take a somewhat reductionist approach in that they only focus on the effect of a few SSc microenvironment representations on a few MSC fibrogenic readouts. While α-SMA expression is considered to be a good indicator of MSC pro-fibrotic activity, it is not sufficient alone to draw the conclusion that under these SSc mimicking conditions, MSCs fully differentiate into myofibroblast-like wound healing pro-fibrotic cells that exacerbate inflammation, fibrosis and tissue scarring, ultimately aggravating SSc progression.

Next generation sequencing (NGS) techniques such as RNAseq as used in this study, allow full analysis of all genes expressed in RNA lysates collected from cultured cells in comparison to a reference human genome. This method, is considerably faster than the use of microarrays and allows more precise quantification of RNA expression. RNAseq can elucidate both coding and non-coding regions of RNA and takes into consideration splicing and some post-transcriptional modifications. But, the main benefit RNAseq has over microarrays is that there is no need to have a pre-conceived notion of potential expression, such that probes are not needed in RNAseq. RNAseq reads millions of short stranded cDNA sections. The RNA obtained from cell cultures is cleaved into short sections, typically between 30 and 100 base pairs long which are amplified by PCR. Fluorescently labelled nucleotides are added to the amplified RNA with DNA polymerase to make a cDNA library of the short strands. One nucleotide is added at a time to increase precision and sensitivity when reading the strands. The fluorescent cDNA is then hydrolysed to become single stranded and the molecules are then aligned to a reference human genome. Paired end sequencing reads aligned sequences from both the 3' and 5' end to give a more accurate reading of longer sequences. Differential

expression is then calculated by the number of reads that have aligned to each locus of the reference genome (Levin et al. 2010) .

6.2 Hypothesis and aims

This Chapter hypothesises that SSc blister fluid will have a differential expression effect on MSCs and fibroblasts compared to healthy control blister fluid, and that increased IL31 in SSc blister fluid accounts for some of the differential effects. The hypothesis was tested through the following aims:

1) To use Illumina RNAseq to determine expression levels of all expressed genes in MSCs in response to blister fluid treatments, and compare with dermal fibroblast expression profile
2) To use Ingenuity Pathway Analysis (IPA) to contextualise and biologically predict functions and pathways causing the differential expression.
3) To use *in vitro* differentiation assays to confirm specific predicted pathways highlighted by IPA analysis.

6.3 Illumina RNAseq results

In this study, an Illumina TruSeq RNAseq analysis was conducted using 43 base pair paired end strands measuring 15 million reads per sample. The study was separated into two groups, one using healthy control dermal fibroblasts, and the other, adipose-derived MSCs, in order to compare the patterns of gene expression in SSc environment activated MSCs with those induced in fibroblasts. Both groups were treated identically with the same number of replicates as follows; 0.2% serum as control, SSc or healthy control blister fluid diluted 1:125, or IL31 (50 ng/ml). As with other blister fluid assays, a different blister fluid sample was used for each of the four replicates to account for the inherent range in blister fluid constituents. The RNAseq was conducted in collaboration with UCL Genomics. Both fibroblasts and MSCs were used to attempt to determine how much an effect was due to the microenvironment, and how much due to intrinsic nature of the cells themselves. In effect, if similar results were obtained for the same gene

expression in both cell types, then it would support the idea that the MSCs are being activated in a fibroblast-like pattern within the disease microenvironment, whereas widely divergent results between the cell types could indicate a specific non-fibroblast role for the activated MSCs.

A heatmap was constructed of the expression of 20 candidate genes, chosen bearing in mind their potential function in SSc pathology, MSC differentiation capabilities or ability to induce pro-fibrotic protein expression (Figure 6.1). The genes chosen were aggrecan *(ACAN),* actin α-2 *(ACTA2, otherwise known as α-SMA),* activated leukocyte cell adhesion molecule *(ALCAM)*, alkaline phosphatase *(ALPL),* cell migration inducing hyalaronan protein *(CEMIP),* collagen type I α1 *(COL1A1),* collagen type IIIα1 *(COL3A1),* collagen type IVα1 *(COL4A1),* connective tissue growth factor *(CTGF),* endoglin *(ENG),* fibronectin 1 *(FN1),* glioma associated oncogene *(GLI1),* insulin-like growth factor binding protein 5 *(IGFBP5),* interleukin 31 *(IL31),* interleukin 31 Receptor A *(IL31RA),* interleukin 6 *(IL6),* 5' nucleotidase-ecto *(NT5E, or CD73),* runt related transcription factor 2 *(RUNX2),* signal transducer and activator of transcription 4 *(STAT4*), transforming growth factor β *(TGFβ1),* transforming growth factor β Receptor 1 *(TGFβR1)* and thymus cell antigen 1 *(THY1).* In fact, surprisingly, when constructing a heatmap without actively choosing the genes to be studied, the majority of the most differentially expressed genes were unidentified pseudogenes.

The heatmap was constructed using R software, which organises genes and samples based on their similarity to each other. The hierarchical dendogram on the left and top of the heatmap illustrates how close genes or samples are, respectively. The distance between genes or samples is reflective of similarity such that the smaller the distance, the shorter the line and the closer the entities. Each is joined to its most similar which are in turn joined to a similar group until a single "parent" is reached. In the heatmap itself, the colour of the block corresponding to the expression of each gene by each sample ranges from blue through yellow to red, with dark blue being the least differentially expressed, getting lighter into yellow, through increased expression

represented by orange, gradually getting darker to red, indicating positive upregulation.

The most striking thing is the complete separation of MSCs from healthy dermal fibroblasts (Figure 6.1). The healthy dermal fibroblasts cluster together to the left of the heatmap while the MSCs, to the right. This shows that the two cells types, even though similar in shape and plastic adherence in culture, have distinct expression profiles, regardless of treatment. Since MSCs are not lineage committed cells, it is expected that they would have an expression profile reflecting their stem-cell pluripotency, while healthy dermal fibroblasts are an established differentiated cell line that express genes related to their function in the skin. In addition to the different cell types clustering separately, within the MSC samples, for the most part, the differently treated samples cluster together, such that all SSc blister fluid treated MSC samples are clustered beside each other, and most of the IL31 treated samples cluster together. This confirms the distinct expression profiles as a result of the treatment rather than the inherent expression of that cell type, and supports the idea that SSc microenvironment and IL31 are capable of inducing specific and consistent changes in MSCs. The results for the treated fibroblasts were not so consistent with considerable overlap between treatment groups, which did not consistently cluster together. These results may indicate less specific responses of the fibroblasts to SSc microenvironment representations. Also, there may be heterogeneity of the dermal fibroblast populations since even the untreated controls did not co-cluster.

Therefore, clustering of the differently treated MSCs is much more precise and distinct than that of dermal fibroblasts. The four different treatments induce four different and separate expression profiles in MSCs with one exception. There is little difference in the expression of these candidate genes between control media and IL31 treatments and as such the line between these two treatments is slightly blurred, although 3 out of the 4 replicates of the IL31 treated MSCs cluster together. Interestingly, although SSc and healthy control blister fluid separate completely, they are clustered beside each other with a more recent “parent” than the control media and IL31 treated MSCs. The latter

two groups also have a common parent, such that the 4 groups share a "grandparent". Both healthy control and SSc blister fluid highly induce *CEMIP*, *IL6* and *ACAN*. The other two treatment groups express these three genes to a much lower extent, and *CEMIP* to an even lower level. Also the expression of *ACTA2*, also known as α-SMA, is slightly higher in SSc blister fluid treated MSCs, compared to healthy control blister fluid treated MSCs, reflective of the Western blots and qPCR assays conducted, described in Chapters 5.4.2, 5.6.2, and 5.7.2. *CTGF* and *COL1A1* are also slightly more expressed in blister fluid treated MSCs compared to IL31 and control media treated cells, this also is similar to the results of the Western blots described in Chapter 5.2 where α-SMA protein is shown to be more differentially expressed than collagen type I or CTGF. *NT5E* is a gene relating to the pluripotency of MSCs. SSc blister fluid treated MSCs express less of this gene than the other treatments, possibly indicating SSc blister fluid induced differentiation of MSCs into myofibroblasts, considering increased α-SMA expression. *ALCAM* is a gene involved in cellular adhesion, particularly during migration. Under blister fluid conditions, expression of this gene is upregulated compared with control media and IL31 treatments. This also is reflective of the scratch wound assays described in Chapter 5.5.3. *IL31RA* gene expression was only slightly increased in response to IL31 treatment, most likely through a positive feedback mechanism, and unlike in the qPCR assay for IL31RA, (Chapter 5.6.3), blister fluid had no noticeable effect on *IL31RA* expression. There was no noticeable difference between all treatments on *TGFβ* or *TGFβR* gene expression. A reduction in *THY1* expression has been shown to be indicative of MSC differentiation, in this assay however, this was not the case, and expression of this gene was not different across all treatments (Moraes et al. 2016). Likewise, fibronectin was not upregulated by any of the treatments, since fibronectin is involved in cell migration, it can be concluded that the migration observed under blister fluid conditions in the scratch wound assays is not due to an increase in fibronectin expression. Although the JAK/STAT pathway is thought to be involved in SSc as part of the IL6 pathway, no increase in STAT4 RNA expression was observed, even under IL31 treatment conditions. *RUNX2* is an osteoblast gene and was investigated as a marker of

MSC to osteoblast differentiation, although no increase in its expression was measured, it is also unlikely that after only 16 hours treatment, there would be any induction in osteoblast differentiation, if anything, expression of this gene would indicate existing osteoblasts in culture, and seeing as how MSCs were cultured on plastic only until confluent, this differentiation was unlikely. Lastly, *COL3A1* and *IGFBP5* expression was downregulated in MSCs to the extent that it was represented as blue under all conditions, but even darker under blister fluid conditions. On the contrary, it is these two genes that are specifically overexpressed in dermal fibroblasts by all treatments.

Unlike the findings with MSCs, dermal fibroblasts seem less responsive to the specific treatments. While some replicates cluster together, others cluster with samples from other treatments and do not share the same expression profile. *ALCAM, COL4A1* and *ENG* expression in fibroblasts was completely opposite to the findings in MSCs. These three genes were downregulated, possibly less so by blister fluid, although the difference is minimal. Like these genes, the upregulated genes in MSCs (*CEMIP, IL6* and *ACAN)* were downregulated in fibroblasts to levels even less than levels observed in IL31 and control media treated MSCs. Notably, α-SMA expression was higher in blister fluid treated fibroblasts than control media treated fibroblasts. This is not unexpected considering the increased level of growth factors in blister fluid.

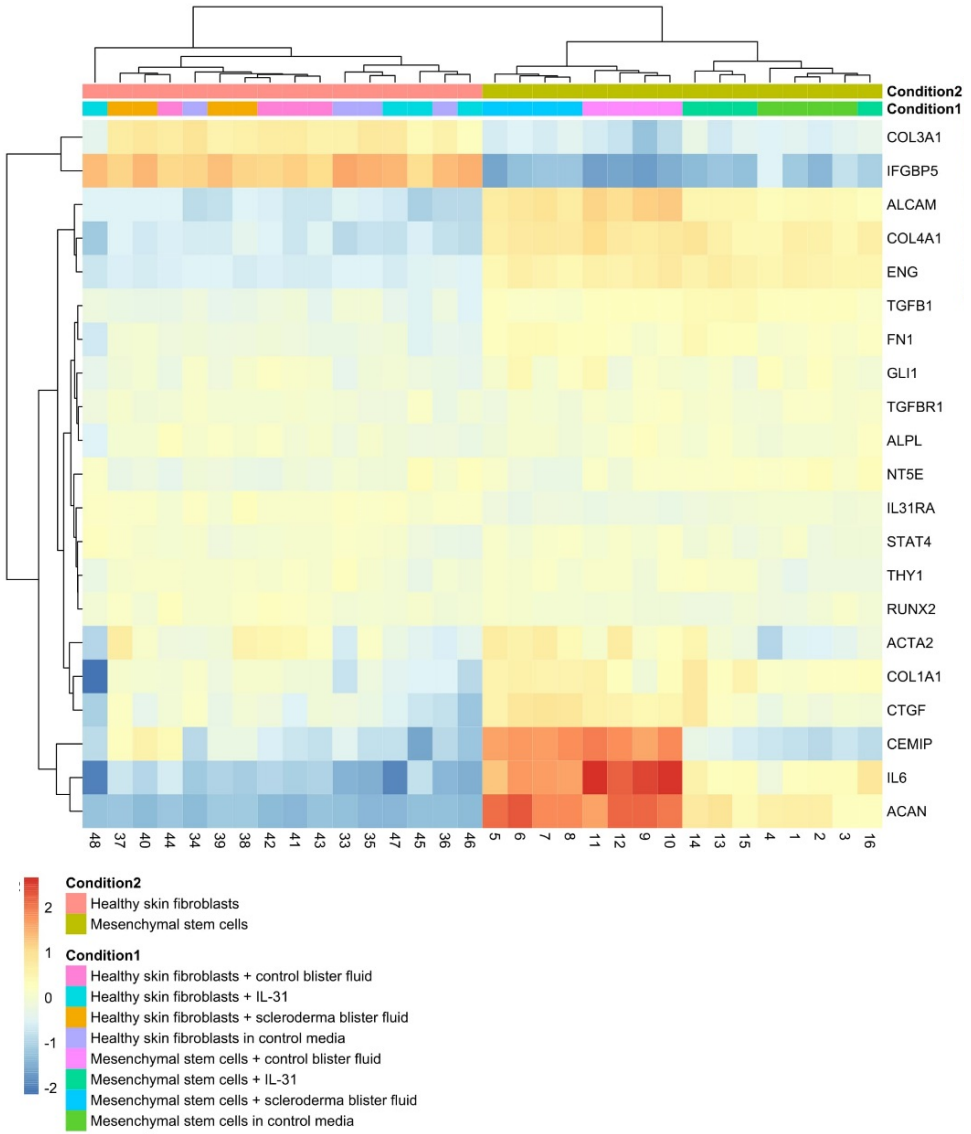

***Figure 6.1* Heatmap and hierarchical clustering of MSCs and dermal fibroblasts treated with SSc microenvironments.** *Both cell types were treated identically with 4 replicates of each treatment. 1-16 are MSC samples and 33-48 are healthy dermal fibroblast RNA samples. Treatments as follows: 1-4 and 33-36 are treated with control 0.2% media, 5-8 and 37-40 are treated with SSc blister fluid (1:125), 9-12 and 41-44 are treated with healthy control blister fluid (1:125) and 13-16 and 45-48 are treated with IL31 (50 ng/ml). Blister fluid and IL31 was diluted in 0.2% serum media. Candidate gene (right) expression analysed for each sample. Samples clustered hierarchically by similarity candidate genes were The genes chosen were aggrecan (ACAN), actin α-2 (ACTA2, otherwise known as α-SMA), activated leukocyte cell adhesion molecule (ALCAM), alkaline phosphatase (ALPL), cell migration inducing hyalaronan protein (CEMIP), collagen type Iα1 (COL1A1), collagen type IIIα1 (COL3A1), collagen type IVα1 (COL4A1), connective tissue growth factor (CTGF), endoglin (ENG), fibronectin 1 (FN1), glioma associated oncogene (GLI1), insulin-like growth factor binding protein 5 (IGFBP5), interleukin 31 (IL31), interleukin 31 Receptor A (IL31RA), interleukin 6 (IL6), 5' nucleotidase-ecto (NT5E, or CD73), runt related transcription factor 2 (RUNX2), signal transducer and activator of transcription 4 (STAT4), transforming growth factor β (TGFβ1), transforming growth factor Receptor 1 (TGFβR1) and thymus cell antigen 1 (THY1).*

Beginning with fibroblasts, principal component analysis identified all the differentially expressed genes in response to each treatment conditions. In this thesis are some of the most differentially expressed, most significant and most interesting expression analyses. Countplots of the number of reads for each gene were constructed and plotted using a regularised logarithmic scale normalised by DEseq2 calculations. This divides the number of RNA counts for each gene per sample divided by a calculated geometric mean for each gene across all the samples. The statistical significance was tested using Wald testing and fits a negative generalised linear model for each gene. This is a statistical transformation to stabilise variance across samples.

While the differences in expression as a result of blister fluid are not obvious from the heatmap (Figure 6.1), dermal fibroblasts cannot be considered unresponsive to SSc blister fluid. Genes upregulated by SSc blister fluid are summarised in Figure 6.2. Although dermal fibroblasts express some α-SMA, their levels are thought to be lower than myofibroblast expression levels. Bearing this in mind, treating fibroblasts with blister fluid increased expression of the *ACTA2* gene encoding α-SMA. Since fibroblasts are terminally differentiated, specific signals are thought to be necessary to induce their differentiation into myofibroblasts. The significantly increased levels of α-SMA under SSc blister fluid conditions indicates as such ($p=0.00364$), although no significant difference was found between SSc and healthy control blister fluid induction ($p=0.9987$).

While in the heatmap (Figure 6.1), *CEMIP* was identified as one of the main downregulated genes in dermal fibroblasts, in comparison with its expression in MSCs it is clear that samples 37 and 40 (fibroblasts treated with SSc blister fluid), express higher levels of *CEMIP* than any other fibroblast sample and this is reflective in the countplot of this gene. SSc blister fluid induces expression of *CEMIP* more than any other treatment ($p=0.0014$). CEMIP is involved in cell migration and its upregulation in response to SSc blister fluid confirms the findings of the preliminary fibroblast scratch wound assays where

SSc blister fluid induced most migration of dermal fibroblasts across a scratch *in vitro* (Chapter 5.2.2). Furthermore, *CEMIP* has recently been identified as one of the most upregulated genes in lung fibrosis in SSc (Verneau 2016)

FBN2 encodes the protein fibrillin-2 (Figure 6.2). This is a large structural protein involved as one of the constituents of the extracellular matrix and plays a role in the mechanical stability and elasticity of the matrix (Ramirez and Dietz 2007). SSc blister fluid induces expression of this gene more than any other treatment ($p=0.0001$). Healthy control blister fluid also increases its expression compared with control media ($p=0.0031$) and IL31 ($p=0.0002$). While SSc blister fluid seemed more apt at *FBN2* gene expression, it was not significantly better at it than healthy control blister fluid.

IL6 is believed to be an important mediator of inflammation and fibrosis in SSc, and therefore was important to determine if the SSc microenvironment of IL31 influenced IL6 expression levels (Khan et al. 2012b). Of note, both SSc and healthy control blister fluid induced IL6 expression significantly ($p=0.0394$ for SSc blister fluid and $p=0.0313$ for healthy control blister fluid), whereas the Il31 treatment did not. This suggests that increased expressed of IL6 by SSc blister fluid is not due to its elevated IL31 levels. This is further confirmed by the similar expression of IL6 in response to healthy control blister fluid, which was not found to have high IL31 levels. Interestingly, IL6 expression seemed somewhat dampened by IL31 (Figure 6.2).

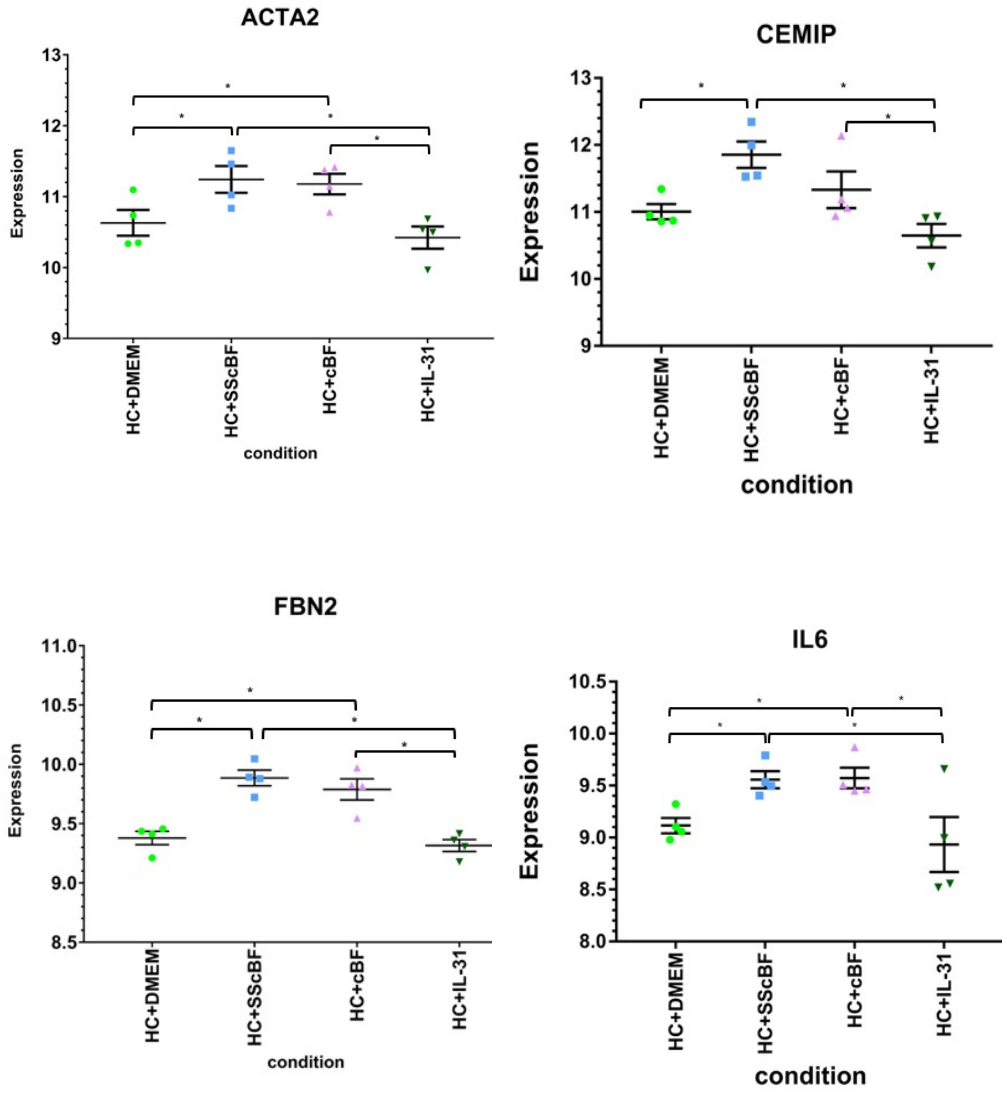

Figure 6.2 ***Genes upregulated in dermal fibroblasts in response to SSc blister fluid detected by RNAseq.*** *RNA expression of genes in Healthy control (HC) dermal fibroblasts treated with 0.2% media (DMEM), SSc blister fluid (SScBF), healthy control blister fluid (cBF) or IL31 (50 ng/ml). ACTA2 (encoding α-SMA) is increased by SSc blister fluid (p=0.00364) and control blister fluid (p=0.0117) when compared to control media and IL31 (p=0.0057 and p=0.0169, respectively). CEMIP expression is increased by SSc blister fluid (p=0.0014) compared to control media and IL31 (p=0.0018). No difference between expression in response to control blister fluid compared with control media but p=0.0012 compared with IL31 treatment. FBN2 expression increased in response to SSc blister fluid (p=0.0001). IL6 expression was increased by SSc and control blister fluid compared with control media (p=0.0394 and p=0.0313), and decreased by IL31 treatment compared with SSc (p=0.0128) and healthy control (p=0.0098) blister fluid. *p<0.05.*

The hypothesis thus far, has been that SSc blister fluid contains factor(s) that are not present, or found at least at lower concentrations in control blister fluid. This sequencing assay put forward the hypothesis that SSc blister fluid may in fact have something missing that is present in control blister fluid.

Growth arrest specific 1 (GAS1) is a protein involved in the arrest of cells in the cell cycle such that most quiescent mammalian cells express this gene. As such, it stands to reason that inhibition of its expression would be seen when cells are undergoing activation. This is seen in response to SSc blister fluid (Figure 6.3). For this reason, it can be suggested that fibroblasts are "activated" by SSc blister fluid more than any other treatment ($p=4.38x10^{-7}$). Healthy control blister fluid and IL31 also inhibit GAS1 expression but not as much as SSc blister fluid (Del et al. 1992)

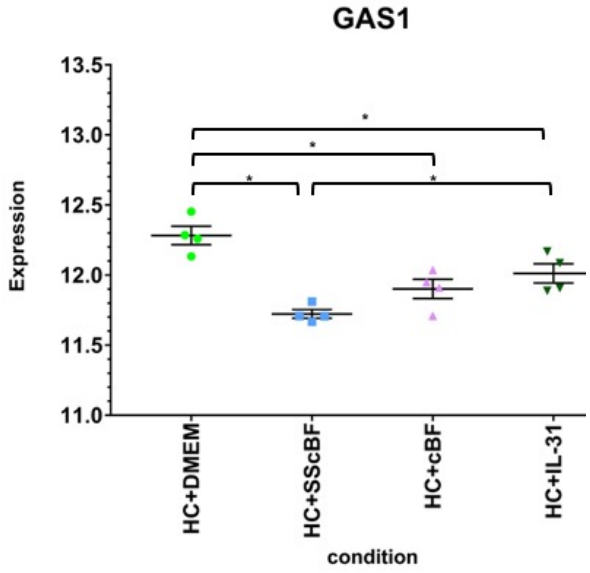

Figure 6.3 ***GAS1 expression is inhibited by SSc blister fluid.*** *SSc blister fluid (SScBF) inhibited GAS1 expression in healthy control (HC)dermal fibroblasts significantly more than serum controls (DMEM) $p=4.38x10^{-7}$. Healthy control blister fluid (cBF) and IL31 also reduced expression (p=0.0029 and p=0.043, respectively.*

As observed in the Western blots of pro-fibrotic protein expression of MSCs (Chapter 5.2), fibroblasts are only minimally induced to express CTGF or collagen type I in response to SSc blister fluid. Since the same results are seen in both cell types, it can be concluded that SSc blister fluid does not contain appropriate stimuli for these proteins to be expressed regardless of cell type. Furthermore, unlike the effects shown on MSCs in Chapter 5.6.3, blister fluid does not alter the expression of IL31RA on fibroblasts (Figure 6.4).

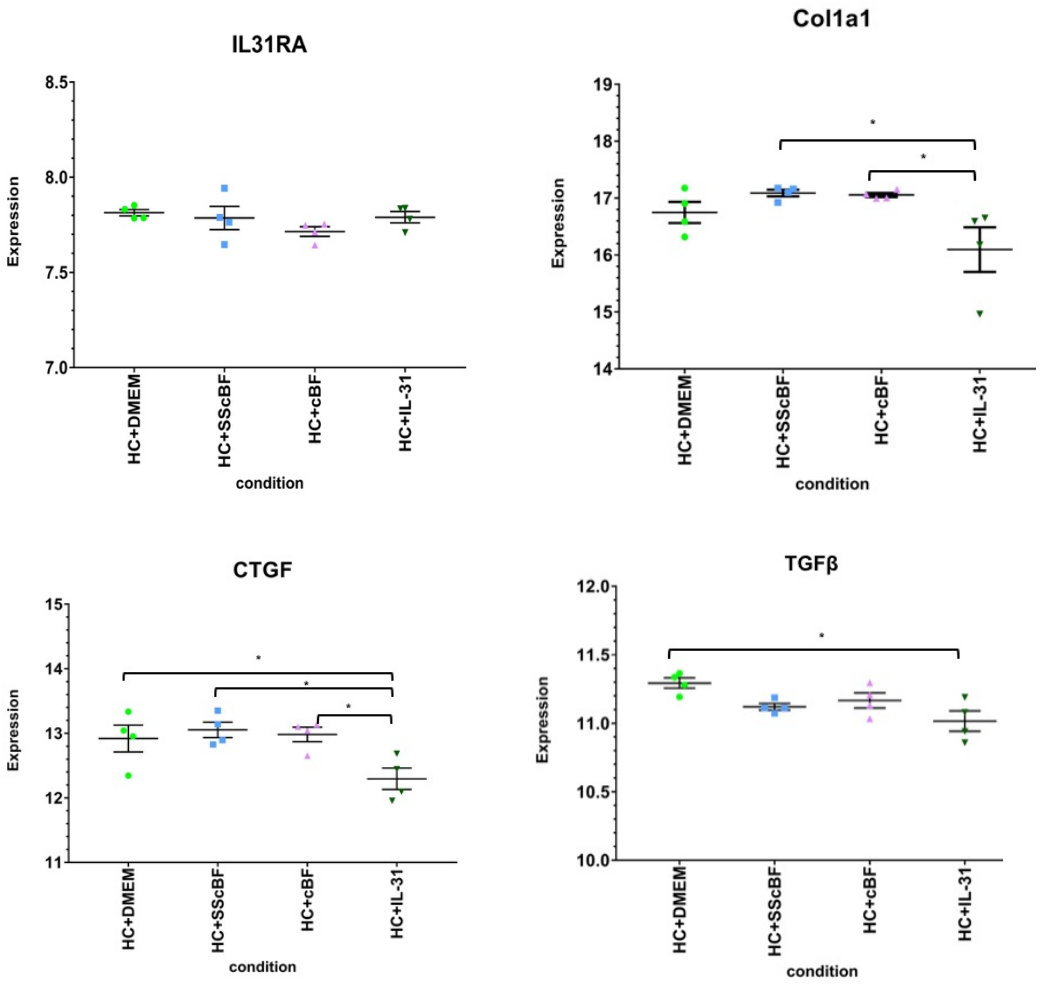

***Figure 6.4* SSc blister fluid does not affect expression of IL31RA, COL1A1, CTGF or TGFβ in dermal fibroblasts as detected by RNAseq.** *IL31 Receptor A (IL31RA) expression is not affect by any treatment. collagen type I (COL1A1) expression is reduced by IL31 in comparison to SSc blister fluid (SScBF p=0.0254) and healthy control blister fluid (cBF p=0.0385). CTGF expression is inhibited by IL31 compared with control media (DMEM p=0.033), SSc blister fluid (p=0.0065) and healthy control blister fluid (p=0.0198). Neither SSc blister fluid nor healthy control blister fluid affected expression of TGFβ. IL31 reduced TGFβ expression compared with control media (p=0.0134).*

While the elevated IL31 in SSc blister fluid did not seem to account for some of the key differences from the effects of healthy control blister fluid, IL31 treatment itself, given at a high concentration (50 ng/ml) had specific effects on RNA expression of dermal fibroblasts (Figure 6.5).

IL13 Receptor A2 (IL13RA2) is a scavenger receptor for interleukin 13 (IL13), which is an inflammatory cytokine produced by CD8-postive T-cells, associated with SSc fibrosis. Moreover, it has been documented that the level of serum IL13 correlates positively with degree of fibrosis severity (Fuschiotti et al. 2013). IL31 treatment of dermal fibroblasts increased expressed of IL13RA2 significantly higher than control media or blister fluid treatments. As such, it can be suggested from this finding that the increased IL31 in SSc microenvironments may modulate the responses to IL13 via upregulation of IL13RA2.

Annexin A1 (ANXA1) is a regulator of inflammation in fibroblasts and has been linked to wound healing. Its inhibition with small-interfering RNA molecules has led to an increase in IL6 production indicating that ANXA1 inhibits IL6 production (Jia et al. 2013). IL31 treatment was found to increase *ANXA1* expression (Figure 6.5). This expression may explain the reduced IL6 levels found in response to IL31 illustrated in Figure 6.5. ANXA1 is also involved in the mediation of VEGF induced cell migration, a process thought to be involved in SSc (Pin et al. 2012)

C-X-C motif chemokine ligand 5 (*CXCL5*) expression was only increased by IL31 treatment of dermal fibroblasts and was unaffected by blister fluid. In comparison with control media, IL31 significantly induced CXCL5 expression ($p=0.0051$). CXCL5 has an effect on neutrophil angiogenic potential and also may play a role in the fibroblast mediated activation of MSCs (Nedeau et al. 2008). Similarly, to CXCL5, IL33 expression was only induced by IL31 treatment. Neither SSc nor healthy control blister fluid had any effect on IL33 expression in comparison to each or to control media. IL33 has been found to be expressed in both dermal and lung fibroblasts in SSc and has been hypothesised to be involved in early endothelial cell activation and damage

which in turn further signals to fibroblasts and myofibroblasts, causing their activation (Manetti et al. 2010).

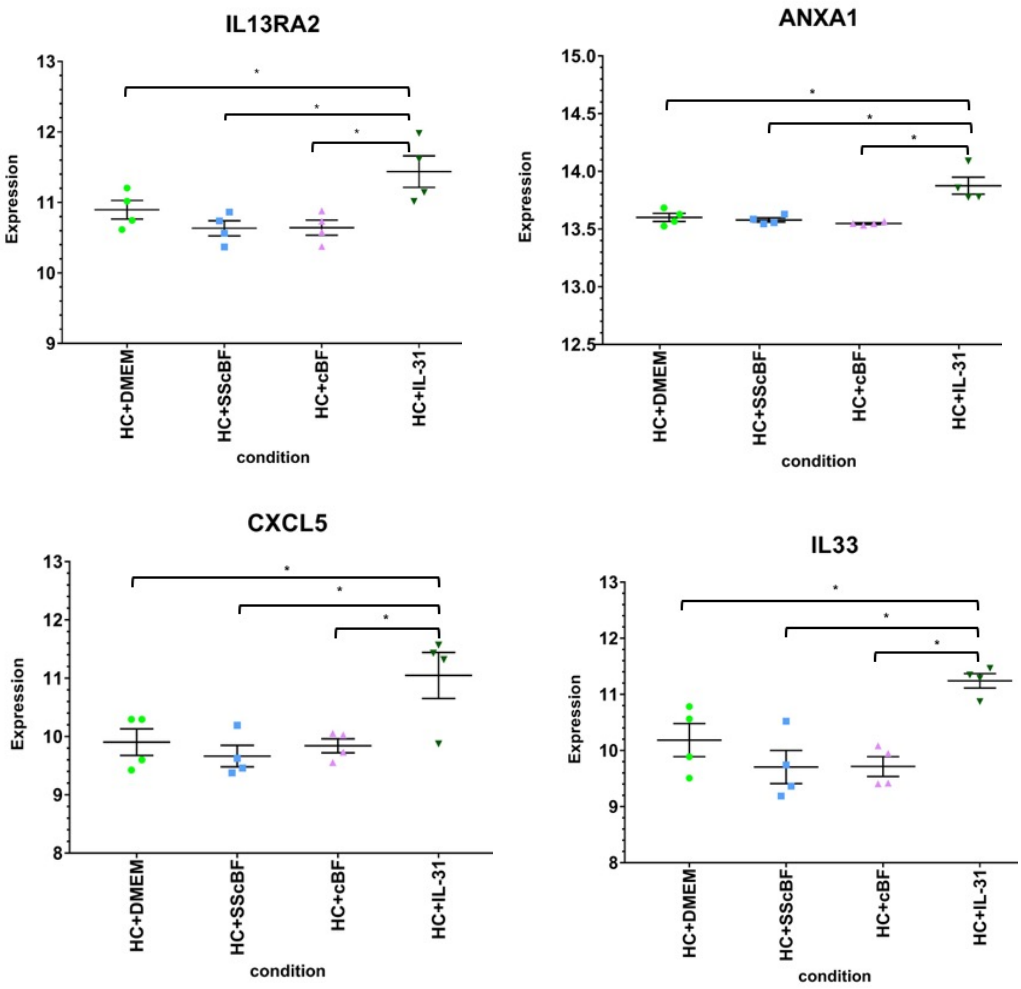

Figure 6.5 ***Effects of IL31 treatment on dermal fibroblast gene expression measured by RNAseq.*** *IL31 increased expression of IL13RA2 more than control media (DMEM p=0.0444), SSc blister Fluid (SScBF p=0.00949) and healthy control blister fluid (cBF p=0.00169). ANXA1 expression was only increased by IL31, significantly more than levels found after DMEM (p=0.0284) SScBF (0.0001) and cBF ($3.48x10^{-5}$) treatments. CXCL5 expression was increased by IL31 compared with DMEM (p=0.0051), SScBF (p=0.00052) and cBF (p=0.0024). IL31 induced expression of IL33 more than DMEM (p=0.045), SScBF (p=0.0019) or cBF (p=0.00193). HC (Healthy control dermal fibroblasts).*

Together these results show how specific SSc microenvironments affect dermal fibroblast expression. The main finding from this assay was the lack of significance found in the different expression between SSc and healthy control blister fluid. While α-*SMA* and *CEMIP* expression hinted at being higher in response to SSc blister fluid, conclusively significant differences were not found. As such, it is difficult to conclude that there is a single entity responsible for the difference in SSc blister fluid constituents compared with healthy control blister fluid influencing gene expression in dermal fibroblasts. One explanation might be that within the disease microenvironment, SSc tissue fluid effects on fibroblasts is through the collective effect of soluble factors together with neighbouring cells and, in the context of SSc specific matrix, or else that microenvironment-fibroblast interaction is not important in the disease.

On the other hand, more definitive results were seen when MSCs were treated with SSc blister fluid. As observed in the heatmap, MSCs respond to SSc blister fluid with a specific and distinct expression profile illustrated in the countplots in Figure 6.6.

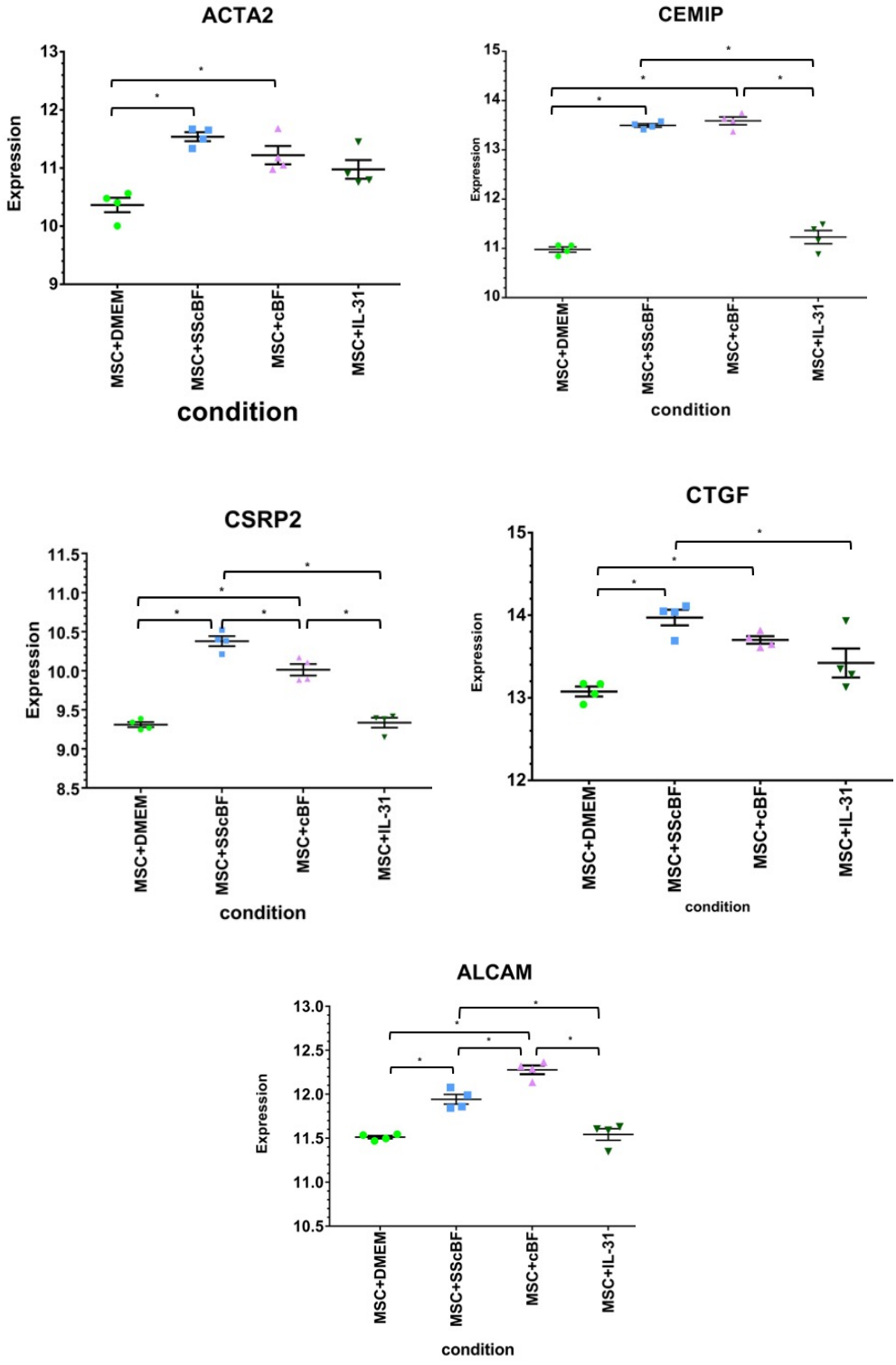
ACTA2
Expression
13
12
11
10
9
MSC+DMEM
MSC+SScBF
MSC+cBF
MSC+IL-31
condition
CEMIP
Expression
15
14
13
12
11
10
MSC+DMEM
MSC+SScBF
MSC+cBF
MSC+IL-31
condition
CSRP2
Expression
11.5
11.0
10.5
10.0
9.5
9.0
8.5
MSC+DMEM
MSC+SScBF
MSC+cBF
MSC+IL-31
condition
CTGF
Expression
15
14
13
12
MSC+DMEM
MSC+SScBF
MSC+cBF
MSC+IL-31
condition
ALCAM
Expression
13.0
12.5
12.0
11.5
11.0
10.5
MSC+DMEM
MSC+SScBF
MSC+cBF
MSC+IL-31
condition

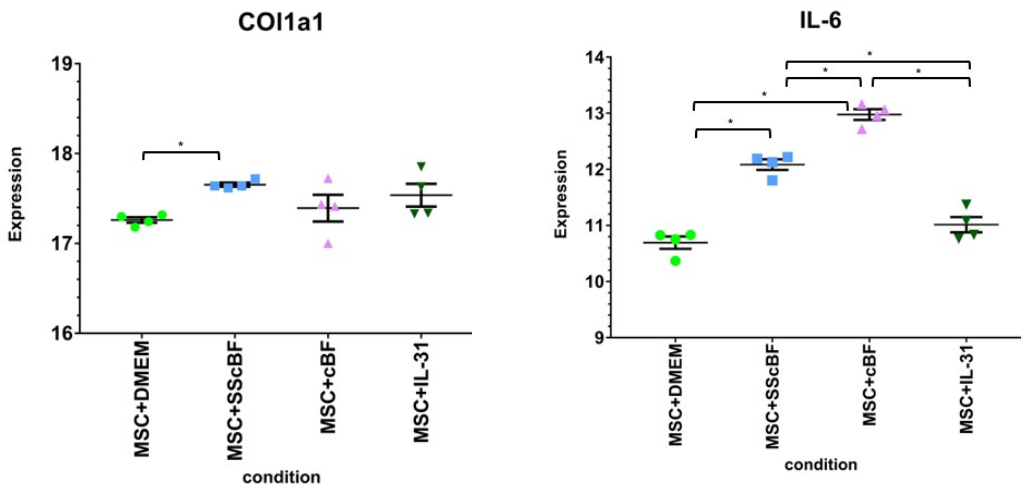

***Figure 6.6* SSc blister fluid increases expression of ACTA2, CEMIP, CSRP2, CTGF, ALCAM, COL1A1 and IL6 in MSCs measured by RNAseq.** *SSc blister fluid (SScBF) induces ACTA2 expression more than control media baseline (DMEM) ($p=4.31x10^{-7}$). Healthy control blister fluid (cBF) also results in ACTA2 expression (p=0.00052). CEMIP expression is increased by both SScBF and cBF compared with DMEM ($p=4.47x10^{-112}$ and $p=9.95x10^{-121}$) and IL31 ($p=2.23x10^{-89}$ and p=0.02203). SScBF induces more CSRP2 than DMEM ($p=1.97x10^{-34}$), cBF (p=0.00324) and IL31 ($p=7.39x10^{-34}$). SSc blister fluid is responsible for increased expression of CTGF compared with DMEM ($p=4.07x10^{-9}$) and IL31 (p=0.002604). cBF also induced CTGF expression higher than baseline (p=0.000188). No significant difference was seen in CTGF expression between SScBF and cBF (p=0.385). cBF induced ALCAM more than DMEM ($p=5.08x10^{-8}$), SScBF (p=0.000595) and IL31 ($p=4.08x10^{-23}$). SScBF stimulates ALCAM expression more than DMEM ($p=5.08x10^{-8}$) and IL31 ($p=4.46x10^{-7}$). Collagen type 1a1 (COL1a1), is stimulated by SScBF only (p=0.0302). Il6 expression is increased by cBF compared with DMEM ($p=8.5x10^{-21}$), SScBF ($p=3.3x10^{-7}$) and IL31 ($p=2.12x10^{-40}$). SScBF also increases IL6 expression compared with DMEM ($p=8.5x10^{-21}$) and IL31 ($p=3.9x10^{-12}$). *p<0.05.*

ACTA2 gene expression of α-SMA was confirmative of the Western blots and qPCR assays conducted investigating SSc blister fluid effect on MSCs (Figure 6.6). As expected SSc blister fluid was responsible for the highest induction of α-SMA ($p=4.31x10^{-7}$). Healthy control blister fluid and IL31 had similar effects on α-SMA expression, again reflective of the Western blots and qPCR assays for α-SMA expression *in vitro*. Also, all treatments expressed α-SMA more than serum controls. While this could indicate common factors between SSc

and healthy control blister fluid, possibly found at higher concentrations in SSc blister fluid, this cannot be fully explained by higher IL31, since the IL31 effects on α-SMA were only partially evoked compared to the full effect seen with SSc blister fluid.

As seen in dermal fibroblasts, SSc blister induced expression of *CEMIP* (Figure 6.6), the protein involved in cell migration, however, contrary to the effects on fibroblasts, healthy control blister fluid also induced a very similar amount. As such, it is difficult to conclude an SSc blister fluid specific protein responsible for this. One explanation is a common factor in both SSc and healthy control blister fluid, possibly found in higher concentrations in SSc blister fluid, but the difference in response between the two cell types could be down to their sensitivity to this factor, possibly a different amount of receptor expression. IL31 had no effect on *CEMIP* expression by MSCs (p=0.42203).
As with dermal fibroblasts, MSCs responded to blister fluid by stimulating expression of IL6. Intriguingly in MSCs, healthy control blister fluid had more of an effect on IL6 expression. With inflammation and fibrosis being almost oppositely occurring phenomena, one theory is that SSc blister fluid could contain factors more conducive to inducing fibrogenic responses whereas the act of taking blister fluid from healthy individuals itself is causation of a wound and warrants an inflammatory response. The blister fluid sampling method, although minimally invasive, may be inducing some degree of tissue damage and eliciting innate responses even in normal skin. Again, IL31 had no effect on IL6 expression (p=0.46367).

CSRP2 (cysteine and glycine rich protein 2) is a gene that was not found to be differentially expressed in dermal fibroblasts. It is documented to be a gene overexpressed over 2-fold more than baseline when MSCs are chemotactically activated by CXCL12 (Stich et al. 2009). This could be one mechanism occurring during MSC migration to wound sites, or over a scratch as modelled *in vitro.* SSc blister fluid induced the highest *CSRP2* expression when compared with control media in comparison to the other treatments ($p=1.97x\ 10^{-34}$) (Figure 6.6).

Western blots in Chapter 5.2 show that after α-*SMA, CTGF* was the next most differentially expressed pro-fibrotic protein of the proteins assayed. This was also shown in the RNA sequencing data with SSc blister fluid inducing expression of CTGF more than any other treatments and significantly higher than control media and IL31 ($p=4.47x10^{-9}$ and $p=0.0076$ respectively) (Figure 6.6). Since CTGF can be induced by PDGF and considering PDGF is increased in SSc blister fluid, it is not surprising that SSc blister fluid would induce expression of this pro-fibrotic protein. Yet, it is one explanation to how MSCs respond to the increased growth factor levels in SSc microenvironments and exacerbate the fibrogenic pathogenicity. There is an interesting contrast between these results and the results obtained with fibroblasts, which did not induce CTGF in response to SSc blister fluid. CTGF is considered a key fibrogenic growth factor in SSc and a biomarker of fibrosis in the disease, and the induction in MSCs by SSc microenvironment may be an important finding.

ALCAM is a cell adhesion gene expressed on stromal pluripotent cells. It is also known as CD166 (Kim et al. 2017). The pattern of differential expression of ALCAM is strange. While control media and IL31 treated MSCs express similar low levels of ALCAM, blister fluid treatment significantly upregulated the expression, particularly healthy control blister fluid which is a better inducer of ALCAM than SSc blister fluid ($p=0.000595$) (Figure 6.6). ALCAM positive cells have been found to have a lower proliferative capacity than ALCAM negative cells, and are also more committed to the myofibroblastic lineage. This finding goes against the theory that SSc blister fluid primes MSCs for myofibroblast commitment more than healthy control blister fluid. Furthermore, ALCAM positive stromal cells are less able to function as epithelial support cells than ALCAM negative cells. In the case of SSc this could be MSCs abandoning their posts as homeostatic maintainers in order to play a more assertive role in pathogenesis (McQualter et al. 2013).

While SSc blister fluid does not have a large effect on collagen type I protein expression (Chapter 5.2), investigating RNA expression may be more

insightful. Like Western blots, the RNA sequencing analysis showed modestly increased *COL1A1* expression in response to SSc blister fluid (Figure 6.6). This was significantly higher than baseline expression under control media conditions (p=0.0302), but was not supportive of MSCs being the sole or main secretors of the excessive collagen deposition responsible for dermal thickening.

Increased IL31 concentrations in SSc blister fluid can be hypothesised to result in increased IL6 expression by MSCs. While blister fluid did indeed increase IL6 expression, this cannot be due to the elevated IL31 in SSc blister fluid for two reasons. The first is that IL31 treatment alone did not have an effect on IL6 expression, and secondly, healthy control blister fluid, found to have less IL31 than SSc blister fluid, was better at inducing IL6 expression of MSCs. Whilst in fibroblasts, both derivations of blister fluid are equally good at inducing IL6 expression (Figure 6.2), MSCs seem to respond differently (Figure 6.6).

SSc blister fluid seems to have no effect on TGFβ expression, nor do other treatments studied (Figure 6.7).

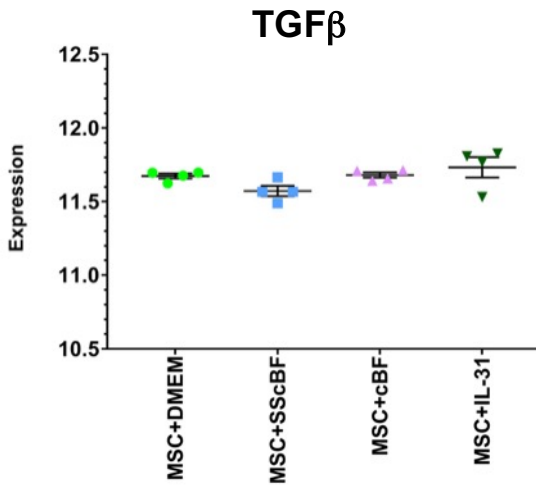

Figure 6.7 TGFβ RNA expression is not affected by SSc microenvironment treatments in MSCs. *SSc blister fluid (SScBF) did not affect TGFβ expression compared with control media (DMEM p=0.3315), healthy control blister fluid (cBF p=0.4785) or IL31 (p=0.06917). cBF also had no effect on expression compared with DMEM (p=0.99099) or IL31 (p=0.7977). Likewise, IL31 had no effect (p=0.9361). *p<0.05.*

Now, considering that TGFβ is not found free-floating in serum, it is unlikely that it will be increased in blister fluid, even if its effects in SSc are prominent. TGFβ is typically found associated with LAP on its C-terminus, making it physiologically silent until a signal transduction event results in dissociation from LAP, allowing TGFβ to act on its receptor (Khalil 1999). An increase in both the latent and free form of TGFβ is likely to be difficult to measure. When in its latent form, it cannot act on its receptors and therefore cannot have any effect on MSCs. This is likely the explanation for a lack of response to blister fluid. Other studies in this thesis (Chapter 5.6.2) have shown that TGFβ treatment significantly affects MSC migration, contraction and α-SMA expression. However, in future studies it would be useful to assay free and total TGFβ in the blister fluid samples.

NT5E is a marker of MSCs and is also known as CD73. MSCs are not considered to be MSCs without surface expression of this marker. As such, theoretically, inhibition of this protein is indicative of MSCs losing their MSC-like phenotype, and possibly differentiating. Interestingly, polymorphisms resulting is reduced activity of the enzyme encoded for by *NT5E* (ecto-5' nucleotidase) have been associated with vascular calcification (Kochan et al. 2016). SSc blister fluid treatment of MSCs significantly reduces expression of NT5E ($p=0.00068$). Healthy control blister fluid also inhibits its expression but does not achieve significance, while IL31 has no effect on MSC NT5E expression ($p=0.0007$) (Figure 6.8).

In addition to *NT5E* gene expression being downregulated by SSc blister fluid, *VEGFC* is likewise affected (Figure 6.8). This gene encodes a protein involved in neo-angiogenesis and vasculogenesis, two processes considerably affected and disrupted in SSc. Raynaud's Phenomenon results in symptoms caused by lack of vasculogenesis in acral regions. Expression of VEGFC is inhibited by SSc blister fluid ($p=0.000247$) and this suggests that SSc microenvironment discourages renewal of vasculature. Further, this is not affected by IL31, indicating that while IL31 is an important part of the SSc microenvironment, it is by no means the sole culprit of SSc microenvironment pathogenicity.

Calcinosis is prevalent in SSc and is a result of increased osteogenic differentiation. Contradictory to this finding, VEGFC induces MSC differentiation into osteoblasts (Murakami et al. 2017). This can be explained by the possibility that MSCs have to commit to either a pro-osteogenic or pro-fibrogenic differentiation pathway. How this commitment is determined is unclear.

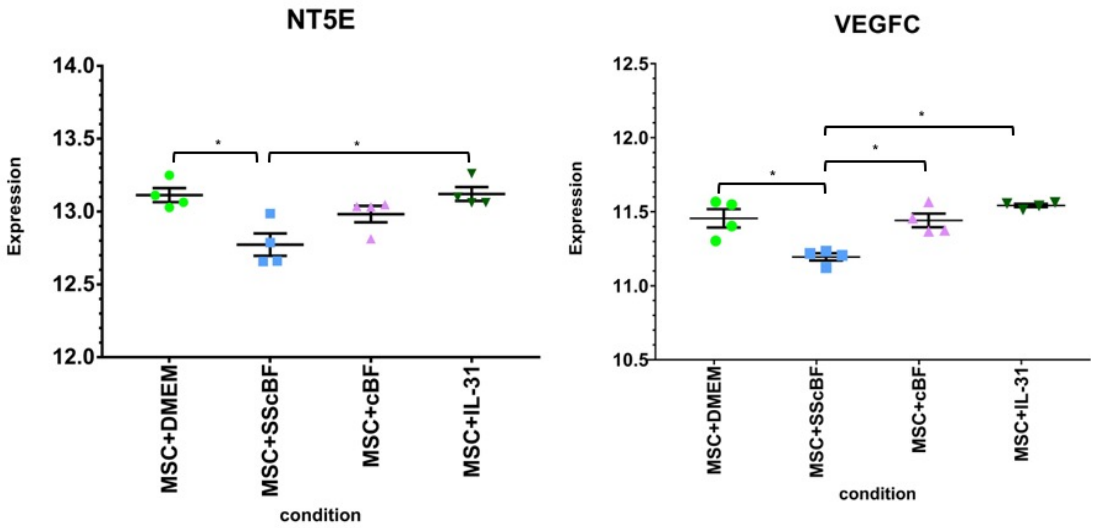

Figure 6.8 ***SSc blister fluid inhibits NT5E and VEGFC expression in MSCs.*** *SSc blister fluid (SScBF) inhibits NT5E expression more than control media (DMEM p=0.00068) and IL31 (p=0.000739). VEGFC expression is decreased by SScBF more than DMEM (p=0.000247), healthy control blister fluid (cBF p=0.0039) and IL31 ($p=3.9x10^{-7}$). *p<0.05.*

Differential expression of these genes were put into context using pathway analysis described in Chapter 6.4.

6.4 Ingenuity Pathway Analysis of SSc microenvironment treatments

Pathway analysis was performed using Ingenuity Pathway Analysis (IPA) software to highlight predicted pathways involved, in the context of their physiological significance. This software uses the differentially expressed genes from the RNAseq data, inputted as FASTQ files, and with its own database called Knowledge Base, predicts the pathways activated or

deactivation, networks of molecules involved and biological function. These predictions are based on existing literature and experimental data. For the purpose of this study, only significantly changed RNA molecules were analysed where $p<0.05$. IPA analysis compares two FASTQ files, and in this study, two comparisons were made; 0.2% media vs SSc blister fluid treated MSCs and, SSc blister fluid vs healthy control blister fluid treated MSCs. These comparisons were chosen to elucidate the specific effects of IL31 on fibroblasts, and compare it to the effects of SSc blister fluid on MSCs. Then to compare the different effects of SSc and healthy control blister fluid on the MSC expression profile.

One of the most beneficial features of the IPA software is its ability to fit the differentially expressed genes into a known canonical pathway and calculate how well the RNAseq data fits into said pathways. Both upregulated and downregulated pathways can be detected as well as the percentage of overlap, depicting how many differentially expressed genes overlap with known genes of the canonical pathway. Significance is calculated by the software as –Log (p-value), and as such, all values above 1.3 are significant, indicating $p<0.05$. Z-scores are computed by the software representing the level of matching between the predicted relationship direction (activation/deactivation) and the observed gene expression. A Z-score of >2 or <-2 is calculated as significant matching.

Figure 6.9 illustrates the top canonical pathways found to be affected by SSc blister fluid on MSCs with regards to the differential expression of RNA. The most significantly activated pathway in response to SSc blister fluid is the integrin linked kinase pathway (ILK). This pathway has a Z-score of -2.52982 with 21.9% overlap between the predicted genes involved and the observed genes. Some of these genes include *ACTA2* and integrins. ILK pathway has been implicated in cell adhesion, motility and wound healing.

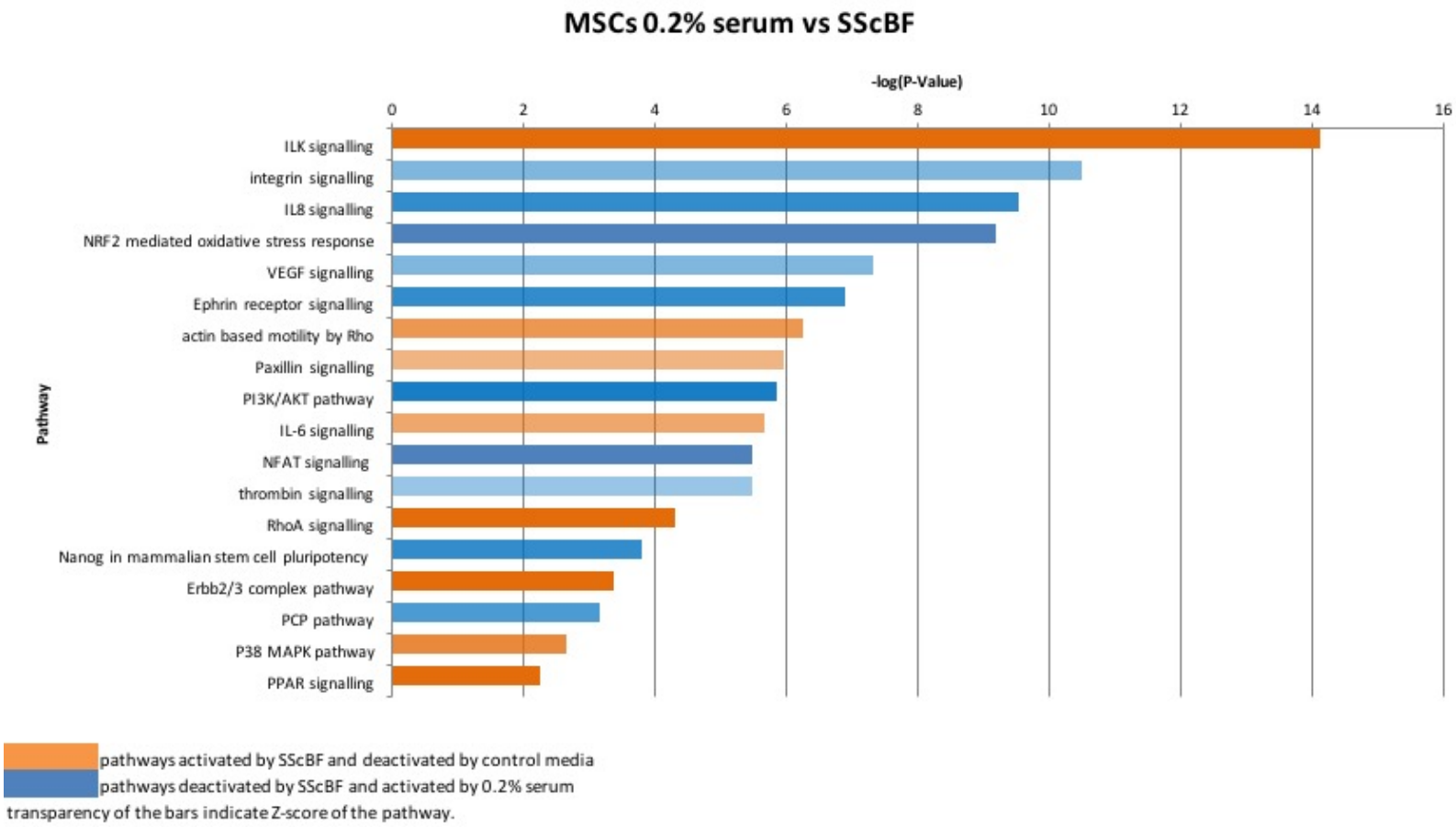

Figure 6.9 ***IPA pathway analsysis of canonical pathways induced in 0.2% serum vs SSc blister fluid treated MSCs.*** *The pathways identified in 0.2% serum or SSc blister fluid(SScBF) treated MSCs were compared. The barplot orders the most activated/deactivated pathways in both conditions. Orange bars depict pathways upregulated by SSc blister fluid. Blue bars depict pathways deactivated by SSc blister fluid. X-axis measures the significance of the activation/deactivation. Transparency of the bars illustrates the z-score calculated, darker bars have darker z-scores meaning more activation/deactivation.*

The VEGF pathway is decreased in response to SSc blister fluid with 21.4% of the known genes of this pathway found differentially expressed in the RNAseq dataset (Figure 6.9). Since vasculogenesis is decreased in SSc and the VEGF pathway is essential for this, inhibition of this pathway in response to SSc microenvironment allows for the conclusion that factors of the soluble microenvironment, even at such high dilution factors, are potent enough to mimic the loss of vasculogenesis of SSc.

Pathways involved in cell migration are upregulated by SSc blister fluid (Figure 6.9). Both actin cytoskeleton remodelling and Rho based motility are pathways found to be significantly involved in MSCs treated with SSc blister fluid. α-SMA was calculated to be involved in both processes. Moreover, MSC differentiation into adipocytes and osteoblasts is regulated via RhoA, which in turn is increased by SSc blister fluid. RhoA has influence on cell shape, signalling and cytoskeletal integrity. Signalling via ROCK, RhoA determines cell shape drives stem cell commitment (Hutchings et al. 2017).

Supportive of MSC differentiation in SSc microenvironments, the NANOG pathway is both significantly involved, and significantly deactivated (Figure 6.9). NANOG is associated with pluripotency of mammalian cells, thus, its inhibition indicates possible loss of pluripotency and therefore, MSC differentiation.

Induction of PPAR pathway by SSc blister fluid was seen (Figure 6.9). The PPAR pathway is involved in lipid metabolism where activation of this pathway induces adipogenesis. Since in SSc, a loss of subcutaneous fat is observed, and *in vitro* adipogenic differentiation assays suggest inhibition of adipogenesis, it seems that this pathway is influenced by more than the soluble factors of SSc blister fluid alone. The software then is able to put these pathways into biological context and predicts function of the pathway together with the genes involved, found differentially expressed in the RNAseq dataset (Table 6.1). The number of molecules involved in each function out of the 1218 significant genes is illustrated in the table.

Categories	Functions	Diseases or Functions Annotation	p-Value	Z-Score	# Molecule
Cell Death and Survival	apoptosis	apoptosis	2.44E-39	-0.103	381
Cellular Assembly and Organization, Cellular Function and Maintenance	organization	organization of cytoplasm	1.49E-27	-0.921	234
Tissue Development	growth	growth of epithelial tissue	3.15E-22	-0.757	119
Cellular Assembly and Organization, Tissue Development	fibrogenesis	fibrogenesis	1.34E-17	-0.42	77
Organismal Injury and Abnormalities	wound	Wound	6.22E-16	-0.204	49
Cellular Movement, Connective Tissue Development and Function	cell movement	cell movement of fibroblast cell lines	1.69E-15	-0.495	48
Cellular Assembly and Organization, Cellular Function and Maintenance, Tissue Development	formation	formation of actin stress fibers	7.15E-15	-1.193	50
Cardiovascular System Development and Function, Cellular Movement	migration	migration of vascular endothelial cells	2.42E-14	-1.335	39
Cellular Development, Connective Tissue Development	differentiation	differentiation of osteoblasts	3.51E-14	0.217	53
Connective Tissue Development and Function, Tissue Morphology	quantity	quantity of connective tissue cells	1.23E-11	-1.309	48
Cellular Movement	cellular infiltration	cellular infiltration	2.65E-10	-1.103	68
Cell-To-Cell Signaling and Interaction, Cellular Assembly and Organization, Cellular Function and Maintenance	formation	formation of focal adhesions	1.24E-13	-1.53	35
Organismal Development	growth	growth of vessel	1.81E-11	1.871	32
Cellular Development, Connective Tissue Development	differentiation	differentiation of adipocytes	1.59E-09	0.069	43
Cellular Development, Connective Tissue Development	differentiation	differentiation of chondrocytes	4.23E-09	0.719	24
Cardiovascular System Development and Function	vascularization	vascularization	5.99E-12	0.383	46

***Table 6.1* IPA Biological context analysis of differentially expressed genes in MSCs treated with SSc blister fluid.** *Rows highlighted in orange are functions predicted to be upregulated by SSc blister fluid while those in blue are downregulated. The P-value takes into consideration the number of genes observed out of the number of genes predicted to be involved in each function. Z-scores >2 or <-2 depict significant deactivation or activation by SSc blister fluid respectively.*

Aside from predicting individual pathways involved in the response of MSCs to SSc blister fluid, the software created networks of focus molecules, known as nodes, linked together based on biological connectivity. A score is algorithmically computed for each network based on the number of nodes, their significance, and directionality. The score indicates the likelihood of connected nodes being generated by chance. A score of above 2 means that there is less than 1 in 100 chance of this. Nodes are either green or red, with green indicating activated by SSc blister fluid, and red, deactivation by blister fluid. The intensity of the colour of each node is a representation of the Z-score, i.e. the directionality of the connection, and how significant it is. Uncoloured, grey nodes are of molecules that were not found to be differentially expressed in the original RNAseq dataset and have been filled in by the software to complete the network. The shapes of the nodes represent the predicted function of that gene including enzymes, protein, receptors, kinases, cytokines, growth factors and transcription factors.

Figure 6.10 shows two significant networks predicted by the software when comparing expression of 0.2% serum and SSc blister fluid treated MSCs. Figure 6.10A is a network predicted to be involved in connective tissue and organismal injury, and cell morphology, with a high score of 37, consisting of 33 focus nodes. It is centralised around the growth factor ERBB2. Other factors of relevance to the finding of SSc blister fluid induced cell migration are Rho GTPases, also highlighted in this network. Furthermore, osteogenic differentiation associated genes fit into this network such as *TWIST2.* The second network is focussed around connective tissue growth and development. This pathway is centred around the *CTGF* gene, and together with *Col1A1*, it is clear that SSc blister fluid induces MSC expression of genes highly associated with SSc. MMPs are also part of this network, supporting migration and tissue remodelling, both of which are implicated in the results of the *in vitro* migration and gel contraction assays.

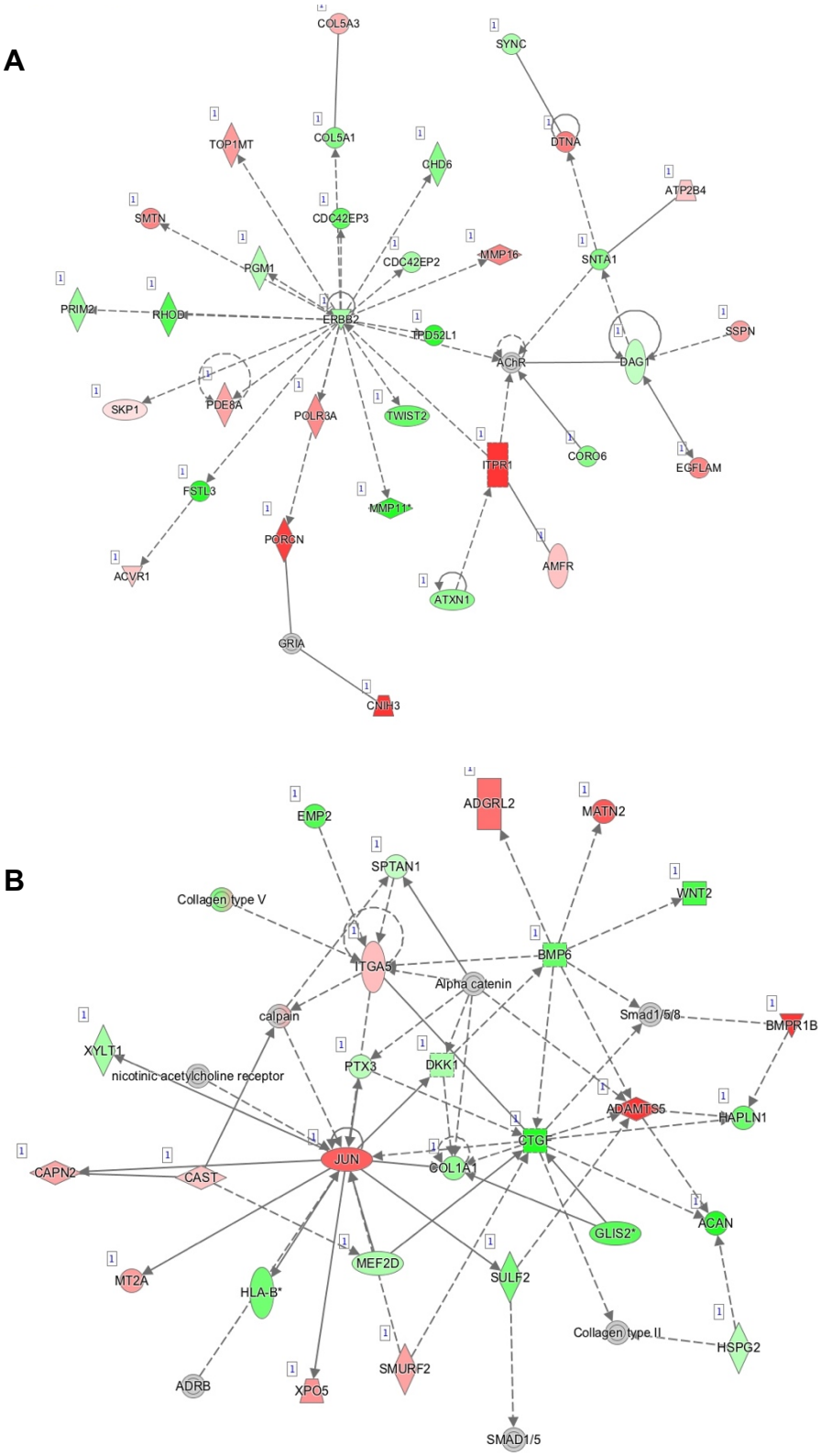

Figure 6.10 ***IPA genetic networks of SSc blister fluid treated MSCs.*** *Connective tissue and organismal injury, and cell morphology pathways are induced by SSc blister fluid (A). Connective tissue development pathways induced by SSc blister fluid illustrated in B. Green nodes are activated by SSc blister fluid, red nodes are deactivated by blister fluid. Grey nodes are involved genes not found to be differentially expressed.*

IPA has the useful ability to predict upstream regulators that explain the differential expression observed in the RNAseq data. The software uses Knowledge base database to predict biological processes being activated or deactivated by certain molecules and their effects on downstream molecules. P-values calculated by this analysis identify how well the RNAseq measured genes are regulated by a specific regulator and is calculated using Fisher's Exact Test where significance is $p<0.01$. The significance does not take into account directionality of the regulation. This is attributed to the Z-score. This numerical value denotes the activation state of the regulator and together with the activation state of a specific gene, the activation of the pathway can be inferred.

TGFβ was measured to be an upstream regulator of over 100 of the differentially expressed genes analysed. These include *ACTA2, ACAN*, collagen genes, Rho GTPases, *TWIST* genes, *NT5E, IL6* and TGFβ receptors where $p=8.62x10^{-30}$ and Z=-0.372. The negative Z-score indicates activation of the regulator by SSc blister fluid where scores below -2 are considered statistically significant.

The oestrogen receptor is also a significant upstream regulator for *ANXA1, CTGF*, collagen molecules, *NT5E* and MMPs. $P=9.95x10^{-15}$ for this regulation and Z=-1.769. This may be relevant to the increased prevalence of SSc in females.

PPARG was found to be a statistically significant upstream regulator of *ACTA2* and *COL1A1* (p=0.00000105 and Z=1.269) with the directionality of this regulation predicted to be inhibitory. *PPARG* is a gene that encodes a protein involved in lipid metabolism. Inhibition of its downstream molecules may be an important factor regarding the loss of MSC adipogenesis seen in SSc.

To assess the expression differences between healthy control and SSc blister fluid induction, the expression profile of both was compared and analysed. The RNAseq data did not highlight specific genes significantly increased in

only SSc blister fluid although there was a trend towards an increase in pro-fibrotic gene expression. The bar plot in Figure 6.11 shows some of the most significant pathways that differ between healthy control and SSc blister fluid treated MSCs. Blue bars indicate pathways activated by SSc blister fluid and deactivated by healthy control blister fluid, while orange pathways indicate the opposite. The transparency of the bars relates to the Z-scores, with darker bars having more significant Z-scores, indicating directionality of the pathway.

IL6 signalling seems to be more highly activated by healthy control blister fluid than SSc blister fluid treatment (See Figure 6.1, 6.6 and 6.11), SSc blister fluid does induce IL6 but not as much as healthy control blister fluid. This pathway is thought to be responsible for the shift from acute inflammation towards fibrogenesis. If the SSc blister fluid alone is responsible for the fibrogenic effects of MSCs, this pathway may have been activated by SSc blister fluid, on the other hand, it is more likely that for SSc blister fluid to have strong fibrogenic effects, a combination of the soluble factors acting together within the physical microenvironment may be needed.

On the other hand, lipid metabolism by activation of the PPAR pathways was amongst the most significantly activated pathways in response to SSc blister fluid. This further confirms that the loss of adipogenesis in SSc is not merely a downstream catabolic effect and is, in fact, part of the pathology most likely a result of the imbalance between differentiation pathways of MSCs. This is further confirmed by the strong activation of the LXR/RXR pathway (Figure 6.11). This pathway is also involved in lipid metabolism and catabolism and in fact, competes with the PPAR pathway to determine the fate of adipogenesis. Either way, the involvement of MSC adipogenic differentiation regulation in SSc microenvironments cannot be disputed (Wu et al. 2009).

ILK signalling is also a significant pathway, however with a Z-score of zero, no directionality of this pathway could be measured (Figure 6.11). With this pathway being significantly activated by SSc blister fluid when compared with 0.2% serum, it stands to reason that activation of the ILK pathway is a result of a commonality between SSc and healthy blister fluid.

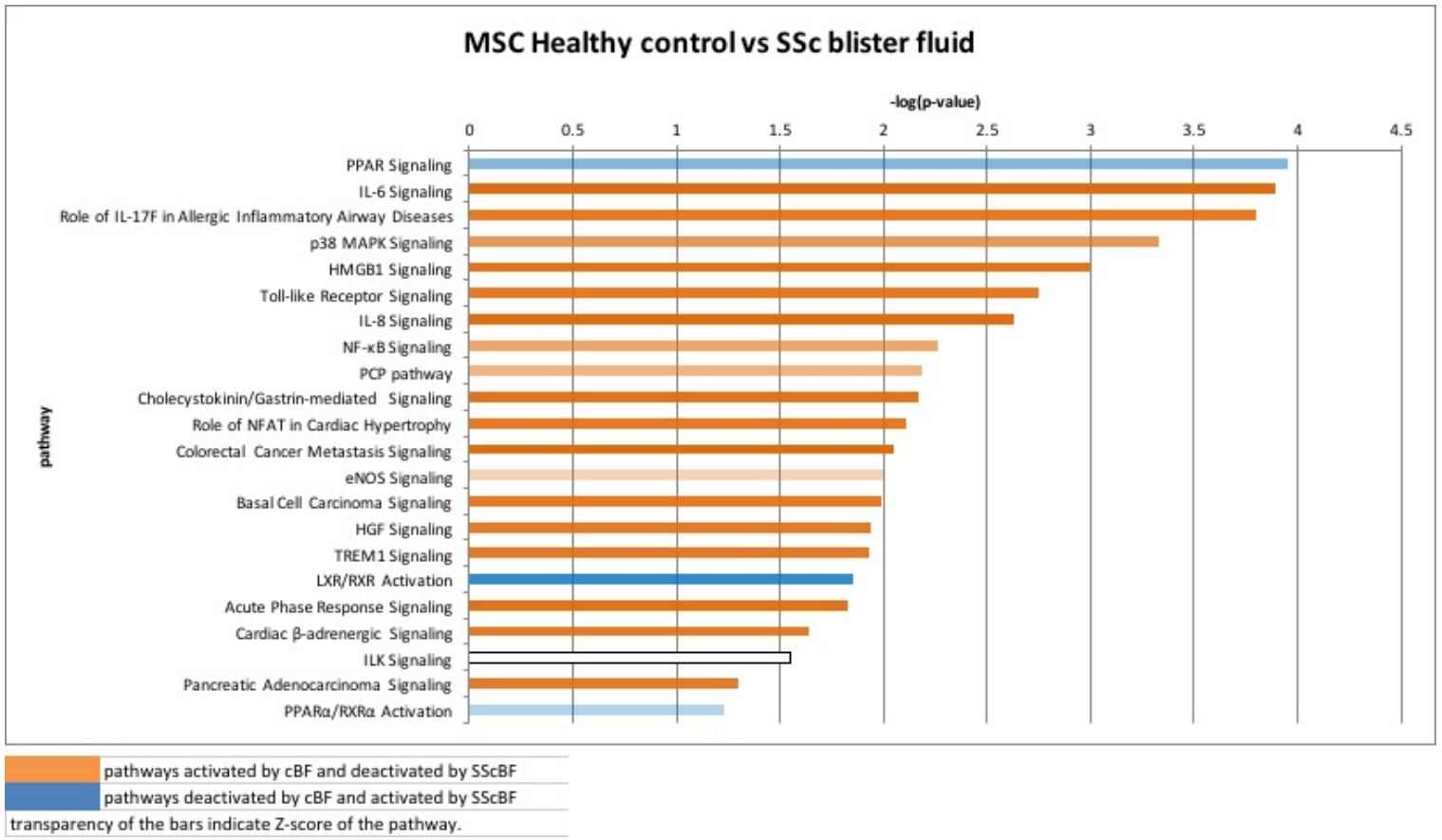

Figure 6.11 ***IPA pathway analysis of canonical pathways in SSc or healthy control blister fluid treated MSCs.*** *Healthy control blister fluid (cBF) induced pathways are highlighted in orange, while SSc blister fluid (SScBF)induced pathways are highlighted in blue. Darker bars indicate higher Z-scores. Length of the bar along the x-axis indicates p-value of overlap between the differentially expressed genes of the RNAseq dataset set, and known genes involved in each pathway.*

Fitting these pathways into biological significance shows that most of the involved functions that differ between the two conditions relate to vasculogenesis and angiogenesis. This is a significant finding and may elucidate the cause of microvascular injury, Raynaud's Phenomenon and lack of vascular repair as a result of SSc. Described in Table 6.2, the biological functions differ between the two treatment conditions. Functions activated by SSc blister fluid include differentiation and proliferation of multilineage progenitor cells, fibrosis and wound healing. All three functions support the hypothesis of this thesis, that SSc blister fluid induces MSCs to differentiate into pro-fibrotic wound healing cells. Furthermore, the functions found to be deactivated by SSc blister fluid included proliferation of endothelial cells. If SSc microenvironments cause endothelial cell damage, it is not surprising that proliferation of these cells is deactivated. As mentioned, many functions regarding the development and maintenance of vasculature were deactivated by SSc blister fluid, including the the formation of new blood vessels.

With regards to upstream regulators, the most interesting finding, was seen when comparing the effects of SSc blister fluid with 0.2% serum, the oestrogen receptor was measured to be a significant upstream regulator of SSc blister fluid induced pathways. With a high Z-score of 2.534 indicating significant activation and a p-value of 2.46×10^{-8} showing a high level of overlap between observed and theoretical pathway activation, this confirms that the higher prevalence of SSc in females may have a cause found in the soluble part of SSc microenvironments.

Categories	Diseases or Functions Annotation	p-Value	Z-score	# Molecules
Cellular Development	differentiation of cells	5.89E-13	3.169	81
Cellular Growth and Proliferation, Organismal Development	proliferation of multilineage progenitor cells	1.28E-07	0.838	9
Organismal Injury and Abnormalities, Tissue Morphology	healing of wound	2.22E-07	1.254	13
Organismal Injury and Abnormalities	Fibrosis	1.03E-08	0.092	29
Cell Death and Survival	necrosis	5.62E-14	0.57	93
Cellular Growth and Proliferation	cell proliferation of vascular endothelial cells	6.74E-07	-0.633	11
Embryonic Development, Organismal Development	development of body axis	7.16E-07	-0.373	40
Organismal Development	formation of vessel	7.25E-07	-0.786	11
Cell-To-Cell Signaling and Interaction, Hematological System	activation of blood cells	7.27E-07	-2.047	27
Hematological System Development and Function, Tissue Morphology	quantity of blood cells	7.54E-07	-1.756	39
Cardiovascular System Development and Function, Organismal Development	angiogenesis	1.53E-16	-2.465	52
Cardiovascular System Development and Function, Organismal Development	vasculogenesis	1.88E-15	-2.615	45
Cardiovascular System Development and Function	development of vasculature	1.83E-14	-2.464	53

Table 6.2 ***IPA biological function of SSc and healthy control blister fluid expressed genes in MSCs.*** *The pathways activated by SSc blister fluid and healthy control blister fluid put into biological context. Blue bars indicate functions associated with genes expressed by SSc blister fluid, and orange those associated with healthy control blister fluid. The P-value takes into consideration the number of genes observed out of the number of genes predicted to be involved in each function. Z-scores<-2 or >2 depict significant deactivation or activation by SSc blister fluid respectively.*

In order to draw comparisons with the effects induced in MSCs by SSc microenvironment factors, and test the theory that MSCs differentiate into fibroblast-like cells, an IPA analysis was conducted comparing the differential expression effects of 0.2% serum and IL31 on healthy dermal fibroblasts (Figure 6.12). The most significantly activated pathways in response to IL31 are integrin, PI3K and IL8 pathways. These are pathways commonly associated with inflammation. Interestingly the PTEN pathway is inhibited, since PTEN itself is an inhibitor of PI3K pathway, the upregulation of PI3K stimulation in response to IL31 may be through inhibition of its inhibitor. In addition to these inflammatory processes, IL31 also seems to trigger pro-fibrotic processes through TGFβ signalling and cell migration through RhoA signalling. The regulation of actin based motility by RhoA explains the enhanced motility of both fibroblasts and MSCs in response to IL31 in the scratch wound assays.

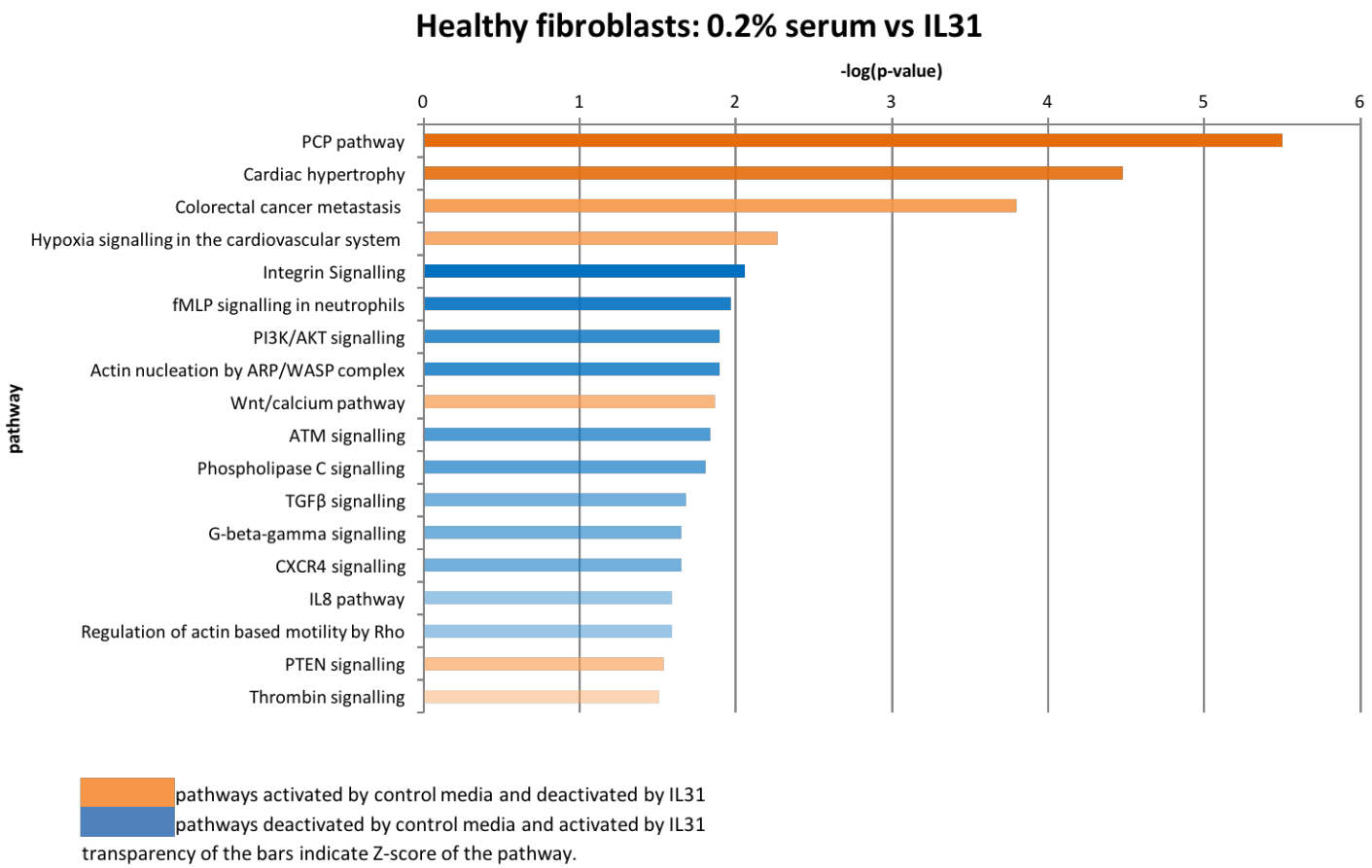

Figure 6.12 ***IPA pathway analysis of canonical pathways activated and deactivated in fibroblasts by IL31 (50 ng/ml) treatment.*** *Healthy dermal fibroblasts treated with either 0.2% serum or IL31. Bars in orange indicated pathways deactivated by IL31 and those in blue, pathways activated by IL31.*

Analysing disease and function of the differential pathways highlighted the effect of lactic acid production (Table 6.3). IL31 induces production of lactic acid, a molecule increased in SSc due to hypoxic conditions. IL31 was also responsible for inducing pathways in dermal fibroblasts predicted to be involved in connective tissue mineralisation, bringing into light its effects on osteogenic differentiation, endothelial and fibroblast cell death. Even though skin thickening is descriptive of SSc, the level of apoptosis, particularly around lesions is high. In Chapter 3, apoptotic and picnotic cell death was observed in only SSc skin biopsies. On the other hand, reflective of the loss of vasculogenesis in SSc, IL31 treatment inhibited pathways involved in angiogenesis and overall homeostasis of the vasculature.

Categories	Diseases or Functions Annotation	p-Value	Z-score	#molecules
Carbohydrate Metabolism, Small Molecule Biochemistry	production of lactic acid	0.00368	-2.021	5
Cellular Growth and Proliferation	proliferation of cells	4.50E-13	-1.589	200
Cell Morphology	mineralization of connective tissue cells	0.000473	-1.358	5
Cell Death and Survival	apoptosis of fibroblast cell lines	0.000175	-1.219	23
Cell Death and Survival, Organismal Injury and Abnormalities	cell death of endothelial cells	0.00612	-0.904	11
Cellular Development, Connective Tissue Development	differentiation of fibroblast cell lines	0.00419	-0.73	12
Cell Death and Survival	apoptosis of fibroblasts	0.000117	-0.694	17
Cardiovascular System Development and Function,	angiogenesis	6.71E-05	0.085	52
Cardiovascular System Development and Function	development of vasculature	6.12E-06	0.106	62
Cardiovascular System Development and Function,	vasculogenesis	0.000631	0.254	41

***Table 6.3* IPA biological function analysis of IL31 treated dermal fibroblasts.** *Functions of pathways activated (blue) and deactivated (orange) by IL31 in healthy dermal fibroblasts. P-value indicates the level of overlap between involved genes from the RNAseq database and genes known to be involved. The Z-score illustrates directionality of the significance, negative Z-scores indicates activation by IL31, positive Z-scores indicate deactivation by IL31.*

Networks created from the differentially expressed gene profile of dermal fibroblasts highlighted two main genetic networks, inflammatory response, cell-to-cell signaling and interaction, and cell movement in cellular development, shown in Figure 6.13. Genes involved in the inflammation network (Figure 6.13A) revolve around IL6 as a central node. IL31 is part of the IL6 family and, therefore, would be expected to activate related genes. Genes involved in cell movement (Figure 6.13B) on the other hand include *ANXA*, *CXCL1* and *dynein* related genes. These centre around ERK1/2, one of the targets of U0126 inhibition used in the scratch wound assays. Both of these networks confirm the IL6-like and migratory inductions of IL31

hypothesised in the models of interaction of SSc. The results overall support an IL6-like effect on fibroblasts, without specific induction of IL6.

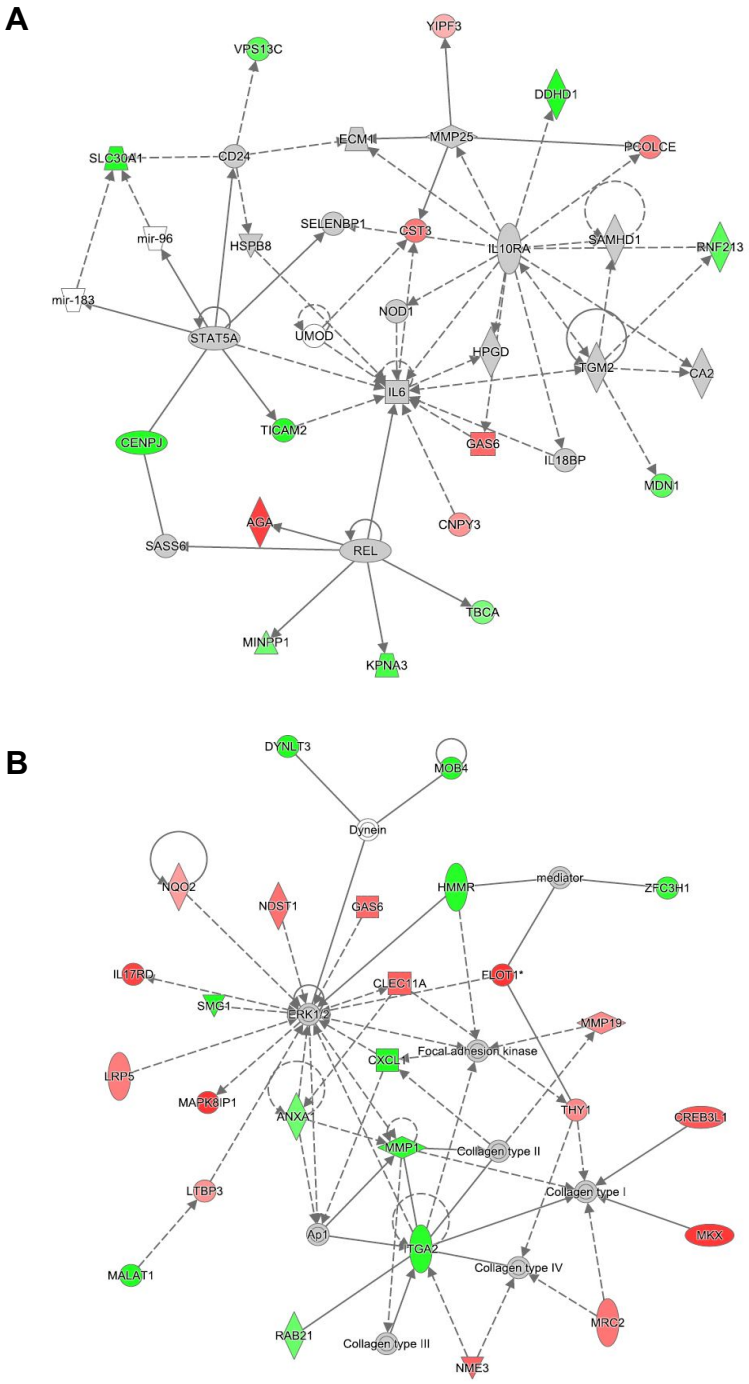

Figure 6.13 ***Networks involved in IL31 treatment of dermal fibroblasts predicted by IPA.*** *Genes involved in the inflammatory response and cell-to-cell interaction, score of 16 with 16 focus molecules (A). Genes involved in cellular movement, score of 33 with 26 focus molecules (B). Nodes in green are activated by IL31. Red nodes are of genes deactivated by IL31. Darkness of the colour illustrates Z-score. Darker colours have more significant directionalities. Grey nodes are filled in by the Ingenuity Knowledge Base.*

The IPA pathway analysis highlighted many pathways associated with SSc, together with many novel pathways that have not been studied yet. This only goes to show the complexity of SSc as a disease with regards to many different cells types, and the difficulty in assigning causality of SSc symptoms to specific pathways. Conversely, it is clear that SSc blister fluid induces a specific set of genes, pathways and networks, many of which are highly associated with fibrosis and differentiation.

Of note, many genes involved in adipogenesis are highlighted by the RNAseq and IPA pathway analysis. Adipogenesis in general is not overlooked in the existing literature with regards to SSc, but the specific effect of MSCs in the adipose metabolism of SSc has not been studied in depth. As such, a novel interaction of SSc blister fluid and MSC adipogenic differentiation potential is studied in the next Chapter.

6.5 Investigating adipogenic differentiation in response to SSc microenvironments

In SSc, a common feature observed is the loss of subcutaneous fat (Bogatkevich 2015). It can be stipulated that the MSCs that reside in subcutaneous adipose tissue, instead of being recruited for adipocyte regeneration and renewal, are otherwise occupied in wound healing and fibrogenesis. If this theory stands true, culturing MSCs in SSc microenvironments should in theory inhibit adipogenic differentiation.

As such, adipose derived MSCs were induced to differentiate into adipocytes by culturing in adipogenic induction media. This media contains high glucose, insulin, indomethacin and IBMX (inhibitor of cyclic nucleotide phosphodiesterases) levels. As a control, MSCs were also cultured in DMEM supplemented with 10% serum. Adipogenic induction media was supplemented with either SSc blister fluid or healthy control blister fluid. To account for differences between individuals, a different sample of blister fluid was used for each of the three replicates. Adipogenic differentiation was allowed to occur for 10 days before staining the cells with Oil Red O staining

solution. This stain is absorbed into adipocytes and, therefore, intensity of staining correlates positively with the level of adipogenic differentiation.

Just looking at the Axioscope microscope images at 2.5x magnification, it is clear that even from as early as day 4, there are some phenotypic morphological changes seen as a result of culturing in adipogenic media, whereas, the cells cultured in 10% serum remained fibroblast-like in morphology. MSCs in adipogenic media became more rounded in shape with fewer elongated projections (Figure 6.14). By day 10 the differences between DMEM treated and adipogenic induction media treated MSCs was stark (Figure 6.15). Cells became oval in shape with a discernable cytoplasm presumably filled with fat, meanwhile MSCs treated with 10% serum showed no change in morphology.

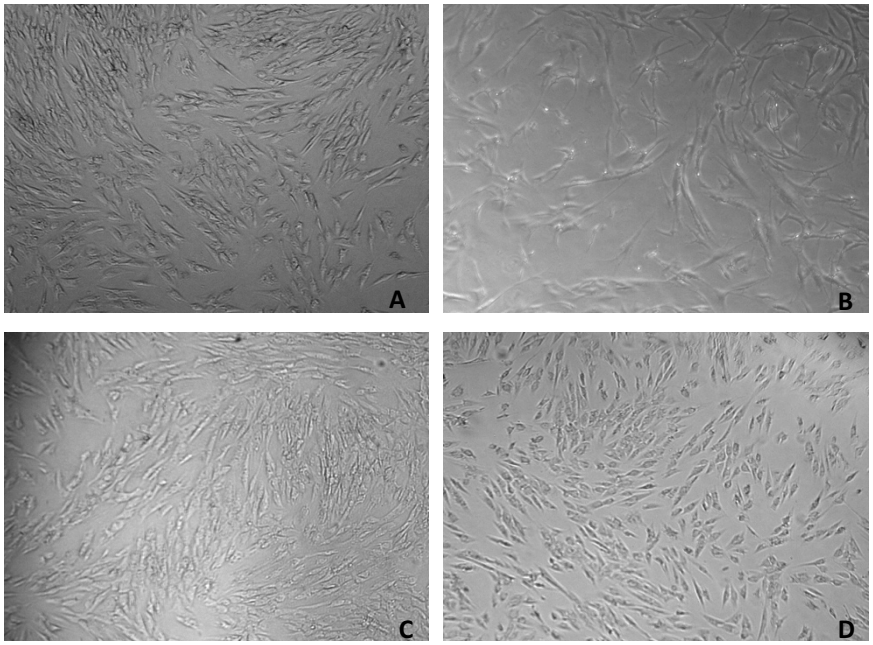

Figure 6.14 ***Day 4 of in vitro adipogenic differentiation of MSCs.*** *Microscope images taken at 2.5x magnification of MSCs cultured in adipogenic induction media only (A), DMEM supplemented with 10% serum (B), adipogenic media + SSc blister fluid (C) or adipogenic media + healthy control blister fluid (D).*

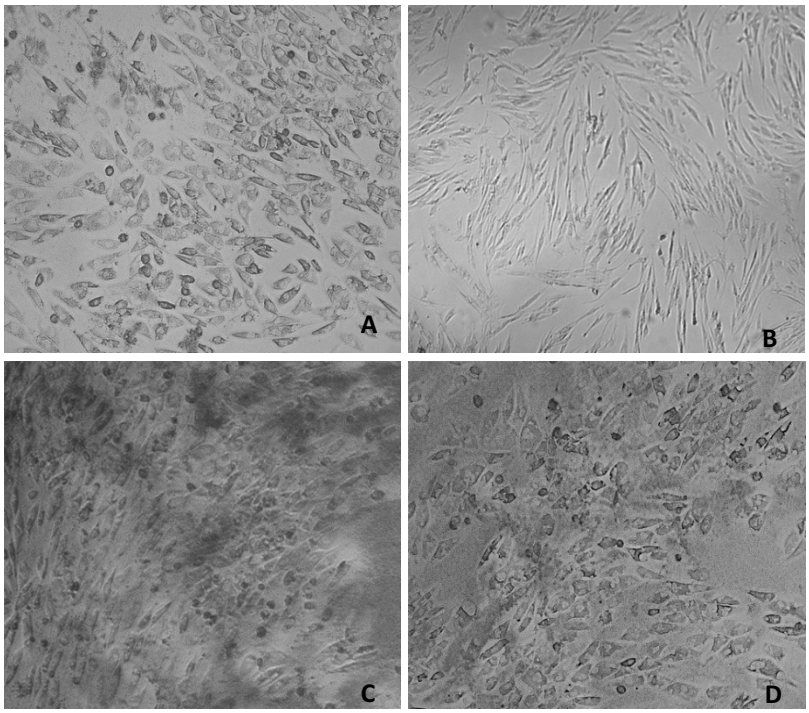

Figure 6.15 ***Day 10 of in vitro adipogenic differentiation of MSCs.*** *Microscope images taken at 2.5x magnification of MSCs cultured in adipogenic induction media only (A), DMEM supplemented with 10% serum (B), adipogenic media + SSc blister fluid (C) or adipogenic media + healthy control blister fluid (D).*

Oil Red O staining allows for semi-quantification of adipogenic differentiation. Since the amount of stain taken up by the cells depends on their differentiation, only adipocytes absorb the stain where measurement of the amount of absorbed stain is a measure of adipocyte presence. The stain is itself red and, therefore, all background staining must be washed off before reaching the stain that has been absorbed into the cells themselves. Absorbed staining was eluted by the addition of isopropanolol and optical density of the eluted stain for each sample was measure at 490 nm. Optical density measurements were corrected against the blank to account for background staining and compared with the non-adipogenic 10% serum supplemented DMEM control to calculate fold change in proportion of adipocytes. Fold changes of over 3 are assumed to indicate adipogenic differentiation (Sadowski et al. 1992).

SSc blister fluid partially inhibited the adipogenic differentiation induced by MSCs cultured in adipogenic media (5.964±1.266 (SEM) to 3.122±0.306

(SEM)) (Figure 6.16). On the other hand, healthy control blister fluid treatment of MSCs did not seem to affect adipogenic differentiation as much. SSc blister fluid did not completely inhibit all adipogenic differentiation and still resulted in a fold change above 3. As such, at this SSc blister fluid concentration (1:125), soluble factors present in SSc blister fluid may not be fully responsible for the loss of adipocytes seen in SSc. However, the fact that some inhibition was observed supports the theory that MSCs are less able to become adipocytes in the SSc microenvironment, possibly being activated as wound healing cells elsewhere.

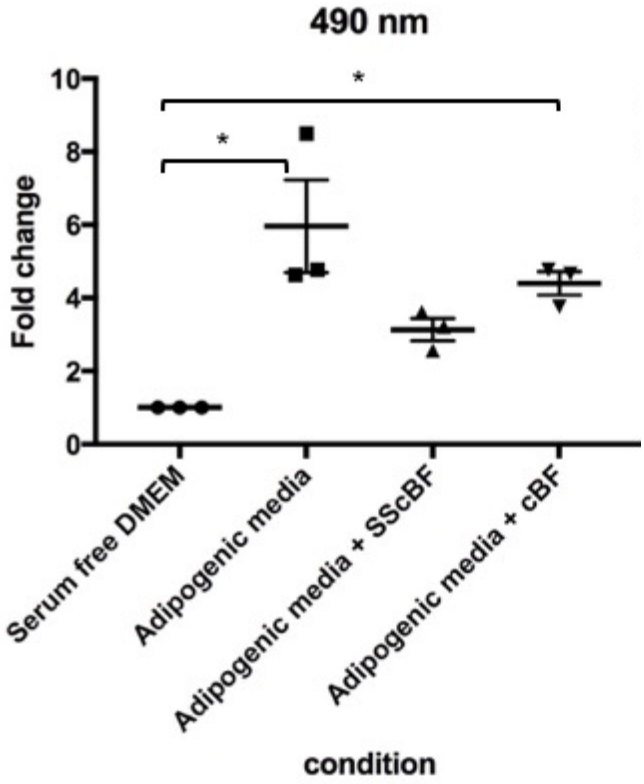

***Figure 6.16* SSc blister fluid inhibits adipogenic differentiation of MSCs.** *SSc blister fluid (SScBF 1:125) reduces adipocyte fold change from 5.964±1.266(SEM) to 3.133±0.362 (SEM). Adipogenic media only and adipogenic media plus healthy control blister fluid (cBF) increased adipocyte fold change significantly (p=0.0035 and p=0.0294 respectively). See appendix for raw data.*

6.6 Conclusion

Taking a more general approach than that of the *in vitro* models, an RNAseq assay attempted to see if not lactate or IL31, which pathways are induced by SSc blister fluid that are different from those induced by healthy control blister fluid.

The most striking result from the RNAseq assay was the difference in expression profile between fibroblasts and MSCs treated identically. Expanding this, MSCs had more distinct responses to SSc blister fluid than dermal fibroblasts. This alone suggests that factors of SSc blister fluid act on MSCs and completely shatter the common thought that MSCs are simply onlookers in SSc and at most, play a secondary role.

SSc blister fluid is responsible for the increased expression of α-*SMA*, *CEMIP* and *IL6* in both MSCs and healthy dermal fibroblasts. The commonalities end there and the two cell types have otherwise opposite expression profiles. In MSCs, CTGF and collagen type I expression was increased in response to SSc blister fluid whereas in fibroblasts, their expression was unaltered and if anything, inhibited by IL31 treatment. IL31 had more of an effect on dermal fibroblasts than MSCs and induced elevated expression of *CXCL5*, *ANXA1* and *IL33* involved in angiogenesis, cell adhesion and inflammation respectively. This hints that even though the elevated IL31 in SSc blister fluid may not have a drastic effect on MSC expression or migration, its importance in SSc pathology should not be overlooked as determined by its strong effect on fibroblasts. On the contrary, in MSCs, SSc blister fluid induced *CSPR1*, involved in MSC migration to wound sites via CXCL12. This migration mechanism is not accounted for by IL31 treatment of MSCs. In fact, IL31 does not seem to have as strong an effect on changing MSC expression profile as it does on dermal fibroblasts. SSc blister fluid had an effect on MSC marker expression. NT5E is an MSC marker, without which an MSC is not deemed to be an MSC. Of note, *NT5E* gene expression is significantly inhibited by SSc blister fluid. It is possible that under SSc blister fluid conditions, MSCs, even as soon as 16 hours after treatment, begin to lose some MSC characteristics

and differentiate. Furthermore, physiologically, MSCs express VEGF molecules as part of their role in endothelial and vascular homeostasis. Expression of *VEGFC* is significantly decreased by SSc blister fluid highlighting the importance of MSCs in the early SSc event of vascular damage. IPA pathway analysis illustrated the complexity of gene expression in response to SSc microenvironments and generated both existing and novel pathways to be associated with SSc pathology. Overall, many pro-fibrotic pathways were predicted by the analysis software, confirming results of the *in vitro* assays at the RNA level. IL31 had its own specific effects on differentiated fibroblasts that also mimic pathways associated with SSc.

Lastly, the loss of subcutaneous fat seen in SSc was modelled by treatment of MSCs with SSc blister fluid. These MSCs partially lost their ability to differentiate into adipocytes, and this inhibition was not seen when MSCs were treated with healthy control blister fluid. This finding is poignant in SSc as this directly links an SSc cause with an SSc effect.

Aside from the role of MSCs in migration and protein/RNA expression as explained in this Chapter, the main role of MSCs as pluripotent stem cells needs to be discussed in the context of SSc. This was illustrated to some extent by the adipogenic differentiation assay, and in the next Chapter will be further examined in relation to osteogenic differentiation. Additionally, whereas the current Chapter mainly focused on the effect of soluble factors on MSC function, it is equally important to address the physical microenvironment of SSc and its effects on MSC function, which is investigated in the next Chapter.

Chapter 7 : Investigating the effect of matrix stiffness on MSCs

7.1 Introduction

Not only is the soluble microenvironment of SSc abnormal, but the physical status of the extracellular matrix is also aberrant. The fibrosis associated with SSc results in significant skin and dermal collagen thickening which, in turn, results in skin stiffness of scores higher than healthy skin when measured using Young's modulus scoring. SSc skin stiffness is measured at between 50-80 kPa compared with the much lower scoring of healthy skin at 4-12 kPa. Skin stiffness of SSc is particularly exacerbated on the face, around the nose and mouth, and forearms (Balbir-Gurman et al. 2002; Sackson et al. 2013).

Skin thickening is a direct consequence of myofibroblast presence due to polymerisation of α-SMA positive contractile fibres pulling the skin tighter. As shown in data presented in Chapter 5, α-SMA is upregulated in MSCs treated with SSc microenvironment soluble representations. For this reason, it is not implausible that these MSCs differentiate into myofibroblasts and are directly responsible for the resultant skin thickening. Furthermore, the excessive expression of collagen type I by MSCs in response to SSc microenvironments can also place MSCs as responsible for the dermal collagen thickening of SSc.

In addition to the soluble factors of SSc causing MSC differentiation into myofibroblasts, the physical stiffness of the extracellular matrix is also thought to play a part, eliciting a positive feedback loop. Stiff matrices could cause MSC to myofibroblast differentiation resulting in collagen deposition causing further stiffness, leading to a continuing cycle. In order for this cycle to ring true, the MSCs must have a way of sensing the stiffness of their surroundings in order to be induced to differentiate. This sensing is thought to occur by MRTFA. As described in Chapter 1, MRTFA is a transcription factor, usually sequestered in the cytoplasm, where upon integrin mediated adhesion and downstream Rho signalling in response to extracellular matrix stiffness, it translocates to the nucleus and functions as a transcription factor for myocardin specific smooth muscle genes such as α-SMA (Asparuhova et al.

2009). Shuttling of MRTFA from the cytoplasm to the nucleus in response to stiff extracellular matrix and mechanical stress is believed to be a product of activation of Rho GTPases at the cell membrane. The result of this is actin cytoskeleton polymerisation into α-SMA positive stress fibres, the conversion of G-actin to F-actin releasing MRTFA, following which MRTFA is transported into the nucleus (Olson and Nordheim 2010).

MRTFA expression has been investigated in the context of SSc and is a mediator of TGFβ-induced myofibroblast differentiation. MRTFA expression in myofibroblasts resulted in increased α-SMA expression even in the absence of TGFβ and when knocking down MRTFA, TGFβ mediated myofibroblast function was decreased, measured by a decrease in α-SMA expression. Further, even under TGFβ conditions, a lack of MRTFA resulted in decreased focal adhesion and contractile force generation (Crider et al. 2011). Additionally, further proving the involvement of MRTFA in myofibroblast differentiation, overexpression of this transcription factor in MRTFA knockout mouse models results in rescue of the otherwise depleted collagen production. Worth noting is that the MRTFA knockout mouse fibroblasts do not produce collagen even upon TGFβ stimulation. This places MRTFA as downstream of TGFβ myofibroblast activation. Moreover, in MRTFA knockout mouse fibroblasts, collagen produced is much looser and thinner in appearance and structure than that produced in MRTFA positive fibroblasts (Luchsinger et al. 2011;Shiwen et al., 2015). Nuclear translocation of MRTFA is found at much higher levels in SSc fibroblasts than healthy fibroblasts indicating a higher baseline levels of nuclear accumulation in SSc, explaining the elevated α-SMA. Nuclear translocation of MRTFA in healthy fibroblasts was present at very low levels and was only increased upon TGFβ stimulation. This indicates that SSc fibroblasts are intrinsically more myofibroblast-like than healthy fibroblasts. Experiments on SSc fibroblasts showed that they contract in floating collagen gels more than healthy control fibroblasts, which can be completely obliterated by the addition of the MRTFA inhibitor CCG-1423. This inhibitor works by preventing the N-terminal of MRFTA from binding to importin α/β1, the shuttling protein responsible for MRTFA localisation (Hayashi et al.

2014). CCG-1423 thereby stops nuclear translocation of MRTFA and in this way inhibits the gene targets of the transcription factor. As such, treating SSc fibroblasts with the inhibitor stopped gel contraction. On the other hand, healthy fibroblast gel contraction was not affected by CCG-1423.

Another SSc symptom is calcinosis. The abnormal deposition of hydroxylapatite and calcium phosphate bone mineral is often associated with SSc disease severity and progression. Studies have implicated IL6 in calcinotic pathology and mineralisation since MSC treatment with IL6 in osteogenic induction media showed increased osteogenic differentiation (Fukuyo et al. 2014). Often the presence of calcinotic lesions coincides with tissue stiffness, occurring at sites of mechanical stress and trauma, and therefore, it is possible that the stiffness of SSc is a contributing factor towards MSC osteogenic differentiation and thus, calcinosis.

7.2 Hypothesis and aims

This Chapter aims to investigate the effect of matrix stiffness on MSC differentiation potential through the following aims:

1) To culture MSCs on Softwell plates of either 4 kPa or 50 kPa stiffness' and measure the RNA expression of myofiboblast pro-fibrotic markers by qPCR.
2) To assess the effect of blister fluid, IL31 and MRTFA pathway on MSC osteogenic differentiation potential.

7.3 Measuring the effect of matrix stiffness of MSC fibrogenic RNA expression

In this Chapter, the effect of tissue stiffness on MSC myofibroblast and osteogenic differentiation is discussed where healthy normal tissue and SSc tissue stiffness is modelled by cell culture on Softwell plates coated with collagen polyacrylamide gels of either 4 or 50 kPa.

Adipose-derived MSCs were cultured on soft (4 kPa) or stiff (50 kPa) Softwell plates and treated with 0.2% serum media, TGFβ or the MRFTA inhibitor CCG-1423. 0.2% serum was used to measure baseline MSC expression levels of the pro-fibrotic α-SMA and CTGF RNA in comparison with *TBP* housekeeping gene by qPCR. TGFβ was used to induce myofibroblast differentiation while CCG-1423 was hypothesised to inhibit the differentiation.

Using α-SMA as a readout of MSC fibrogenic activity (Figure 7.1), it was found that under basal conditions using 0.2% serum media, relatively low levels of α-SMA RNA expression was observed in MSCs on both soft and stiff plates. Treating MSCs with TGFβ significantly induced high α-SMA expression on stiff plates ($p=0.025$) and while TGFβ treatment did induce some α-SMA on soft plates, this was not nearly as much as that seen on stiff plates (stiff mean 101.7 ± 40.67 (SEM), soft mean 4.501 ± 2.417 (SEM), $p=0.036$). On both matrices, the inhibition of MRFTA with the use of CCG-1423 reverted any α-SMA induction and this was particularly noticeable in MSCs cultured on stiff matrices ($p=0.031$).

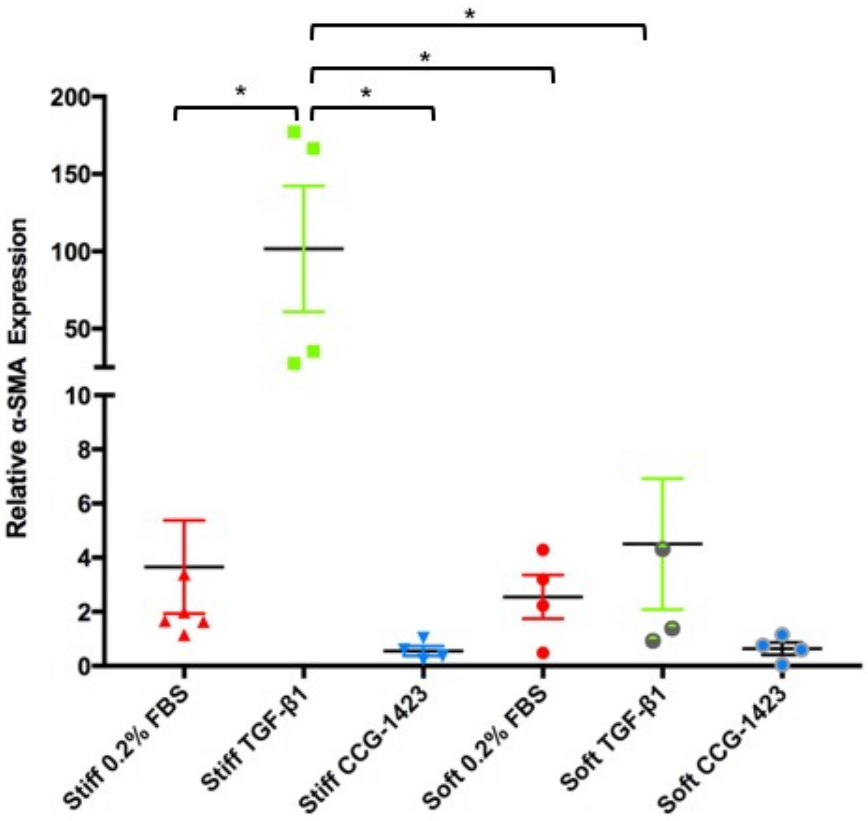

***Figure 7.1* CCG-1423 inhibited the TGFβ mediated α-SMA expression of MSCs.** *MSCs treated with 0.2% serum (FBS), TGFβ (4 ng/ml) or CCG-1423 (10 μM) were analysed for α-SMA RNA expression by qPCR. TGFβ induced more α-SMA on stiff matrices than 0.2% serum on soft and stiff tissues (p=0.025 and p=0.034) and TGFβ on soft matrices (stiff mean 101.7 ± 40.67 (SEM), soft mean 4.501 ± 2.417 (SEM),p=0.036). CCG-1423 inhibited expression on stiff matrices (p=0.031). N=4 for all conditions. TGFβ and CCG-1423 treatments were diluted in 0.2% FBS. *p<0.05.*

Myofibroblasts are known to express CTGF, releasing it into the microenvironment when depositing collagen and therefore, if MSCs are differentiating into myofibroblasts on stiff matrices, they are expected to be expressing CTGF. Like the findings with α-SMA, CTGF expression was most expressed by MSCs when treated with TGFβ on stiff matrices. Further, this was abolished when cells were treated with CCG-1423 indicating that MRFTA in MSCs works downstream of TGFβ during myofibroblast differentiation. Unlike α-SMA, matrix stiffness seemed to be less important in regards to CTGF expression with expression in response to TGFβ being similar on both

soft and stiff matrices, although the induction was less consistent with the soft matrices (2 out of 4 replicates showed induction) (Figure 7.2).

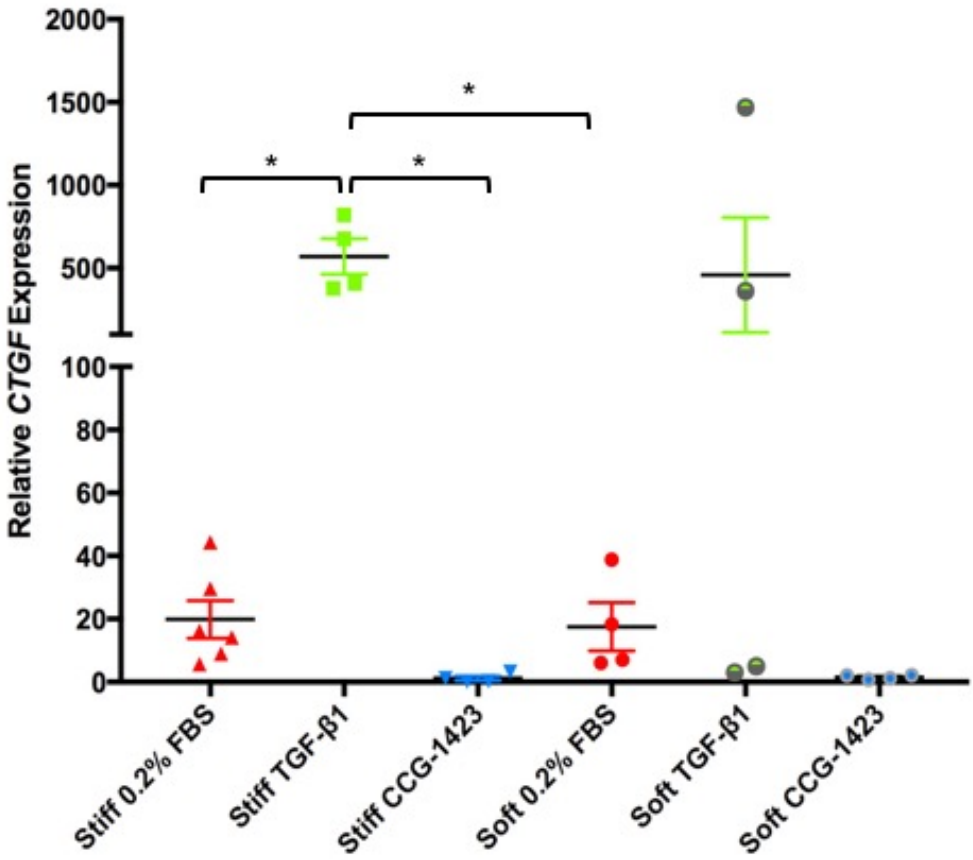

***Figure 7.2** **Matrix stiffness does not affect TGFβ induced CTGF expression of MSCs.** MSCs treated with 0.2% serum (FBS), TGFβ (4 ng/ml) or CCG-1423 (10μM) on soft (4 kPa) or stiff (50 kPa) matrices. CTGF expression was increased by TGFβ on stiff matrices (p=0.043) compared with 0.2% FBS. CCG-1423 inhibited this expression on both soft and stiff matrices (p=0.05). N=4 for all conditions. TGFβ and CCG-1423 treatments were diluted in 0.2% FBS. *p<0.05.*

An obvious further experiment would be to evaluate the effect of adding SSc or control blister fluid to these experiments and measuring the effect on α-SMA and CTGF on stiff and soft matrices. However, time constraints and the scarce and valuable nature of the blister fluid limited these experiments. Since matrix stiffness determines MSC to myofibroblast differentiation to some extent, the

following experiments sought out to determine how it affects MSC to osteogenic differentiation.

7.4 Measuring the effect on matrix stiffness on MSC osteogenic differentiation

With calcinosis being prevalent in SSc, and the ability of MSCs to differentiate into osteoblasts, a differentiation assay was conducted to elucidate the effect of soluble factors on MSC to osteoblast differentiation compared with the effect of the matrix stiffness. Considering experiments have shown that MSCs cultured on stiff matrices preferentially differentiate into osteoblasts, this was put into the context of SSc (Engler et al. 2006).

MSCs cultured on soft or stiff gel matrices mimicking healthy and SSc skin respectively, were subject to osteogenic differentiation in osteogenic induction media (OIM). This culture media contains high levels of dexamethasone and β-glycerophosphate conducive to encouraging osteogenic differentiation. Since IL6 has been found to affect osteogenic differentiation, the family member IL31 was investigated in this assay considering its elevation in SSc blister fluid. The effect of IL31 on osteogenic differentiation was compared with the effect of SSc blister fluid on differentiation to elucidate to what degree IL31 in SSc blister fluid was responsible for osteogenic differentiation of MSCs. Further, to test the effect matrix stiffness has on differentiation, the MRTFA inhibitor CCG-1423 was used to inhibit the ability of MSCs to sense the stiffness of the matrix and react accordingly. Osteogenic induction media was supplemented with TGFβ, IL31, CCG-1423 or SSc or healthy control blister fluid. Treatments continued for 12 days before the cells were stained with Alizarin Red S solution. This stain is absorbed by hydroxylapatite crystals formed by differentiated osteoblasts.

Figure 7.3 illustrates the effects of TGFβ, IL31 and CCG-1423 on MSC osteogenic differentiation. It is worth noting that the collagen matrix of the Softwell plates in the absence of cells also absorbed the red stain and produced a pink or purple background (Figure 7.5) and as such calcification was measured as the presence of individual red speckles. Denser areas of

differentiation were seen as dark red blotches. The most striking observation was the increased number of calcified cells on the stiff plate compared with the soft plate. This was clear even under untreated osteogenic induction media conditions. While TGFβ induced some calcification on soft matrices, this was much more evident on the stiff matrices indicating enhanced TGFβ mediated osteogenic differentiation on stiff matrices. On soft plates IL31 induced little if any osteogenic differentiation. The complete opposite was seen on stiff matrices where IL31 treatment of MSCs resulted in osteogenic differentiation and calcification to levels similar to TGFβ. Fitting with the theory that the stiffness is enhancing differentiation, inhibition of nuclear localisation of MRFTA and, therefore, lack of mechanosensing by CCG-1423 treatment reduced differentiation to negligible levels on both soft and stiff matrices, to levels less than the basal levels with osteogenic media alone.

Since mechanical stiffness has a marked effect on MSC differentiation, blister fluid was added to MSCs cultured in osteogenic induction media on soft or stiff gels in order to better model the effect of the disease microenvironment on differentiation (Figure 7.4). The induction of osteogenic differentiation in response to blister fluid was less obvious than that in response to TGFβ and IL31 alone, although it was clear that SSc blister fluid induced more osteogenic differentiation of MSC than healthy control blister fluid. There was not an apparent difference between induction effects of SSc blister fluid on differentiation between the two stiffness's. On the other hand, healthy control blister fluid had no effect on differentiation on either soft or stiff matrices.

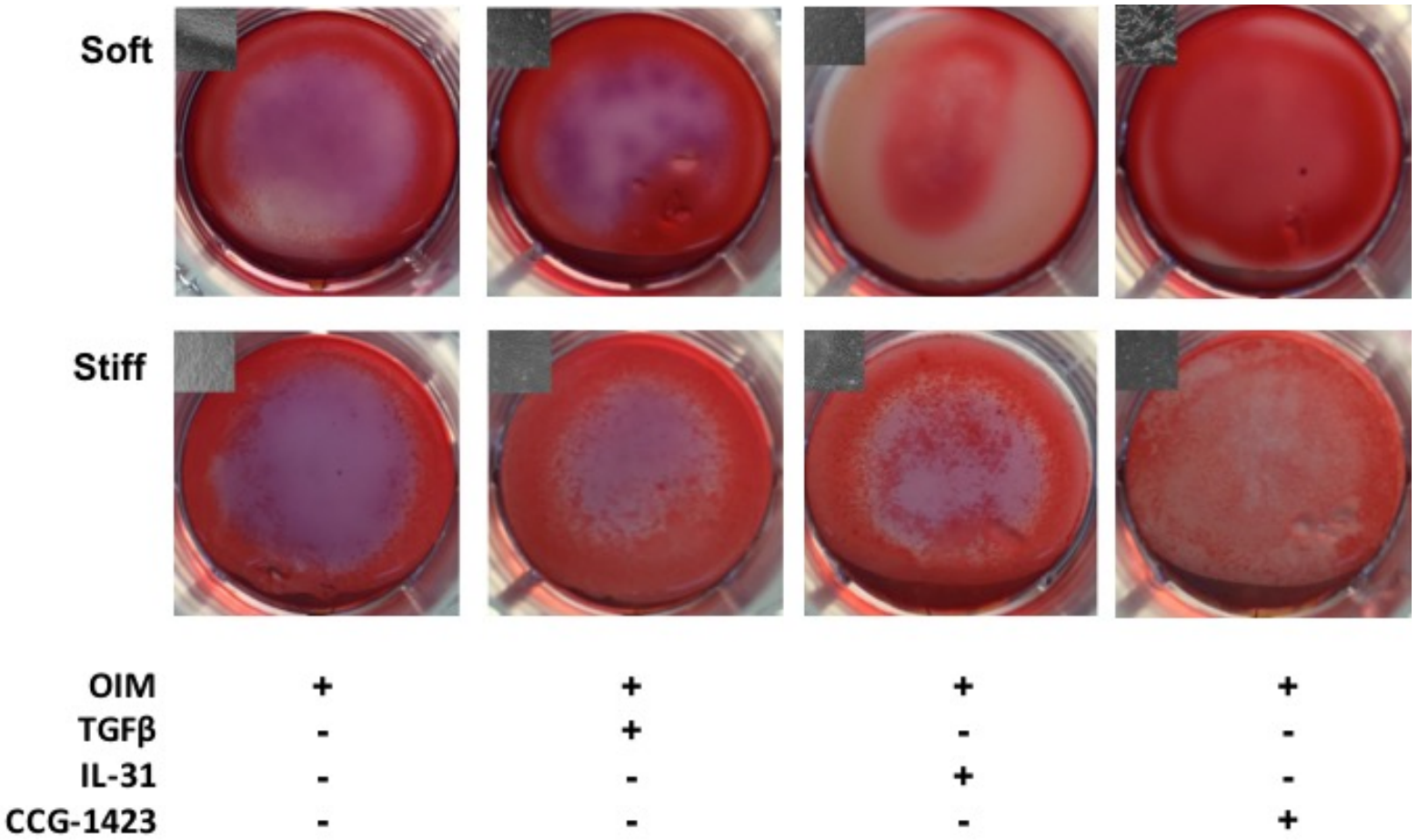

Figure 7.3 ***Osteogenic differentiation of MSCs in response to TGFβ, IL31 and CCG-1423.*** *MSCs were cultured on soft (4 kPa) or stiff (50 kPa) plates in osteogenic induction media (OIM) for 12 days. OIM was supplemented with TGFβ (4 ng/ml), IL31 (50 ng/ml) or CCG-1423 (10 μM). 2.5x magnification light microscope images shown in top left of each image. Individual red speckles indicate osteogenic differentiation of MSCs into osteoblasts stained with Alizarin Red S solution for hydroxyapatite crystals. N=3 for each treatment.*

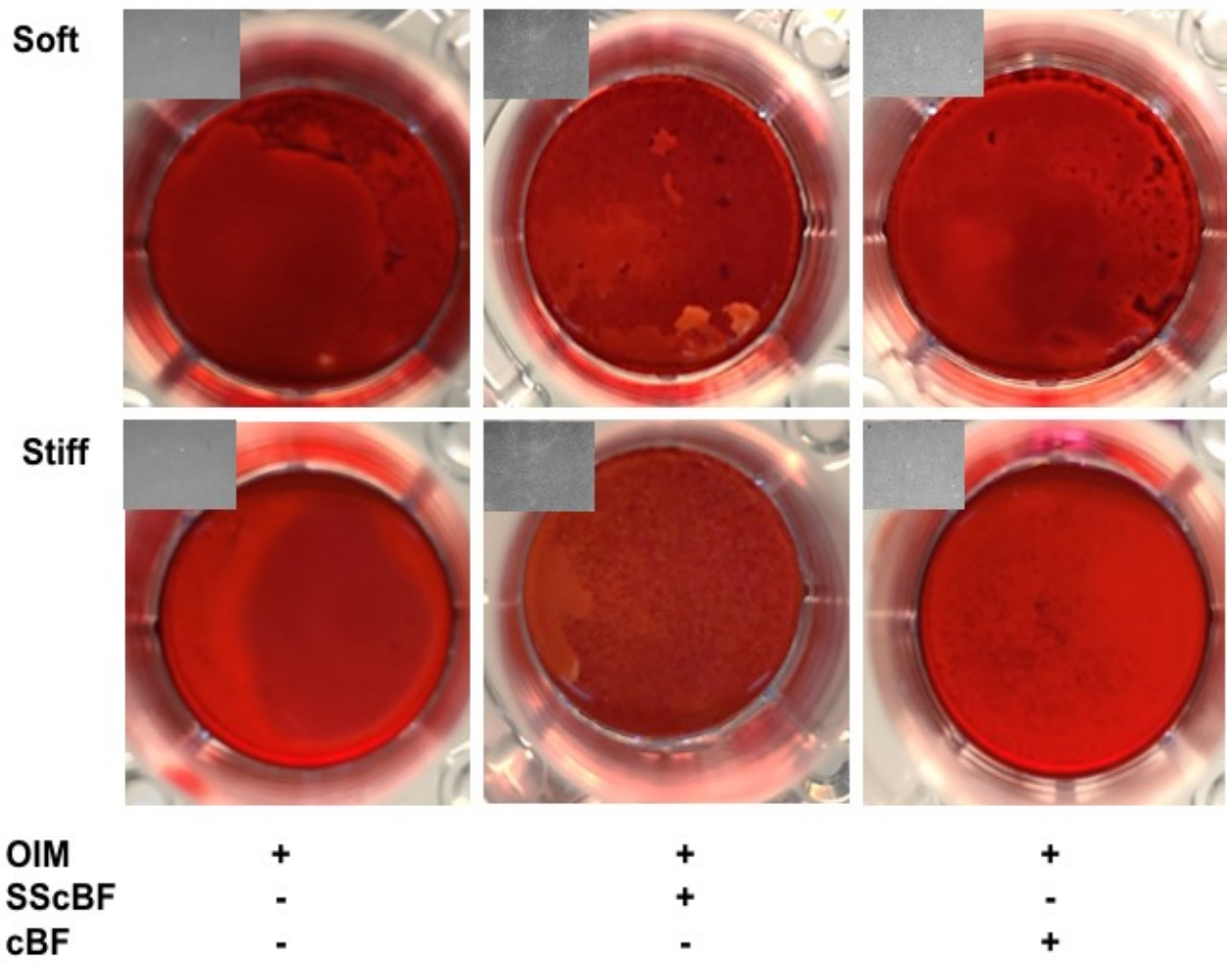

Figure 7.4 ***Osteogenic differentiation of MSCs in response to SSc and healthy control blister fluid.*** *MSCs cultured for 12 days in osteogenic induction media (OIM) with or without SSc or healthy control blister fluid (SScBF, cBF) diluted 1:50. Alizarin Red S staining for osteoblast production of hydroxylapatite crystals show as red speckles. 2.5x magnification microscope images shown in top left of each picture. N=3 for each treatment.*

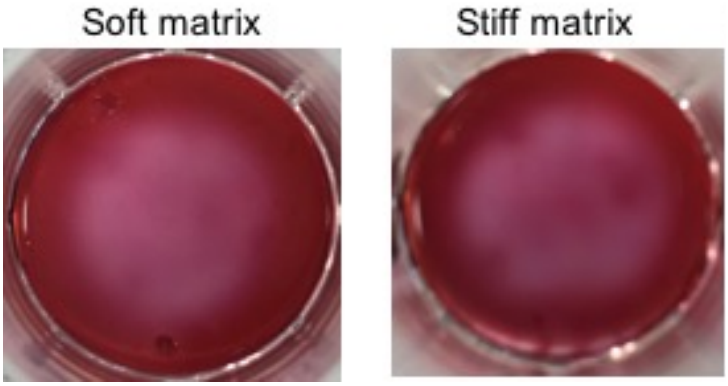

Figure 7.5 ***Background staining of collagen gel matrix of the Softwell plates.*** *Matrix stains red with Alizarin Red S solution without the presence of cells.*

To ensure red speckles were indeed osteoblasts forming from MSCs and that the adipose-derived MSCs were pluripotent enough to differentiate into osteoblasts, healthy dermal fibroblasts were cultured alongside the MSCs on hard plastic (>50 kPa). As expected, no osteogenic differentiation of these lineage committed, fully differentiated cells was observed (Figure 7.6).

Figure 7.6 ***Healthy dermal fibroblasts treated with osteogenic induction media are not able to differentiate into osteoblasts.*** *No red staining is observed when healthy control dermal fibroblasts were cultured in vitro for 12 days in osteogenic induction media.*

7.5 Conclusion

This Chapter sought to investigate the effect of matrix stiffness on the ability of MSCs to differentiate into osteoblasts, bringing together two SSc features, stiff extracellular matrix surrounding cells, and calcinosis.

Firstly, the ability of MSCs to respond to mechanical stress in surrounding extracellular matrix was tested using myofibroblast differentiation as the determinant of mechanosensing. MSCs cultured on stiff matrices respond to TGFβ by significantly upregulating α-SMA expression. Since α-SMA expression is an important myofibroblast marker, this assay not only confirmed that MSCs can differentiate into α-SMA expressing myofibroblast-like cells, but that they are encouraged to do so in stiff microenvironments. The effect of TGFβ on α-SMA expression on soft substrates was much lower. On the other hand, even though CTGF is expressed by myofibroblasts the difference in stiffness between the two substrates did not have an effect on CTGF expression. Expression of both pro-fibrotic molecules was completely inhibited upon CCG-1423 addition. Thus, for expression of these molecules, MSCs need to be able to respond to the surrounding tissue stiffness. With regards for CTGF, although the difference between the substrates was not noticeable, the fact that CCG-1423 inhibited its expression even on soft substrates means that some degree of mechanosensing is not involved in CTGF expression, and it is likely that 4 kPa is sufficient to induce CTGF. It can therefore, be concluded that the TGFβ mediated α-SMA and CTGF expression is a result of MRTFA signalling in MSCs eliciting their expression.

Furthermore, osteogenic differentiation was clearly highly dependent on matrix stiffness since, in all treatment conditions, the MSCs cultured on stiff substrates demonstrated more osteogenic potential than their soft substrate counterparts. As such, it is likely that the stiff collagen layer in SSc creates the optimal environment for MSC osteogenic differentiation into osteoblasts, which in turn, cause deposition of the hydroxylapatite crystals and calcinotic lesions. This theory is reinforced by the observation that calcinosis is more typically

seen in sites of mechanical stress, skin tightening and dermal collagen thickening.

Not only is TGFβ a potent stimulator of pro-fibrotic genes, it is also clearly involved in MSC differentiation on stiff substrates. This highlights the heterogeneity of MSCs where the same signal can elicit multiple responses, context dependent on tissue and soluble microenvironment. It can, therefore, be theorised that the TGFβ prominent in SSc microenvironments acts on MSCs in two very different ways, either myofibroblastic or osteogenic. Perhaps it is the co-signalling of other factors in the microenvironment that determine the pathway the MSC takes.

IL31 has potent effects on MSC osteogenic differentiation on stiff matrices similar to TGFβ. This pro-inflammatory cytokine therefore, has been shown to play a potential role in SSc aside from the established pruritus and inflammatory response. Further, while IL31 effects in SSc are often limited to fibroblasts and immune cells, this study supports the notion that IL31 effects on MSCs could be equally important in SSc pathology.

Most strikingly in these assays is the effect of CCG-1423 and the suggestion that mechanosensing by MSCs is such an imperative phenomenon that inhibiting it may be able to override stiffness signals. CCG-1423 should therefore, be of interest in therapeutic use to prevent stiffness induced myofibroblast differentiation, extracellular matrix escalation and MSC osteogenic differentiation.

This thesis has established IL31 as an important part of the SSc microenvironment constitution. To date IL31 has not been investigated in a mouse model in the context of collagen thickening of SSc. A manuscript prepared by the author of this thesis and co-workers describing a new mouse model for SSc focussing on the effect of IL31 on dermal thickening, collagen cross-linking and expression of SSc related growth factors is presented in the Appendix as supplementary data to this thesis.

Chapter 8 : Discussion

The aim of this thesis was to try and model the interaction between MSCs and SSc microenvironments using a number of different methods. To date, SSc has no specific curative treatments due to a lack of well defined causative mechanisms. For the most part, MSCs are considered to be a tool that can be exploited as an SSc therapy, rather than an integral part of the pathology, and only recently, have there been investigations regarding the role of MSCs in SSc. Even in these studies, the main factor studied is the pluripotency of MSCs rather than their pro-fibrotic and pro-inflammatory potential (Capelli et al. 2017b;Fonteneau et al. 2017). In fact, very little data exists surrounding the behavioural effects of MSCs in SSc environments. If true elucidation of SSc causation is to be achieved, the role of MSCs needs to be considered as more than merely secondary or tertiary, or even therapeutic. A recent study, and one of the few of its kind, has attempted to look at the function of MSCs in SSc serum conditions with regards to its promotion of oxidative stress reactions. This study concluded that while MSCs are somewhat affected by SSc serum, they can still function therapeutically (Fonteneau et al. 2017). Essentially, the studies of this thesis suggest the opposite and indicate the potential for MSCs to become pathogenic within the context of SSc. Such contradictions only stress the need for more MSC studies in the context of SSc, before their widespread use, therapeutically, is recommended

8.1 Determining whether activated MSCs are present within the fibrotic environment of SSc patients' skin lesions

Much of the work on MSCs in SSc has been investigating these cells as therapeutic agents. Such investigations often are *in vitro* with MSCs treated in tissue culture. Particularly considering the fact that these are stem cells, *in vitro* work takes a reductionist approach being somewhat unrepresentative. This is because MSCs which have been cultured and allowed to proliferate *in vitro*, will inevitably be induced to change phenotype by the growth factors used and tissue culture microenvironment. This means the serum, growth factors, cytokines, the lack of other cellular components and the extracellular matrix must all be considered as limitations to this approach. For this reason,

identifying potential MSCs *in situ* within biopsies taken directly from SSc patients, bridges the gap and limitations that are a result of *in vitro* work.

It is known that physiologically, MSCs can reside in the adipose tissue, where they are mostly quiescent until being signalled to participate in adipogenic differentiation, or wound healing. MSCs *in vivo* are thought to have a morphology similar to fibroblasts, with a thin, elongated body. It is hypothesised however, that when these cells are activated, they adopt a nuclear morphology that allows them to partake in metakaryotic stem cell division. This type of division is neither mitosis nor meiosis and is in fact termed amitosis, a process that caters for both symmetrical and asymmetrical stem cell division. Such divisions are characterised by the presence of large, hollow, bell-shaped nuclei, where rather than even chromosome dispersion, the DNA content is concentrated in a ring on the 'open' end of the bell. Studies of these cells have implicated them in wound healing conducted by α-SMA positive myofibroblast-like wound healing cells (Pasquinelli et al. 2017). Since MSCs are postulated to be myofibroblast-like when activated, and the fact that they express higher levels of α-SMA under SSc conditions, highly suggests that these MSCs also undergo metakaryotic cell division.

While the main aim of this study was to quantify the number of metakaryotic nuclei in SSc skin, other striking differences in appearance between the healthy and SSc sections should not be ignored. One of the main differences was the appearance of the collagen matrix. Typically, histology of SSc skin takes a sideways approach, visualising all the skin layers in sections which are aligned vertically through the skin showing all layers from epidermis to deep dermis. The approach used in Chapter 3 of this thesis, looked at the skin in gradually deepening layers, visualised in thick sections cut parallel to the skin surface, and using partial digestion with collagenase to expand the extracellular matrix. The collagen therefore can be visualised as individual fibres, rather than a whole layer and thereby, more than just the thickness can be commented on. This is particularly important in SSc, where dermal collagen thickening is not only a result of increased collagen production and secretion,

but also possibly abnormal cross-linking of the collagen, leading to the thick bundles and the parallel alignment of collagen observed in the images of Chapter 3 (Cao et al., 2017).

One of the most interesting findings of Chapter 3, aside from the presence of metakaryotic nuclei in SSc tissue only, was the presence of many osteoclasts also found only in SSc tissue, together with the presence of bone material. While osteoclasts and bone material seem to suggest opposing processes, osteoclasts digest bone, and bone material suggests activation of osteoblasts, in fact this observation is emulous of the calcinosis together with osteoporosis in SSc patients (Valenzuela and Chung 2015). The finding of osteoclasts in this fibrotic disorder is analogous to the findings in rheumatoid arthritis where the aberrant synovial fibroblasts are implicated in promoting osteoclasts via myostatin and RANKL (Dankbar et al. 2015). It is possible that the disease fibroblasts in SSc are releasing these factors to induce local macrophages to differentiate into osteoclasts. In keeping with this idea, peripheral blood monocytes from SSc patients with acroosteolysis can be readily differentiated in tissue culture to an osteoclast phenotype (Park et al., 2016). Also, serum levels of RANKL are higher in SSc patients consistent with systemic activation of osteoclast responses (Dovio et al. 2008).

No metakaryotic nuclei were observed at any level examined in healthy skin biopsies. Considering the fact that MSCs are still present in healthy skin, these results suggest that they are remaining quiescent in the subcutaneous fat, whereas the presence of these nuclei in disease tissue indicates that in SSc, these stem cells are being activated. This activation results in their proliferation, migration and division. The fact that these nuclei are seen in the middle and bottom layers of the SSc biopsy also highlights their probable migration from the subcutaneous fat below to the next nearest layer, rather than to the uppermost layer.

This is a completely novel method for studying MSCs in SSc. A possible further refinement to this method would be to use antibodies against some MSC markers and look for co-localisation of the bell-shaped nuclei with positive

staining. Possible makers for MSCs could include Gli1. Staining for α-SMA would theoretically co-localise with both MSCs and fibroblasts, and staining for RANK or calcitonin would confirm the bi-nucleated cells to be osteoclasts (Kramann et al. 2015). Immunohistochemistry could be combined with the method used in Chapter 3 to give higher specificity to the findings.

The images of the metakaryotic nuclei near blood vessels may illustrate the MSC-endothelial cell relationship. Furthermore, seeing as MSCs were often found embedded in collagen fibres, the question arises as to whether the fibrotic extracellular matrix of SSc attracts and recruits MSCs to the lesion or MSCs themselves are somehow involved in the deposition of extracellular matrix proteins. It might be possible to model this using SSc tissue culture in MSC populated gels and to track migration of MSCs into the disease tissue.

The findings presented in Chapter 3 confirmed that the role that MSCs take in SSc pathogenesis is worth investigating and that this role is probably different from their role in healthy skin. The results supported the reasoning behind elucidating their function in the context of SSc microenvironments. To fulfil the aim of the thesis, investigating the interaction between MSCs and SSc microenvironment, three steps were conducted. The first was, to confirm the presence of dividing activated MSCs in SSc tissue. The second to define what the SSc microenvironment is. And the third was to put the two together in models of interaction. Chapter 3 successfully completed the first of these steps.

8.2 Profiling the tissue fluid to determine the factors present

Aside from the physical symptoms, SSc is commonly diagnosed by analysing components of the patients' blood, particularly looking at autoantibodies. Blood offers a global and systemic representation of bodily processes and therefore does not draw attention to red flags that are localised and specific to certain organs or areas. Such red flags include increased levels of soluble proteins in the interstitial fluid. One way of overcoming the issues relating to blood samples is by using blister fluid. This sampling method consists of

creating a blister on the forearm of patients, a commonly affected area in SSc, and aspirating the fluid that accumulated in the blister. Unlike blood, this is the fluid that is in direct contact with the cells that play the largest role in SSc, and as such it offers direct insight into the microenvironment the cells are in, within SSc fibrotic lesions.

Conversely, a major limitation of using blister fluid as a direct representation of the environment surrounding the cells in SSc, is the comparison with healthy samples. The act of taking the blister fluid itself creates a minor wound, and thereby results in some degree of tissue injury and likely acute inflammatory response in the area of the blister. This may result in the increase of pro-inflammatory and inflammatory soluble factors in the blister fluid that otherwise would not be induced. In keeping with this, the data in Chapter 4 indicates the presence of some innate inflammatory proteins in the healthy control samples. While a large difference still exists between healthy and SSc blister fluid samples, it is unclear to what extent the healthy samples are representative of normal quiescent healthy skin conditions. This is a possible explanation for some of the observed biologic effects of healthy blister fluid samples on MSCs.

The starting point for Chapter 4 came from the paper published by colleagues that used a Luminex assay to measure the concentrations of 41 growth factors, cytokines and chemokines (Clark et al, 2015). They observed differences between SSc and healthy blister fluid samples in IL6, IL15, IFNγ, IL17A, MCP-3 and PDGF-AA. IL17A has been implicated in pruritus. Since IL31 has also been connected with pruritus in models of atopic dermatitis, and it is also part of the IL6 superfamily, its levels in blister fluid were measured (Dillon et al. 2004). Ultimately, the goal would be to elucidate all factors differentially expressed in SSc blister fluid compared with healthy blister fluid, and assess their downstream functions, before creating a compound designed to inhibit or activate a factor increased or decreased in SSc blister fluid that may be responsible for its differing effects from healthy blister fluid. This might be achievable with the very recent technology such as SOMA scan, although the cost of this is well beyond the resources available during this thesis.

Originally, IL31 levels were found to be significantly elevated in both blister fluid and plasma of SSc patients. The only limitation of measuring IL31 in blister fluid in this way is that an ELISA, is not directly comparable to a Luminex assay, and therefore, the conclusion of IL31 being the most highly increased of all factors measured in SSc blister fluid, cannot be made with absolute certainty. Nonetheless, IL31 was evidently increased in SSc blister fluid in comparison with healthy control blister fluid. This result would possibly support the use of IL31, or IL31RA neutralising antibody, to be used on SSc patients in order to control and treat the pruritus and inflammatory effects of increased IL31. As the sample size of the healthy cohort was increased, a few volunteers with high IL31 in their blister fluid skewed the mean concentrations, although there is clearly a trend towards higher IL31 in SSc.

Likewise, a positive correlation was found between the level of IL31 in the blister fluid of SSc patients, and their itch score, determined by a questionnaire (see Appendix). This correlation was not found in plasma, most likely due to itching being a relatively acute and localised phenomenon, and as mentioned, not accounted for by the systemic approach of plasma sampling. These results highlight the importance of IL31 in a common SSc symptom, and alone, are supportive of anti-IL31 compounds being developed to treat the pruritic symptoms of SSc.

Rather interestingly, was the increased expression of the IL31RA found in SSc fibroblasts. If this is the mechanism by which the increased IL31 is functioning to result in SSc pruritus, it could also be considered a target for treatment of this symptom. It is plausible that SSc cells express more IL31 receptors than healthy cells, but a more striking finding was that the MSC expression of the receptor was akin to those of SSc cells, even though these MSCs themselves were from healthy individuals. This was one of the first indications that MSCs and IL31 have a relationship that can fit into the story of SSc pathology.

While the increased IL31 may be an indicator of SSc, alone, it is not sufficient as it neglects the large subgroup of SSc patients that do not have elevated dermal IL31, and also those that do not suffer from significant pruritus. As

such, IL31 alone is not sufficient to account for all the differences between healthy and SSc blister fluid. Raynaud's Phenomenon is an even more common symptom of SSc than pruritus, affecting approximately 95% of the SSc population. This symptom is caused by severe vasoconstriction of the digital circulation as well as microcapillary abnormalities in the extremities leading to hypoxia, ischaemia and even avascularisation.

Hypoxia is easily measured using a Fingertip Lacticemy. This is where lactate concentration is measured in the blood collected from a small fingertip prick. Higher lactate concentrations suggest ischaemia. This procedure is routinely conducted to measure the efficiency of vascular perfusion. It therefore, could easily be incorporated into the diagnosis of SSc, and potentially may indicate Raynaud's phenomenon early in the process, allowing for more effective treatment before avascularisation results in necrotic lesions, often leading to amputation. In blister fluid, although not significant, there is a clear trend towards increased lactate in SSc samples as compared to healthy samples and with a larger sample size, it would not be surprising if significance was achieved. Reassuringly, results in literature conclude increased lactate to be a sign of increased glycolysis in fibroblasts, which in turn, is one of the first steps of myofibroblast differentiation. This glycolytic reprogramming was found to augment lung fibrosis, and further, inhibition of the glycolytic response significantly inhibited fibroblast to myofibroblast differentiation (Xie et al. 2015). One limitation in measuring the lactate in the blister fluid almost contradicts the advantages of blister fluid itself. Blister fluid is collected from the anterior forearm. Although the skin in this area is often scarred and tightened, the main vascular complications arise in the fingertips and digits where capillaries are smaller and more prone to problems from the vasoconstriction. Since blister fluid takes a localised approach to the microenvironment of the site of collection, if there is lactate build up in the fingers, the blister fluid would not necessarily reflect this, whereas a Fingertip Lacticemy is more likely to measure local increases in lactate, as a result of anaerobic respiration (Pucinelli et al. 2002). Regardless, the IL31 and lactate ELISAs in Chapter 4 show that the constituents of blister fluid are considerably different between SSc and healthy individuals.

Since this thesis aims to bring together MSCs and SSc microenvironment, it is worth investigating whether each of these entities, alone, is pathological, in order to validly assign causation. While some experiments document changes in SSc derived MSCs as compared to healthy MSCs, these changes, are often able to be overridden (Capelli et al. 2017). As such, a more likely hypothesis is that the MSCs in SSc patients are inherently normal, whereas the microenvironment is pathological. What may be occurring is the MSCs residing in such an abnormal environment become primed to certain soluble and physical factors, in turn, altering their phenotype. An interesting question is whether newly "born" MSCs in SSc, i.e. MSCs that have not had prior exposure to SSc microenvironment, are different from healthy MSCs. This could potentially be addressed by sampling from clinically uninvolved sites.

8.3 Evaluating the effects of disease microenvironment on MSCs

Now that actively dividing MSCs have been confirmed to be present in SSc, and some indication of the constituents of the SSc microenvironment have been elucidated, Chapter 5 attempts to fit the two together in many models of interaction. It is difficult to reflect all SSc microenvironment characteristics into one model of interaction and therefore, often only specific microenvironment features were studied at once. This makes many of the models of interaction highly reductionist in their approach.

The role of MSCs in SSc discussed in this thesis focusses on external skin fibrosis, and as such, the use of adipose-derived MSCs rather than bone marrow-derived MSCs was preferred. Furthermore, adipose-derived MSC populations have been shown to contain more committed progenitor cells than bone marrow-derived cells whilst maintaining the immunosuppressive fingerprint of bone marrow derived cells (Bourin et al. 2013).

In this thesis the first study of MSC activation by SSc microenvironment factors is presented and the various strengths and weaknesses of the preliminary findings will be discussed. The nomenclature surrounding MSCs is likely to be

a factor contributing to the difficulty faced in elucidation of their activity. The adipose-derived MSCs used in this thesis lack the inherent definition of stem cells in that they do not produce the range of cells associated with truly pluripotent stem cells. They are somewhat already lineage committed. Thus these MSCs are more specifically known as multipotent mesenchymal stromal cells lacking haematopoietic markers.

The promiscuity of MSC function is in part due to the effects of the microenvironment. This poses the question of the effects of the SSc microenvironment composition. Perhaps it is not only the presence/absence of a particular growth factor or cytokine in the microenvironment that is responsible for MSC activation, rather it may be the overall effect of all microenvironment components that, only when together in a certain balance, do they induce the typically quiescent MSCs to become activated. This thesis aimed to begin unfolding this question by making and using different microenvironment representations and selecting specific components used individually to decipher their role.

One hypothesis is that SSc microenvironment has an effect on healthy MSCs in stimulating their differentiation into myofibroblasts. This has been documented in the current literature, and the most common way this is measured is by the cells' increased expression of α-SMA. This protein is highly expressed by myofibroblasts, and is mostly polymerised into the actin cytoskeleton during turnover, giving these fibroblast-like cells a myocyte phenotype. The actin in these cells is able to give the cells contractile and tensile strength. As such, α-SMA was used as the main readout of MSC to myofibroblast differentiation.

One way this was measured was by analysing α-SMA protein expression of MSCs in response to blister fluid and IL31. If MSCs were indeed differentiating into myofibroblasts, then it was expected that the α-SMA expression would be higher in response to SSc blister fluid. Indeed, this effect was seen, although not significantly. The lack of significance is most likely due to the following reasons, a low number of replicates, high dilution factor of blister fluid such

that pipetting errors were more likely, and the short treatment time. Considering it takes MSCs approximately 10 days to differentiate into osteoblast and adipocytes, only 24 hours' treatment is relatively short, even considering the similarities between MSCs and fibroblasts. The other measure of myofibroblast differentiation was the expression of CTGF and collagen type I. The increase of these in response to SSc blister fluid was not as strong as α-SMA, further suggesting that if the MSCs were differentiating into myofibroblasts, this had not fully taken place. Overall the results of the Western blots were particularly encouraging as they were consistent with the results observed by Boris Hinz, regarding MSC differentiation into myofibroblasts, with particular emphasis on the overexpression of α-SMA (Talele et al. 2015).

An early problem encountered was the difficulty in obtaining a regular source of blister fluid and therefore, often, high dilution factors were used. In order to ensure that the results, or lack thereof, of the blister fluid were not due to its dilution, and in fact results of blister fluid on MSCs, cells were treated with blister fluid of different concentrations. A dose response curve was generated, using α-SMA expression as a measure of MSC response to blister fluid. Dilutions ranged from 1:5 through 1:125, to completely serum free media with no blister fluid. Confirmative of the Western blot analyses, SSc blister fluid was responsible for consistently higher α-SMA expression than healthy control blister fluid at all doses. More interestingly was the apparent lack of an optimum dose, where higher concentrations at lower dilution factors did not necessarily result in more α-SMA expression. For this reason, most experiments were conducted using blister fluid diluted 1:125, at which there was a maximal difference between control and SSc samples based on the dose response curve.

Collagen alignment of SSc skin is proposed to be different to that of healthy skin, aside from its thickness. Glass slides coated with collagen either mimic SSc or healthy skin with regards to the pattern of collagen. SSc models consist of collagen fibres arranged in parallel, whereas collagen in healthy skin should

be woven into braids. The difference in collagen configuration was seen in the biopsy histology in Chapter 3, where these parallel collagen fibres were observed in SSc skin. As such, the collagen coated glass slides were considered to be a valid representation, and possibly would elucidate whether collagen configuration has an effect on MSC migration. The main problem faced with the used of these slides was the lack of adherence of the cells to the collagen. Human integrins are thought to be able to bind to bovine collagen, as advised by the manufacturer of the slides, however, *in vitro*, fibroblasts seeded on the slides at many different densities, to account for contact inhibition, were unable to adhere. For this reason, other migration assays were considered. One of which was the scratch wound assay conducted on both fibroblasts in preliminary experiments, and MSCs under SSc blister fluid conditions. The measure of migration in these assays was the remaining area of the scratch, with the change in area being the most reliable way to determine migration. Although care was taken to create all scratches of equal widths, the reduction in scratch size is a more valid measure of cell migration than final scratch size. The main goal of these assays was to assess the specific effect of IL31 on migration in comparison to blister fluid, with and without IL31 signalling pathway inhibitors. With barely any published literature available on the effect of IL31 on cell migration, this assay showed that IL31, through both the PI3K and MAPK pathways induces migration of both fibroblasts and MSCs. The fact that both cell types behave similarly is indicative of their similarities being associated with more than just morphology. Cell migration is likely a pathological phenomenon of SSc, with many cells infiltrating into sites of wound healing, inflammation or fibrosis (Ahmed Abdi et al. 2017). This raises the question that if cells were denied migration into these sites, possibly through the blockade of the chemokine attraction from the sites, or indeed through antagonists of IL31, would the decrease in cellular infiltrates result in alleviation of the chronic wound healing process associated with SSc?

A consideration of these assays was the extent of which cell proliferation accounts for closing of the “wound”. Often, in such assays, mitomycin C is used to prevent proliferation in order to assess migration alone. Mitomycin C was not used in these assays, for several reasons. The first of which is that

wound healing *in vivo* is a result of both proliferation and migration, if this model was to successfully model wound healing, both processes would need to be considered. Secondly, there are studies that suggest mitomycin C may even stop MSC migration by inhibiting RNA synthesis (Glenn et al. 2016). And lastly, for the effect of proliferation to be stronger than the effect of migration, the assays would need to take place for over 24 hours. This short incubation time allows for a maximum of one cell cycle.

The scratch wound assays took place on hard, plastic substrates. This thesis showed the large effect of substrate stiffness on MSC function. For this reason, and to incorporate the migration assay into a 3D models, gel contraction assays were conducted. On plastic, the cells most likely use the turnover of focal adhesions and Rho GTPases for migratory processes. On such 2D substrates, contractile strength is not as necessary as it is in 3D substrates. Collagen gels therefore make a better representation of cell migration in skin than does plastic. In collagen gels, in order to migrate, cells create contractile fibres, and connect to the collagen, thereby pulling on the collagen as they move, expelling media in the process, resulting in smaller gels. The formation of these contractile fibres rely on incorporation of α-SMA into polymerising actin subunits. This is a more accurate representation of possible myofibroblast differentiation than 2D migration assays. It is also a better model of wound healing, as tightening of the gel mimics the tightening of the skin surrounding the wound, with skin being stretched over the wound to close and heal it.

In these 3D models, many different representations of SSc microenvironment were used; SSc blister fluid, IL31 and lactate alone and together, and well as TGFβ, which was used as a positive control. Using factors of SSc blister fluid individually allowed assessment of their individual effects in SSc blister fluid. Lactate was used at concentrations similar to those found in SSc blister fluid, but IL31 was used at concentrations well over *in vivo* levels (50 ng/ml whereas the highest levels seen in SSc blister fluid were 38 ng/ml). In addition to these treatments, inhibitors for each were used on blister fluid, to assess their

function in blister fluid, and as food for thought for use of these inhibitors therapeutically. This particularly resonates following the finding that therapeutic inhibition of lactate, inhibits myofibroblast differentiation and possible resultant pulmonary fibrosis (Kottmann et al. 2015). Results of these contraction assays showed that all representations of SSc blister fluid induce some degree of MSC migration and contraction. SSc blister fluid had more of an effect than all other individual representations of the microenvironment at inducing cell migration. Although the individual effects of TGFβ, IL31 and lactate should not be ignored and clearly have an effect. All three SSc microenvironment representations had positive effects on MSC migration and gel contraction and therefore are valid targets in SSc pathology. One thing to consider when analysing the effects of inhibitors on gel contraction is that the seemingly low inhibition may in fact be due to difficulty of the inhibitors entering the polymerised collagen gels. This theory was reinforced when the same treatments were analysed in MSCs cultured in monolayers, and analysed for α-SMA expression rather than gel contraction as measures of MSC myofibroblast activity. In the qPCR assays for α-SMA, the TGFβ, PI3K and MAPK pathways, as well as lactate transport, were shown to have an effect on α-SMA expression in the monolayer experiments. An interesting result of this assay was that lactate treatment of MSCs results in modest upregulation of α-SMA expression, while inhibiting lactate transport in lactate treated MSCs, resulted in complete inhibition of all α-SMA expression, below baseline levels. This can be explained by lactate added to the media, possibly being only partially transported into MSCs, whereas inhibiting the transporter itself may inhibit the function of lactate already in the MSCs. It would be worth adding the inhibitor to serum free media treated MSCs to assess to what extent added lactate has an effect on MSC expression.

Still, blister fluid alone was more effective at inducing all pro-fibrotic readouts of MSCs. As such, it was hypothesised that the combination of factors in blister fluid is responsible for SSc blister fluid induction. For this reason, assays for α-SMA were conducted with inhibition of the TGFβ, PI3K and MAPK pathways together. In fact, the hypothesis was proved incorrect, since inhibition of all

three pathways together did not result in different induction in expression than inhibition of any one alone. This was further confirmed by the observation that both lactate and IL31 treatments together had no significant effect on gel contraction compared with their individual effects. Of note, though α-SMA is a good readout of contractile fibre polymerisation, it is worth considering the fact that prior to culture in the collagen suspension, the MSCs were cultured on hard plastic until highly confluent, in 10% serum. These conditions themselves may have had an effect on MSC phenotype that the 48 hours in soft collagen may not have overridden. To try and avoid MSC differentiation on plastic, all MSCs studied in the collagen gel and α-SMA qPCR assays had been through the same number of passages, were frozen at the same time, and cultured for the same amount of time on plastic.

These models of interaction provide novel data regarding MSC activation in SSc environments. While individual SSc blister fluid components alone cannot be entirely responsible for SSc blister fluid effects, their role is undoubtedly of potential importance for consideration when designing ways to inhibit the pathogenicity of SSc blister fluid.

8.4 Next Generation Sequencing of MSCs in SSc microenvironments

All the *in vitro* models of interaction of Chapter 5 looked at specific aspects of the SSc microenvironments, and used a small number of readouts believed to resemble the activation state of MSCs in the disease. They were aimed at elucidating the extent of TGFβ, IL31 and lactate on migration, contraction, protein and RNA expression. While results of these assays were positive and encouraging, giving insight into the specific roles of these SSc factors not often explored, alone, they could not account for the whole SSc blister fluid effects. As such, taking a broader approach, the large next generation sequencing assay was developed. The main goal of this assay was to identify all the genes differentially expressed in MSCs in response to SSc blister fluid and compare them to those expressed by healthy control blister fluid and IL31. This was hoped to identify key pathways initiated by SSc blister fluid and from this, possible therapeutic targets. Also, more broadly, if the SSc blister fluid is

having disease specific effects, then a differential pattern of gene expression would be predicted. Rather than assessing the individual functions of all possible elevated factors, the approach taken by the next generation sequencing gave much more comprehensive results. Combining these results with Ingenuity Pathway Analysis, the differentially expressed genes were put into biological context. Thus, not only were up/down-regulated genes identified, but the pathways and genetic networks these genes were involved in, together with their known association in diseases, and physiological functions were also established.

Arguably the most important finding from this assay was that the expression profile of MSCs was completely different from that of fibroblasts, and within MSCs, all four treatments resulted in distinct genetic expression. This is the first time it has been shown that the microenvironment of SSc has effects on MSCs that consistently differ from the effects of healthy microenvironment. As such, it can be safely concluded that the differences in the constitution of SSc blister fluid is responsible for MSC activation. This places significant liability on the SSc microenvironment as being the primary pathology of SSc, rather than an inherent abnormality in the function of MSCs. In fact, this is also the case in fibroblasts, where blister fluid induces expression of some pro-fibrotic proteins, namely α-SMA, CTGF and collagen type I. Therapeutically, therefore, MSC transplantation as an SSc treatment, would not be useful with regards to long term treatment. This is confirmed by the relatively short beneficial effects of MSC transplantation. The effects seen are not inconsistent with the findings in practice. Healthy, transplanted MSCs are likely to induce positive immunomodulatory effects in SSc before being negatively affected by the microenvironment, thus explaining the early optimism surrounding the beneficial effects of transplantation. In the more recent transplantation trials, there has been a shift in the expected functions of MSC. Rather than exploiting their pluripotency, studies are now more interested in their immunomodulatory functions. The results of this thesis may explain why *in vitro*, at least, MSCs take longer to be induced to differentiate, than they do to express immunoregulatory factors. As such, at least in the beginning, the transplanted

MSCs may be expressing such factors, which result in short term localised alleviation of SSc symptoms. However, as observed in many MSC clinical trials in SSc, the beneficial effects wear off, and even sometimes worsen symptoms (Granel et al. 2015). Possible explanations of this may be differentiation of these MSCs in response to SSc microenvironments, into possible pro-fibrotic phenotypes.

In this thesis, the expression of α-SMA is used as the main measure of MSC myofibroblast differentiation. Evidence of the deleterious effects of SSc microenvironments is highlighted by similar reactions of both MSCs and fibroblasts with regards to α-SMA. The SSc microenvironment therefore, has an effect on both MSCs and fibroblasts. Since normal physiological effects of fibroblasts in SSc are also thought to be relatively impaired, this is further evidence confirming the theory of an abnormal microenvironment being one of the primary SSc pathologies. Although fibroblasts have been documented as possible myofibroblast precursors, MSCs seem to be more responsive to SSc blister fluid than fibroblasts with regards to expression of myofibroblast markers. This finding supports the notion that MSCs might be important effector cells within the SSc microenvironment, as compared to the fully differentiated, fully committed tissue fibroblasts.

α-SMA is an established SSc marker, but its expression is often a downstream effect of CTGF and TGFβ, and therefore, its direct inhibition has not been studied. On the other hand, clinical trials of drugs inhibiting the TGFβ pathway have failed to result in successful results, with cytotoxicity, and lack of complete inhibition, the main concerns (Varga and Pasche 2009). For this reason, advances in SSc research often focusses on identifying new targets of inhibition. The RNAseq assay of this thesis identified *CEMIP, IL6* and *ACAN* as highly upregulated genes in response to SSc blister fluid in MSCs. *CEMIP*, interestingly, has very recently been identified as being involved in pulmonary fibrosis (Verneau 2016). No other studies have implicated this gene in SSc, and so the findings of the RNAseq assay present *CEMIP* as a novel target in SSc, with particular effect on MSCs.

Interestingly, the more common SSc-associated genes, are not as significantly upregulated in MSCs or fibroblasts in response to SSc blister fluid, possibly explaining the limited effect of their inhibition in clinical trials. Another novel gene is *CSRP2*. While studies exist investigating its effect in fibrosis, its specific effect in SSc is largely neglected (Herrmann et al. 2004). Furthermore, its expression in this assay was limited to MSCs. Since SSc studies mostly look at the effect of factors on fibroblasts, macrophages and endothelial cells, it is not surprising the effects of CSPR2 in SSc are overlooked.

IL31 seems to have very different effects on fibroblasts than it does on MSCs. In fibroblasts, it has strong effects on the IL6, IL8 and integrin pathways, all of which can be associated with SSc. In MSCs, on the other hand, the effects of IL31 are more subtle, with slight increases in α-SMA and CTGF, plus enhancement of migration and osteogenic differentiation. If an IL31 inhibitor were developed for SSc treatment, it would likely treat symptoms caused by fibroblast activity, in addition to pruritus, whereas its effect on pathogenesis of MSCs, is likely to be less obvious, perhaps reducing their migration into the fibrotic lesions or dampening their osteogenic polarisation at sites of pressure or trauma.

Some of the most useful information obtained from the IPA analysis was regarding the function of MSCs in vasculogenesis. The cause of Raynaud's phenomenon in SSc is often put down to hypoxia and ischemia of the digits resulting the vascular damage. Although the primary cause of this vascular damage is still up for debate, IPA analysis of blister fluid treated MSCs placed high importance on how well the expression profile of these MSCs fit into known processes in vascular damage. Particularly as explanations for the differences between SSc and healthy control blister fluid treated MSCs. Furthermore, for the first time, a significant result was found directly linking SSc treated MSCs to fibrogenesis (Table 6.1). The software was also able to pinpoint the specific genes responsible for categorising the MSCs as fibrogenic. While many of these genes are known to be implicated in

fibrogenesis, some new genes were identified that have not been studied in the context of SSc. Over 70 fibrogenic genes were highlighted, and aside from the expected role of *CTGF* and collagen, *SMAD3, DKK1 and WNT11* genes were implicated as genes involved in the fibrogenic response of MSCs to SSc blister fluid.

One of the biological functions the IPA software associated with SSc blister fluid treated MSCs, was a decrease in adipogenesis. With loss of subcutaneous fat, a common SSc symptom, and with MSC adipogenic potential, the adipogenic differentiation assay in Chapter 5.8 aimed at elucidating the direct effect of SSc blister fluid on MSC adipogenic differentiation. As predicted, SSc blister fluid modestly inhibited the ability of MSC differentiation. As discussed in the literature review there is a precarious balance between MSC adipogenic and osteogenic differentiation, which likely explains both adipogenesis and osteogenesis being highlighted as implicated functions in response to SSc blister fluid in the IPA analysis. In the differentiation assay, this balance was pushed towards adipogenesis by culturing MSCs in media, conducive for adipogenic encouragement. In spite of this, SSc blister fluid was better than healthy control blister fluid at inhibiting this differentiation. Although the loss of subcutaneous fat in SSc is not a symptom that is often considered as needing treatment, with it not having deleterious effects on patient well-being, this assay implicated the pathogenicity of MSCs in a new context. As such, aside from MSCs impairing normal wound healing responses, differentiating into myofibroblasts, and being responsible for fibrogenesis, they also are responsible for the loss of fat, and their role in SSc ought to be more significant in SSc research endeavours.

In summary, comparing SSc and healthy blister fluid, pathway analysis highlighted a potentially important mechanism of how the SSc interstitial microenvironment causes vascular damage. Again fibrosis was calculated to be an important function of SSc blister fluid treated MSCs. This analysis, with the differential expression profile together with results of the *in vitro* assay, provides evidence beyond reasonable doubt that MSCs, when placed in SSc microenvironments, have less than favourable effects and may promote the

pathogenesis of SSc. As such, the true extent of their pathogenicity in SSc should be assessed in much greater depth before transplantation of MSCs should be considered as a routine treatment.

8.5 Investigating the effect of matrix stiffness on MSCs

The majority of publications investigating MSCs, often focus on one MSC function at a time, working under the reductionist assumption that different MSC roles are distinct. This thesis takes a novel approach and assesses many MSC functions in response to the same stimulus, taking into considering the highly heterogeneic and pleiotropic nature of these cells. Their propensity to turn into myofibroblasts, express pro-fibrotic genes, take part in cytokine and immunomodulatory processes and failure to differentiate into adipocytes have all been studied under SSc blister fluid conditions. The results of these assays indicate that in response to the same stimulus, MSCs simultaneously function in different ways. This stimulus itself is also somewhat reductionist, only considering the soluble SSc microenvironment. For this reason, the assays on different matrix stiffness's was conducted.

Adding to the already convincing evidence that MSCs adopt some form of myofibroblast-like phenotype in response to SSc microenvironments, is the qPCR assay for the expression of α-SMA and CTGF by MSCs cultured on matrices of different stiffness. The main conclusions drawn from these experiments is that with regards to both genes, their expression is increased in response to TGFβ. This in itself is not novel, and is in fact a well established fact (Ide et al. 2017). What is original is the ability of soft matrices to override the TGFβ induction of α-SMA. With expression of these genes being the main measure of myofibroblast differentiation, it stands to reason that differentiation of MSCs into this fibrogenic cell type relies on more than just the soluble cues. On the other hand, CTGF expression in response to TGFβ does not seem to rely so much on matrix stiffness. This being said, inhibiting the ability of the cell to transduce the mechanosensing signal to the nucleus by MRTFA significantly inhibited expression of both pro-fibrotic genes. So rather than concluding that CTGF expression is not related to matrix stiffness, it is more

likely that soft 4 kPa matrices are sufficient in inducing its expression. In addition to investigating the effect of matrix stiffness on MSC expression of pro-fibrotic genes, Chapter 6 also studies how matrix stiffness affects the osteogenic differentiation potential of MSCs. TGFβ is documented to be both an inducer of myofibroblast and osteogenic differentiation; another example of how the same stimulus can result in completely different MSC responses. The osteogenic differentiation assay firstly confirmed that the commercially obtained MSCs were indeed pluripotent, and had not become lineage committed throughout passages, although care was taken to use the MSCs at low passage numbers, particularly in the differentiation assays of this thesis. One of the main technical difficulties of the osteogenic differentiation of MSCs on the Softwell collagen plates was the background staining. When cultured on plastic, the staining for osteoblasts, can be measured by the amount of red staining remaining after thorough washing of the well. However, the collagen substrates, particularly the softer wells, seemed to absorb much of the stain, resulting in relatively strong background staining. For this reason, it is likely that the level of differentiation may have been underestimated. In this assay, to account for the background staining, individual dots of staining were considered positive. Aside from this, the results were still striking. The effects of TGFβ on osteogenic differentiation were much stronger on stiff substrates than on soft, and even stronger than the effects of the osteogenic induction media alone. What was more striking however, was the extent of differentiation in response to IL31, to some degree higher than that of TGFβ. Indeed, IL31 is related to IL6, which in turn has been shown to affect osteogenic differentiation of MSCs (Yoon et al. 2014). But more noteworthy is the fact that IL31 is found in higher levels in SSc microenvironments than IL6, and so the fact that it has such a positive effect on the osteogenic potential places IL31 as a major factor in MSC driven calcinosis. As such, especially considering its effects on MSC cell migration, and differentiation, IL31 should be considered in SSc for much more than merely a driver of pruritus. The stiffness of the substrates on which MSCs are cultured seems to play more of a role when it comes to differentiation than it does in α-SMA and CTGF expression since inhibition of mechanosensing is more effective in inhibiting differentiation on stiff

substrates. In saying that, the differentiation on soft plates was minimal and therefore could explain why inhibition was not obvious. SSc blister fluid, on the other hand, was better at inducing differentiation, even on soft substrates, although not as much as on the stiff. SSc blister fluid was also considerably more effective than healthy control blister fluid, which had no effect on inducing differentiation.

The main take home message of these matrix assays was that with regards to both gene expression and differentiation, matrix stiffness was an essential factor in MSC stimulation. Furthermore, when it comes to gene expression, matrix stiffness can, to some extent override soluble stimuli, like it did for α-SMA expression, while with regards to differentiation, the soluble stimuli seem to be more important, and, especially considering the effects of blister fluid, the stiffness was not able to override soluble stimuli.

In both cases, the effect of matrix stiffness is clearly a major factor in the determination of MSC function. Therefore, it should be as important as the soluble microenvironment when considering treatments, since theoretical inhibition of TGFβ, as a pro-fibrotic factor, will not override the effects of the matrix stiffness of SSc on MSC fibrogenesis and calcinosis for example. As such, inhibition of mechanosensing by using CCG-1423, or similar more recently developed and more specific derivatives, is a valid option with regards to treatment of SSc specific symptoms, but its effects on physiological mechanosensing should be considered (Hutchings et al. 2017).

Overall, this thesis has shown compelling evidence towards the consideration of activated MSCs as much more pathogenic than they are beneficial in the case of SSc. Taking into account many MSC processes and functions, MSCs have been shown to have deleterious effects that easily fit into SSc pathology and it is likely that this will be the case when other MSC functions are studied in response to SSc microenvironments. A major drawback in the field of MSC studies is the fact that there is, to date, no direct *in vivo* evidence that MSCs themselves can act as collagen depositors through myofibroblast

differentiation, or not. If this can be demonstrated, MSCs should be highlighted as majorly pathogenic in SSc and should be studied as a therapeutic target.

8.6 Final conclusions and future work

In order to develop appropriate and effective treatments for SSc, robust elucidation of its cause is needed. And in turn, before this can be determined, it is necessary to discover the cellular and molecular participants of this disease and the roles they play.

MSCs, are not a new discovery. Their pleiotropy, heterogeneity, pluripotency and self-renewal properties have long been identified as possible targets, and the use of MSC transplantation is the current “hot topic” in many auto-immune and degenerative disease. In theory it seems perfect; healthy MSCs, which do not mount an immune response can be transplanted into patients where they carry out regenerative, wound healing and immunomodulatory functions to treat and cure the symptoms of their condition. In fact, the few clinical trials that have been conducted, yield somewhat optimistic results (Christopeit et al. 2008; Granel et al. 2015). While this may be the case in some diseases, in SSc the case for using MSCs therapeutically is far more complicated. In this complex and multifactorial disease, MSCs need to be considered as more than a potentially beneficial treatment. Based on the findings of this thesis, the cells themselves are involved in SSc pathogenicity and so the practice of transplanting MSCs into SSc patients’ lesions raises questions. In the case that SSc MSCs are themselves depleting or non-functioning, it is understandable why transplantation of healthy allogeneic MSC are likely to be beneficial. This may be relevant to late stage SSc, where in some cases the skin becomes atrophic and non-healing ulcers are a significant clinical burden. However, is seems likely that the SSc MSCs are, for the most part, healthy, and therefore unlikely that transplantation will result in more than temporary short term benefits. The theory assumed in this thesis, is that the MSCs themselves are completely physiological, but the microenvironment they reside in has deleterious induction effects, stimulating the MSCs to adopt a pathological chronic wound healing and fibrogenic phenotype.

This thesis presents the first data that activated, metakaryotically dividing MSCs are present in abundance in SSc skin, while being completely absent in healthy skin. To date, such activation was only documented in cancerous tumours, and during embryonic development (Gostjeva et al. 2009).

SSc MSCs are theorised to be physiologically normal, and therefore, there must be something inducing them to act abnormally. Based on the findings of this thesis, this "something" is the unique constitution of the SSc microenvironment and for the purpose of this thesis, is represented by blister fluid, some of its elevated components IL31 and lactate and the physical culture matrix.

The main readout of the SSc models of interaction was MSC to myofibroblast differentiation, measured by increased α-SMA expression, as well as migration and collagen contraction. SSc blister fluid, and its individual components, induced all readout measurements. IL31 and lactate alone were responsible for increased α-SMA expression and MSC migration both on plastic and in 3D collagen matrices but SSc blister fluid was found to be a better inducer. Three pathways predicted to be involved in SSc blister fluid effects were inhibited, the TGFβ pathway with 1D11, PI3K pathway with Wortmmanin and MAPK pathway with U0126. Since inhibition of all three pathways results in only modest inhibition of myofibroblast differentiation readouts, it is safe to conclude other factors in SSc blister fluid, absent in healthy blister fluid, must be responsible. This unknown factor(s) might even be the underlying cause to SSc pathology. Theoretically, inhibiting it would treat SSc at the root. Considering the relatively high dilution factors used in this thesis, it is highly unlikely that the "cause of SSc" is merely increased a few-fold in SSc blister fluid compared to healthy blister fluid. It is more plausible that this unknown factor(s) is elevated hundreds of times in SSc blister fluid. Likewise, it is also possible the factor may be able to work at relatively low concentrations with possible candidates being autoantibodies and miRNA.

Whatever the factor, it is likely that it is responsible for the novel pathways identified by the RNAseq next generation sequencing assay. This assay proved some of the most convincing evidence for SSc blister fluid being significantly different from healthy control blister. But more interestingly, is the stark effect it has on MSCs in comparison to fibroblasts. It is commonly believed that fibroblasts are the main pathological cell type in SSc, being collagen secretors, fibrogenic and possible myofibroblast precursors. As such it was somewhat surprising that the effect of SSc blister fluid on fibroblasts was much less marked than its effects on MSCs, leading to the possibility that MSCs are in fact the recipients of the effects of SSc microenvironments and are thus, the main pathological cell type mediating SSc processes. IL31 did indeed account for some of the SSc blister fluid induced pathways, but there were many pathways induced by SSc blister fluid alone. One of the most potentially important findings being the induction of CEMIP. Only recently weakly associated with pulmonary fibrosis, this gene was measured as one of the most differentially expressed in response to SSc blister fluid. With many SSc pathways having unknown causes, it is not difficult to believe that CEMIP is responsible for at least some of them. IL6 signalling was also significantly increased by both healthy control and SSc blister fluid highlighting that at the same time these cells are secreting fibrogenic molecules and differentiating, they also are involved in immunomodulation. When comparing SSc to healthy control blister fluid, the majority of the differences were with respect to vasculogenesis. Raynaud's phenomenon is of unknown aetiology and the IPA analysis of this thesis strongly places SSc blister fluid effects on MSCs as a potential cause.

MSC pluripotency was not overlooked in this thesis. Their potential for differentiation is often neglected when being considered for transplantation, likely because of limited engraftment in the target site *in vivo*. For this reason, when developing MSCs for transplantation trials, their immunomodulatory function is mainly exploited. In SSc however, MSC differentiation is implicated in three ways; differentiation into myofibroblasts, resulting in fibrosis, osteoblasts, resulting in calcinosis, and inhibition of differentiation into adipocytes, resulting in the loss of subcutaneous fat. As mentioned, evidence

for MSCs being myofibroblast precursors was demonstrated by the increased α-SMA expression, cell migration and collagen contraction. Osteogenic differentiation was increased by SSc blister fluid, TGFβ and IL31, while adipogenic differentiation was decreased by SSc blister fluid. It is, therefore, conceivable that the SSc microenvironment shifts the osteogenic-adipogenic balance towards osteoblast differentiation, resulting in deposition of calcium minerals and hydroxyapatite, and ultimately, painful calcinotic lesions.

In an attempt to take the most holistic approach possible, the assays of this investigation addressed many of the MSC related pathogenic processes of SSc. The results have been collated to develop a schematic of how MSCs might be acting as key players in SSc (Figure 8.1).

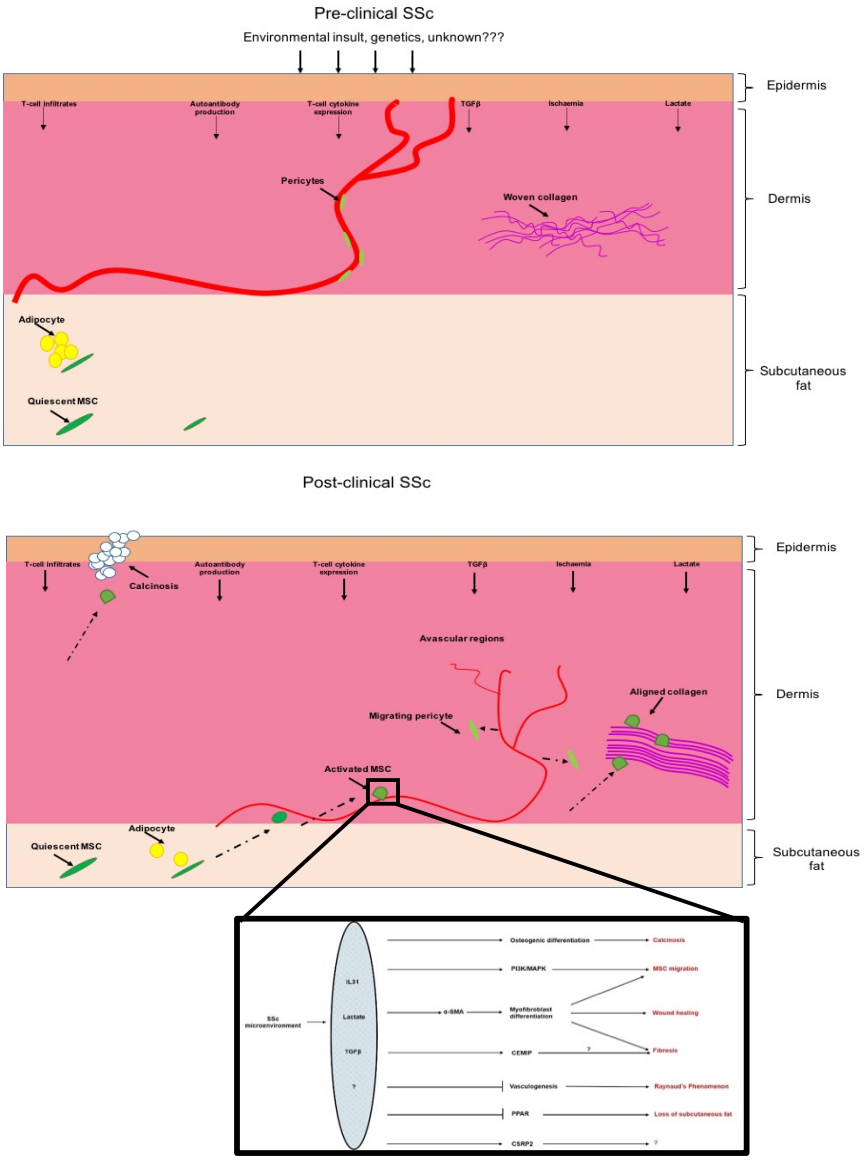

***Figure 8.1* MSCs as key players in SSc.** *Pre-clinical SSc is caused by environmental insult and/or genetic predisposition leading to auto-immunity. Vasculature is intact and collagen in the dermis is fine and woven. Subcutaneous fat is maintained by adipogenic differentiation. MSCs are quiescent with a fibroblast-like morphology. Post-clinical SSc presents with loss of subcutaneous fat due to inhibited MSC adipogenic differentiation. Quiescent MSCs migrate into the dermis with bell shaped nuclear morphology. Dermal thickening due to increased collagen and MSC myofibroblast differentiation. Collagen found as thick fibrils aligned in parallel. Vasculature is damaged resulting eventual Raynaud's phenomenon. MSC osteogenic differentiation resulting in calcinosis. MSCs react to increased IL31, lactate, TGFβ, and stiff matrix as illustrated in the magnified box, leading to increased osteogenic differentiation, and migration, partially via the PI3K and MAPK pathways. MSCs are induced to express CEMIP, resulting in fibrosis, and CSRP2 with unknown consequences to date. The PPAR and VEGFC pathways are inhibited leading to reduced adipogenic differentiation and vasculogenesis causing Raynaud's Phenomenon.*

The thesis heavily points to there being a factor(s) in SSc blister fluid responsible for MSC pathological effects in SSc. One step towards identification of this factor is by first elucidating its nature. It would be useful if SSc blister fluid was treated in such a way to produce four different blister fluid versions, to identify the bioactive component; whole blister fluid, blister fluid lacking proteins, blister fluid lacking immunoglobulins and blister fluid with miRNA molecules removed. Similar assays to those described in the studies of this thesis would be conducted and theoretically would elucidate whether the “unknown” factor of SSc blister fluid is a protein, immunoglobulin or miRNA.

The effect of IL31 in SSc blister fluid must not be neglected and it is clear that its role in SSc expands to more than pruritus. For this reason, an IL31 mouse model was developed to study, *in vivo*, the specific effects of the IL31 found significantly elevated in blister fluid. Results of this mouse model are described in the Appendix demonstrating that *in vivo* administration of IL31 into the subcutaneous tissue leads to dermal fibrosis and enhances systemic inflammation, including elevated IL6, thus resembling SSc.

Furthermore, results of this thesis provide evidence that MSCs are contributing to fibrosis, immunomodulation, calcinosis, loss of subcutaneous fat, and wound healing, in response to the SSc microenvironment. These processes cover almost all pathological aspects of the disease and therefore, these findings not only raise the question of how MSCs are considered to be beneficial to SSc, nor only how much a part these cells play in SSc, but how likely it is that MSCs are responsible for much of SSc pathogenicity. This thesis puts forward the theory that MSCs, through their pleiotropy, are highly influenced by the SSc microenvironment and possibly very early in pathogenesis, are induced into becoming pathogenic themselves, exacerbating the disease from early, manageable autoimmunity, into aggressive systemic fibrosis.

References

Ahmed, A.B., Lopez, H., Karrar, S., Renzoni, E., Wells, A., Tam, A., Etomi, O., Hsuan, J.J., Martin, G.R., Shiwen, X., Denton, C.P., Abraham, D., & Stratton, R. 2017. Use of Patterned Collagen Coated Slides to Study Normal and Scleroderma Lung Fibroblast Migration. *Sci.Rep.*, 7, (1) 2628 available from: PM:28572686

Akhmetshina, A., Venalis, P., Dees, C., Busch, N., Zwerina, J., Schett, G., Distler, O., & Distler, J.H. 2009. Treatment with imatinib prevents fibrosis in different preclinical models of systemic sclerosis and induces regression of established fibrosis. *Arthritis Rheum.*, 60, (1) 219-224 available from: PM:19116940

Ankrum, J.A., Ong, J.F., & Karp, J.M. 2014. Mesenchymal stem cells: immune evasive, not immune privileged. *Nat.Biotechnol.*, 32, (3) 252-260 available from: PM:24561556

Asparuhova, M.B., Gelman, L., & Chiquet, M. 2009. Role of the actin cytoskeleton in tuning cellular responses to external mechanical stress. *Scand.J.Med.Sci.Sports*, 19, (4) 490-499 available from: PM:19422655

Balbir-Gurman, A., Denton, C.P., Nichols, B., Knight, C.J., Nahir, A.M., Martin, G., & Black, C.M. 2002. Non-invasive measurement of biomechanical skin properties in systemic sclerosis. *Ann.Rheum.Dis.*, 61, (3) 237-241 available from: PM:11830429

Ball, S.G., Shuttleworth, C.A., & Kielty, C.M. 2010. Platelet-derived growth factor receptors regulate mesenchymal stem cell fate: implications for neovascularization. *Expert.Opin.Biol.Ther.*, 10, (1) 57-71 available from: PM:20078229

Barnes, J. & Mayes, M.D. 2012. Epidemiology of systemic sclerosis: incidence, prevalence, survival, risk factors, malignancy, and environmental triggers. *Curr.Opin.Rheumatol.*, 24, (2) 165-170 available from: PM:22269658

Baroni, S.S., Santillo, M., Bevilacqua, F., Luchetti, M., Spadoni, T., Mancini, M., Fraticelli, P., Sambo, P., Funaro, A., Kazlauskas, A., Avvedimento, E.V., & Gabrielli, A. 2006a. Stimulatory autoantibodies to the PDGF receptor in systemic sclerosis. *N.Engl.J.Med.*, 354, (25) 2667-2676 available from: PM:16790699

Baroni, S.S., Santillo, M., Bevilacqua, F., Luchetti, M., Spadoni, T., Mancini, M., Fraticelli, P., Sambo, P., Funaro, A., Kazlauskas, A., Avvedimento, E.V., & Gabrielli, A. 2006b. Stimulatory autoantibodies to the PDGF receptor in

systemic sclerosis. *N.Engl.J.Med.*, 354, (25) 2667-2676 available from: PM:16790699

Battula, V.L., Chen, Y., Cabreira, M.G., Ruvolo, V., Wang, Z., Ma, W., Konoplev, S., Shpall, E., Lyons, K., Strunk, D., Bueso-Ramos, C., Davis, R.E., Konopleva, M., & Andreeff, M. 2013. Connective tissue growth factor regulates adipocyte differentiation of mesenchymal stromal cells and facilitates leukemia bone marrow engraftment. *Blood*, 122, (3) 357-366 available from: PM:23741006

Behfar, A., Crespo-Diaz, R., Terzic, A., & Gersh, B.J. 2014. Cell therapy for cardiac repair--lessons from clinical trials. *Nat.Rev.Cardiol.*, 11, (4) 232-246 available from: PM:24594893

Bell, E., Ivarsson, B., & Merrill, C. 1979. Production of a tissue-like structure by contraction of collagen lattices by human fibroblasts of different proliferative potential in vitro. *Proc.Natl.Acad.Sci.U.S.A*, 76, (3) 1274-1278 available from: PM:286310

Bellido, T., Borba, V.Z., Roberson, P., & Manolagas, S.C. 1997. Activation of the Janus kinase/STAT (signal transducer and activator of transcription) signal transduction pathway by interleukin-6-type cytokines promotes osteoblast differentiation. *Endocrinology*, 138, (9) 3666-3676 available from: PM:9275051

Bergmann, C. & Distler, J.H. 2016. Canonical Wnt signaling in systemic sclerosis. *Lab Invest*, 96, (2) 151-155 available from: PM:26752744

Bilsborough, J., Leung, D.Y., Maurer, M., Howell, M., Boguniewicz, M., Yao, L., Storey, H., LeCiel, C., Harder, B., & Gross, J.A. 2006. IL-31 is associated with cutaneous lymphocyte antigen-positive skin homing T cells in patients with atopic dermatitis. *J.Allergy Clin.Immunol.*, 117, (2) 418-425 available from: PM:16461143

Bogatkevich, G.S. 2015. Editorial: fate of fat tissue adipocytes: do they transform into myofibroblasts in scleroderma? *Arthritis Rheumatol.*, 67, (4) 860-861 available from: PM:25504912

Borue, X., Lee, S., Grove, J., Herzog, E.L., Harris, R., Diflo, T., Glusac, E., Hyman, K., Theise, N.D., & Krause, D.S. 2004. Bone marrow-derived cells contribute to epithelial engraftment during wound healing. *Am.J.Pathol.*, 165, (5) 1767-1772 available from: PM:15509544

Bourin, P., Bunnell, B.A., Casteilla, L., Dominici, M., Katz, A.J., March, K.L., Redl, H., Rubin, J.P., Yoshimura, K., & Gimble, J.M. 2013. Stromal cells from the adipose tissue-derived stromal vascular fraction and culture expanded adipose tissue-derived stromal/stem cells: a joint statement of the

International Federation for Adipose Therapeutics and Science (IFATS) and the International Society for Cellular Therapy (ISCT). *Cytotherapy.*, 15, (6) 641-648 available from: PM:23570660

Bray, N.L., Pimentel, H., Melsted, P., & Pachter, L. 2016. Near-optimal probabilistic RNA-seq quantification. *Nat.Biotechnol.*, 34, (5) 525-527 available from: PM:27043002

Bruno, S., Deregibus, M.C., & Camussi, G. 2015. The secretome of mesenchymal stromal cells: Role of extracellular vesicles in immunomodulation. *Immunol.Lett.*, 168, (2) 154-158 available from: PM:26086886

Capelli, C., Zaccara, E., Cipriani, P., Di, B.P., Maglione, W., Andracco, R., Di, L.G., Pignataro, F., Giacomelli, R., Introna, M., Vitali, C., & Del, P.N. 2017a. Phenotypical and Functional Characteristics of In Vitro-Expanded Adipose-Derived Mesenchymal Stromal Cells From Patients With Systematic Sclerosis. *Cell Transplant.*, 26, (5) 841-854 available from: PM:28139194

Capelli, C., Zaccara, E., Cipriani, P., Di, B.P., Maglione, W., Andracco, R., Di, L.G., Pignataro, F., Giacomelli, R., Introna, M., Vitali, C., & Del, P.N. 2017b. Phenotypical and Functional Characteristics of In Vitro-Expanded Adipose-Derived Mesenchymal Stromal Cells From Patients With Systematic Sclerosis. *Cell Transplant.*, 26, (5) 841-854 available from: PM:28139194

Caplan, A.I. 2008. All MSCs are pericytes? *Cell Stem Cell*, 3, (3) 229-230 available from: PM:18786406

Cenit, M.C., Simeon, C.P., Vonk, M.C., Callejas-Rubio, J.L., Espinosa, G., Carreira, P., Blanco, F.J., Narvaez, J., Tolosa, C., Roman-Ivorra, J.A., Gomez-Garcia, I., Garcia-Hernandez, F.J., Gallego, M., Garcia-Portales, R., Egurbide, M.V., Fonollosa, V., Garcia, d.l.P., Lopez-Longo, F.J., Gonzalez-Gay, M.A., Hesselstrand, R., Riemekasten, G., Witte, T., Voskuyl, A.E., Schuerwegh, A.J., Madhok, R., Fonseca, C., Denton, C., Nordin, A., Palm, O., van Laar, J.M., Hunzelmann, N., Distler, J.H., Kreuter, A., Herrick, A., Worthington, J., Koeleman, B.P., Radstake, T.R., & Martin, J. 2012. Influence of the IL6 gene in susceptibility to systemic sclerosis. *J.Rheumatol.*, 39, (12) 2294-2302 available from: PM:23027890

Cepeda, E.J. & Reveille, J.D. 2004. Autoantibodies in systemic sclerosis and fibrosing syndromes: clinical indications and relevance. *Curr.Opin.Rheumatol.*, 16, (6) 723-732 available from: PM:15577611

Chamberlain, G., Fox, J., Ashton, B., & Middleton, J. 2007. Concise review: mesenchymal stem cells: their phenotype, differentiation capacity, immunological features, and potential for homing. *Stem Cells*, 25, (11) 2739-2749 available from: PM:17656645

Chen, C., Wang, D., Moshaverinia, A., Liu, D., Kou, X., Yu, W., Yang, R., Sun, L., & Shi, S. 2017a. Mesenchymal stem cell transplantation in tight-skin mice identifies miR-151-5p as a therapeutic target for systemic sclerosis. *Cell Res.*, 27, (4) 559-577 available from: PM:28106077

Chia, J.J., Zhu, T., Chyou, S., Dasoveanu, D.C., Carballo, C., Tian, S., Magro, C.M., Rodeo, S., Spiera, R.F., Ruddle, N.H., McGraw, T.E., Browning, J.L., Lafyatis, R., Gordon, J.K., & Lu, T.T. 2016. Dendritic cells maintain dermal adipose-derived stromal cells in skin fibrosis. *J.Clin.Invest*, 126, (11) 4331-4345 available from: PM:27721238

Chieco, P. & Derenzini, M. 1999. The Feulgen reaction 75 years on. *Histochem.Cell Biol.*, 111, (5) 345-358 available from: PM:10403113

Christopeit, M., Schendel, M., Foll, J., Muller, L.P., Keysser, G., & Behre, G. 2008. Marked improvement of severe progressive systemic sclerosis after transplantation of mesenchymal stem cells from an allogeneic haploidentical-related donor mediated by ligation of CD137L. *Leukemia*, 22, (5) 1062-1064 available from: PM:17972956

Cipriani, P., Di, B.P., Ruscitti, P., Campese, A.F., Liakouli, V., Carubbi, F., Pantano, I., Berardicurt, O., Screpanti, I., & Giacomelli, R. 2014. Impaired endothelium-mesenchymal stem cells cross-talk in systemic sclerosis: a link between vascular and fibrotic features. *Arthritis Res.Ther.*, 16, (5) 442 available from: PM:25248297

Clark, K.E., Lopez, H., Abdi, B.A., Guerra, S.G., Shiwen, X., Khan, K., Etomi, O., Martin, G.R., Abraham, D.J., Denton, C.P., & Stratton, R.J. 2015a. Multiplex cytokine analysis of dermal interstitial blister fluid defines local disease mechanisms in systemic sclerosis. *Arthritis Res.Ther.*, 17, 73 available from: PM:25885360

Clark, K.E., Lopez, H., Abdi, B.A., Guerra, S.G., Shiwen, X., Khan, K., Etomi, O., Martin, G.R., Abraham, D.J., Denton, C.P., & Stratton, R.J. 2015b. Multiplex cytokine analysis of dermal interstitial blister fluid defines local disease mechanisms in systemic sclerosis. *Arthritis Res.Ther.*, 17, 73 available from: PM:25885360

Crider, B.J., Risinger, G.M., Jr., Haaksma, C.J., Howard, E.W., & Tomasek, J.J. 2011. Myocardin-related transcription factors A and B are key regulators of TGF-beta1-induced fibroblast to myofibroblast differentiation. *J.Invest Dermatol.*, 131, (12) 2378-2385 available from: PM:21776010

Dankbar, B., Fennen, M., Brunert, D., Hayer, S., Frank, S., Wehmeyer, C., Beckmann, D., Paruzel, P., Bertrand, J., Redlich, K., Koers-Wunrau, C., Stratis, A., Korb-Pap, A., & Pap, T. 2015. Myostatin is a direct regulator of osteoclast differentiation and its inhibition reduces inflammatory joint

destruction in mice. *Nat.Med.*, 21, (9) 1085-1090 available from: PM:26236992

Deidda, M., Piras, C., Cadeddu, D.C., Locci, E., Barberini, L., Orofino, S., Musu, M., Mura, M.N., Manconi, P.E., Finco, G., Atzori, L., & Mercuro, G. 2017. Distinctive metabolomic fingerprint in scleroderma patients with pulmonary arterial hypertension. *Int.J.Cardiol.*, 241, 401-406 available from: PM:28476520

Del, S.G., Ruaro, M.E., Philipson, L., & Schneider, C. 1992. The growth arrest-specific gene, gas1, is involved in growth suppression. *Cell*, 70, (4) 595-607 available from: PM:1505026

Denton, C.P. 2015. Advances in pathogenesis and treatment of systemic sclerosis. *Clin.Med.(Lond)*, 15 Suppl 6, s58-s63 available from: PM:26634684

di Bonzo, L.V., Ferrero, I., Cravanzola, C., Mareschi, K., Rustichell, D., Novo, E., Sanavio, F., Cannito, S., Zamara, E., Bertero, M., Davit, A., Francica, S., Novelli, F., Colombatto, S., Fagioli, F., & Parola, M. 2008. Human mesenchymal stem cells as a two-edged sword in hepatic regenerative medicine: engraftment and hepatocyte differentiation versus profibrogenic potential. *Gut*, 57, (2) 223-231 available from: PM:17639088

Di, N.M., Carlo-Stella, C., Magni, M., Milanesi, M., Longoni, P.D., Matteucci, P., Grisanti, S., & Gianni, A.M. 2002. Human bone marrow stromal cells suppress T-lymphocyte proliferation induced by cellular or nonspecific mitogenic stimuli. *Blood*, 99, (10) 3838-3843 available from: PM:11986244

Dillon, S.R., Sprecher, C., Hammond, A., Bilsborough, J., Rosenfeld-Franklin, M., Presnell, S.R., Haugen, H.S., Maurer, M., Harder, B., Johnston, J., Bort, S., Mudri, S., Kuijper, J.L., Bukowski, T., Shea, P., Dong, D.L., Dasovich, M., Grant, F.J., Lockwood, L., Levin, S.D., LeCiel, C., Waggie, K., Day, H., Topouzis, S., Kramer, J., Kuestner, R., Chen, Z., Foster, D., Parrish-Novak, J., & Gross, J.A. 2004. Interleukin 31, a cytokine produced by activated T cells, induces dermatitis in mice. *Nat.Immunol.*, 5, (7) 752-760 available from: PM:15184896

Ding, R., Darland, D.C., Parmacek, M.S., & D'Amore, P.A. 2004. Endothelial-mesenchymal interactions in vitro reveal molecular mechanisms of smooth muscle/pericyte differentiation. *Stem Cells Dev.*, 13, (5) 509-520 available from: PM:15588508

Dovio, A., Data, V., Carignola, R., Calzolari, G., Vitetta, R., Ventura, M., Saba, L., Severino, A., & Angeli, A. 2008. Circulating osteoprotegerin and soluble

RANK ligand in systemic sclerosis. *J.Rheumatol.*, 35, (11) 2206-2213 available from: PM:18843778

Eckes, B., Moinzadeh, P., Sengle, G., Hunzelmann, N., & Krieg, T. 2014. Molecular and cellular basis of scleroderma. *J.Mol.Med.(Berl)*, 92, (9) 913-924 available from: PM:25030650

Engler, A.J., Sen, S., Sweeney, H.L., & Discher, D.E. 2006. Matrix elasticity directs stem cell lineage specification. *Cell*, 126, (4) 677-689 available from: PM:16923388

Errea, A., Cayet, D., Marchetti, P., Tang, C., Kluza, J., Offermanns, S., Sirard, J.C., & Rumbo, M. 2016. Lactate Inhibits the Pro-Inflammatory Response and Metabolic Reprogramming in Murine Macrophages in a GPR81-Independent Manner. *PLoS.One.*, 11, (11) e0163694 available from: PM:27846210

Fleischmajer, R. & Perlish, J.S. 1984. The pathophysiology of the fibrosis in scleroderma skin. *Prog.Clin.Biol.Res.*, 154, 381-404 available from: PM:6382305

Fonteneau, G., Bony, C., Goulabchand, R., Maria, A.T.J., Le, Q.A., Riviere, S., Jorgensen, C., Guilpain, P., & Noel, D. 2017. Serum-Mediated Oxidative Stress from Systemic Sclerosis Patients Affects Mesenchymal Stem Cell Function. *Front Immunol.*, 8, 988 available from: PM:28919892

Friedenstein, A.J., Deriglasova, U.F., Kulagina, N.N., Panasuk, A.F., Rudakowa, S.F., Luria, E.A., & Ruadkow, I.A. 1974. Precursors for fibroblasts in different populations of hematopoietic cells as detected by the in vitro colony assay method. *Exp.Hematol.*, 2, (2) 83-92 available from: PM:4455512

Fritzius, T. & Moelling, K. 2008. Akt- and Foxo1-interacting WD-repeat-FYVE protein promotes adipogenesis. *EMBO J.*, 27, (9) 1399-1410 available from: PM:18388859

Fukuyo, S., Yamaoka, K., Sonomoto, K., Oshita, K., Okada, Y., Saito, K., Yoshida, Y., Kanazawa, T., Minami, Y., & Tanaka, Y. 2014. IL-6-accelerated calcification by induction of ROR2 in human adipose tissue-derived mesenchymal stem cells is STAT3 dependent. *Rheumatology.(Oxford)*, 53, (7) 1282-1290 available from: PM:24599911

Fuschiotti, P. 2017. Current perspectives on the role of CD8+ T cells in systemic sclerosis. *Immunol.Lett.* available from: PM:28987475

Fuschiotti, P., Larregina, A.T., Ho, J., Feghali-Bostwick, C., & Medsger, T.A., Jr. 2013. Interleukin-13-producing CD8+ T cells mediate dermal fibrosis in

patients with systemic sclerosis. *Arthritis Rheum.*, 65, (1) 236-246 available from: PM:23001877

Gabrielli, A., Avvedimento, E.V., & Krieg, T. 2009. Scleroderma. *N.Engl.J.Med.*, 360, (19) 1989-2003 available from: PM:19420368

Ghannam, S., Pene, J., Moquet-Torcy, G., Jorgensen, C., & Yssel, H. 2010. Mesenchymal stem cells inhibit human Th17 cell differentiation and function and induce a T regulatory cell phenotype. *J.Immunol.*, 185, (1) 302-312 available from: PM:20511548

Gheisari, Y., Azadmanesh, K., Ahmadbeigi, N., Nassiri, S.M., Golestaneh, A.F., Naderi, M., Vasei, M., Arefian, E., Mirab-Samiee, S., Shafiee, A., Soleimani, M., & Zeinali, S. 2012. Genetic modification of mesenchymal stem cells to overexpress CXCR4 and CXCR7 does not improve the homing and therapeutic potentials of these cells in experimental acute kidney injury. *Stem Cells Dev.*, 21, (16) 2969-2980 available from: PM:22563951

Glenn, H.L., Messner, J., & Meldrum, D.R. 2016. A simple non-perturbing cell migration assay insensitive to proliferation effects. *Sci.Rep.*, 6, 31694 available from: PM:27535324

Glenn, J.D. & Whartenby, K.A. 2014. Mesenchymal stem cells: Emerging mechanisms of immunomodulation and therapy. *World J.Stem Cells*, 6, (5) 526-539 available from: PM:25426250

Goritz, C., Dias, D.O., Tomilin, N., Barbacid, M., Shupliakov, O., & Frisen, J. 2011. A pericyte origin of spinal cord scar tissue. *Science*, 333, (6039) 238-242 available from: PM:21737741

Gostjeva, E.V., Koledova, V., Tomita-Mitchell, A., Mitchell, M., Goetsch, M.A., Varmuza, S., Fomina, J.N., Darroudi, F., & Thilly, W.G. 2009. Metakaryotic stem cell lineages in organogenesis of humans and other metazoans. *Organogenesis.*, 5, (4) 191-200 available from: PM:20539738

Granel, B., Daumas, A., Jouve, E., Harle, J.R., Nguyen, P.S., Chabannon, C., Colavolpe, N., Reynier, J.C., Truillet, R., Mallet, S., Baiada, A., Casanova, D., Giraudo, L., Arnaud, L., Veran, J., Sabatier, F., & Magalon, G. 2015. Safety, tolerability and potential efficacy of injection of autologous adipose-derived stromal vascular fraction in the fingers of patients with systemic sclerosis: an open-label phase I trial. *Ann.Rheum.Dis.*, 74, (12) 2175-2182 available from: PM:25114060

Grinnell, F. 1994. Fibroblasts, myofibroblasts, and wound contraction. *J.Cell Biol.*, 124, (4) 401-404 available from: PM:8106541

Hawkins, K.E., Sharp, T.V., & McKay, T.R. 2013. The role of hypoxia in stem cell potency and differentiation. *Regen.Med.*, 8, (6) 771-782 available from: PM:24147532

Hawro, T., Saluja, R., Weller, K., Altrichter, S., Metz, M., & Maurer, M. 2014. Interleukin-31 does not induce immediate itch in atopic dermatitis patients and healthy controls after skin challenge. *Allergy*, 69, (1) 113-117 available from: PM:24251414

Hayashi, K., Watanabe, B., Nakagawa, Y., Minami, S., & Morita, T. 2014. RPEL proteins are the molecular targets for CCG-1423, an inhibitor of Rho signaling. *PLoS.One.*, 9, (2) e89016 available from: PM:24558465

Hegner, B., Schaub, T., Catar, R., Kusch, A., Wagner, P., Essin, K., Lange, C., Riemekasten, G., & Dragun, D. 2016a. Intrinsic Deregulation of Vascular Smooth Muscle and Myofibroblast Differentiation in Mesenchymal Stromal Cells from Patients with Systemic Sclerosis. *PLoS.One.*, 11, (4) e0153101 available from: PM:27054717

Hegner, B., Schaub, T., Catar, R., Kusch, A., Wagner, P., Essin, K., Lange, C., Riemekasten, G., & Dragun, D. 2016b. Intrinsic Deregulation of Vascular Smooth Muscle and Myofibroblast Differentiation in Mesenchymal Stromal Cells from Patients with Systemic Sclerosis. *PLoS.One.*, 11, (4) e0153101 available from: PM:27054717

Hermanns, H.M. 2015. Oncostatin M and interleukin-31: Cytokines, receptors, signal transduction and physiology. *Cytokine Growth Factor Rev.*, 26, (5) 545-558 available from: PM:26198770

Herrmann, J., Arias, M., Van de Leur, E., Gressner, A.M., & Weiskirchen, R. 2004. CSRP2, TIMP-1, and SM22alpha promoter fragments direct hepatic stellate cell-specific transgene expression in vitro, but not in vivo. *Liver Int.*, 24, (1) 69-79 available from: PM:15102003

Higashi-Kuwata, N., Makino, T., Inoue, Y., Takeya, M., & Ihn, H. 2009. Alternatively activated macrophages (M2 macrophages) in the skin of patient with localized scleroderma. *Exp.Dermatol.*, 18, (8) 727-729 available from: PM:19320738

Hinz, B. 2009. Tissue stiffness, latent TGF-beta1 activation, and mechanical signal transduction: implications for the pathogenesis and treatment of fibrosis. *Curr.Rheumatol.Rep.*, 11, (2) 120-126 available from: PM:19296884

Ho, Y.Y., Lagares, D., Tager, A.M., & Kapoor, M. 2014. Fibrosis--a lethal component of systemic sclerosis. *Nat.Rev.Rheumatol.*, 10, (7) 390-402 available from: PM:24752182

Hong, Y.J., Kim, J., Oh, B.R., Lee, Y.J., Lee, E.Y., Lee, E.B., Lee, S.H., & Song, Y.W. 2012. Serum elastin-derived peptides and anti-elastin antibody in patients with systemic sclerosis. *J.Korean Med.Sci.*, 27, (5) 484-488 available from: PM:22563211

Huaux, F., Liu, T., McGarry, B., Ullenbruch, M., Xing, Z., & Phan, S.H. 2003. Eosinophils and T lymphocytes possess distinct roles in bleomycin-induced lung injury and fibrosis. *J.Immunol.*, 171, (10) 5470-5481 available from: PM:14607953

Hugle, T., O'Reilly, S., Simpson, R., Kraaij, M.D., Bigley, V., Collin, M., Krippner-Heidenreich, A., & van Laar, J.M. 2013. Tumor necrosis factor-costimulated T lymphocytes from patients with systemic sclerosis trigger collagen production in fibroblasts. *Arthritis Rheum.*, 65, (2) 481-491 available from: PM:23045159

Hutchings, K.M., Lisabeth, E.M., Rajeswaran, W., Wilson, M.W., Sorenson, R.J., Campbell, P.L., Ruth, J.H., Amin, A., Tsou, P.S., Leipprandt, J.R., Olson, S.R., Wen, B., Zhao, T., Sun, D., Khanna, D., Fox, D.A., Neubig, R.R., & Larsen, S.D. 2017. Pharmacokinetic optimitzation of CCG-203971: Novel inhibitors of the Rho/MRTF/SRF transcriptional pathway as potential antifibrotic therapeutics for systemic scleroderma. *Bioorg.Med.Chem.Lett.*, 27, (8) 1744-1749 available from: PM:28285914

Ide, M., Jinnin, M., Tomizawa, Y., Wang, Z., Kajihara, I., Fukushima, S., Hashizume, Y., Asano, Y., & Ihn, H. 2017. Transforming growth factor beta-inhibitor Repsox downregulates collagen expression of scleroderma dermal fibroblasts and prevents bleomycin-induced mice skin fibrosis. *Exp.Dermatol.* available from: PM:28418584

Ip, W.K., Wong, C.K., Li, M.L., Li, P.W., Cheung, P.F., & Lam, C.W. 2007. Interleukin-31 induces cytokine and chemokine production from human bronchial epithelial cells through activation of mitogen-activated protein kinase signalling pathways: implications for the allergic response. *Immunology*, 122, (4) 532-541 available from: PM:17627770

Jia, Y., Morand EF FAU - Song, W., Song, W.F., Cheng, Q.F., Stewart, A.F., & Yang, Y.H. 2013. Regulation of lung fibroblast activation by annexin A1. *J.Cell Physiol* (1097-4652 (Electronic))

Jingjing Han, Nishanth V.Menon, Yuejun Kang, & Shang-you Tee 2014. An *in vitro* study on the collective tumor cell migration on nanoroughened poly(dimethylsiloxane) surfaces. *Journal of Materials Chemistry B*, 3, 1565-1572

Juric, V., Chen, C.C., & Lau, L.F. 2009. Fas-mediated apoptosis is regulated by the extracellular matrix protein CCN1 (CYR61) in vitro and in vivo. *Mol.Cell Biol.*, 29, (12) 3266-3279 available from: PM:19364818

Kahaleh, M.B. & LeRoy, E.C. 1999. Autoimmunity and vascular involvement in systemic sclerosis (SSc). *Autoimmunity*, 31, (3) 195-214 available from: PM:10739336

Kasraie, S., Niebuhr, M., & Werfel, T. 2010. Interleukin (IL)-31 induces pro-inflammatory cytokines in human monocytes and macrophages following stimulation with staphylococcal exotoxins. *Allergy*, 65, (6) 712-721 available from: PM:19889120

Kasraie, S., Niebuhr, M., & Werfel, T. 2013a. Interleukin (IL)-31 activates signal transducer and activator of transcription (STAT)-1, STAT-5 and extracellular signal-regulated kinase 1/2 and down-regulates IL-12p40 production in activated human macrophages. *Allergy*, 68, (6) 739-747 available from: PM:23621408

Kasraie, S., Niebuhr, M., & Werfel, T. 2013b. Interleukin (IL)-31 activates signal transducer and activator of transcription (STAT)-1, STAT-5 and extracellular signal-regulated kinase 1/2 and down-regulates IL-12p40 production in activated human macrophages. *Allergy*, 68, (6) 739-747 available from: PM:23621408

Keyszer, G., Christopeit, M., Fick, S., Schendel, M., Taute, B.M., Behre, G., Muller, L.P., & Schmoll, H.J. 2011. Treatment of severe progressive systemic sclerosis with transplantation of mesenchymal stromal cells from allogeneic related donors: report of five cases. *Arthritis Rheum.*, 63, (8) 2540-2542 available from: PM:21547891

Khalil, N. TGF-beta: from latent to active. (1286-4579 (Print))

Khan, K., Xu, S., Nihtyanova, S., Derrett-Smith, E., Abraham, D., Denton, C.P., & Ong, V.H. 2012a. Clinical and pathological significance of interleukin 6 overexpression in systemic sclerosis. *Ann.Rheum.Dis.*, 71, (7) 1235-1242 available from: PM:22586157

Khan, K., Xu, S., Nihtyanova, S., Derrett-Smith, E., Abraham, D., Denton, C.P., & Ong, V.H. 2012b. Clinical and pathological significance of interleukin 6 overexpression in systemic sclerosis. *Ann.Rheum.Dis.*, 71, (7) 1235-1242 available from: PM:22586157

Kim, R., Park, S.I., Lee, C.Y., Lee, J., Kim, P., Oh, S., Lee, H., Lee, M.Y., Kim, J., Chung, Y.A., Hwang, K.C., Maeng, L.S., & Chang, W. 2017. Alternative new mesenchymal stem cell source exerts tumor tropism through ALCAM and

N-cadherin via regulation of microRNA-192 and -218. *Mol.Cell Biochem.*, 427, (1-2) 177-185 available from: PM:28039611

Kochan, Z., Karbowska, J., Gogga, P., Kutryb-Zajac, B., Slominska, E.M., & Smolenski, R.T. 2016. Polymorphism in exon 6 of the human NT5E gene is associated with aortic valve calcification. *Nucleosides Nucleotides Nucleic Acids*, 35, (10-12) 726-731 available from: PM:27906615

Kottmann, R.M., Trawick, E., Judge, J.L., Wahl, L.A., Epa, A.P., Owens, K.M., Thatcher, T.H., Phipps, R.P., & Sime, P.J. 2015. Pharmacologic inhibition of lactate production prevents myofibroblast differentiation. *Am.J.Physiol Lung Cell Mol.Physiol*, 309, (11) L1305-L1312 available from: PM:26408551

Kramann, R., Schneider, R.K., DiRocco, D.P., Machado, F., Fleig, S., Bondzie, P.A., Henderson, J.M., Ebert, B.L., & Humphreys, B.D. 2015. Perivascular Gli1+ progenitors are key contributors to injury-induced organ fibrosis. *Cell Stem Cell*, 16, (1) 51-66 available from: PM:25465115

Lafyatis, R. 2014. Transforming growth factor beta--at the centre of systemic sclerosis. *Nat.Rev.Rheumatol.*, 10, (12) 706-719 available from: PM:25136781

Lambova, S. & Muller-Ladner, U. 2017. Nailfold Capillaroscopy Within and Beyond the Scope of Connective Tissue Diseases. *Curr.Rheumatol.Rev.* available from: PM:28641551

Lee, S., Choi, E., Cha, M.J., & Hwang, K.C. 2015. Cell adhesion and long-term survival of transplanted mesenchymal stem cells: a prerequisite for cell therapy. *Oxid.Med.Cell Longev.*, 2015, 632902 available from: PM:25722795

LeRoy, E.C., Black, C., Fleischmajer, R., Jablonska, S., Krieg, T., Medsger, T.A., Jr., Rowell, N., & Wollheim, F. 1988. Scleroderma (systemic sclerosis): classification, subsets and pathogenesis. *J.Rheumatol.*, 15, (2) 202-205 available from: PM:3361530

Levin, J.Z., Yassour, M., Adiconis, X., Nusbaum, C., Thompson, D.A., Friedman, N., Gnirke, A., & Regev, A. 2010. Comprehensive comparative analysis of strand-specific RNA sequencing methods. *Nat.Methods*, 7, (9) 709-715 available from: PM:20711195

Li, H., Li, T., Wang, S., Wei, J., Fan, J., Li, J., Han, Q., Liao, L., Shao, C., & Zhao, R.C. 2013. miR-17-5p and miR-106a are involved in the balance between osteogenic and adipogenic differentiation of adipose-derived mesenchymal stem cells. *Stem Cell Res.*, 10, (3) 313-324 available from: PM:23399447

Li, Z., Xu, X., Wang, W., Kratz, K., Sun, X., Zou, J., Deng, Z., Jung, F., Gossen, M., Ma, N., & Lendlein, A. 2017. Modulation of the mesenchymal stem cell migration capacity via preconditioning with topographic microstructure. *Clin.Hemorheol.Microcirc.* available from: PM:28869459

Liang, J., Zhang, H., Hua, B., Wang, H., Lu, L., Shi, S., Hou, Y., Zeng, X., Gilkeson, G.S., & Sun, L. 2010. Allogenic mesenchymal stem cells transplantation in refractory systemic lupus erythematosus: a pilot clinical study. *Ann.Rheum.Dis.*, 69, (8) 1423-1429 available from: PM:20650877

Luchsinger, L.L., Patenaude, C.A., Smith, B.D., & Layne, M.D. 2011. Myocardin-related transcription factor-A complexes activate type I collagen expression in lung fibroblasts. *J.Biol.Chem.*, 286, (51) 44116-44125 available from: PM:22049076

Lygoe, K.A., Wall, I., Stephens, P., & Lewis, M.P. 2007. Role of vitronectin and fibronectin receptors in oral mucosal and dermal myofibroblast differentiation. *Biol.Cell*, 99, (11) 601-614 available from: PM:17516912

Manetti, M., Ibba-Manneschi, L., Liakouli, V., Guiducci, S., Milia, A.F., Benelli, G., Marrelli, A., Conforti, M.L., Romano, E., Giacomelli, R., Matucci-Cerinic, M., & Cipriani, P. 2010. The IL1-like cytokine IL33 and its receptor ST2 are abnormally expressed in the affected skin and visceral organs of patients with systemic sclerosis. *Ann.Rheum.Dis.*, 69, (3) 598-605 available from: PM:19778913

Marangoni, R.G., Korman, B.D., Wei, J., Wood, T.A., Graham, L.V., Whitfield, M.L., Scherer, P.E., Tourtellotte, W.G., & Varga, J. 2015. Myofibroblasts in murine cutaneous fibrosis originate from adiponectin-positive intradermal progenitors. *Arthritis Rheumatol.*, 67, (4) 1062-1073 available from: PM:25504959

Massague, J. 2012. TGFbeta signalling in context. *Nat.Rev.Mol.Cell Biol.*, 13, (10) 616-630 available from: PM:22992590

McQualter, J.L., McCarty, R.C., Van, d., V, O'Donoghue, R.J., Asselin-Labat, M.L., Bozinovski, S., & Bertoncello, I. 2013. TGF-beta signaling in stromal cells acts upstream of FGF-10 to regulate epithelial stem cell growth in the adult lung. *Stem Cell Res.*, 11, (3) 1222-1233 available from: PM:24029687

Meirelles, L.S., Fontes, A.M., Covas, D.T., & Caplan, A.I. 2009. Mechanisms involved in the therapeutic properties of mesenchymal stem cells. *Cytokine Growth Factor Rev.*, 20, (5-6) 419-427 available from: PM:19926330

Moodley, Y.P., Misso, N.L., Scaffidi, A.K., Fogel-Petrovic, M., McAnulty, R.J., Laurent, G.J., Thompson, P.J., & Knight, D.A. 2003. Inverse effects of interleukin-6 on apoptosis of fibroblasts from pulmonary fibrosis and

normal lungs. *Am.J.Respir.Cell Mol.Biol.*, 29, (4) 490-498 available from: PM:12714376

Moraes, D.A., Sibov, T.T., Pavon, L.F., Alvim, P.Q., Bonadio, R.S., Da Silva, J.R., Pic-Taylor, A., Toledo, O.A., Marti, L.C., Azevedo, R.B., & Oliveira, D.M. 2016. A reduction in CD90 (THY-1) expression results in increased differentiation of mesenchymal stromal cells. *Stem Cell Res.Ther.*, 7, (1) 97 available from: PM:27465541

Murakami, J., Ishii, M., Suehiro, F., Ishihata, K., Nakamura, N., & Nishimura, M. 2017. Vascular endothelial growth factor-C induces osteogenic differentiation of human mesenchymal stem cells through the ERK and RUNX2 pathway. *Biochem.Biophys.Res.Commun.*, 484, (3) 710-718 available from: PM:28163024

Nedeau, A.E., Bauer, R.J., Gallagher, K., Chen, H., Liu, Z.J., & Velazquez, O.C. 2008. A C. *Exp.Cell Res.*, 314, (11-12) 2176-2186 available from: PM:18570917

Nuttall, M.E. & Gimble, J.M. 2000. Is there a therapeutic opportunity to either prevent or treat osteopenic disorders by inhibiting marrow adipogenesis? *Bone*, 27, (2) 177-184 available from: PM:10913909

O'Reilly, S., Cant, R., Ciechomska, M., & van Laar, J.M. 2013. Interleukin-6: a new therapeutic target in systemic sclerosis? *Clin.Transl.Immunology*, 2, (4) e4 available from: PM:25505952

Olivares-Navarrete, R., Lee, E.M., Smith, K., Hyzy, S.L., Doroudi, M., Williams, J.K., Gall, K., Boyan, B.D., & Schwartz, Z. 2017. Substrate Stiffness Controls Osteoblastic and Chondrocytic Differentiation of Mesenchymal Stem Cells without Exogenous Stimuli. *PLoS.One.*, 12, (1) e0170312 available from: PM:28095466

Olson, E.N. & Nordheim, A. 2010. Linking actin dynamics and gene transcription to drive cellular motile functions. *Nat.Rev.Mol.Cell Biol.*, 11, (5) 353-365 available from: PM:20414257

Park, J.K., Fava, A., Carrino, J., Del, G.F., Rosen, A., & Boin, F. 2016. Association of Acroosteolysis With Enhanced Osteoclastogenesis and Higher Blood Levels of Vascular Endothelial Growth Factor in Systemic Sclerosis. *Arthritis Rheumatol.*, 68, (1) 201-209 available from: PM:26361270

Park, J.S., Chu, J.S., Tsou, A.D., Diop, R., Tang, Z., Wang, A., & Li, S. 2011. The effect of matrix stiffness on the differentiation of mesenchymal stem cells in response to TGF-beta. *Biomaterials*, 32, (16) 3921-3930 available from: PM:21397942

Pasquinelli, G., Thilly, W.G., Gostjeva, E.V., Todeschini, P., Cianciolo, G., Ronco, C., & La, M.G. 2017. Restenosis in Hemodialytic Fistulas and Chronic Kidney Disease-Associated Vascular Disease: Two Pathologies Driven by Metakaryotic Stem Cells. *Contrib.Nephrol.*, 190, 96-107 available from: PM:28535522

Pavlides, S., Tsirigos, A., Vera, I., Flomenberg, N., Frank, P.G., Casimiro, M.C., Wang, C., Fortina, P., Addya, S., Pestell, R.G., Martinez-Outschoorn, U.E., Sotgia, F., & Lisanti, M.P. 2010. Loss of stromal caveolin-1 leads to oxidative stress, mimics hypoxia and drives inflammation in the tumor microenvironment, conferring the "reverse Warburg effect": a transcriptional informatics analysis with validation. *Cell Cycle*, 9, (11) 2201-2219 available from: PM:20519932

Pin, A.L., Houle, F., Fournier, P., Guillonneau, M., Paquet, E.R., Simard, M.J., Royal, I., & Huot, J. 2012. Annexin-1-mediated endothelial cell migration and angiogenesis are regulated by vascular endothelial growth factor (VEGF)-induced inhibition of miR-196a expression. *J.Biol.Chem.*, 287, (36) 30541-30551 available from: PM:22773844

Pittenger, M.F., Mackay, A.M., Beck, S.C., Jaiswal, R.K., Douglas, R., Mosca, J.D., Moorman, M.A., Simonetti, D.W., Craig, S., & Marshak, D.R. 1999. Multilineage potential of adult human mesenchymal stem cells. *Science*, 284, (5411) 143-147 available from: PM:10102814

Prey, S., Ezzedine, K., Doussau, A., Grandoulier, A.S., Barcat, D., Chatelus, E., Diot, E., Durant, C., Hachulla, E., de Korwin-Krokowski, J.D., Kostrzewa, E., Quemeneur, T., Paul, C., Schaeverbeke, T., Seneschal, J., Solanilla, A., Sparsa, A., Bouchet, S., Lepreux, S., Mahon, F.X., Chene, G., & Taieb, A. 2012. Imatinib mesylate in scleroderma-associated diffuse skin fibrosis: a phase II multicentre randomized double-blinded controlled trial. *Br.J.Dermatol.*, 167, (5) 1138-1144 available from: PM:23039171

Pucinelli, M.L., Fontenelle, S., & Andrade, L.E. 2002. Determination of fingertip lacticemy before and after cold stimulus in patients with primary Raynaud's phenomenon and systemic sclerosis. *J.Rheumatol.*, 29, (7) 1401-1403 available from: PM:12136896

Raimondo, A., Lembo, S., Di, C.R., Donnarumma, G., Monfrecola, G., Balato, N., Ayala, F., & Balato, A. 2017. Psoriatic cutaneous inflammation promotes human monocyte differentiation into active osteoclasts, facilitating bone damage. *Eur.J.Immunol.*, 47, (6) 1062-1074 available from: PM:28386999

Rajkumar, V.S., Sundberg, C., Abraham, D.J., Rubin, K., & Black, C.M. 1999. Activation of microvascular pericytes in autoimmune Raynaud's phenomenon and systemic sclerosis. *Arthritis Rheum.*, 42, (5) 930-941 available from: PM:10323448

Raker, V., Haub, J., Stojanovic, A., Cerwenka, A., Schuppan, D., & Steinbrink, K. 2017. Early inflammatory players in cutanous fibrosis. *J.Dermatol.Sci.*, 87, (3) 228-235 available from: PM:28655471

Ramirez, F. & Dietz, H.C. 2007. Fibrillin-rich microfibrils: Structural determinants of morphogenetic and homeostatic events. *J.Cell Physiol*, 213, (2) 326-330 available from: PM:17708531

Razykov, I., Thombs, B.D., Hudson, M., Bassel, M., & Baron, M. 2009. Prevalence and clinical correlates of pruritus in patients with systemic sclerosis. *Arthritis Rheum.*, 61, (12) 1765-1770 available from: PM:19950328

Roccaro, A.M., Sacco, A., Maiso, P., Azab, A.K., Tai, Y.T., Reagan, M., Azab, F., Flores, L.M., Campigotto, F., Weller, E., Anderson, K.C., Scadden, D.T., & Ghobrial, I.M. 2013. BM mesenchymal stromal cell-derived exosomes facilitate multiple myeloma progression. *J.Clin.Invest*, 123, (4) 1542-1555 available from: PM:23454749

Ronda, N., Gatti, R., Giacosa, R., Raschi, E., Testoni, C., Meroni, P.L., Buzio, C., & Orlandini, G. 2002. Antifibroblast antibodies from systemic sclerosis patients are internalized by fibroblasts via a caveolin-linked pathway. *Arthritis Rheum.*, 46, (6) 1595-1601 available from: PM:12115191

Roumm, A.D., Whiteside, T.L., Medsger, T.A., Jr., & Rodnan, G.P. 1984. Lymphocytes in the skin of patients with progressive systemic sclerosis. Quantification, subtyping, and clinical correlations. *Arthritis Rheum.*, 27, (6) 645-653 available from: PM:6375682

Ruaro, B., Smith, V., Sulli, A., Decuman, S., Pizzorni, C., & Cutolo, M. 2015. Methods for the morphological and functional evaluation of microvascular damage in systemic sclerosis. *Korean J.Intern.Med.*, 30, (1) 1-5 available from: PM:25589827

Sacchetti, B., Funari, A., Michienzi, S., Di, C.S., Piersanti, S., Saggio, I., Tagliafico, E., Ferrari, S., Robey, P.G., Riminucci, M., & Bianco, P. 2007. Self-renewing osteoprogenitors in bone marrow sinusoids can organize a hematopoietic microenvironment. *Cell*, 131, (2) 324-336 available from: PM:17956733

Sacchetti, B., Funari, A., Remoli, C., Giannicola, G., Kogler, G., Liedtke, S., Cossu, G., Serafini, M., Sampaolesi, M., Tagliafico, E., Tenedini, E., Saggio, I., Robey, P.G., Riminucci, M., & Bianco, P. 2016a. No Identical "Mesenchymal Stem Cells" at Different Times and Sites: Human Committed Progenitors of Distinct Origin and Differentiation Potential Are Incorporated as Adventitial Cells in Microvessels. *Stem Cell Reports.*, 6, (6) 897-913 available from: PM:27304917

Sacchetti, B., Funari, A., Remoli, C., Giannicola, G., Kogler, G., Liedtke, S., Cossu, G., Serafini, M., Sampaolesi, M., Tagliafico, E., Tenedini, E., Saggio, I., Robey, P.G., Riminucci, M., & Bianco, P. 2016b. No Identical "Mesenchymal Stem Cells" at Different Times and Sites: Human Committed Progenitors of Distinct Origin and Differentiation Potential Are Incorporated as Adventitial Cells in Microvessels. *Stem Cell Reports.*, 6, (6) 897-913 available from: PM:27304917

sackson I, Wener M, Pollock P.S, & Dighe M.K. Shear wave elastography: a quantitative approach for evaluating scleroderma skin. Arthritus and Rheumatism . 2013.
Ref Type: Abstract

Sadowski, H.B., Wheeler, T.T., & Young, D.A. 1992. Gene expression during 3T3-L1 adipocyte differentiation. Characterization of initial responses to the inducing agents and changes during commitment to differentiation. *J.Biol.Chem.*, 267, (7) 4722-4731 available from: PM:1371508

Saitta, B., Gaidarova, S., Cicchillitti, L., & Jimenez, S.A. 2000. CCAAT binding transcription factor binds and regulates human COL1A1 promoter activity in human dermal fibroblasts: demonstration of increased binding in systemic sclerosis fibroblasts. *Arthritis Rheum.*, 43, (10) 2219-2229 available from: PM:11037881

Sakkas, L.I., Chikanza, I.C., & Platsoucas, C.D. 2006. Mechanisms of Disease: the role of immune cells in the pathogenesis of systemic sclerosis. *Nat.Clin.Pract.Rheumatol.*, 2, (12) 679-685 available from: PM:17133253

Santiago, B., Galindo, M., Rivero, M., & Pablos, J.L. 2001. Decreased susceptibility to Fas-induced apoptosis of systemic sclerosis dermal fibroblasts. *Arthritis Rheum.*, 44, (7) 1667-1676 available from: PM:11465719

Sato, S., Hamaguchi, Y., Hasegawa, M., & Takehara, K. 2001. Clinical significance of anti-topoisomerase I antibody levels determined by ELISA in systemic sclerosis. *Rheumatology.(Oxford)*, 40, (10) 1135-1140 available from: PM:11600743

Schurgers, E., Kelchtermans, H., Mitera, T., Geboes, L., & Matthys, P. 2010. Discrepancy between the in vitro and in vivo effects of murine mesenchymal stem cells on T-cell proliferation and collagen-induced arthritis. *Arthritis Res.Ther.*, 12, (1) R31 available from: PM:20175883

Shiwen, X., Stratton, R., Nikitorowicz-Buniak, J., Ahmed-Abdi, B., Ponticos, M., Denton, C., Abraham, D., Takahashi, A., Suki, B., Layne, M.D., Lafyatis, R., & Smith, B.D. 2015a. A Role of Myocardin Related Transcription Factor-A

(MRTF-A) in Scleroderma Related Fibrosis. *PLoS.One.*, 10, (5) e0126015 available from: PM:25955164

Shiwen, X., Stratton, R., Nikitorowicz-Buniak, J., Ahmed-Abdi, B., Ponticos, M., Denton, C., Abraham, D., Takahashi, A., Suki, B., Layne, M.D., Lafyatis, R., & Smith, B.D. 2015b. A Role of Myocardin Related Transcription Factor-A (MRTF-A) in Scleroderma Related Fibrosis. *PLoS.One.*, 10, (5) e0126015 available from: PM:25955164

Sondergaard, K., Stengaard-Pedersen, K., Zachariae, H., Heickendorff, L., Deleuran, M., & Deleuran, B. 1998. Soluble intercellular adhesion molecule-1 (sICAM-1) and soluble interleukin-2 receptors (sIL-2R) in scleroderma skin. *Br.J.Rheumatol.*, 37, (3) 304-310 available from: PM:9566672

Soneson, C., Love, M.I., & Robinson, M.D. 2015. Differential analyses for RNA-seq: transcript-level estimates improve gene-level inferences. *F1000Res.*, 4, 1521 available from: PM:26925227

Stich, S., Haag, M., Haupl, T., Sezer, O., Notter, M., Kaps, C., Sittinger, M., & Ringe, J. 2009. Gene expression profiling of human mesenchymal stem cells chemotactically induced with CXCL12. *Cell Tissue Res.*, 336, (2) 225-236 available from: PM:19296133

Strutt, B., Khalil, W., & Killinger, D. 1996. Growth and differentiation of human adipose stromal cells in culture. *Methods Mol.Med.*, 2, 41-51 available from: PM:21359732

Sugihara, H., Yonemitsu, N., Miyabara, S., & Yun, K. 1986. Primary cultures of unilocular fat cells: characteristics of growth in vitro and changes in differentiation properties. *Differentiation*, 31, (1) 42-49 available from: PM:3732657

Talele, N.P., Fradette, J., Davies, J.E., Kapus, A., & Hinz, B. 2015. Expression of alpha-Smooth Muscle Actin Determines the Fate of Mesenchymal Stromal Cells. *Stem Cell Reports.*, 4, (6) 1016-1030 available from: PM:26028530

Tarte, K., Gaillard, J., Lataillade, J.J., Fouillard, L., Becker, M., Mossafa, H., Tchirkov, A., Rouard, H., Henry, C., Splingard, M., Dulong, J., Monnier, D., Gourmelon, P., Gorin, N.C., & Sensebe, L. 2010. Clinical-grade production of human mesenchymal stromal cells: occurrence of aneuploidy without transformation. *Blood*, 115, (8) 1549-1553 available from: PM:20032501

Theofilopoulos, A.N. & Dixon, F.J. 1985. Murine models of systemic lupus erythematosus. *Adv.Immunol.*, 37, 269-390 available from: PM:3890479

Thilly, W.G., Gostjeva, E.V., Koledova, V.V., Zukerberg, L.R., Chung, D., Fomina, J.N., Darroudi, F., & Stollar, B.D. 2014. Metakaryotic stem cell nuclei use pangenomic dsRNA/DNA intermediates in genome replication and segregation. *Organogenesis.*, 10, (1) 44-52 available from: PM:24418910

Todorovic, V., Chen, C.C., Hay, N., & Lau, L.F. 2005. The matrix protein CCN1 (CYR61) induces apoptosis in fibroblasts. *J.Cell Biol.*, 171, (3) 559-568 available from: PM:16275757

Tyndall, A. 2014. Mesenchymal stem cell treatments in rheumatology: a glass half full? *Nat.Rev.Rheumatol.*, 10, (2) 117-124 available from: PM:24217581

Uccelli, A., Moretta, L., & Pistoia, V. 2008. Mesenchymal stem cells in health and disease. *Nat.Rev.Immunol.*, 8, (9) 726-736 available from: PM:19172693

Uysal, C.A., Tobita, M., Hyakusoku, H., & Mizuno, H. 2014. The Effect of Bone-Marrow-Derived Stem Cells and Adipose-Derived Stem Cells on Wound Contraction and Epithelization. *Adv.Wound.Care (New Rochelle.)*, 3, (6) 405-413 available from: PM:24940554

Valenzuela A, Cuomo G, Sutton E, Gordon J, Spiera R, & Rodriguez-Reyna TS. Frequency of calcinosis in a multi-center international cohort of patients with systemic sclerosis: a Scleroderma Clinical Trials Consortium Study. Presented at the 13th International Workshop on Scleroderma Research . 2013.
Ref Type: Abstract

Valenzuela, A., Baron, M., Herrick, A.L., Proudman, S., Stevens, W., Rodriguez-Reyna, T.S., Vacca, A., Medsger, T.A., Jr., Hinchcliff, M., Hsu, V., Wu, J.Y., Fiorentino, D., & Chung, L. 2016. Calcinosis is associated with digital ulcers and osteoporosis in patients with systemic sclerosis: A Scleroderma Clinical Trials Consortium study. *Semin.Arthritis Rheum.*, 46, (3) 344-349 available from: PM:27371996

Valenzuela, A. & Chung, L. 2015. Calcinosis: pathophysiology and management. *Curr.Opin.Rheumatol.*, 27, (6) 542-548 available from: PM:26352733

Valvona, C.J., Fillmore, H.L., Nunn, P.B., & Pilkington, G.J. 2016. The Regulation and Function of Lactate Dehydrogenase A: Therapeutic Potential in Brain Tumor. *Brain Pathol.*, 26, (1) 3-17 available from: PM:26269128

van den Hoogen, F., Khanna, D., Fransen, J., Johnson, S.R., Baron, M., Tyndall, A., Matucci-Cerinic, M., Naden, R.P., Medsger, T.A., Jr., Carreira, P.E.,

Riemekasten, G., Clements, P.J., Denton, C.P., Distler, O., Allanore, Y., Furst, D.E., Gabrielli, A., Mayes, M.D., van Laar, J.M., Seibold, J.R., Czirjak, L., Steen, V.D., Inanc, M., Kowal-Bielecka, O., Muller-Ladner, U., Valentini, G., Veale, D.J., Vonk, M.C., Walker, U.A., Chung, L., Collier, D.H., Csuka, M.E., Fessler, B.J., Guiducci, S., Herrick, A., Hsu, V.M., Jimenez, S., Kahaleh, B., Merkel, P.A., Sierakowski, S., Silver, R.M., Simms, R.W., Varga, J., & Pope, J.E. 2013. 2013 classification criteria for systemic sclerosis: an American College of Rheumatology/European League against Rheumatism collaborative initiative. *Arthritis Rheum.*, 65, (11) 2737-2747 available from: PM:24122180

Vanneaux, V., Farge-Bancel, D., Lecourt, S., Baraut, J., Cras, A., Jean-Louis, F., Brun, C., Verrecchia, F., Larghero, J., & Michel, L. 2013. Expression of transforming growth factor beta receptor II in mesenchymal stem cells from systemic sclerosis patients. *BMJ Open.*, 3, (1) available from: PM:23299111

Varet, H., Brillet-Gueguen, L., Coppee, J.Y., & Dillies, M.A. 2016. SARTools: A DESeq2- and EdgeR-Based R Pipeline for Comprehensive Differential Analysis of RNA-Seq Data. *PLoS.One.*, 11, (6) e0157022 available from: PM:27280887

Varga, J. & Pasche, B. 2009. Transforming growth factor beta as a therapeutic target in systemic sclerosis. *Nat.Rev.Rheumatol.*, 5, (4) 200-206 available from: PM:19337284

Velayos, E.E., Robinson, H., Porciuncula, F.U., & Masi, A.T. 1971. Clinical correlation analysis of 137 patients with Raynaud's phenomenon. *Am.J.Med.Sci.*, 262, (6) 347-356 available from: PM:5146924

Verneau, J. Identification of Novel Mediators in Lung Fibrosis. American Journal of Respiratory and Critical Care Medicine 193. 2016.
Ref Type: Abstract

Walenda, G., Abnaof, K., Joussen, S., Meurer, S., Smeets, H., Rath, B., Hoffmann, K., Frohlich, H., Zenke, M., Weiskirchen, R., & Wagner, W. 2013. TGF-beta1 does not induce senescence of multipotent mesenchymal stromal cells and has similar effects in early and late passages. *PLoS.One.*, 8, (10) e77656 available from: PM:24147049

Westermann, W., Schobl, R., Rieber, E.P., & Frank, K.H. 1999. Th2 cells as effectors in postirradiation pulmonary damage preceding fibrosis in the rat. *Int.J.Radiat.Biol.*, 75, (5) 629-638 available from: PM:10374945

Wu, M., Melichian, D.S., Chang, E., Warner-Blankenship, M., Ghosh, A.K., & Varga, J. 2009. Rosiglitazone abrogates bleomycin-induced scleroderma and blocks profibrotic responses through peroxisome proliferator-

activated receptor-gamma. *Am.J.Pathol.*, 174, (2) 519-533 available from: PM:19147827

Yan, X., Liu, Y., Han, Q., Jia, M., Liao, L., Qi, M., & Zhao, R.C. 2007. Injured microenvironment directly guides the differentiation of engrafted Flk-1(+) mesenchymal stem cell in lung. *Exp.Hematol.*, 35, (9) 1466-1475 available from: PM:17637496

Yang, C., Tibbitt, M.W., Basta, L., & Anseth, K.S. 2014. Mechanical memory and dosing influence stem cell fate. *Nat.Mater.*, 13, (6) 645-652 available from: PM:24633344

Yoon, D.S., Kim, Y.H., Lee, S., Lee, K.M., Park, K.H., Jang, Y., & Lee, J.W. 2014. Interleukin-6 induces the lineage commitment of bone marrow-derived mesenchymal multipotent cells through down-regulation of Sox2 by osteogenic transcription factors. *FASEB J.*, 28, (7) 3273-3286 available from: PM:24719354

Youd, M., Blickarz, C., Woodworth, L., Touzjian, T., Edling, A., Tedstone, J., Ruzek, M., Tubo, R., Kaplan, J., & Lodie, T. 2010. Allogeneic mesenchymal stem cells do not protect NZBxNZW F1 mice from developing lupus disease. *Clin.Exp.Immunol.*, 161, (1) 176-186 available from: PM:20456409

Zanotti, L., Angioni, R., Cali, B., Soldani, C., Ploia, C., Moalli, F., Gargesha, M., D'Amico, G., Elliman, S., Tedeschi, G., Maffioli, E., Negri, A., Zacchigna, S., Sarukhan, A., Stein, J.V., & Viola, A. 2016. Mouse mesenchymal stem cells inhibit high endothelial cell activation and lymphocyte homing to lymph nodes by releasing TIMP-1. *Leukemia*, 30, (5) 1143-1154 available from: PM:26898191

Zhou, B.R., Xu, Y., Guo, S.L., Xu, Y., Wang, Y., Zhu, F., Permatasari, F., Wu, D., Yin, Z.Q., & Luo, D. 2013a. The effect of conditioned media of adipose-derived stem cells on wound healing after ablative fractional carbon dioxide laser resurfacing. *Biomed.Res.Int.*, 2013, 519126 available from: PM:24381938

Zhou, B.R., Xu, Y., Guo, S.L., Xu, Y., Wang, Y., Zhu, F., Permatasari, F., Wu, D., Yin, Z.Q., & Luo, D. 2013b. The effect of conditioned media of adipose-derived stem cells on wound healing after ablative fractional carbon dioxide laser resurfacing. *Biomed.Res.Int.*, 2013, 519126 available from: PM:24381938

Appendix

Supplemental material for Chapter 3

Tukey's multiple comparisons test	Mean Diff.	95.00% CI of diff.	Significant?	Adjusted P Value
Top vs. Middle	-0.8	-1.24 to -0.3599	Yes	0.0001
Top vs. Bottom	-0.7528	-1.205 to -0.3007	Yes	0.0004
Middle vs. Bottom	0.04722	-0.4049 to 0.4993	No	0.9666
Test details	**Mean 1**	**Mean 2**	**Mean Diff.**	**SE of diff.**
Top vs. Middle	0.025	0.825	-0.8	0.1851
Top vs. Bottom	0.025	0.7778	-0.7528	0.1901
Middle vs. Bottom	0.825	0.7778	0.04722	0.1901

Table S1 ***Two-way ANOVA with Tukey's Post Hoc test for number of metakaryotic nuclei in SSc skin biopsies***

Supplemental material for Chapter 4

PRURITUS QUESTIONNAIRE
5D Scale

1. During the last 2 weeks, how many hours a day have you been itching?
   <6
   6-12
   12-18
   18-23
   All day

2. Please rate the intensity of your itching over the past 2 weeks

   Nil
   Mild
   Moderate
   Severe
   Unbearable

3. Over the past 2weeks has your itching gotten better or worse compared to the previous month?

   Completely resolved
   Much better but still present
   Little better but still present
   Unchanged
   Worsening

4. Rate of impact on the following Activities

	N/A	Never	Rarely	Occasionally	Frequently	Always
Sleep						
Leisure						
Housework						
Work						

5. Distribution

Head/Scalp	Soles
Face	Palms
Chest	Tops of hands
Abdomen	Fore-arms
Back	Upper arms
Buttocks	Points of contact with clothing
Thighs	Groin
Lower legs	
Tops of feet	

6. What treatments have you had in the past?
   Hydroxyzine Hydroxychloride
   Fexofenadine
   Chlorephenamine
   Montelukast
   Liquid paraffin
   Aqueous cream
   Own creams (Shea butter)

Savlon healing gel (over the counter)

7. Which was most beneficial?
   None
   Antihistamines
   Liquid Paraffin/Aqueous cream
   Double base

8. Ethnic Origin?
9. Pakistani
   Caucasian
   Afro-Caribbean
   African
   Middle eastern

10. Pigment change?

    Yes No

11. Severity of pigment change?

    2/10
    4/10
    5/10
    6/10
    7/10
    8/10
    9/10
    10/10

12. Average skin scores?

Figure S1 ***Itch Score questionnaire***

5.5.5 Dermal Fibroblast scratch wound assays

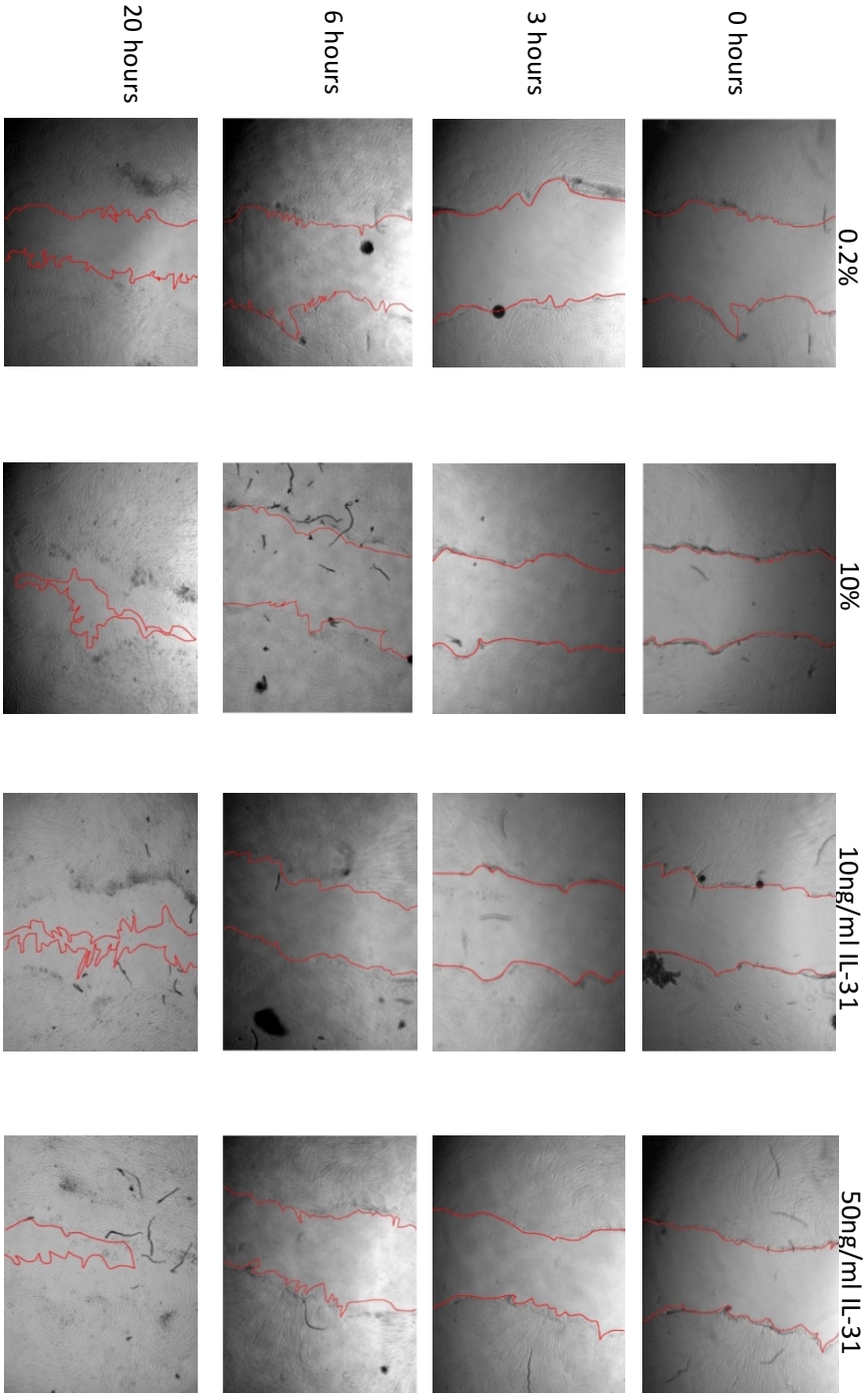

Figure S2 ***Images of scratches at 0, 3, 6, 20, 24 and 30 hours post treatment with 0.2% serum, 10% serum, 10ng/ml IL-31 and 50ng/ml IL-31.*** *Red outlines the remaining area of the scratch. Continued on next page.*

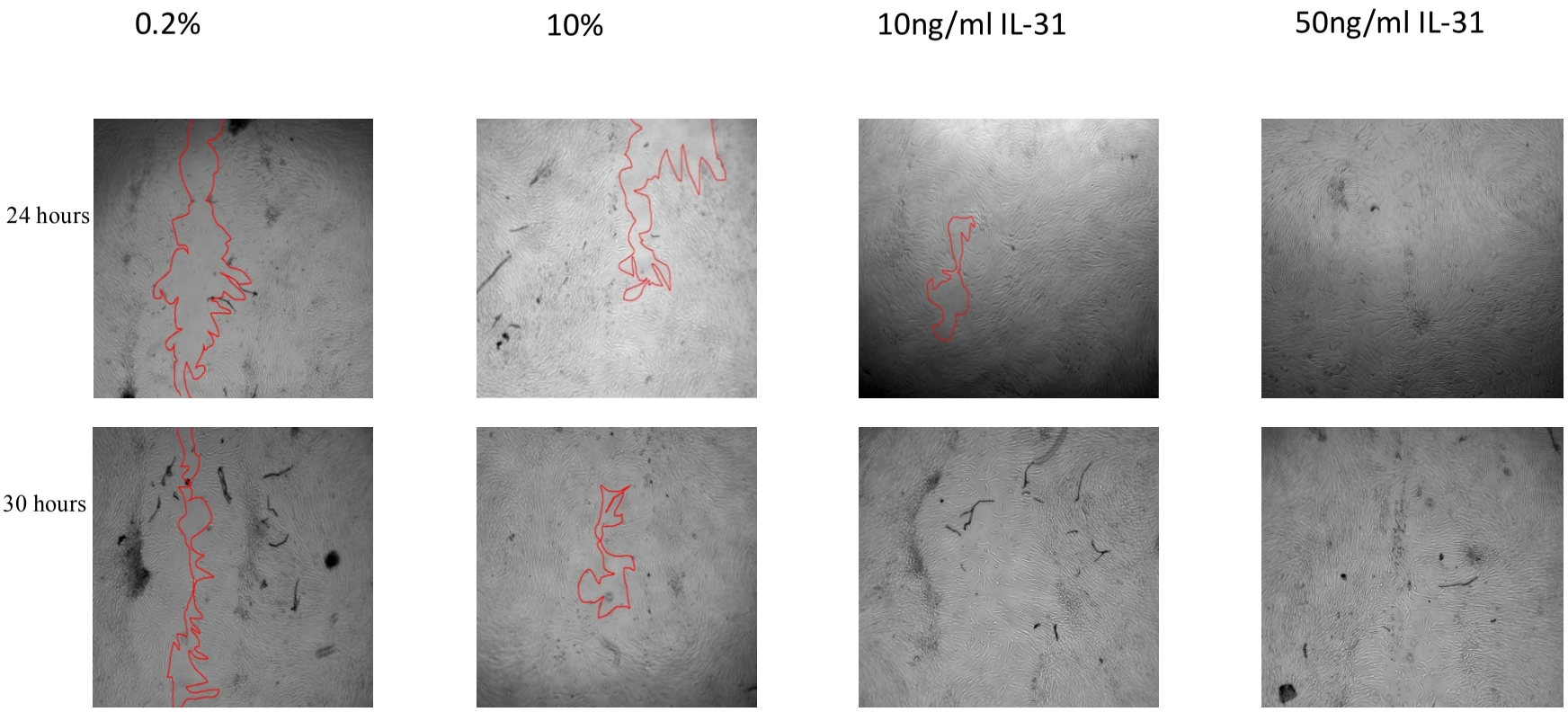
0.2%
10%
10ng/ml IL-31
50ng/ml IL-31
24 hours
30 hours

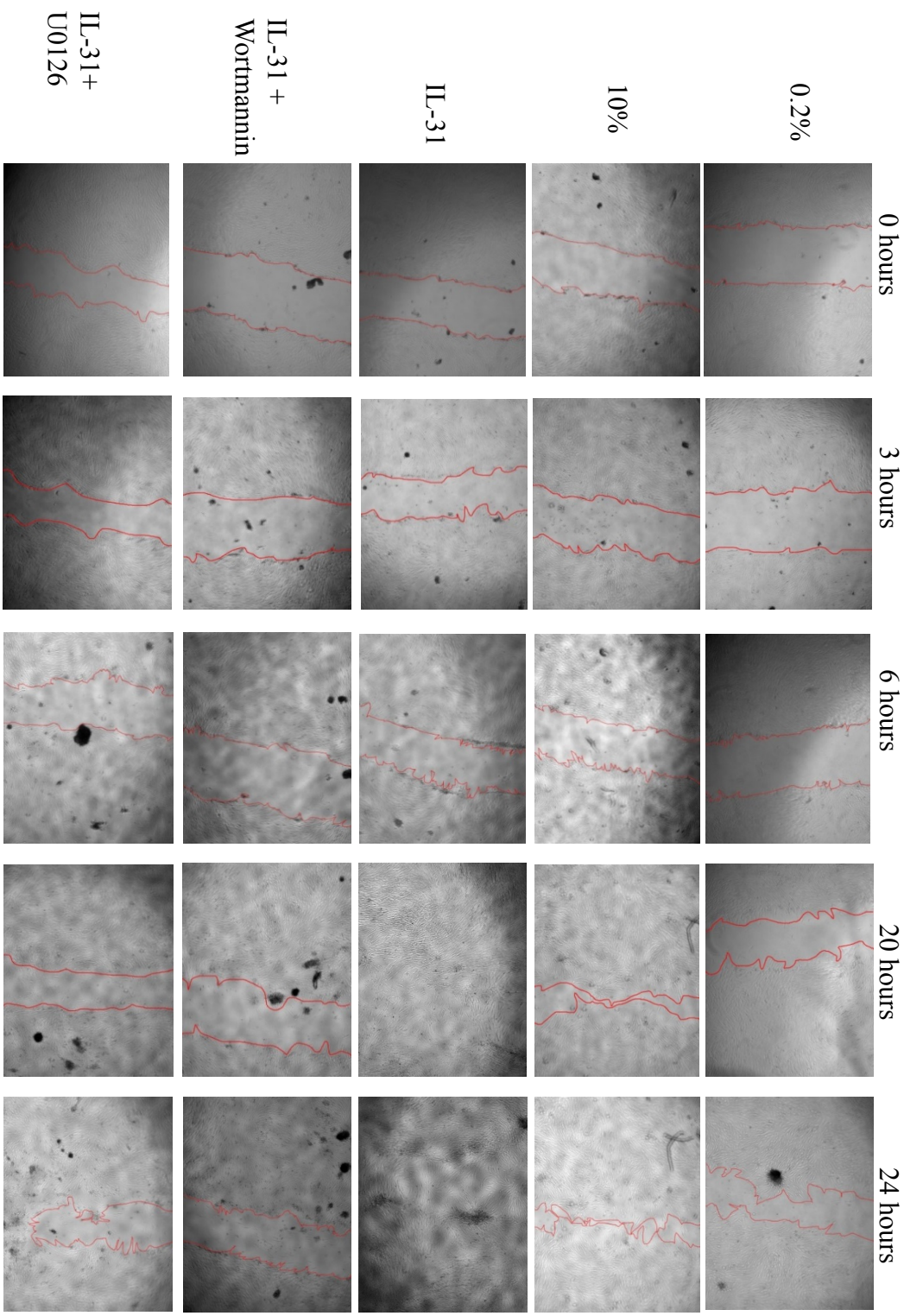

Figure S3 ***IL-31 at 50ng/ml enhances healthy control dermal fibroblast migration across a wound (red) in vitro from as soon as 6 hours post treatment.***

5.6.1 Collagen gel contraction and IL31

Treatment	1	2	3	Average
Serum free media	0.354	0.394	0.392	0.38
TGFβ	0.158	0.154	0.159	0.157
SScBF	0.14	0.139	0.128	0.136
cBF	0.16	0.193	0.146	0.166
SScBF + 1D11	0.182	0.174	0.152	0.169
cBF + 1D11	0.162	0.194	0.161	0.172
SScBF + Wortmannin	0.153	0.149	0.16	0.154
cBF + Wortmannin	0.166	0.196	0.162	0.175
SScBF + U0126	0.152	0.149	0.148	0.15
cBF + U0126	0.162	0.202	0.174	0.179
IL31 + Wortmannin	0.27	0.282	0.223	0.258

Table S2 ***Raw data and statistical analysis for Figure 5.10.*** *MSC populated gels were treated with serum free media, 10% serum, SSc blister fluid (SScBF 1:125), control blister fluid (cBF 1:125) or IL31 (50 ng/ml) with or without Wortmannin (100 nM). Wortmannin was added 1 hour prior to IL31 and other treatments. One-way ANOVA multiple comparisons is shown on the next page.*

Tukey's multiple comparisons test	Mean Diff.	95.00% CI of diff.	Significant?	Adjusted P Value
serum free media vs. 10% serum	0.03667	0.009881 to 0.06345	Yes	0.0062
serum free media vs. SScBF	0.04233	0.01555 to 0.06912	Yes	0.002
serum free media vs. cBF	0.01867	-0.008119 to 0.04545	No	0.2505
serum free media vs. IL31	0.02	-0.006786 to 0.04679	No	0.1961
serum free media vs. IL31+ Wortmannin	-0.001	-0.02779 to 0.02579	No	>0.9999
10% serum vs. SScBF	0.005667	-0.02112 to 0.03245	No	0.977
10% serum vs. cBF	-0.018	-0.04479 to 0.008786	No	0.2818
10% serum vs. IL31	-0.01667	-0.04345 to 0.01012	No	0.3528
10% serum vs. IL31+ Wortmannin	-0.03767	-0.06445 to -0.01088	Yes	0.0051
SScBF vs. cBF	-0.02367	-0.05045 to 0.003119	No	0.0954
SScBF vs. IL31	-0.02233	-0.04912 to 0.004452	No	0.1248
SScBF vs. IL31+ Wortmannin	-0.04333	-0.07012 to -0.01655	Yes	0.0016
cBF vs. IL31	0.001333	-0.02545 to 0.02812	No	>0.9999
cBF vs. IL31+ Wortmannin	-0.01967	-0.04645 to 0.007119	No	0.2087
IL31 vs. IL31+ Wortmannin	-0.021	-0.04779 to 0.005786	No	0.1621

Treatment	1 (g)	2 (g)	3 (g)	Average weight of gel (g)
Serum free media	0.354	0.394	0.392	0.38
TGFβ	0.158	0.154	0.159	0.157
SScBF	0.14	0.139	0.128	0.136
cBF	0.16	0.193	0.146	0.166
SScBF + 1D11	0.182	0.174	0.152	0.169
cBF + 1D11	0.162	0.194	0.161	0.172
SScBF + Wortmannin	0.153	0.149	0.16	0.154
cBF + Wortmannin	0.166	0.196	0.162	0.175
SScBF + U0126	0.152	0.149	0.148	0.15
cBF + U0126	0.162	0.202	0.174	0.179

***Table S3* Raw data for Figure 5.10 and ANOVA statistical analysis on next page.** *MSC populated collagen gels were treated with serum free media, TGFβ (4 ng/ml), SSc blister fluid (SScBF 1:50) or healthy control blister fluid (cBF 1:50) with or without TGFβ neutralising antibody 1D11 (10 ng/ml), PI3K inhibitor Wortmannin (100 nM) or MAPK inhibitor U0126 (5 μM). All treatments were in serum free media conditions.*

Tukey's multiple comparisons test	adjusted p-value
serum free vs. TGFb	< 0.0001
serum free vs. SScBF	< 0.0001
serum free vs. cBF	< 0.0001
serum free vs. SScBF+1D11	< 0.0001
serum free vs. cBF+1D11	< 0.0001
serum free vs. SScBF+ Wortmannin	< 0.0001
serum free vs. cBF+ Wortmannin	< 0.0001
serum free vs. SScBF+ U0126	< 0.0001
serum free vs. cBF+U0126	< 0.0001
serum free vs. IL31+Wortmannin	< 0.0001
TGFb vs. SScBF	0.7793
TGFb vs. cBF	0.9991
TGFb vs. SScBF+1D11	0.9917
TGFb vs. cBF+1D11	0.9625
TGFb vs. SScBF+ Wortmannin	> 0.9999
TGFb vs. cBF+ Wortmannin	0.9128
TGFb vs. SScBF+ U0126	0.9999
TGFb vs. cBF+U0126	0.7332
TGFb vs. IL31+Wortmannin	< 0.0001
SScBF vs. cBF	0.3316
SScBF vs. SScBF+1D11	0.2243
SScBF vs. cBF+1D11	0.1456
SScBF vs. SScBF+ Wortmannin	0.8934
SScBF vs. cBF+ Wortmannin	0.1017
SScBF vs. SScBF+ U0126	0.9794
SScBF vs. cBF+U0126	0.0473
SScBF vs. IL31+Wortmannin	< 0.0001
cBF vs. SScBF+1D11	> 0.9999
cBF vs. cBF+1D11	> 0.9999
cBF vs. SScBF+ Wortmannin	0.9917
cBF vs. cBF+ Wortmannin	0.9997
cBF vs. SScBF+ U0126	0.9375
cBF vs. cBF+U0126	0.9878
cBF vs. IL31+Wortmannin	< 0.0001
SScBF+1D11 vs. cBF+1D11	> 0.9999
SScBF+1D11 vs. SScBF+ Wortmannin	0.9625
SScBF+1D11 vs. cBF+ Wortmannin	> 0.9999
SScBF+1D11 vs. SScBF+ U0126	0.8478
SScBF+1D11 vs. cBF+U0126	0.9984
SScBF+1D11 vs. IL31+Wortmannin	< 0.0001
cBF+1D11 vs. SScBF+ Wortmannin	0.8934
cBF+1D11 vs. cBF+ Wortmannin	> 0.9999
cBF+1D11 vs. SScBF+ U0126	0.7172

cBF+1D11 vs. cBF+U0126	> 0.9999
cBF+1D11 vs. IL31+Wortmannin	< 0.0001
SScBF+ Wortmannin vs. cBF+ Wortmannin	0.8081
SScBF+ Wortmannin vs. SScBF+ U0126	> 0.9999
SScBF+ Wortmannin vs. cBF+U0126	0.583
SScBF+ Wortmannin vs. IL31+Wortmannin	< 0.0001
cBF+ Wortmannin vs. SScBF+ U0126	0.6
cBF+ Wortmannin vs. cBF+U0126	> 0.9999
cBF+ Wortmannin vs. IL31+Wortmannin	< 0.0001
SScBF+ U0126 vs. cBF+U0126	0.3737
SScBF+ U0126 vs. IL31+Wortmannin	< 0.0001
cBF+U0126 vs. IL31+Wortmannin	< 0.0001

5.6.2 Investigating α-SMA expression of MSCs treated with blister fluid and inhibitors

Sample	a-SMA Ct	TBP Ct	ΔCT	2^-ΔCT	Average	SEM
serum free	13.48	17.65	-4.17	18.0009357	16.8358302	1.1651054 9
serum free	13.54	17.51	-3.97	15.6707247		
TGFβ	12.75	17.79	-5.04	32.8996424	34.7020406	1.8023982 2
TGFβ	12.68	17.87	-5.19	36.5044389		
SScBF	13.35	18.17	-4.82	28.2464958	29.3654559	1.1189600 2
SScBF	13.19	18.12	-4.93	30.4844159		
cBF	18.07	22.67	-4.6	24.2514650	22.3931397	1.8583253 5
cBF	18.25	22.61	-4.36	20.5348143		
SScBF+1d11	15.03	18.45	-3.42	10.7034204	10.3450324	0.3583880 2
SScBF+1d11	15.09	18.41	-3.32	9.98664439		
cBF+1d11	14.26	18.47	-4.21	18.5070109	18.8333351 1	0.3263241 66
cBF+1d11	14.39	18.65	-4.26	19.1596592 7		
SScBF+W	14.3	17.82	-3.52	11.4716419 8	11.2762588 6	0.1953831 2
SScBF+W	14.3	17.77	-3.47	11.0808757 4		
cBF+W	15.34	20.03	-4.69	25.8125363	23.2450907 9	2.5674455 02
cBF+W	15.43	19.8	-4.37	20.6776452 9		
SScBF+U0126	14.3	17.93	-3.63	12.3805199 5	11.7692346 4	0.6112853 09
SScBF+U0126	14.32	17.8	-3.48	11.1579493 3		
cBF+U0126	16.23	20.3	-4.07	16.7954669 4	16.0188374 5	0.7766294 85
cBF+U0126	16.17	20.1	-3.93	15.2422079 7		
SScBF+x3	14.22	17.92	-3.7	12.9960383 4	12.0001864 4	0.9958518 98

SScBF+x3	14.32	17.78	-3.46	11.00433455		
cBF+x3	14.41	18.76	-4.35	20.39297004	20.04564033	0.347329712
cBF+x3	14.39	18.69	-4.3	19.69831061		

Table S4 **qPCR data for Figure 5.11. α-SMA expression of MSCs in response to blister fluid with 1D11, Wortmmanin and U0126 inhibitors. One-way ANOVA with Tukey's post hoc on next page.**

Tukey's multiple comparisons test	Mean Diff.	95.00% CI of diff.	Significant ?	P Value
serum free media vs. TGFβ	-17.87	-24.79 to -10.94	Yes	<0.0001
serum free media vs. SScBF	-12.53	-19.46 to -5.603	Yes	0.0004
serum free media vs. cBF	-5.557	-12.48 to 1.37	No	0.1667
serum free media vs. SScBF + 1D11	6.491	-0.4363 to 13.42	No	0.074
serum free media vs. cBF + 1D11	-1.998	-8.925 to 4.93	No	0.9846
serum free media vs. SScBF + Wortmannin	5.56	-1.367 to 12.49	No	0.1664
serum free media vs. cBF + Wortmannin	-6.409	-13.34 to 0.5178	No	0.0796
serum free media vs. SScBF + U0126	5.067	-1.86 to 11.99	No	0.2487
serum free media vs. cBF + U0126	0.817	-6.11 to 7.744	No	>0.9999
serum free media vs. SScBF + x3	4.836	-2.091 to 11.76	No	0.2972
serum free media vs. cBF + x3	-3.21	-10.14 to 3.717	No	0.7728
TGFβ vs. SScBF	5.337	-1.59 to 12.26	No	0.2002
TGFβ vs. cBF	12.31	5.382 to 19.24	Yes	0.0005
TGFβ vs. SScBF + 1D11	24.36	17.43 to 31.28	Yes	<0.0001
TGFβ vs. cBF + 1D11	15.87	8.942 to 22.8	Yes	<0.0001
TGFβ vs. SScBF + Wortmannin	23.43	16.5 to 30.35	Yes	<0.0001
TGFβ vs. cBF + Wortmannin	11.46	4.53 to 18.38	Yes	0.001
TGFβ vs. SScBF + U0126	22.93	16.01 to 29.86	Yes	<0.0001
TGFβ vs. cBF + U0126	18.68	11.76 to 25.61	Yes	<0.0001
TGFβ vs. SScBF + x3	22.7	15.77 to 29.63	Yes	<0.0001
TGFβ vs. cBF + x3	14.66	7.729 to 21.58	Yes	<0.0001
SScBF vs. cBF	6.972	0.04525 to 13.9	Yes	0.048
SScBF vs. SScBF + 1D11	19.02	12.09 to 25.95	Yes	<0.0001
SScBF vs. cBF + 1D11	10.53	3.605 to 17.46	Yes	0.0021
SScBF vs. SScBF + Wortmannin	18.09	11.16 to 25.02	Yes	<0.0001

SScBF vs. cBF + Wortmannin	6.12	-0.8067 to 13.05	No	0.1027
SScBF vs. SScBF + U0126	17.6	10.67 to 24.52	Yes	<0.0001
SScBF vs. cBF + U0126	13.35	6.42 to 20.27	Yes	0.0002
SScBF vs. SScBF + x3	17.37	10.44 to 24.29	Yes	<0.0001
SScBF vs. cBF + x3	9.32	2.393 to 16.25	Yes	0.0058
cBF vs. SScBF + 1D11	12.05	5.121 to 18.98	Yes	0.0006
cBF vs. cBF + 1D11	3.56	-3.367 to 10.49	No	0.6653
cBF vs. SScBF + Wortmannin	11.12	4.19 to 18.04	Yes	0.0013
cBF vs. cBF + Wortmannin	-0.852	-7.779 to 6.075	No	>0.9999
cBF vs. SScBF + U0126	10.62	3.697 to 17.55	Yes	0.0019
cBF vs. cBF + U0126	6.374	-0.5528 to 13.3	No	0.0821
cBF vs. SScBF + x3	10.39	3.466 to 17.32	Yes	0.0023
cBF vs. cBF + x3	2.348	-4.58 to 9.275	No	0.9548
SScBF + 1D11 vs. cBF + 1D11	-8.488	-15.42 to -1.561	Yes	0.0122
SScBF + 1D11 vs. SScBF + Wortmannin	-0.9312	-7.858 to 5.996	No	>0.9999
SScBF + 1D11 vs. cBF + Wortmannin	-12.9	-19.83 to -5.973	Yes	0.0003
SScBF + 1D11 vs. SScBF + U0126	-1.424	-8.351 to 5.503	No	0.999
SScBF + 1D11 vs. cBF + U0126	-5.674	-12.6 to 1.253	No	0.1511
SScBF + 1D11 vs. SScBF + x3	-1.655	-8.582 to 5.272	No	0.9963
SScBF + 1D11 vs. cBF + x3	-9.701	-16.63 to -2.774	Yes	0.0042
cBF + 1D11 vs. SScBF + Wortmannin	7.557	0.63 to 14.48	Yes	0.0282
cBF + 1D11 vs. cBF + Wortmannin	-4.412	-11.34 to 2.515	No	0.4033
cBF + 1D11 vs. SScBF + U0126	7.064	0.137 to 13.99	Yes	0.0442
cBF + 1D11 vs. cBF + U0126	2.814	-4.113 to 9.742	No	0.875
cBF + 1D11 vs. SScBF + x3	6.833	-0.09392 to 13.76	No	0.0544
cBF + 1D11 vs. cBF + x3	-1.212	-8.139 to 5.715	No	0.9998

SScBF + Wortmannin vs. cBF + Wortmannin	-11.97	-18.9 to -5.042	Yes	0.0006
SScBF + Wortmannin vs. SScBF + U0126	-0.493	-7.42 to 6.434	No	>0.9999
SScBF + Wortmannin vs. cBF + U0126	-4.743	-11.67 to 2.184	No	0.3186
SScBF + Wortmannin vs. SScBF + x3	-0.7239	-7.651 to 6.203	No	>0.9999
SScBF + Wortmannin vs. cBF + x3	-8.769	-15.7 to -1.842	Yes	0.0095
cBF + Wortmannin vs. SScBF + U0126	11.48	4.549 to 18.4	Yes	0.001
cBF + Wortmannin vs. cBF + U0126	7.226	0.2992 to 14.15	Yes	0.0381
cBF + Wortmannin vs. SScBF + x3	11.24	4.318 to 18.17	Yes	0.0011
cBF + Wortmannin vs. cBF + x3	3.199	-3.728 to 10.13	No	0.7758
SScBF + U0126 vs. cBF + U0126	-4.25	-11.18 to 2.677	No	0.4494
SScBF + U0126 vs. SScBF + x3	-0.231	-7.158 to 6.696	No	>0.9999
SScBF + U0126 vs. cBF + x3	-8.276	-15.2 to -1.349	Yes	0.0147
cBF + U0126 vs. SScBF + x3	4.019	-2.908 to 10.95	No	0.5192
cBF + U0126 vs. cBF + x3	-4.027	-10.95 to 2.9	No	0.5166
SScBF + x3 vs. cBF + x3	-8.045	-14.97 to -1.118	Yes	0.0182

5.7.1 Lactate in blister fluid and MSC collagen gel contraction

Condition	1 (g)	2 (g)	Average weight of gel (g)
serum free media	0.102	0.153	0.1275
10% serum	0.06	0.052	0.056
lactate	0.089	0.126	0.1075
lactate + aCHCA	0.174	0.179	0.1765
SScBF	0.086	0.073	0.0795
cBF	0.1625	0.166	0.16425
SScBF + aCHCA	0.072	0.112	0.092
cBF + aCHCA	0.106	0.125	0.1155

Table S8.1 Raw data for Figure 5.13. *MSC populated collagen gels were treated with serum free media, 10% serum, Lactate (25 mM) with or without αCHCA (5 mM) and SSc or healthy control blister fluid (diluted 1:50) with or without αCHCA. One-way ANOVA analysis on next page.*

Tukey's multiple comparisons test	Significant?	P Value
serum free media vs. 10% serum	No	0.0757
serum free media vs. lactate	No	0.9587
serum free media vs. lactate + aCHCA	No	0.3157
serum free media vs. SScBF	No	0.3347
serum free media vs. cBF	No	0.6014
serum free media vs. SScBF + aCHCA	No	0.6349
serum free media vs. cBF + aCHCA	No	0.9976
10% serum vs. lactate	No	0.2718
10% serum vs. lactate + aCHCA	Yes	0.0040
10% serum vs. SScBF	No	0.9132
10% serum vs. cBF	Yes	0.0078
10% serum vs. SScBF + aCHCA	No	0.6215
10% serum vs. cBF + aCHCA	No	0.1648
lactate vs. lactate + aCHCA	No	0.0891
lactate vs. SScBF	No	0.8259
lactate vs. cBF	No	0.1963
lactate vs. SScBF + aCHCA	No	0.9891
lactate vs. cBF + aCHCA	No	0.9998
lactate + aCHCA vs. SScBF	Yes	0.0152
lactate + aCHCA vs. cBF	No	0.9973
lactate + aCHCA vs. SScBF + aCHCA	Yes	0.0328
lactate + aCHCA vs. cBF + aCHCA	No	0.1496
SScBF vs. cBF	Yes	0.0323
SScBF vs. SScBF + aCHCA	No	0.9969
SScBF vs. cBF + aCHCA	No	0.6215
cBF vs. SScBF + aCHCA	No	0.0721
cBF vs. cBF + aCHCA	No	0.3204
SScBF + aCHCA vs. cBF + aCHCA	No	0.9132

5.7.2 Investigating α-SMA expression in response to Lactate

Sample	a-SMA Ct	TBP Ct	ΔCT	2^-ΔCT	Average
serum free	19.15	24.8	-5.65	50.21338227	43.98601322
serum free	19.16	24.79	-5.63	49.52207979	
serum free	19.86	24.87	-5.01	32.2225776	
10%	18.86	25.23	-6.37	82.71058116	71.46247872
10%	18.83	24.79	-5.96	62.24991663	
10%	18.84	24.42	-5.58	47.83517596	
10%	18.64	25.18	-6.54	93.05424111	
Lactate	20.78	25.95	-5.17	36.00187151	52.85151262
Lactate	20.63	25.95	-5.32	39.94657756	
Lactate	20.26	26.27	-6.01	64.4451552	
Lactate	20.18	26.33	-6.15	71.01244621	
Lactate + aCHCA	23.25	25.64	-2.39	5.241573615	8.196984477
Lactate + aCHCA	22.78	25.66	-2.88	7.361501205	
Lactate + aCHCA	21.81	24.79	-2.98	7.889861636	
Lactate + aCHCA	21.27	24.89	-3.62	12.29500145	
SScBF	18.86	24.93	-6.07	67.18186775	57.31641855
SScBF	18.87	24.66	-5.79	55.3303828	
SScBF	18.87	24.79	-5.92	60.54768939	
SScBF	18.88	24.41	-5.53	46.20573426	
cBF	20.18	25.24	-5.06	33.35890435	27.90948255
cBF	20	25.44	-5.44	43.41133848	
cBF	20.59	24.9	-4.31	19.8353232	
cBF	20.74	24.65	-3.91	15.03236399	

SScBF + aCHCA	22.18	25.69	-3.51	11.39240156	15.55436309
SScBF + aCHCA	22.06	25.38	-3.32	9.986644391	
SScBF + aCHCA	22.79	26.3	-3.51	11.39240156	
SScBF + aCHCA	21.58	26.46	-4.88	29.44600482	
cBF + aCHCA	20.07	25.76	-5.69	51.62507259	38.46283382
cBF + aCHCA	19.57	25.35	-5.78	54.94818793	
cBF + aCHCA	21.8	24.94	-3.14	8.815240927	

Table S8.2 *Confluent MSCs were treated with serum free media, 10% serum, lactate (25mM) with or without αCHCA (5 mM) and SSc or healthy control blister fluid (SScBF, cBF 1:50) with or without αCHCA. One-way ANOVA results on next page.*

Tukey's multiple comparisons test	Significant?	Adjusted P Value
serum free media vs. 10% serum	No	0.3060
serum free media vs. lactate	No	0.9936
serum free media vs. lactate + aCHCA	No	0.0843
serum free media vs. SScBF	No	0.9394
serum free media vs. cBF	No	0.8568
serum free media vs. SScBF + aCHCA	No	0.2688
serum free media vs. cBF + aCHCA	No	0.9497
10% serum vs. lactate	No	0.6714
010% serum vs. lactate + aCHCA	**Yes**	**0.0001**
10% serum vs. SScBF	No	0.8851
10% serum vs. cBF	**Yes**	**0.0101**
10% serum vs. SScBF + aCHCA	**Yes**	**0.0007**
10% serum vs. cBF + aCHCA	**Yes**	**0.0201**
lactate vs. lactate + aCHCA	**Yes**	**0.0079**
lactate vs. SScBF	No	0.9999
lactate vs. cBF	No	0.3283
lactate vs. SScBF + aCHCA	**Yes**	**0.0374**
lactate vs. cBF + aCHCA	No	0.4947
lactate + aCHCA vs. SScBF	**Yes**	**0.0030**
lactate + aCHCA vs. cBF	No	0.6086
lactate + aCHCA vs. SScBF + aCHCA	No	0.9967
lactate + aCHCA vs. cBF + aCHCA	No	0.4273
SScBF vs. cBF	No	0.1641
SScBF vs. SScBF + aCHCA	**Yes**	**0.0148**
SScBF vs. cBF + aCHCA	No	0.2748
cBF vs. SScBF + aCHCA	No	0.9390
cBF vs. cBF + aCHCA	No	>0.9999
SScBF + aCHCA vs. cBF + aCHCA	No	0.8267

5.7.3 Investigating the collective effects of lactate and IL31 on MSC collagen gel contraction

Condition	1 (g)	2 (g)	3 (g)	Average weight of gel(g)
serum free media	0.106	0.107		0.1065
10% serum	0.042	0.045		0.0435
lactate	0.102	0.089	0.091	0.094
IL31	0.109	0.101	0.082	0.097333333
lactate + IL31	0.071	0.092		0.0815

Tukey's multiple comparisons test	Significant?	Adjusted P Value
serum free media vs. 10% serum	Yes	0.0026
serum free media vs. lactate	No	0.6671
serum free media vs. IL31	No	0.8485
serum free media vs. lactate + IL31	No	0.1978
10% serum vs. lactate	Yes	0.0056
10% serum vs. IL31	Yes	0.0039
10% serum vs. lactate + IL31	Yes	0.0391
lactate vs. IL31	No	0.9930
lactate vs. lactate + IL31	No	0.6671
IL31 vs. lactate + IL31	No	0.4773

Table S8.3 ***Raw data for Figure 5.15.*** *MSC populated collagen gels were treated with serum free media, 10% media, lactate (25 mM) and IL31 (50 ng/ml), both alone and together. One-way ANOVA with Tukey's' post hoc data is shown.*

6.3 Investigating adipogenic differentiation in response to SSc microenvironments

Media				Average	corrected for blank	fold difference	
serum only	0.148	0.17	0.15	0.156	0.027666667	1	
adipogenic media only	0.262	0.248	0.37	0.293333333	0.165	5.963855422	
adipogenic media + sscBF	0.219	0.191	0.235	0.215	0.086666667	3.13253012	
adipogenic media + cBF	0.259	0.252	0.239	0.25	0.121666667	4.397590361	
blank	0.13	0.12	0.135	0.128333333	0		

Tukey's multiple comparisons test	Significant?	Adjusted P Value
Serum free DMEM vs. Adipogenic media	Yes	0.0035
Serum free DMEM vs. Adipogenic media + SScBF	No	0.1898
Serum free DMEM vs. Adipogenic media + cBF	Yes	0.0294
Adipogenic media vs. Adipogenic media + SScBF	No	0.0679
Adipogenic media vs. Adipogenic media + cBF	No	0.4052
Adipogenic media + SScBF vs. Adipogenic media + cBF	No	0.5689

Table S8.4 ***Raw data for Figure 6.16.*** *MSCs cultured in serum free media, adipogenic media with or without SSc or healthy control blister fluid (1:125). N=3. Optical density measured at 490 nm. Fold changes >3 indicates adipogenic differentiation. One-way ANOVA with Tukey's post hoc test conduction.*

Royal Free & Medical School Local Research Ethics Committee

NHS

Please reply to:

Ethics Department
Royal Free Hospital
Pond Street
London
NW3 2QG

Telephone: 020 7830 2746
Fax: 020 7830 2961
E-mail: rosemary.brown@royalfree.nhs.uk

14 December 2006

Prof Carol M Black,
Department of Rheumatology
The Royal Free & University Medical School
Pond Street
Hampstead
London
NW3 2QG

Dear Prof Black,

REC Ref: 6398 **Elucidating the pathogenesis of systemic sclerosis by studying skin, blood and tissue samples from scleroderma patients and healthy volunteers**

Amendment number:2
Amendment date:31.10.2006

The above amendment was reviewed by the Sub-Committee of the Research Ethics Committee at the meeting held on 13.12.2006
Ethical opinion

The members of the Committee present gave a favourable ethical opinion of the amendment on the basis described in the notice of amendment form and supporting documentation.

Approved documents

The documents reviewed and approved at the meeting were:

Healthy Volunteer information sheet version 2 dated 31.10.06 with tracked changes
Patient information sheet version 2 dated 31.10.06 with tracked changes
Control consent version 2 dated 31.10.06 with tracked changes
patient consnet version 2 dated 31.10.06 with tracked changes
Ethics application form version 2 dated 31.10.06 with tracked changes

Membership of the Committee

The members of the Ethics Committee who were present at the meeting are

Dr Michael Pegg -- Chair
Mr John Farrell
Mrs Wendy Spicer
Marissa Kaye

Management approval

Before implementing the amendment, you should check with the host organisation whether it affects their approval of the research.

Statement of compliance (from 1 May 2004)

Manuscript

Interleukin 31 promotes pathogenic mechanisms in systemic sclerosis and induces skin fibrosis in mice

Taki Z[1], Zafar S[1], Rosario H[1], Black S[1], Etomi O[1], Abdi Ahmed B[1], Tam A[1], Scolamiero L[1], Hart A[1], Arumala N[1], Renzoni E[3], Nicholson A[3], Abraham D[1], Denton C[1], Venturini C[1], Mohamed A[1], Mazumder N[1], Shiwen X[1], Xing F[1], Lopez H[2], Stratton R[1]

[1]Centre for Rheumatology and Connective Tissue Disease, Royal Free Hospital Campus, University College Medical School, Rowland Hill Street, London, NW3 2PF, UK, [2]MuriGenics, Inc., 941 Railroad Avenue, Vallejo, CA, 94592, USA, [3]Imperial College London, Royal Brompton Campus, Sydney Street,London SW3 6NP, UK

Abstract

In scleroderma, an autoimmune process leads to progressive fibrosis of the skin and internal organs, which is resistant to therapy. Cytokines released by infiltrating T cells may provide a mechanistic link between the autoimmunity and the persistent fibroblast activation seen. We investigated the role of IL-31, a Th2 cytokine, implicated in other pruritic skin conditions. IL-31 was present at high levels in plasma and skin lesions of scleroderma patients, and the receptor, IL-31RA, overexpressed by downstream effector cells relevant to the disease process, including skin and lung fibroblasts, epidermal cells and fat derived mesenchymal stem cells (MSCs). Treatment of skin fibroblasts with IL-31 induced gene expression profiles linked to integrin signalling, growth, actin polymerisation, motility, plus Wnt and TGFβ signalling, and induced phenotypic changes including migration and collagen protein release, resembling the activation state in the disease. MSCs derived from subcutaneous fat were induced to migrate and differentiate by IL-31. In mice, IL-31 caused skin fibrosis more than the pro-fibrotic growth factor TGFβ, and led to increased cytokine and growth factor levels in a scleroderma-like pattern. IL-31 appears to act as a central mediator in scleroderma skin fibrosis and is confirmed as a target for specific therapies.

Introduction

ln scleroderma (also called systemic sclerosis, SSc), progressive fibrosis of the skin and internal organs resistant to current therapy remains a significant clinical problem linked to severe disability and increased mortality (1, 2). Whereas progress has been made in the treatment of pulmonary hypertension, renal crisis and peripheral ischaemia, current treatments for fibrosis have limited efficacy and are associated with toxicity. Immunosuppressive regimens, such as methotrexate or cyclophosphamide, have a modest effect against skin fibrosis and may cause sepsis or myelosuppression

(3, 4). Autologous haematopoietic stem cell therapy following high intensity immunosupression, has shown long term clinical benefit but is associated with up to 10% increase in mortality in the first year (5). Improved understanding of underlying biomechanisms might lead to a more selective and effective anti-fibrotic treatment.

The mechanisms underlying SSc pathogenesis are, however, complex and incompletely understood. Large systematically designed genomic studies have implicated immunogenetic and immunoregulatory factors in the disease, at least in subsets (6). Gene polymorphism associated with SSc include HLA DR subtypes, IRF5, STAT4, CD247, TNIP, IRF8, IL12RB2, CSK, KIAA0319L, PXK, JAZF1, BLK, ITGAM, TNRFAIP3(7, 8). In particular, the role of Th cell dependent mechanisms in SSc is supported by a number of observations, including the genetic associations with HLA-DR alleles, infiltration of involved tissues by Th cells as well as macrophages in approximately 50% of patients, restricted T cell receptor repertoire in involved tissue and downstream antigen-specific B cell responses (reviewed in (9)). More specifically, Th2 cells are capable of stimulating fibroblasts directly through cytokine production or indirectly through polarisation of macrophages to the alternatively activated ("M2") subtype (10-13).

The heterogeneity of SSc makes therapeutic trials challenging, as beneficial effects may only be seen in certain subgroups. Gene expression profiling of lesional RNA from SSc patients, has indicated patient-specific inflammatory, fibroproliferative, limited, and normal-like patterns (14). Response to therapy might also be predictable on the basis of these classifications (15). Recent attempts at therapy have focused on clinically defined subsets such as those patients with raised C-reactive protein, in whom the use of anti-IL6 receptor antibody trended towards clinical benefit (16). For this reason, biological definition of subgroups may further benefit clinical trial design in SSc, especially for more targeted therapies.

Of the clinical features of SSc, severe and intractable itch or pruritus poses a significant problem in a sub-population of patients, which may be resistant to conventional treatment. The severity of itch varies in intensity from a mild discomfort to a disabling symptom associated with a significant psychosocial burden, impacting negatively on quality of life. Razykov et al. estimated the prevalence of pruritus at 43%, in one epidemiological study of 959 scleroderma patients. Although prevalence did not change with disease duration (46% at 1.0 – 4.9 years vs. 41% ≥ 5.0 years since onset of disease from first non-Raynaud's symptom), pruritus was independently

associated with greater skin and gastro-intestinal involvement(17). Patients with scleroderma who reported higher pain and itch severity were also more likely to have more severe depressive symptoms, overall disability, and sleep and fatigue problems, even when demographic measures were controlled for (18).

Pruritus is also a prominent feature of other chronic skin conditions, including atopic eczema, nodular prurigo, and T cell lymphoma. Mast cell recruitment, histamine release and inflammatory cytokine production are the mechanisms which have been implicated in pruritus (reviewed in (19)). One particular cytokine, Interleukin-31 (IL-31), which was recently identified as a member of the four-helix bundle structure IL-6 family of cytokines, is now considered an important itch-inducing factor (20). IL-31 is predominantly Th2 secreted and signals via a heterodimeric receptor, composed of the oncostatin M receptor (OSMR) and interleukin 31 receptor alpha (IL-31RA). It has been shown to be strongly associated with pruritic skin conditions including atopic dermatitis and cutaneous T-cell lymphoma, and induces itching behaviour in mouse models (20-23). IL-31 is known to signal through the JAK-STAT, RAS/ERK and PI3K/AKT pathways (24, 25).

Since Th2 responses have been implicated in SSc, we studied the levels of IL-31 in tissue fluid and plasma and sought correlation with itch severity. In addition we assayed levels of the IL-31 receptor IL-31RA in target cells from patients and investigated whether recombinant IL-31 induced gene expression and phenotypic changes linked to the SSc disease process. The fibrogenic potential of IL-31 has not been previously evaluated and we investigated the capacity of recombinant IL-31 to induce skin fibrosis in mice.

Results

IL-31in plasma and skin of scleroderma patients IL-31 concentrations were measured in plasma and blister fluid of 43 SSc patients and 27 healthy controls. Plasma IL-31 was elevated in SSc (HC range 0-792, mean 196, SEM 48, SSc range 0-17764, mean 1370, SEM 567, $p<0.048$). BF IL-31 trended towards elevation in SSc but did not reach significance (HC 0-2777, mean 196, SEM 139, SSc 0-38222, mean1203, SEM 872 pg/ml, pNS) (Figure 1). IL-31 was present in BF at over 1000pg/ml in a subgroup of 5 SSc patients (Table 1). These patients were from both limited and diffuse scleroderma subgroups, but had high itch scores (median 5D score 23 range 16-24).

Age	Gender	Disease	Autoantibody profile	Disease duration (months)	Itch Score	Hb (g/L)	Plt (x109/L)	ESR	CRP	mRSS
59	Female	Diffuse	Scl70, RF	72	18	122	188	12	1	20
44	Female	Limited	ANA, ACA	118	16	122	279	5	2	11
65*	Male	Diffuse	RNA Pol III	74	23	130	276	5	2	21
66*	Female	Diffuse	RNA Pol III	26	23	102	319	27	2	10
60*	Male	Limited	ACA	74	24	130	172	22	22	4

Table 1 Clinical and laboratory characteristics of scleroderma patients with dermal blister fluid IL-31 >1000 pg/ml. A subgroup of patients was identified with high blister fluid IL-31. These patients were from both diffuse and limited cutaneous subsets and early and late disease, but had in common very high 5D itch scores. In general marked systemic inflammatory features such as high CRP, anaemia or high platelet count, associated with a high IL-6 phenotype, were not seen. (Scl70=anti-topoisomerase, ANA=antinuclear antibody, ACA=anti-centromere, RNA PolIII=anti-RNA polymerase III, RhF=rheumatoid factor, mRSS=modified Rodnan Skin Score).

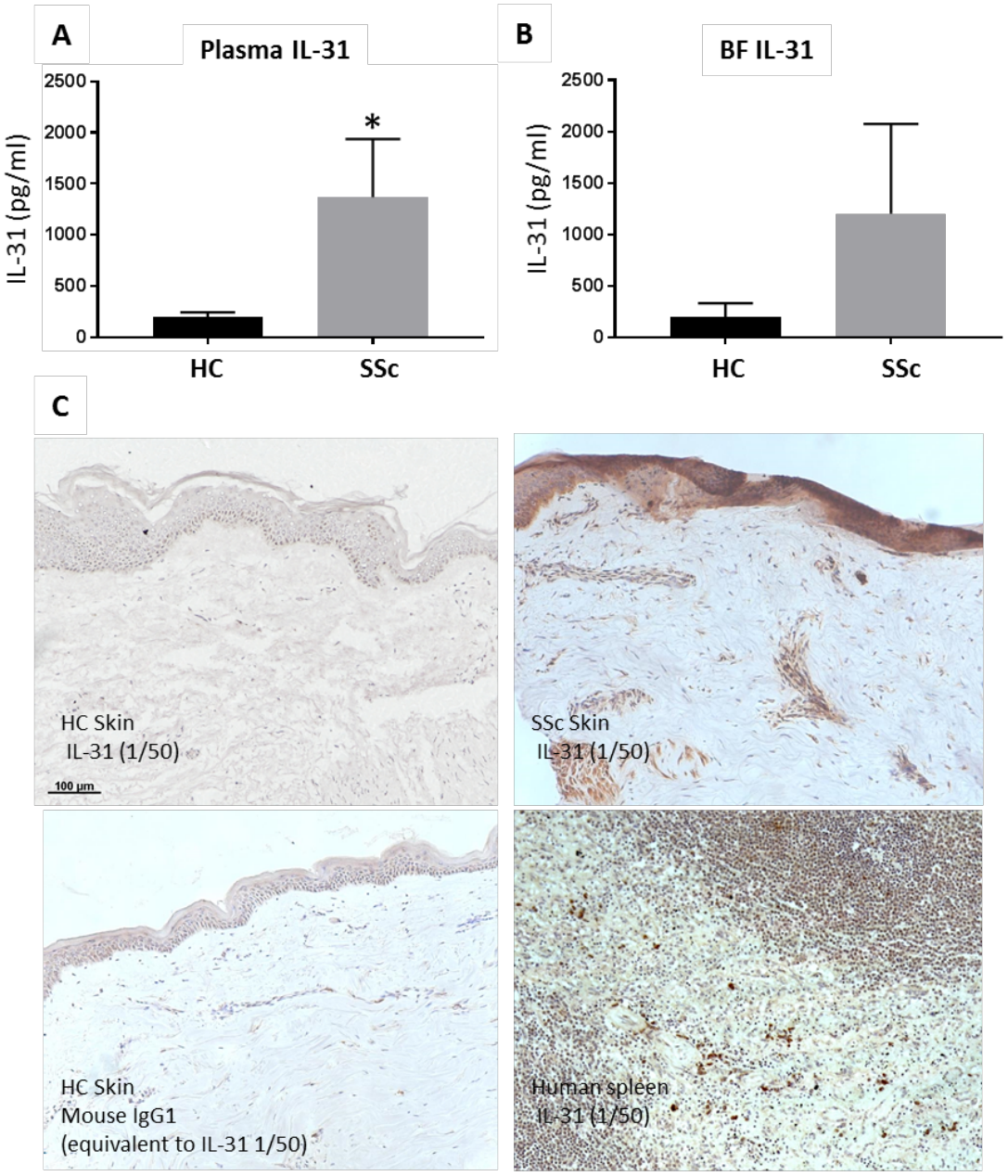

Figure 1 Elevated IL-31 in plasma and skin lesions of scleroderma patients. (**A, B**) IL-31 was assayed by ELISA of plasma and synchronous dermal blister fluid (BF) of SSc patients and healthy controls (SSc N=43 HC N=27). IL-31 was significantly elevated in plasma of SSc patients and BF IL-31 trended towards elevation in SSc but did not reach significance. (**C**) Involved forearm skin biopsy material from SSc patients and biopsies from the normal forearm skin of healthy controls were frozen in OCT and cut as frozen sections, and then immunostained with anti-IL-31. No positive staining was identified in healthy control sections, or with control mouse polyclonal IgG. However, in the SSc lesions strong perivascular and epidermal positive staining was identified. Human spleen tissue was used as positive control.

IL31 is present in SSc skin To ascertain whether increased IL-31 levels were present in SSc skin, biopsies taken from patients with recent onset diffuse SSc experiencing

severe pruritus, were stained for IL-31 (Figure 1C). IL-31 expression was mainly localised to the epidermis in SSc skin and around blood vessels. IL-31 expression in healthy skin was not seen. The specific upregulation and localisation to the epidermis may account for the severe pruritus experienced by the SSc patients.

IL-31 Receptor expression in downstream effector cells In order to more fully explore the IL-31 axis in SSc cells and tissue, a range of candidate downstream effector cells were evaluated for expression levels of the IL-31 receptor, IL-31RA. The lL-31RA mRNA expression levels were increased in SSc dermal and lung fibroblasts, and also expressed by fat derived MSCs (Figure 2A). Furthermore, IL-31RA trended to being increased in SSc epidermal tissue samples (Figure 2B).

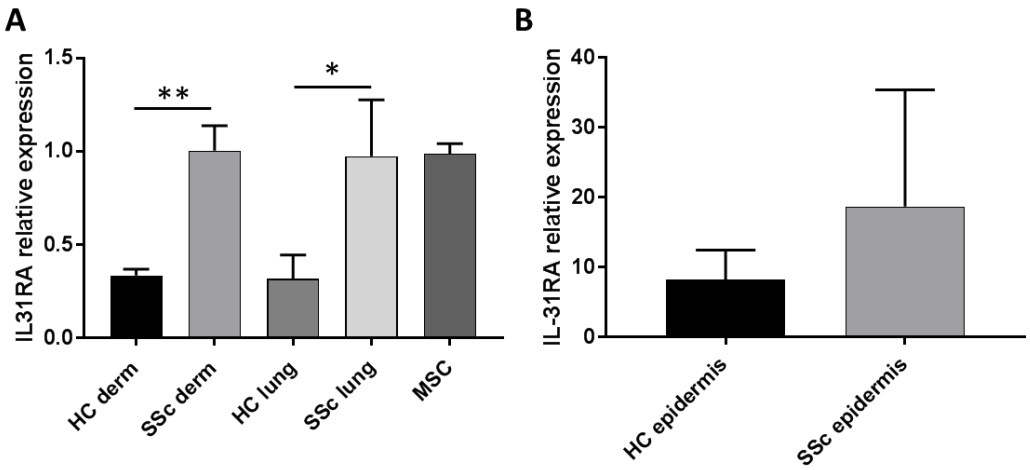

Figure 2 Expression levels of IL-31RA by target cells and tissue. (**A**) Potential effector cells downstream of IL-31 were profiled for expression of the receptor IL-31RA. Cells cultured in vitro including healthy control and SSc dermal and lung fibroblasts (N=4 lines for both SSc and HC), as well as fat derived MSCs (healthy control only) were assessed by qPCR. Expression relative to TBP is shown. IL-31RA was elevated in SSc dermal and lung fibroblasts and expressed by fat derived MSCs at a level similar to SSc fibroblasts. (**B**) Also, whole tissue extracts of SSc epidermis sampled during the blister fluid protocol (n=8 SSc and HC), were lysed and assayed for IL-31 RA. There was a trend towards increased IL-31RA in SSc tissue extracts but this did not reach statistical significance. **P<0.001, * P<0.05.

IL31 induces phenotypic changes in fibroblasts and MSCs Furthermore, we suspected that IL-31 might be involved in pathologic changes in addition to its known pruritogenic properties, and we went on to study the effect of recombinant human IL-31 on target cells relevant to scleroderma**.** Control dermal fibroblasts were switched to low serum media containing ascorbate overnight and then treated with the known fibrogenic growth factor

TGFβ (4ng/ml), or recombinant IL-31 (1-50 ng/ml), or both and then lysed for RNA and protein extraction. As expected TGFβ induced collagen I protein as well CTGF, a downstream fibrosis enhancing factor, at both mRNA and protein level (Figure 3). However the responses induced by IL-31 were distinct from the TGFβ induced changes. IL-31 provoked collagen I release from these cells but did not significantly induce CTGF or mRNA for collagen I or CTGF (Figure 3D). Since STAT3 is implicated in both the response to IL-31 as well as in the overall pro-fibrotic phenotype of SSc cells, the STAT3 inhibitor SD1029 was evaluated. Treatment with SD1029 blocked collagen induction by both IL-31 and TGFβ, implicating STAT3 signalling in the fibrotic responses (Figure 3C).

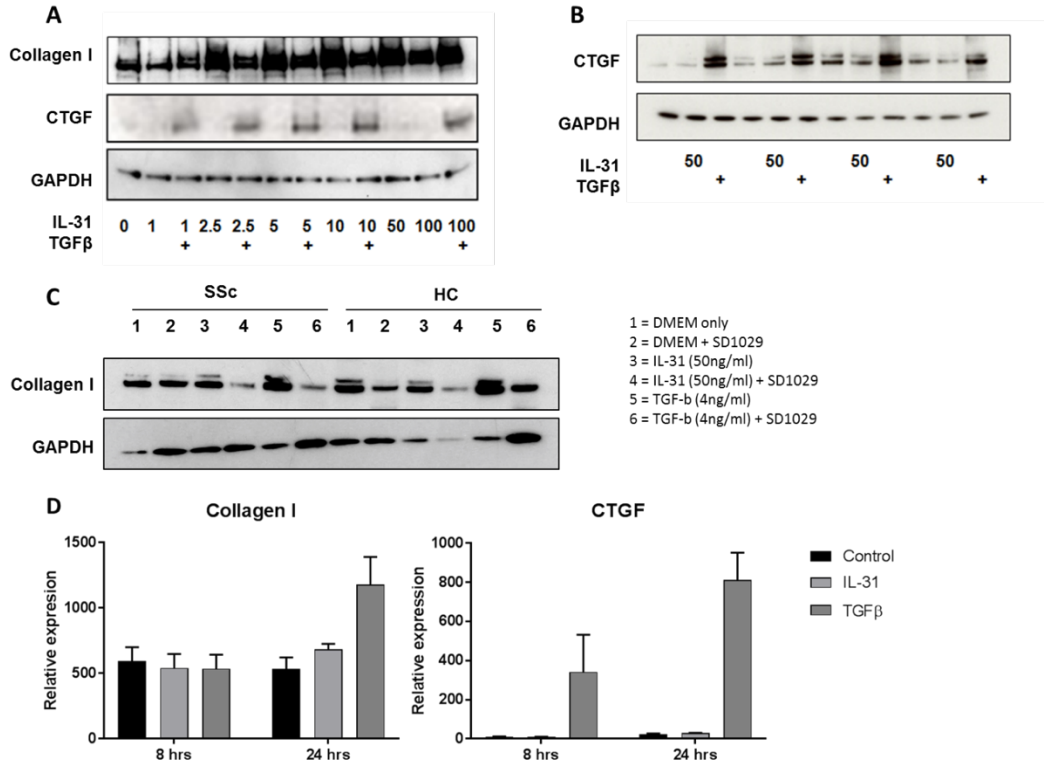

Figure 3 Effect of IL-31 on collagen and CTGF expression in normal skin fibroblasts. (**A**) Treatment of normal dermal fibroblasts under low serum conditions with various doses of IL-31 (1-100ng/ml) led to release of collagen I protein maximal at 50 ng/ml and comparable but not additive to the effect of TGFβ. (**B**) However CTGF protein levels did not increase following treatment with IL-31, but were increased as expected by TGFβ. (**C**) The STAT3 inhibitor SD1029, blocked induction of collagen I by both IL-31 and TGFβ and reduced basal collagen secretion by these cells. (**D**) Collagen I and CTGF gene expression assayed by qPCR, which were as induced by TGFβ as expected but were not affected by IL-31.

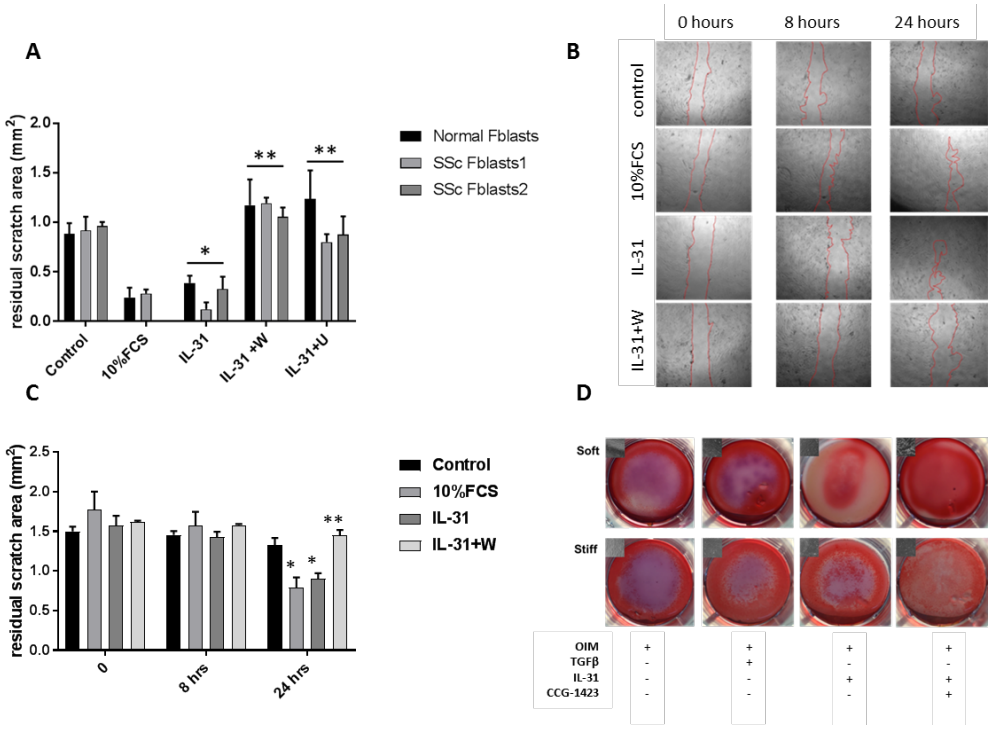

Figure 4 IL-31 induces migration of fibroblasts and MSCs and promotes osteogenic differentiation **(A)** Since IL-31 signals via PI3 K a pathway known to be involved in migration of fibroblasts, a migration assay was performed. Healthy control dermal fibroblasts (NF25) and SSc dermal fibroblasts (SScF1/F2) were treated with 50 ng/ml IL31, with or without the PI3K inhibitor, Wortmannin (W, 100nM) or MEK/ERK inhibitor U0126 (U, 5μM). IL-31 led to enhanced migration of normal and SSc skin fibroblasts inhibited by both antagonists. (**B,C**) Furthermore, a similar effect was seen with MSCs which were strongly induced to migrate by IL-31, inhibited by W. (**D**) In MSCs grown in osteogenic media (OIM) IL-31 (50 ng/ml) enhanced osteogenic polarisation identified by Alluzarin red stain on stiff 50kPa substrates but not 4 kPa substrates, appearance at day 12 shown. The stiff substrates model the stiffness of lesional fibrotic skin in SSc. CCG-1423 10μM, an inhibitor of the mechano-sensing MRTF-A pathway, blocked the osteogenic differentiation induced by IL-31. * P<0.05 versus control, ** P<0.05 vs IL-31 treatment

IL31 induces osteogenic differentiation of MSCs IL6 is known to affect MSC osteogenic differentiation. As IL31 is an IL-6 related protein, present at high levels in the SSc microenvironment, its effects on the ability of MSCs to differentiate into osteoblasts were investigated. MSCs cultured on stiff (50 KPa) substrates in osteogenic induction media (OIM) were found to take up more Alizarin red stain than those of soft substrates (4 KPa) at day 12 (Figure 7). Furthermore, IL-31 induced differentiation to a similar extent as the TGFβ positive control. Inhibiting the ability of the cells to respond to the stiffness of the extracellular matrix by adding the MRTF-A inhibitor CCG-1243 reduced the differentiation potential of the cells

(26). TGFβ and IL31 treatment result in the most differentiation into osteoblasts resembling the calcinosis which occurs at the sites of pressure and minor trauma.

The results indicate that both the biochemical constituents of the environment together with the physical extracellular environment are important in influencing MSC differentiation potential.

IL31 induces differential RNA expression of cytokines in healthy control dermal fibroblast

Next generation sequencing using Illumina TruSeq highlighted specific RNA molecules expressed by healthy control dermal fibroblasts in response to IL31. Interleukin-33 (IL33), Matrix metallopeptidase 10 (MMP10), CXCL5 and Annexin 1 (ANXA1), were the most differentially expressed (Figure 5A). IL33 is a member of the Interleukin- 1 family and induces the production of many T-helper 2 cytokines. *In vivo* these cytokines indicate the activation of inflammatory processes and most interestingly, IL33 has been associated with pruritus in dermatitis models.

Ingenuity Pathway Analysis (IPA) pathway analysis was performed highlighting the physiological and disease association to the differentially expressed genes (Figure 5B). In the IPA data below, significance values were set at a threshold of $p<0.05$ using Walds statistic. Z-scores highlight directionality of the pathway such that in this case, negative z-scores show upregulated in response to IL-31, and positive score indicates a downregulated pathway. The Z-score is a statistical measure of the match between the predicted and expected direction of the regulation of the pathway, and the gene expression observed. The Z-score is calculated by using existing literature and published findings (Table 2).

The positive effect seen on the PI3K pathway in response to IL31 is notable, highlighting this pathway's importance in the downstream effects of this cytokine and supporting the use of Wortmannin as an IL31 inhibitor is the migration and protein expression experiments. Furthermore, PTEN, an inhibitor of the PI3K pathway, is itself inhibited by IL31, possibly elucidating the mechanism of PI3K pathway activation by IL31.

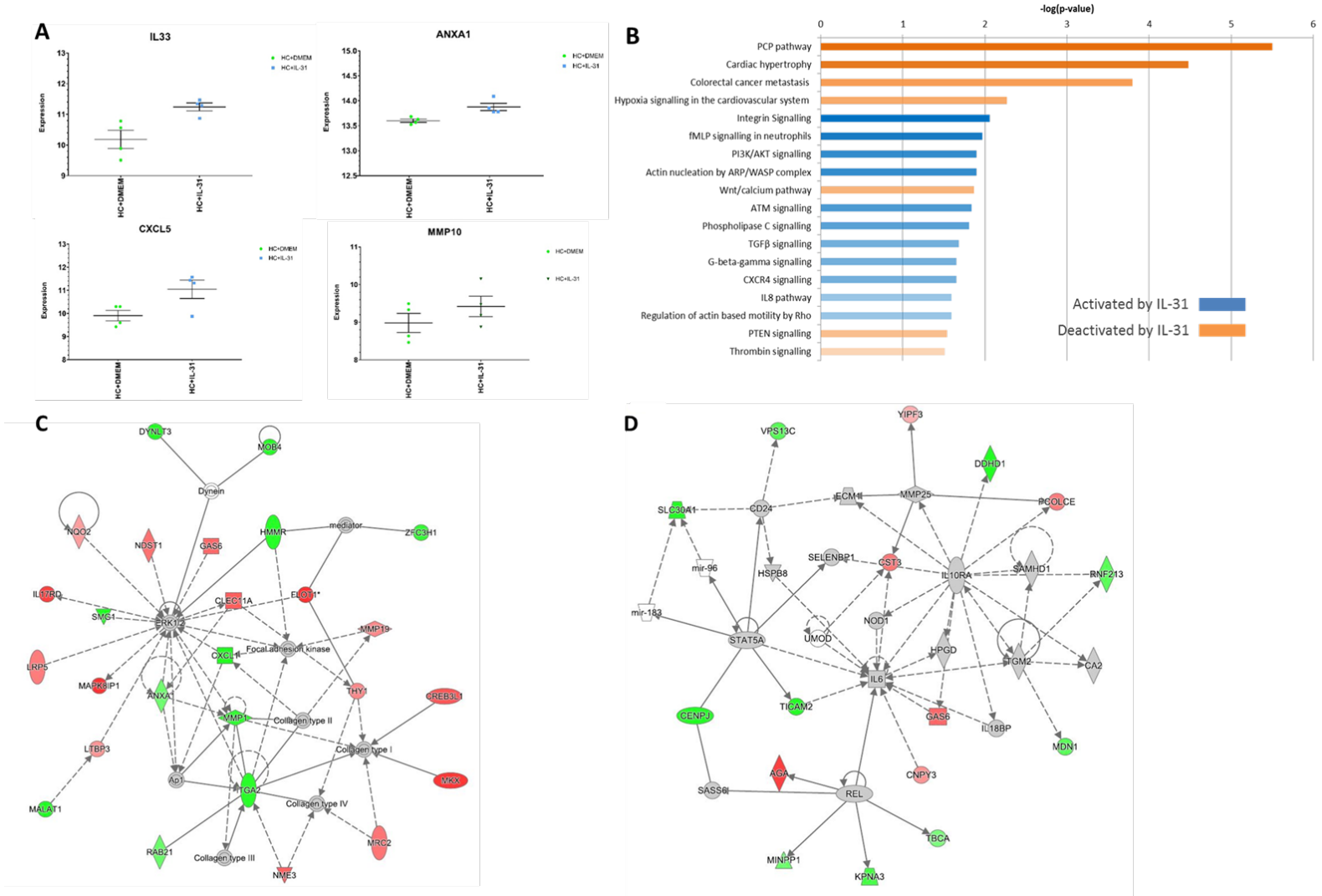

Figure 5 Next generation sequencing analysis of IL-31 treated fibroblasts. (**A**) Healthy control dermal fibroblasts were treated with IL-31 (50 ng/m) for 16 hours and then lysed for RNA extraction followed by NGS. Key responsive genes are shown. IL33, ANXA1, and CXCL5 were significantly increased in IL-31 treated cells (p= 0.043, p= 0.02, p= 0.005) and MMP10 expression was also higher in response to IL31 than serum free controls, although not significantly so (p= 0.26.). (**B**)

Significantly altered canonical pathways in response to IL-31 treatment are shown. The significance threshold was set at $p < 0.05$. Blue bars indicate pathway positively upregulated by IL31 and the orange, the pathways negatively regulated. The transparency of the bars indicate the Z-score with more opaque bars showing pathways with higher z-scores. (**C**) IPA pathway analysis identified a non-directional gene interaction map network with a score of 33 and 26 focus molecules. These proteins have been identified as being involved in cellular movement, cell-to-cell signalling and interaction, and cellular development. Of note are the fibrillary collagens I and III, as major constituents of the extracellular matrix, as well as the ERK1/2 signalling pathway implicated in myofibroblast activation in SSc. (**D**) IPA pathway analysis identified a non-directional gene interaction map network with a score of 16 and 16 focus molecules. These proteins have been identified as being involved in the inflammatory response, cell-to-cell signalling and interaction, haematological system development and function. IL-6 , known to implicated in SSc pathogenesis, features as a central node in the network. Green symbols indicate activated by IL31, and the red indicate inactivated by IL31.

Canonical pathway	-log(p-value)	Z-score	ratio of overlap	Genes
PCP pathway	5.5	1.889822	0.159	ROCK1,ROR2,SDC2,EFNB1,CTHRC1,JUND,SDC3,FZD2,FZD7,HSPB1
Colorectal Cancer Metastasis Signalling	3.8	0.27735	0.0688	LRP5,AKT2,GNAS,NRAS,BAD,RHOJ,GNG10,GNG11,MSH2,TGFB1,FZD2,MMP1,RALGDS,GNG12,FZD7,ATM,MMP19
Hypoxia Signaling in the Cardiovascular System	2.27	1	0.0923	BIRC6,ATF4,LDHA,UBE2D1,ATM,PTEN
Integrin Signalling	2.06	-0.33333	0.0548	ROCK1,TSPAN3,AKT2,NRAS,ITGA11,ITGA2,ARPC3,RHOJ,GSN,NEDD9,ATM,PTEN
fMLP Signalling in Neutrophils	1.97	-1.63299	0.0661	NRAS,GNAS,GNG11,NFAT5,ARPC3,GNG12,GNG10,ATM
PI3K/AKT Signalling	1.91	-1.41421	0.0645	AKT2,RHEB,NRAS,YWHAG,BAD,ITGA2,MAPK8IP1,PTEN
Actin Nucleation by ARP-WASP Complex	1.9	-1.34164	0.0893	ROCK1,NRAS,ITGA2,ARPC3,RHOJ
Wnt/Ca+ pathway	1.87	1.341641	0.0877	NFAT5,PDIA3,ATF4,FZD2,FZD7
Phospholipase C Signalling	1.81	-0.37796	0.0506	MARCKS,NRAS,GNAS,GNG11,NFAT5,ITGA2,HDAC7,ATF4,RHOJ,GNG12,RALGDS,GNG10
TGF-β Signalling	1.68	-0.44721	0.069	NRAS,BMP4,TGFB1,BMPR1B,ACVR2A,PMEPA1
G Beta Gamma Signalling	1.65	-0.8165	0.0682	AKT2,NRAS,GNAS,GNG11,GNG12,GNG10
CXCR4 Signalling	1.65	-0.37796	0.0545	ROCK1,AKT2,NRAS,GNAS,GNG11,RHOJ,GNG12,GNG10,ATM
IL-8 Signalling	1.59	-0.70711	0.0508	ROCK1,AKT2,NRAS,GNAS,GNG11,CXCL1,RHOJ,GNG12,GNG10,ATM
Regulation of Actin-based Motility by Rho	1.59	-0.44721	0.0659	ROCK1,PIP5K1C,ITGA2,ARPC3,RHOJ,GSN
PTEN Signalling	1.54	0.377964	0.0588	AKT2,NRAS,BAD,ITGA2,BMPR1B,FGFRL1,PTEN
Thrombin Signalling	1.51	0.377964	0.0493	ROCK1,AKT2,NRAS,GNAS,GNG11,PDIA3,RHOJ,GNG12,GNG10,ATM
Cardiac Hypertrophy Signalling	1.48	0.333333	0.0468	ROCK1,NRAS,GNAS,GNG11,TGFB1,PDIA3,RHOJ,GNG12,GNG10,ATM,HSPB1

Table 2 Canonical pathway analysis of IL-31 treated dermal fibroblasts assayed by RNAseq. 4 control dermal fibroblast lines were treated with IL-31 (50ng/ml) over 16 hours and then lysed for RNA extraction and subject to next generation sequencing. IPA software was used with IPA Knowledge Base as its reference to identify signalling pathways induced in the target fibroblasts, based on the profile of induced gene expression. Pathways ranked by p values, those highlighted orange

are inactivated by IL31 and those in blue are activated by IL31. The –log(p-value) indicates significance. The p-value significance threshold was set at $p<0.05$ and as such –log(0.05)= 1.3. all pathways with –log(p-values) of more than 1.3 are shown in the table. The z-score is the predicted directionality of the pathway. Negative z-scores are for pathways activated by IL31. The ratio of overlap indicates how well the predicted pathway fits with known pathways found in the literature and experimentally.

Categories	Functions	Diseases or Functions Annotation	p-Value	Z-score	number of molecules involved/561
Carbohydrate Metabolism, Small Molecule Biochemistry	production	production of lactic acid	0.00368	-2.021	5
Cellular Growth and Proliferation	proliferation	proliferation of cells	4.5E-13	-1.589	200
Cell Morphology	mineralization	mineralization of connective tissue cells	0.000473	-1.358	5
Cell Death and Survival	apoptosis	apoptosis of fibroblast cell lines	0.000175	-1.219	23
Cell Death and Survival, Organismal Injury and Abnormalities	cell death	cell death of endothelial cells	0.00612	-0.904	11
Cellular Development, Connective Tissue Development and Function	differentiation	differentiation of fibroblast cell lines	0.00419	-0.73	12
Cell Death and Survival	apoptosis	apoptosis of fibroblasts	0.000117	-0.694	17
Cardiovascular System Development and Function, Organismal Development	angiogenesis	angiogenesis	6.71E-05	0.085	52
Cardiovascular System Development and Function	development	development of vasculature	6.12E-06	0.106	62
Cardiovascular System Development and Function, Organismal Development	vasculogenesis	vasculogenesis	0.000631	0.254	41

Table 3 Disease and functional analysis of gene expression in IL-31 treated dermal fibroblasts. Based on the above next generation sequencing, analysis was performed relevant to function during pathogeneic states of the target cell. Disease and function analysis predicts the affected biological processes based on gene expression and the directional changes. Negative z-values indicate activation by IL-31. 561 molecules were found to be differentially expressed upon IL-31 addition ($p<0.05$) and the table indicates how many of these 561 are predicted to be involved in each of the associated diseases and functions. Functions highlighted in blue are predicted to be upregulated by Il31, and those in orange to be downregulated.

In addition to canonical pathways affected by IL-31, the software can also predict functionality of the genes expressed in relation to whole system physiology and the number of genes out of those differentially expressed by IL-31 that fit into the known genes involved in the annotated functions (Table 3). Consistent with a role for IL-31 in SSc pathophysiology was the reduction in "development of vasculature" function, of relevance to the microvascular injury and failure of neoangiogenesis considered to be a ubiquitous finding in SSc patients. Also of note IL-31 enhanced gene expression patterns linked to apoptosis and lactic acid production possibly relevant to the ischaemic microenvironment.

The IPA software was also able to group molecules predicted to work together, based on existing literature and published experimental data, into networks. Biological function and molecular relationship is represented as a line between two molecules and any grey molecules are those filled in by the Knowledge Base software. The differently shaped focus molecules denote enzymes, kinases, receptors, cytokines and growth factors. Figures 5C and 5D depict the most significantly and highly scored networks illustrating functions in cell movement and inflammatory process respectively.

IL-31 induces fibrosis in mice A widely used mouse model of SSc fibrosis consists of daily subcutaneous injections of the clastogen bleomycin over 3 or more weeks to induce tissue injury, leading to dermal fibrosis and inflammation. Marked macrophage infiltration is seen by day 3, and progressive fibrosis is apparent by day 14. On day 21 histologic changes showing epidermal hypertrophy, dermal fibrosis, and an accumulation of myofibroblasts, collagen and dense extracellular matrix material, and adipose atrophy are seen, thus resembling SSc skin pathology. Biopsy of lesional skin shows upregulated TGFβ1, and increased nuclear phosphorylated SMAD2/3 in fibroblasts (27), and upregulated CTGF (28). However, the initiating tissue damage in this model is non-specific and unrelated to SSc and the bleomycin model responds to anti-inflammatory therapies that are less effective in the human disease. We developed a mouse model whereby IL-31 was delivered continuously for 14 days into the subcutaneous tissues by an implanted minpump. Comparison was made with the effects of treatment with the known pro-fibrotic TGFβ, and possible synergy was investigated by giving both agents together. Dermal thickening was seen following IL-31 treatment, and piscosirius red (PSR) staining for collagen revealed increased dermal collagen cross linking. No change in lung histology was seen. In general

TGFβ failed to induce fibrotic changes and did not synergise with IL-31 treatment (Figure 6 A,B). Treatment with IL-31 led to a significant increase in plasma IL-6 and a trend towards increased PDGF-BB and TGFβ1 (Figure 6 C,D,E).

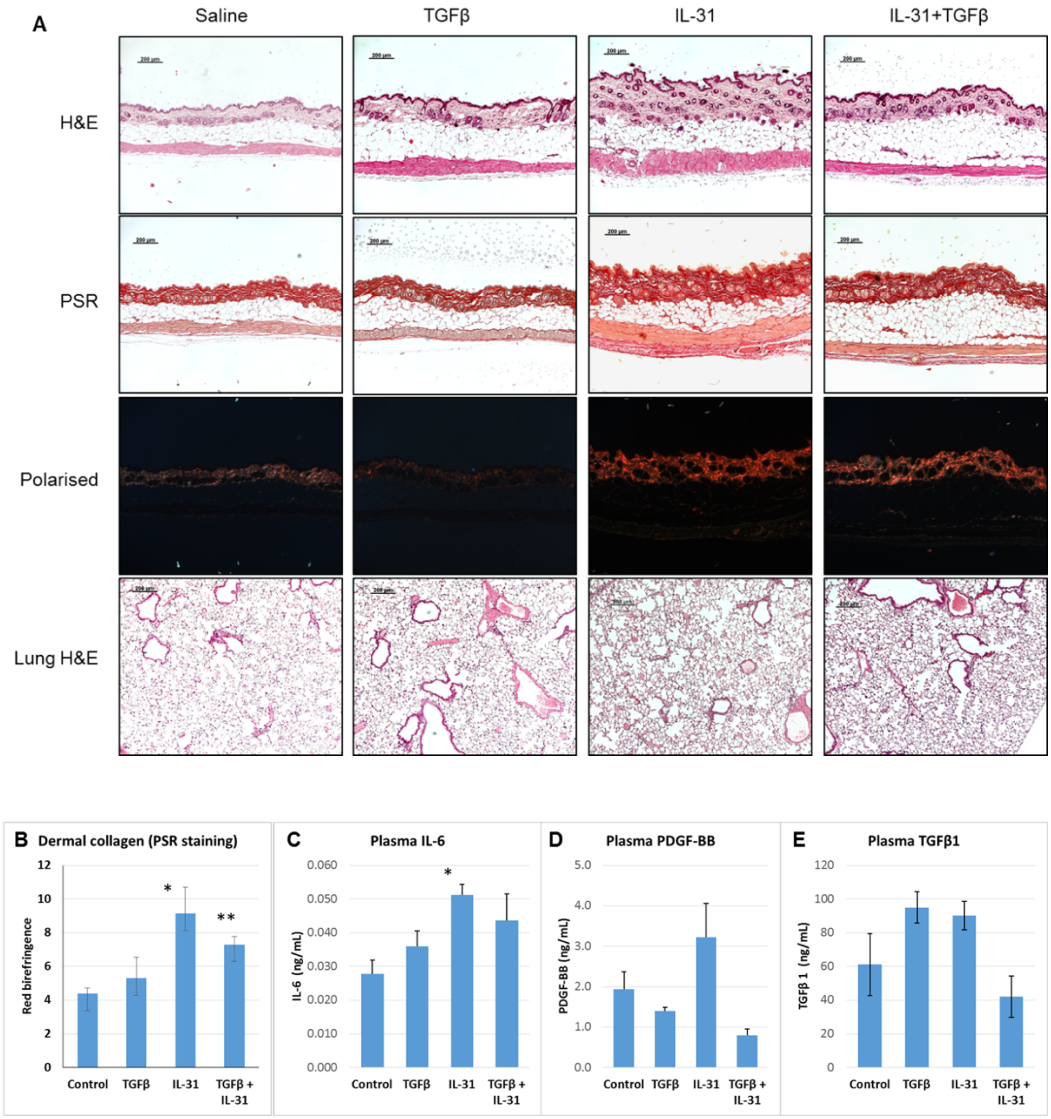

Figure 6 IL-31 induces dermal fibrosis in mice. (**A**) IL-31 with or without TGFβ was given by continuous subcutaneous mini pump in wild type Balb/c mice (N=6-7 per group) for 14 days, which were euthanised at 21 days. Skin and lung biopsy material obtained at 21 days are shown. Lung histology was not affected. (**B**) Treatment with IL-31 led to significantly increased dermal thickness plus increased picrosirius red (PSR) stain and enhanced cross linking of collagen as assayed by polaroid imaging of sections. (**C, D, E**) Analysis of cytokines and growth factors revealed elevated IL-6 in the IL-31 treated mice, and trend towards elevated PDGF-BB and TGFβ in these mice. *P<0.03, **P<0.002.

Discussion

Treating progressive skin and organ based fibrosis in SSc remains a significant unmet need. It is possible that the complex pathology developing in SSc fibrotic lesions is irreversible because of the chaotic cellular and cytokine environment, plus the severe mechanical stress-related changes that evolve. However, other complex rheumatic disorders have turned out to be treatable and reversible through specific treatments inhibiting key pathogenic cytokines or cell populations, and both of these approaches have shown promise against SSc (16, 29). In this paper we present data implicating the IL-31/IL-31RA axis in multiple pathogenic steps in this disease, including fibroblast activation via multiple pathways, enhancement of migratory behaviour by fibroblasts and fibroblast precursors, osteogenic differentiation of these cells of relevance to the calcinosis, and stimulation of collagen release independent of gene expression. Since cytokines may be involved in T cell-fibroblast cross talk in this disease IL-31 was evaluated further as a pathogenic factor. These studies reveal that the receptor was present on multiple candidate cells relevant to the disease process. Epidermal tissues, fat derived MSCs, as well as dermal and lung derived fibroblasts were found to express the IL-31 receptor. It is possible that elevated IL-31 is promoting known pathogenic mechanisms including activation of the epidermis (30), mobilisation and activation of subcutaneous fat derived precursor cells (31), as well as having a direct effect on tissue fibroblasts. Interestingly IL-31 triggered collagen I protein release without altering mRNA levels, although the non-transcriptional regulation of collagen I is a well-known phenomenon (32). Furthermore, we showed that in dermal fibroblasts IL-31 induced multiple fibrosis relevant pathways including Wnt, PI3K, and TGFβ itself, well established as central to the pro-fibrotic phenotype (33, 34). IL-31 induced patterns of gene expression associated with apoptosis of endothelial cells and suppression of angiogenesis, also relevant to the disease (35). Based on these findings it is proposed that IL-31 is a key central cytokine involved in persistent skin and lung fibrosis in a disease subgroup.

Limitations of our study include the relatively small number of tissue fluid samples analysed and the cross sectional but non longitudinal nature of the data, which could

be extended. However, the seminal work implicating IL-31 in atopic dermatitis has led to specific clinical trials of the monoclonal against IL-31RA (20, 36). A single dose of anti-IL31RA monoclonal was shown to have a lasting benefit extending up to 12 weeks. This treatment could be assessed in patients with SSc and high itch scores or those with high blister fluid IL-31, adding a single infusion of the anti-IL31Ra to a standard treatment, and would be the clearest experiment to fully establish the role of this factor in SSc pathogenesis. Blister fluid sampling before and after therapy could provide useful biomarker data. It is possible that IL-31 is a key central pathogenic cytokine in this disease and this idea is favoured by the very high blister fluid levels seen, which greatly exceed those of other cytokines including IL-6, as assayed by us previously (37) , and the multiple pathogenic effects described. Reservations would include the absence of a clear IL-31/IL-31RA signal in previous gene arrays studies, although there is some support for an OSMR increase in disease cells (14, 38, 39).

When first identified as a pathogenic cytokine, it was shown that IL-31 induces inflammation and itching behaviour relevant to atopic dermatitis(20). However, the fibrogenic activity of IL-31 was not evaluated in these studies. Since SSc is both pruritic and fibrotic we thought that IL-31 could be promoting multiple aspects of the disease, and we have modelled this, delivering IL-31 subcutaneously in wild type mice with or without additional TGFβ. This method has led to a fibrotic change in the mouse dermis, where increased dermal thickness and enhanced mature cross linked collagen was observed. Furthermore, an SSc-like pattern of cytokine induction was seen, with high levels of plasma IL-6. However, fibrosis in the deep fascia was observed and loss of subcutaneous fat absent, in contrast to the typical changes of SSc. However, this may reflect the route of administration of the drug which is preferentially into the subcutaneous tissue, whereas the SSc pathology is initiated in perivascular regions in the dermis and at the dermo-epidermal junction. Other competing models for SSc skin fibrosis include the bleomycin induced model which recapitulates dermal fibrosis and inflammation, but is initiated by a non-specific clastogenic stimulus, as well as hypochlorite induced skin fibrosis, which has been shown to induce scleroderma-like auto-antibody reactions(40). Possible merits of the current IL-31 induced model include disease-specific cytokine induction, the relatively non-invasive method which involves a single subcutaneous implantation

under anaesthesia, and clearly reproducible results in terms of the plasma IL-6 induction and dermal thickening.

Th2 responses have evolved as critical in host defence mechanisms against parasitic infections, promoting specific immune-allergic reactions as well as pro-fibrotic responses downstream that are essentially required for containment of focal invasion in the skin, gut, liver and elsewhere. We believe that IL-31 could have a similar role, inducing itching as a danger signal in the skin and also inducing fibroblasts and mobilising MSCs, in order to wall off invasion from pathogens.

It may be possible to target the IL-31 pathway in scleroderma patients, and therapeutic blockade with a neutralizing anti-IL-31RA or other specific approaches may treat severe pruritus and attenuate fibroblast activation in a subset of patients, possibly identified by severe pruritus and high dermal IL-31. The anti-IL-31 RA antibody nemolizumab has recently been shown to benefit itch and extent of skin involvement in atopic dermatitis (36). We propose to study this or similar therapy in patients with SSc-related pruritus using itch severity as well as biomarkers of skin fibrosis as endpoints. In addition we have previously shown that the dermal blister fluid method can be used to assay protein biomarkers, which now include IL-31 (37).

Methods

Patients studied All donors who provided peripheral blood, skin biopsy or dermal blister fluid samples did so with written informed consent to a study approved by the NHS Health Research Authority, NRES Committee London-Hampstead, HRA, reference number 6398. All samples were collected at the Royal Free Hospital Centre for Rheumatology and Connective Tissue Disease. Scleroderma patients met internationally agreed criteria for diagnosis. Clinical itch severity was assessed using a standardised 5D Pruritus questionnaire (41). In total plasma was sampled from 43 scleroderma patients and 27 healthy controls, and blister fluid from 44 scleroderma patients and 22 healthy controls (Table 4)

Scleroderma patients	
Male	8
Female	48
Average age (years)	57.7 (27-80)
Diffuse	26
Diffuse overlap	5
Limited	25
ACA	17

Scl70	14
RNA Pol	9
SNP	1
Ro	4
ANA only	8
RNP	7
Disease duration (years)	13.64 (2.0-37)
Mean itch score	12.2 (5.0-24)
Mean RSS	14.3(3.0-38)
Mean Hb (g/L)	122 (9.0-148)
Number of patients with clinical anaemia	10
Mean platelets ($x10^9$/L)	270 (76-447)
Number with thrombocytosis	2
Mean CRP (mg/dl)	4.64
Mean ESR (mm/hour)	15.23
Number with raised inflammatory markers	22
Healthy Controls	
Male	10
Female	12
Average age (years)	41.42

Table 4 Clinical and laboratory characteristics of patients studied.

Sample Collection: Interstitial fluid samples from the forearm skin of patients with scleroderma and healthy controls were collected using the dermal suction blister method as previously described (42). This involved using dermal suction machine with an 8mm orifice adhering to sterilised forearm skin. The machine was attached to a vacuum line, and left for 3.5 hours with suction pressure of 280-310 mmHg. Interstitial fluid was removed from the blister using a 23 gauge needle and syringe, before being stored in aliquots at -80°C. At the end of the procedure the epidermal tissue roof of the blister was dissected from the skin with a scalpel and stored in RNA later prior to RNA extraction by Qiagen miniRNA kit. In total 44 SSc and 27 healthy control samples were analysed. Plasma samples were obtained synchronous to the time of blister sampling. Plasma was aliquoted and frozen for later analysis at -80°C.

Clinical details on the patients were collected, including type of disease, gender, age, duration of disease onset, antibody status, current treatment, prior treatment, organ involvement, most recent FVC and FEV1, recent creatinine, recent estimated pulmonary artery pressure on echocardiogram, and recent NT-BNP results.

Assay of IL-31 and IL-31RA ELISA was employed to determine the concentration of IL -31 in plasma and blister fluid samples (R&D systems). RNA from 4 SSc and healthy control skin and lung fibroblast cell lines was extracted, along with RNA from

2 lines of adipose derived MSCs, and assayed for IL31 receptor expression using qPCR. Primers for the receptor were designed using NCBI q bank. Qiagen Quantifast SYBR Green kit was used for the assay, with TBP expression used as a control housekeeping gene to normalise IL31 receptor expression. Rotogene6000 series software 1.7 was used to analyse the results and Graphpad prism 7 was used to conduct ANOVA statistical analysis.

Protein assays for CTGF and Collagen I in IL31 treated fibroblasts Dermal fibroblasts were cultured from 4mm skin biopsies taken from the involved forearm skin of SSc patients and healthy controls and the fibroblast outgrowth was used at early passage number 3-4 as described previously (43). Fibroblasts were cultured initially in DMEM supplemented with 10% FCS plus penicillin/streptomycin, and then switched to serum free DMEM overnight prior to treatment with IL-31 at increasing concentrations (1/2.5/5/10/50/100 ng/ml). TGFβ (4ng/ml) was used as positive control alone and together with IL31. Collagen and CTGF induction were assayed by Western blot of cell lysates using a standard method (43), as well as by qPCR. Nitrocellulose blots were probed with anti-collagen I (Abcam ab34710), anti-CTGF (Santa Cruz sc14939) and anti-GAPDH (Abcam ab8245) polyclonals.

IL31 in SSc Skin 4mm punch biopsies from healthy volunteer and SSc patients were taken from the anterior forearm before freezing and sectioning. Mouse anti-human IL31 primary antibody (1:50) and horse anti-mouse secondary antibody (1:200) were used. Sections were immersed in xylene and mounted before imaging.

IL31 mouse model To determine whether IL31 induces multiple pro-fibrotic pathways that are distinct from the effects of TGFβ in inducing fibrosis, IL31 was pumped into mouse skin over 21 days. A mini ALZA osmotic pump embedded into the skin of 6-8 week old male Balb/c mice (Charles River Laboratories, CA) delivered 0.2 μg IL31 (Peprotech #210-31-10) per day over 24 hours (0.008 μg/hour) (n=7). Mice were also treated with 800 ng TGFβ per day (Prosec #cyt-8585b) (n=6). Mice either received IL31 or TGFβ treatments alone or together (n=6) and compared to saline control treated mice (n=7). Treatments were every day for 14 days before removing the pumps and allowing 1 week recovering before euthanisation on day 21. Paraffin embedded sections were prepared of the skin and lung tissue for analysis of collagen content, loss of subcutaneous fat, PSR staining for increased dermal thickness and Masson's Trichrome.

IL31 migration assay Fibroblast migration was studied using a scratch migration assay(44). 1 healthy control (NF25) and 2 SSc (SScF1 and SScF2) cell lines were cultured in three 24 well plates. All cells were at passage 4. Once confluent, cells were serum starved overnight before making a scratch of the diameter of each well using a p200 pipette tip. Cells were treated as follows with 4 replicates of each treatment: 0.2% serum, 10% serum, 50ng/ml IL31 in 0.2% serum, 50ng/ml IL31 plus Wortmannin 100 nM(PI3K inhibitor) or U0126 10μM (ERK pathway inhibitor) (45, 46). Migration was quantified by imaging the cells at 0, 3, 6, 20 and 24 hours using Axioscope light microscope at 2.5x magnification and The same protocol was used for one MSC cell line treated as follows in replicates of 3: 0.2% serum, 10% serum, 50 ng/ml IL31 in 0.2% serum, 50 ng/ml IL31 plus Wortmannin 100nM. Wells were imaged at 0, 8 and 24 hours in the same way as the fibroblasts. The area of the scratch was measured using NIH ImageJ software followed by ANOVA with Tukey's post hoc statistical analysis using SPSS software.

Next generation sequencing Healthy dermal fibroblast and fat derived MSCs were cultured in 24 well plastic plates until fully confluent. After overnight serum starvation, both cell lines were treated in replicates of 4 as follows; 0.2% serum , SSc or healthy control blister fluid (1:125), or IL31 (50 ng/ml). Blister fluid and IL31 were added to 0.2% serum conditions. A different sample of blister fluid was used for each replicate for both cell lines. Cells were treated for 16 hours and lysed for RNA extraction using Qiagen RNeasy extraction kit and protocol. In collaboration with UCL Genomics, RNA extractions were assayed using Illumina TrueSeq standards library with 15 million reads per sample. Quality control of the samples was performed using the High Sensitivity Tapestation kit and 43 paired end sequencing.

Transcriptome analysis Paired end reads were mapped to the Ensembl human transcriptome reference sequence (latest version available during analysis: GRCh38 (47). Mapping and generation of read counts per transcript were done using Kallisto (doi:10.1038/nbt.3519), based on the novel idea of pseudoalignment. R/Bioconductor package tximport was used to import the mapped counts data and summarise the transcripts-level data into gene level as described in this paper Further analyses were run using DESeq2 package (48)https://doi.org/10.1371/journal.pone.0157022). Some advantages of this method includes (i) correction for potential changes in gene length across samples (i.e. from differential isoform usage), (ii) Kallisto is faster and require

less memory and disk usage compared to alignment-based method. Normalization and differential analysis are carried out according to the DESeq2 model by use of negative binomial generalized linear model. The estimates of dispersion and logarithmic fold changes incorporate data-driven prior distributions. Using this method, we compared the two conditions for each experiment and we extracted a result table with log2fold changes, Wald test p values and adjusted p values (according to false discovery rate). Mapped reads for each sample ranged between 12 and 21 million. Principal component analysis was used as a quality control assessment.

Functional classification of genes' list was performed using Ingenuity Pathway analysis (IPA, https://www.qiagenbioinformatics.com/). The "core analysis" function was used to interpret the data in the context of biological processes, pathways and networks. Both up and down regulated identifiers were defined as value parameters for the analysis. Significance of the biofunctions and the canonical pathways were tested by the Fisher Exact test p-value. The more interconnected the network is, the more likely it represents a significant physiological process or function. The network is constructed using the focus molecules from the dataset obtained from the NGS and the database used by the IPA software, Knowledge Base, fills in areas lacking connectivity with predicted non-focus molecules.

The networks were then scored based on an algorithm which ranks different networks by function based on significance of connectivity and relatively to focus molecules from the dataset. The score is based on the number of focus molecules and the overall size of the network for a specific function compared with how close the network is to the focus genes of the original dataset. Countplots of differentially expressed genes were produced using Graphpad prism 7.0.

Osteogenic differentiation study In order to induce osteogenic differentiation, adipose derived MSCs were cultured in osteogenic induction media (OIM) containing 50 mM ascorbic acid, 10 mM b-glycerophosphoric acid and 0.1 mM dexamethasone (Life technologies; Paisley) with or without TGF-β1 (4ng/ml) or IL-31 (50 ng/ml) (R&D systems; Minneapolis, USA). Cells were cultured on either soft (4 KPa) or stiff (50 KPa) collagen matrices mimicking healthy or SSc skin respectively. Calcification was examined using Alizarin Red S (ARS) staining (Sigma-Aldrich; Missouri, USA). The culture media was changed and replaced with the new addition of TGF-β1 and IL-31 as above, every three days, over nine days. Photographs were made using a

light microscope and Axiovision Rel 4.5, on day 9 to confirm that cells were present prior to the mineralisation assay. On day 9 of culture, which is a known intermediate time-point of osteogenic differentiation, Briefly, cells were fixed with 4% formaldehyde (CellPath; Newtown, UK) for 20 minutes and rinsed with deionised water before adding 4 pipette droplets of 1% ARS solution (pH 4.1) per well. Following incubation at room temperature for 15 minutes, the cells were washed thoroughly with deionised water to remove all non-specific staining. Differentiation was visualised by the identification of red dots.

References:

1. Denton CP, and Khanna D. Systemic sclerosis. *Lancet (London, England).* 2017.
2. Nihtyanova SI, Schreiber BE, Ong VH, Rosenberg D, Moinzadeh P, Coghlan JG, Wells AU, and Denton CP. Prediction of pulmonary complications and long-term survival in systemic sclerosis. *Arthritis & rheumatology (Hoboken, NJ).* 2014;66(6):1625-35.
3. van den Hoogen FH, Boerbooms AM, Swaak AJ, Rasker JJ, van Lier HJ, and van de Putte LB. Comparison of methotrexate with placebo in the treatment of systemic sclerosis: a 24 week randomized double-blind trial, followed by a 24 week observational trial. *British journal of rheumatology.* 1996;35(4):364-72.
4. Tashkin DP, Elashoff R, Clements PJ, Roth MD, Furst DE, Silver RM, Goldin J, Arriola E, Strange C, Bolster MB, et al. Effects of 1-year treatment with cyclophosphamide on outcomes at 2 years in scleroderma lung disease. *American journal of respiratory and critical care medicine.* 2007;176(10):1026-34.
5. van Laar JM, Naraghi K, and Tyndall A. Haematopoietic stem cell transplantation for poor-prognosis systemic sclerosis. *Rheumatology (Oxford, England).* 2015;54(12):2126-33.
6. Bossini-Castillo L, Lopez-Isac E, and Martin J. Immunogenetics of systemic sclerosis: Defining heritability, functional variants and shared-autoimmunity pathways. *Journal of autoimmunity.* 2015;64(53-65.
7. Mayes MD, Bossini-Castillo L, Gorlova O, Martin JE, Zhou X, Chen WV, Assassi S, Ying J, Tan FK, Arnett FC, et al. Immunochip analysis identifies multiple susceptibility loci for systemic sclerosis. *American journal of human genetics.* 2014;94(1):47-61.
8. Lopez-Isac E, Campillo-Davo D, Bossini-Castillo L, Guerra SG, Assassi S, Simeon CP, Carreira P, Ortego-Centeno N, Garcia de la Pena P, Beretta L, et al. Influence of TYK2 in systemic sclerosis susceptibility: a new locus in the IL-12 pathway. *Annals of the rheumatic diseases.* 2015.
9. O'Reilly S, Hugle T, and van Laar JM. T cells in systemic sclerosis: a reappraisal. *Rheumatology (Oxford, England).* 2012;51(9):1540-9.
10. O'Reilly S. Role of interleukin-13 in fibrosis, particularly systemic sclerosis. *BioFactors (Oxford, England).* 2013;39(6):593-6.
11. Greenblatt MB, Sargent JL, Farina G, Tsang K, Lafyatis R, Glimcher LH, Whitfield ML, and Aliprantis AO. Interspecies comparison of human and murine scleroderma reveals IL-13 and CCL2 as disease subset-specific targets. *The American journal of pathology.* 2012;180(3):1080-94.
12. Hasegawa M, Fujimoto M, Kikuchi K, and Takehara K. Elevated serum levels of interleukin 4 (IL-4), IL-10, and IL-13 in patients with systemic sclerosis. *The Journal of rheumatology.* 1997;24(2):328-32.

13. Wermuth PJ, and Jimenez SA. The significance of macrophage polarization subtypes for animal models of tissue fibrosis and human fibrotic diseases. *Clin Transl Med.* 2015;4(2.
14. Milano A, Pendergrass SA, Sargent JL, George LK, McCalmont TH, Connolly MK, and Whitfield ML. Molecular subsets in the gene expression signatures of scleroderma skin. *PloS one.* 2008;3(7):e2696.
15. Hinchcliff M, Huang CC, Wood TA, Matthew Mahoney J, Martyanov V, Bhattacharyya S, Tamaki Z, Lee J, Carns M, Podlusky S, et al. Molecular signatures in skin associated with clinical improvement during mycophenolate treatment in systemic sclerosis. *The Journal of investigative dermatology.* 2013;133(8):1979-89.
16. Khanna D, Denton CP, Jahreis A, van Laar JM, Frech TM, Anderson ME, Baron M, Chung L, Fierlbeck G, Lakshminarayanan S, et al. Safety and efficacy of subcutaneous tocilizumab in adults with systemic sclerosis (faSScinate): a phase 2, randomised, controlled trial. *Lancet (London, England).* 2016.
17. Razykov I, Levis B, Hudson M, Baron M, and Thombs BD. Prevalence and clinical correlates of pruritus in patients with systemic sclerosis: an updated analysis of 959 patients. *Rheumatology (Oxford, England).* 2013;52(11):2056-61.
18. Racine M, Hudson M, Baron M, and Nielson WR. The Impact of Pain and Itch on Functioning and Health-Related Quality of Life in Systemic Sclerosis: An Exploratory Study. *Journal of pain and symptom management.* 2016;52(1):43-53.
19. Haber JS, Valdes-Rodriguez R, and Yosipovitch G. Chronic Pruritus and Connective Tissue Disorders: Review, Gaps, and Future Directions. *American Journal of Clinical Dermatology.* 2016;17(5):445-9.
20. Dillon SR, Sprecher C, Hammond A, Bilsborough J, Rosenfeld-Franklin M, Presnell SR, Haugen HS, Maurer M, Harder B, Johnston J, et al. Interleukin 31, a cytokine produced by activated T cells, induces dermatitis in mice. *Nature immunology.* 2004;5(7):752-60.
21. Grimstad O, Sawanobori Y, Vestergaard C, Bilsborough J, Olsen UB, Gronhoj-Larsen C, and Matsushima K. Anti-interleukin-31-antibodies ameliorate scratching behaviour in NC/Nga mice: a model of atopic dermatitis. *Experimental dermatology.* 2009;18(1):35-43.
22. Bilsborough J, Leung DY, Maurer M, Howell M, Boguniewicz M, Yao L, Storey H, LeCiel C, Harder B, and Gross JA. IL-31 is associated with cutaneous lymphocyte antigen-positive skin homing T cells in patients with atopic dermatitis. *J Allergy Clin Immunol.* 2006;117(2):418-25.
23. Singer EM, Shin DB, Nattkemper LA, Benoit BM, Klein RS, Didigu CA, Loren AW, Dentchev T, Wysocka M, Yosipovitch G, et al. IL-31 is produced by the malignant T-cell population in cutaneous T-Cell lymphoma and correlates with CTCL pruritus. *The Journal of investigative dermatology.* 2013;133(12):2783-5.
24. Kasraie S, Niebuhr M, and Werfel T. Interleukin (IL)-31 activates signal transducer and activator of transcription (STAT)-1, STAT-5 and extracellular signal-regulated kinase 1/2 and down-regulates IL-12p40 production in activated human macrophages. *Allergy.* 2013;68(6):739-47.
25. Ip WK, Wong CK, Li ML, Li PW, Cheung PF, and Lam CW. Interleukin-31 induces cytokine and chemokine production from human bronchial epithelial cells through activation of mitogen-activated protein kinase signalling pathways: implications for the allergic response. *Immunology.* 2007;122(4):532-41.
26. Shiwen X, Stratton R, Nikitorowicz-Buniak J, Ahmed-Abdi B, Ponticos M, Denton C, Abraham D, Takahashi A, Suki B, Layne MD, et al. A Role of Myocardin Related Transcription Factor-A (MRTF-A) in Scleroderma Related Fibrosis. *PloS one.* 2015;10(5):e0126015.

27. Takagawa S, Lakos G, Mori Y, Yamamoto T, Nishioka K, and Varga J. Sustained activation of fibroblast transforming growth factor-β/Smad signaling in a murine model of scleroderma. *Journal of investigative dermatology.* 2003;121(1):41-50.
28. Mori Y, Hinchcliff M, Wu M, Warner-Blankenship M, Lyons K, and Varga J. Connective tissue growth factor/CCN2-null mouse embryonic fibroblasts retain intact transforming growth factor-β responsiveness. *Experimental cell research.* 2008;314(5):1094-104.
29. Jordan S, Distler JH, Maurer B, Huscher D, van Laar JM, Allanore Y, and Distler O. Effects and safety of rituximab in systemic sclerosis: an analysis from the European Scleroderma Trial and Research (EUSTAR) group. *Annals of the rheumatic diseases.* 2015;74(6):1188-94.
30. Aden N, Nuttall A, Shiwen X, de Winter P, Leask A, Black CM, Denton CP, Abraham DJ, and Stratton RJ. Epithelial cells promote fibroblast activation via IL-1alpha in systemic sclerosis. *The Journal of investigative dermatology.* 2010;130(9):2191-200.
31. Wu M, Melichian DS, Chang E, Warner-Blankenship M, Ghosh AK, and Varga J. Rosiglitazone abrogates bleomycin-induced scleroderma and blocks profibrotic responses through peroxisome proliferator-activated receptor-gamma. *The American journal of pathology.* 2009;174(2):519-33.
32. Wong S, Botelho FM, Rodrigues RM, and Richards CD. Oncostatin M overexpression induces matrix deposition, STAT3 activation, and SMAD1 Dysregulation in lungs of fibrosis-resistant BALB/c mice. *Laboratory investigation; a journal of technical methods and pathology.* 2014;94(9):1003-16.
33. Lafyatis R. Transforming growth factor beta--at the centre of systemic sclerosis. *Nature reviews Rheumatology.* 2014;10(12):706-19.
34. Beyer C, Schramm A, Akhmetshina A, Dees C, Kireva T, Gelse K, Sonnylal S, de Crombrugghe B, Taketo MM, Distler O, et al. beta-catenin is a central mediator of pro-fibrotic Wnt signaling in systemic sclerosis. *Annals of the rheumatic diseases.* 2012;71(5):761-7.
35. Manetti M, Guiducci S, and Matucci-Cerinic M. The crowded crossroad to angiogenesis in systemic sclerosis: where is the key to the problem? *Arthritis research & therapy.* 2016;18(36.
36. Ruzicka T, Hanifin JM, Furue M, Pulka G, Mlynarczyk I, Wollenberg A, Galus R, Etoh T, Mihara R, Yoshida H, et al. Anti-Interleukin-31 Receptor A Antibody for Atopic Dermatitis. *The New England journal of medicine.* 2017;376(9):826-35.
37. Clark KE, Lopez H, Abdi BA, Guerra SG, Shiwen X, Khan K, Etomi O, Martin GR, Abraham DJ, Denton CP, et al. Multiplex cytokine analysis of dermal interstitial blister fluid defines local disease mechanisms in systemic sclerosis. *Arthritis research & therapy.* 2015;17(1):73.
38. Assassi S, Swindell WR, Wu M, Tan FD, Khanna D, Furst DE, Tashkin DP, Jahan-Tigh RR, Mayes MD, Gudjonsson JE, et al. Dissecting the heterogeneity of skin gene expression patterns in systemic sclerosis. *Arthritis & rheumatology (Hoboken, NJ).* 2015;67(11):3016-26.
39. Whitfield ML, Finlay DR, Murray JI, Troyanskaya OG, Chi JT, Pergamenschikov A, McCalmont TH, Brown PO, Botstein D, and Connolly MK. Systemic and cell type-specific gene expression patterns in scleroderma skin. *Proceedings of the National Academy of Sciences of the United States of America.* 2003;100(21):12319-24.
40. Batteux F, Kavian N, and Servettaz A. New insights on chemically induced animal models of systemic sclerosis. *Current opinion in rheumatology.* 2011;23(6):511-8.
41. Elman S, Hynan LS, Gabriel V, and Mayo MJ. The 5-D itch scale: a new measure of pruritus. *Br J Dermatol.* 2010;162(3):587-93.

42. Sondergaard K, Stengaard-Pedersen K, Zachariae H, Heickendorff L, Deleuran M, and Deleuran B. Soluble intercellular adhesion molecule-1 (sICAM-1) and soluble interleukin-2 receptors (sIL-2R) in scleroderma skin. *British journal of rheumatology.* 1998;37(3):304-10.
43. Stratton R, Shiwen X, Martini G, Holmes A, Leask A, Haberberger T, Martin GR, Black CM, and Abraham D. Iloprost suppresses connective tissue growth factor production in fibroblasts and in the skin of scleroderma patients. *The Journal of clinical investigation.* 2001;108(2):241-50.
44. Donovan J, Shiwen X, Norman J, and Abraham D. Platelet-derived growth factor alpha and beta receptors have overlapping functional activities towards fibroblasts. *Fibrogenesis & tissue repair.* 2013;6(1):10.
45. Chen Y, Leask A, Abraham DJ, Pala D, Shiwen X, Khan K, Liu S, Carter DE, Wilcox-Adelman S, Goetinck P, et al. Heparan sulfate-dependent ERK activation contributes to the overexpression of fibrotic proteins and enhanced contraction by scleroderma fibroblasts. *Arthritis and rheumatism.* 2008;58(2):577-85.
46. Shi-Wen X, Chen Y, Denton CP, Eastwood M, Renzoni EA, Bou-Gharios G, Pearson JD, Dashwood M, du Bois RM, Black CM, et al. Endothelin-1 promotes myofibroblast induction through the ETA receptor via a rac/phosphoinositide 3-kinase/Akt-dependent pathway and is essential for the enhanced contractile phenotype of fibrotic fibroblasts. *Molecular biology of the cell.* 2004;15(6):2707-19.
47. Soneson C, Love MI, and Robinson MD. Differential analyses for RNA-seq: transcript-level estimates improve gene-level inferences. *F1000Research.* 2015;4(1521.
48. Varet H, Brillet-Gueguen L, Coppee JY, and Dillies MA. SARTools: A DESeq2- and EdgeR-Based R Pipeline for Comprehensive Differential Analysis of RNA-Seq Data. *PloS one.* 2016;11(6):e0157022.